# Assessing ocean alkalinity for carbon storage


**Sarah Gore**

School of Earth and Environmental Sciences

Cardiff University

Submitted in partial fulfilment of the requirements for the degree of

*Doctor of Philosophy*

November 2021

# Abstract

Proposals to remove $CO_2$ from the atmosphere are becoming increasingly important in climate change policy. However, considerable uncertainty remains regarding the cost, scalability, and socioenvironmental consequences. One proposal for removing $CO_2$ from the atmosphere involves increasing total alkalinity (TA) in the ocean. This is known as ocean alkalinity enhancement (OAE) and involves the oceanic uptake of $CO_2$ from the atmosphere and its' conversion to carbonate ($CO_3^{2-}$) or bicarbonate ($HCO_3^-$) ions. Increasing ocean TA, pH, and calcium carbonate saturation state ($\Omega_{CaCO3}$) could potentially alleviate sensitive ecosystems from ocean acidification. However, OAE could raise pH and $\Omega_{CaCO3}$ well above modern day levels and there is little data on the environmental impact of this. These potential perturbations could substantially influence marine biology, particularly those taxa found in coastal environments as these regions are a favourable site for TA addition. This thesis sets out to determine how elevated TA influences the physiology of two important coastal taxa, a benthic calcifying macroalgae found on rocky shores of the continental shelf (*Corallina* spp.) and *Synechococcus* 8806, a calcifying pico-sized phytoplankton found in the surface of deeper continental shelf waters. How elevated TA affects the growth rates, calcification rates, productivity rates and photophysiology of these two physiologically different species was investigated as part of four separate ex-situ experiments. The results from this thesis provide the first insights to the practical use of OAE as a carbon dioxide removal approach in terms of the response of the marine environment. Results show that increasing seawater TA significantly increases *Corallina* spp. calcification rates and productivity rates and so could potentially lessen the impacts of ocean acidification. Furthermore, these results suggest that elevated TA increases *Synechococcus* 8806 growth and under elevated TA higher rates of $CaCO_3$ precipitation rates occurred. However, the results from this thesis do not show whether this was due to *Synechococcus* 8806 growth. The results show that OAE would not be intrinsically detrimental for *Corallina* spp. and *Synechococcus* 8806 in terms of direct effects to physiology. However, further research is needed to determine what the indirect effects of elevated TA are and how this could impact *Corallina* spp. and *Synechococcus* 8806.

# Lay summary

The research undertaken for this thesis is based around a “carbon dioxide removal” technology. To reduce the negative effects caused by global temperature rise, greenhouse gasses such as $CO_2$ need to be removed from the atmosphere as well as heavily reducing the amount of $CO_2$ (and other greenhouse gases) we release into the atmosphere. This thesis specialises in an ocean-based carbon dioxide removal approach known as “ocean alkalinity enhancement”.

The oceans currently naturally store vast amounts $CO_2$ (there is 40 times more CO2 in the ocean than there is in the atmosphere) and has the capability to store much more for a very long time. Since humans first started burning fossil fuels and releasing CO2 into the atmosphere, the oceans have taken up one third of all human CO2 emissions. This means the ocean is a perfect place to store the excess CO2 emissions we’ve pumped into the atmosphere but the rate at which the oceans take up atmospheric $CO_2$ needs to be sped up and ocean alkalinity enhancement works by speeding that process up.

$CO_2$ molecules are constantly moving from the surface ocean into the atmosphere and from the atmosphere back into the surface ocean. When there are more $CO_2$ molecules in the atmosphere, they move to the ocean. When there are more $CO_2$ molecules in the ocean, they move to the atmosphere. The bigger the difference in $CO_2$ molecules between the surface ocean and the atmosphere, the more $CO_2$ can be taken up by the ocean. So to get the ocean to take up more atmospheric $CO_2$ there needs to be fewer $CO_2$ molecules in the surface ocean compared to the atmosphere. This can be done by changing seawater chemistry. If certain “alkaline minerals” are added to the surface ocean, when $CO_2$ molecules move from the atmosphere into the surface ocean, they are then stored as “alkalinity” (i.e. stored as $CO_3^{2-}$ and $HCO_3^-$ molecules). This means that even though the ocean is taking up more CO2 from the atmosphere, there are less CO2 molecules stored in the surface ocean. This has the added effect of making the seawater less acidic (increases the pH of the surface ocean) and so means that ocean alkalinity enhancement can be used to help reduce the effects of “ocean acidification”. This is when the ocean takes up $CO_2$ without the addition of alkaline minerals. In this case, the $CO_2$ molecules stay as $CO_2$ and do not get stored as alkalinity. This results in surface seawater $CO_2$ concentration to increase and pH to decrease, which has been shown to have a negative impact on marine biology.

Before ocean alkalinity enhancement can be used at a large scale all across the globe to reduce atmospheric $CO_2$, more research needs to be done to work out whether this is a practicable option for helping reduce the impacts of climate change. For example, how the change in seawater chemistry is going to affect marine ecosystems needs to be better understood. Therefore, this thesis set out to answer the following question:

How does the marine environment respond to increased alkalinity?

To answer this, laboratory experiments were carried out where two very different types of marine plants were grown under different alkalinity conditions and how they responded was carefully monitored. The two organisms investigated were:

1. A red seaweed (*Corallina*)

2. A microscopic “blue-green algae” (cyanobacteria)

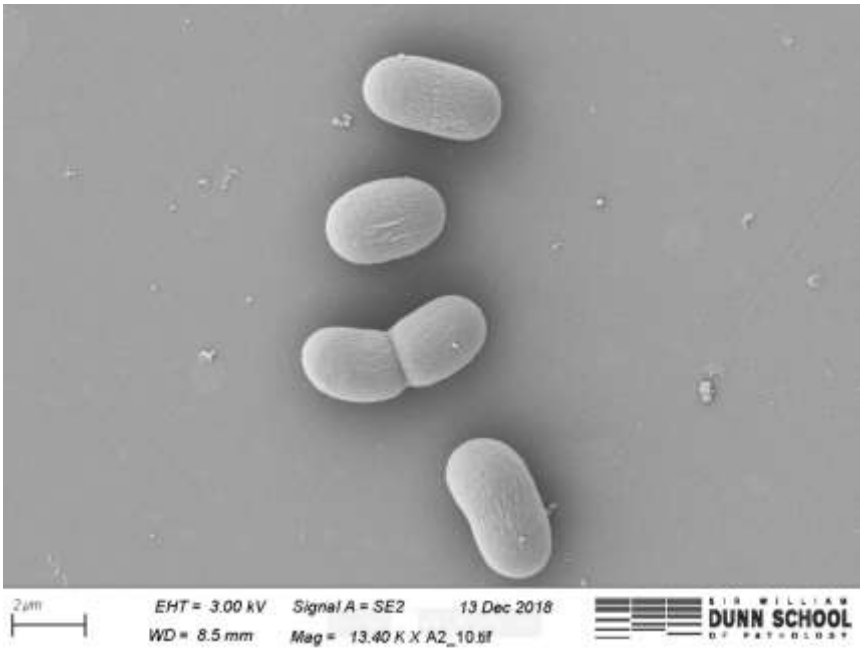


In the simplest terms, the results from the experiments showed that increasing alkalinity did not harm the growth of either type of organisms. In fact, it enhanced their growth. This means that ocean alkalinity enhancement does not appear to be detrimental to the marine environment and could also be used for ocean acidification mitigation. However, only two species were studies and there are many more species in the ocean and so a lot more work needs to be done before we can say for sure than ocean alkalinity enhancement is truly safe.

# Author contribution to publications

Chapter 2 has been published as:

Gore S. J., Renforth, P. and Perkins, R. (2019) The potential environmental response to increasing ocean alkalinity for negative emissions. Mitigation and Adaptation Strategies for Global Change (2019) 24:1191–1211. doi: 10.1007/s11027-018-9830-z

N.B. Since publication, an accuracy issue with respect to the pH electrode measurements has been identified. See Section 6.4. for further discussion on this.

# Acknowledgements

First of all, I would like to thank my supervisors Phil Renforth and Roo Perkins. Thank you for the support you have given me throughout my time at Cardiff. Thank you, Phil, for supporting me in taking the research in the direction I wanted and thank you to Roo for agreeing to be part of this project and providing the technical knowledge and contacts I needed to be able to do so. Also, thanks to Stephen Barker for his help at the start of my PhD.

I have been incredibly lucky and been able to spend time at other universities with other research groups whilst studying for my PhD. I would like to thank the Ocean Bugs research group at Oxford University for allowing me to visit in 2018 and 2019. In particular, I want to say a huge thank you to Sophie Gill for setting me up in the lab and being so welcoming and to Ros Rickaby for your support whilst I was visiting. Thanks to Phil Holdship and Errin Johnson for helping me with my analyses at Oxford. Also, I would like to thank Doug Campbell and Max, Alysosn, Mirere, Miranda, and Matt at Mount Alison University, New Brunswick for all your help whilst working in your lab. Finally, thank you to all the staff at Cardiff University School of Earth and Ocean Sciences (now School of Earth and Environmental Sciences). In particular, Xiaohong Tang, Jen Pinion and Huw Pullin.

I would like to thank my friends, family and colleagues who have provided constant reassurance and encouragement throughout my PhD. A huge thank you goes to my mum, dad, and sisters, Katey and Mollie for their continuous love and support. I also want to thank the Birds, for all their support over the years. Thank you to all my friends outside university for showing me there is much more to life than academia; in particular, Beth, Jenny, and Zoë. Thanks also to my PhD cohort for all the fun over the years. I want to especially thank Chantelle Roeslefse for being such a good friend and for always saying yes when I asked for a coffee break. Finishing this PhD would have been much harder without your support.

My acknowledgements would not be complete without thanking Sam. Thank you for being my biggest supporter and for taking that leap of faith with me by agreeing to leave your job in Southampton to move to Cardiff. Thank you for your patience, support, and encouragement while I have been writing this thesis and thank you for always making me a cup of tea in the morning. I honestly could not have done this without you.

Finally, I must thank my grandad. Without your financial support, I would not have been able to do my masters and so would never have started this PhD and so I dedicate this thesis to you.

# Table of Contents

# List of Figures

# List of Tables

# List of Equations

# Notations

| | |
|---|---|
| CDR | Carbon dioxide removal |
| OAE | Ocean alkalinity enhancement |
| EW | Enhanced weathering |
| TA | Total alkalinity |
| CA | Carbonate alkalinity |
| $TA_{con}$ | Conservative alkalinity |
| DIC | Dissolved inorganic carbon |
| $pCO_2$ | Partial pressure of $CO_2$ |
| $\Omega_{CaCO3}$ | The saturation state of calcium carbonate in solution |
| $\Omega_{Ca}$ | The saturation state of calcite in solution, see Section 1.3.3 |
| $\Omega_{Ar}$ | The saturation state of aragonite in solution, see Section 1.3.3 |
| $CO_2$ | Carbon dioxide |
| $CO_3^{2-}$ | Carbonate ion |
| $HCO_3^-$ | Bicarbonate ion |
| $CaCO_3$ | Calcium carbonate (typically as calcite or aragonite polymorphs) |
| [*x*] | Concentration of *x* |
| µEq $L^{-1}$ | Microequivalents per litre (units of alkalinity; equivalent to 0.001 mmol $L^{-1}$) |
| µmol $L^{-1}$ | Micromoles per litre (units of concentration; equivalent to 0.001 mmol $L^{-1}$) |
| µatm | Microatmospheres (units of pressure) |
| psu | Practical salinity unit (units of salinity) |
| °C | Degrees Celsius (units of temperature) |
| gDW | Grams dry weight |
| NCR | Net calcification rate |
| ppm | Parts per million; equivalent to mg $L^{-1}$ |
| NPP | Net primary production |
| Chl-*a* | Chlorophyll *a* |
| IGR | Instantaneous growth rate |
| µ | Growth rate constant |
| RLC | Rapid light curve |
| PAM | Pulse Amplitude Modulation |
| $rETR_{max}$ | Relative maximum electron transport rate |
| α | Coefficient of light use efficiency, see Section 2.3.4 |
| $E_k$ | Light saturation coefficient, see Section 2.3.4 |
| $F_v/F_m$ | The Genty parameter, see Section 2.3.4 |
| FRRf | Fast repetition rate fluorometry |

For FFRf parameters see Table 4.2, Section 4.3.3, page 84.

# Chapter 1.

# General Introduction

## 1.1. Status of the climate emergency and the need for carbon dioxide removal

Anthropogenic climate change is defined as the shift in climate patterns mainly caused by greenhouse gas emissions from human activities such as energy production, industrial activities and those related to forestry, land use and land-use change (Edenhofer et al. 2014). This shift is accelerating and in 2019, the UK was the first parliament to declare a "climate emergency" (Labour 2019).

Greenhouse gases trap heat in the Earth's atmosphere, which is the main driving force behind global warming. The main greenhouse gases defined by the Kyoto protocol are carbon dioxide ($CO_2$), methane ($CH_4$), nitrous oxide ($N_2O$), and the fluorinated gases such as hydrofluorocarbons (HFCs), perfluorocarbons (PFCs) and sulphur hexafluoride ($SF_6$) (Change 2008; UNFCCC 2008). This thesis will focus on $CO_2$ because it has the most impact on the changing climate due to its longevity in the atmosphere. In 2018, $CO_2$ emissions accounted for approximately three quarters of the total global greenhouse gas emissions (United Nations Environment Programme; 2019). Present-day atmospheric $CO_2$ concentrations are nearly 50% higher than preindustrial concentrations (Doney et al. 2020) $CO_2$ and other GHG emissions from anthropogenic activities are thought to have already caused ~1.0 °C of global warming above pre-industrial temperatures and is likely to reach 1.5 °C between 2030 and 2052 if the current emission rate continues (IPCC 2018).

Increases in temperature are directly related to an increase in risk associated with climate hazards such as droughts, floods, hurricanes, severe storm events, heatwaves, wildfires, extreme cold spells and landslides (Giles 2015). Climate related hazards have a considerable social, economic, and environmental impact. For example, in 2018 natural disasters affected 68.5 million people and cost ~$132 billion in damages (CRED 2009). Other risks associated with temperature rise include sea level rise, loss of life due to health hazards and natural disasters, increased ecosystem stress, increased food and water security stress, increased migration, and increased geopolitical tensions (WEF 2020). The risk imposed by these impacts is lower when temperature rise is limited to 1.5 °C compared to 2 °C warming (IPCC 2018). Therefore, the 2015 Paris agreement proposes to limit global temperature rise well

below 2 °C above pre-industrial levels and to pursue efforts to limit the temperature increase even further to 1.5 °C (UNFCCC 2015).

To meet the 1.5 °C target by the end of the century, greenhouse gas emissions need to be reduced to 25–30 $GtCO_2$ eq $year^{-1}$ by 2030 (IPCC 2018). To achieve this, there needs to be a 45% decline in anthropogenic greenhouse gas emissions by 2030 (compared to 2010 levels), and net-zero emissions must be achieved by 2050 (or 25% and by 2070 to meet the 2 °C target by 2100) (IPCC 2018). Unfortunately, atmospheric $CO_2$ is still accumulating by approximately 0.5% each year (~2 ppm/year) (Le Quéré et al. 2018) and so the current mitigation efforts and future emissions commitments are not sufficient to achieve these temperature goals (Lawrence et al. 2018; Nieto et al. 2018). However, carbon dioxide removal approaches (CDR, also known as 'negative emission technologies') could be used to significantly reduce $CO_2$ emissions (Keith 2000); (Fuss et al. 2018; Minx et al. 2018; Nemet et al. 2018). Further, Peters et al. (2013) suggest that CDR will be needed (in addition to substantially reduced greenhouse gas emissions) to keep to the 2015 Paris agreement targets.

CDR involves removing $CO_2$ from the atmosphere and the main proposals include: bioenergy carbon capture and storage, biochar, enhanced weathering, direct air carbon capture and storage, ocean fertilization, soil carbon sequestration, afforestation and reforestation, wetland construction and restoration, and ocean alkalinity enhancement (McGlashan et al. 2012; McLaren 2012; Lawrence et al. 2018; Lenzi et al. 2018; Royal Society 2018; Lin and Zhu 2019; Palmer 2019; Pires 2019; Goglio et al. 2020) For more information, please see the three-part review where several CDR approached are evaluated and their costs, potentials, side-effects, and their potential for upscaling are estimated (Fuss et al. 2018; Minx et al. 2018; Nemet et al. 2018).

## 1.2. Ocean alkalinity enhancement

A proposal to remove $CO_2$ from the atmosphere involves increasing total alkalinity (TA) in the ocean. This is known as ocean alkalinity enhancement (OAE) and involves the oceanic uptake of $CO_2$ from the atmosphere and when $CO_2$ is stored in the ocean as carbonate ($CO_3^{2-}$) or bicarbonate ($HCO_3^-$) ions. The chemistry of which is explained in further detail below in Section 1.3.

The idea of increasing ocean TA by adding solid alkaline materials, or their dissolution products into the oceans was first introduced by Kheshgi (1995). He proposed adding lime (CaO) or portlandite ($Ca(OH)_2$) to the surface oceans. Rau and Caldeira (1999) proposed the

idea of artificially enhancing mineral carbonate dissolution by exposing carbonate minerals to flue gasses ($CO_2$ rich waste gas) and seawater, which mimics the natural weathering of limestone. Another approach to increase ocean TA is to add naturally occurring and abundant alkaline minerals, such as forsteritic olivine ($Mg_2SiO_4$) (Köhler et al. 2010), limestone ($CaCO_3$) (Harvey 2008), or basalt (Beerling et al. 2018; Rigopoulos et al. 2018; Beerling et al. 2020) to the ocean or land surfaces (Hartmann et al. 2013). An alternative technique is the electrolysis of seawater which involves electrochemically removing HCl from the oceans which result in an increase in TA (House et al. 2007). Table 1.1 summarises the different methods of artificially increasing ocean TA. The overall objective of each of these approaches is to accelerate the natural weathering reactions which would otherwise take tens to hundreds of thousands of years (Archer 2005; Lord et al. 2016) to occur in a policy relevant timescale.

The ocean currently stores ~140,000 $GtCO_2$, (~40,000 GtC primarily as $HCO_3^-$ and $CO_3^-$ ) and through OAE it may be able to store trillions of tons of $CO_2$ for tens of thousands of years in the form of dissolved inorganic carbon (Renforth and Henderson 2017). The cost of OAE will depend on the approach utilized in producing, transporting and distributing the alkaline material and is estimated to be between \$10 and \$190/$tCO_2$ captured, (Renforth and Henderson 2017). OAE is still a relatively new concept, and most of the research is still at early stages of development.

*Table 1.1. Summary of Ocean Alkalinity Enhancement (OAE) methods.*

| OAE approach | Description | CDR Potential | Additional Perturbations | Advantages | Disadvantages | Reference |
|---|---|---|---|---|---|---|
| Enhanced Weathering of Silicates- Open Ocean | Finely ground silicate minerals applied evenly over the open ocean. The silicate minerals dissolve directly in surface seawater releasing cations (e.g. $Mg^{2+}$) which cause TA to increase. | 3.4 moles of $CO_2$ uptake per mole of olivine (forsterite) dissolved | Silicate rock dissolution products (e.g. $SiO_2$, Mg, Ni, Fe) | • Silicate minerals are abundant and already mined on a large scale.<br>• Homogenous application would result in less severe perturbations to marine carbonate chemistry<br>• Increased $SiO_2$ and Fe could have a fertilising effect and also increase $CO_2$ uptake through enhancing the biological carbon pump. | • Potentially large volumes of silicate rocks needed to be mined and processed (expensive and energy intrusive)<br>• Dissolution products could potentially impact on marine biology.<br>• Silicate powders would need to be fine in order to stop them sinking to the deep ocean and this would be an energy intensive process<br>• Even distribution over entire ocean regions is unfeasible.<br>• An enormous infrastructure needed to transport mined silicate minerals. | Köhler et al. (2013) |

| | | | | | | |
|---|---|---|---|---|---|---|
| Enhanced Weathering of Silicates- Coastal | Silicate minerals applied to beaches or shallow shelf seas on the continental shelf. The silicate minerals dissolve in coastal seawater releasing cations (e.g. $Mg^{2+}$) which cause TA to increase in coastal regions eventually dispersing throughout the ocean. | 3.4 moles of $CO_2$ uptake per mole of olivine (forsterite) dissolved | Silicate rock dissolution products (e.g. $SiO_2$, Mg, Ni, Fe) | • Silicate minerals are abundant and already mined on a large scale<br>• Because the coast is a more energy intensive environment, then not as much grinding needed.<br>• Coastal regions are also well mixed which will help increase the efficiency of ocean carbon uptake.<br>• Increased $SiO_2$ and Fe could have a fertilising effect and also increase $CO_2$ uptake through enhancing the biological carbon pump. | • Potentially large volumes of silicate rocks needed to be mined and processed (expensive and energy intrusive)<br>• Dissolution products could potentially impact on marine biology<br>• An enormous infrastructure needed to transport mined silicate minerals. | Meysman and Montserrat (2017)<br><br>Montserrat et al.(2017)<br><br>Hangx and Spiers (2009)<br><br>Feng et al. (2017) |
| Enhanced Weathering of Silicates- Land | Finely ground silicate minerals applied over land surfaces, where the silicate minerals dissolve and then the dissolution products (e.g. $Mg^{2+}$) are discharged into the ocean via rivers. | 3.4 moles of $CO_2$ uptake per mole of olivine (forsterite) dissolved | Silicate rock dissolution products (e.g. $SiO_2$, Mg, Ni, Fe) | • If combined with agriculture crop yields could be enhanced and soil erosion prevented.<br>• Silicate minerals are abundant and already mined on a large scale.<br>• Increased $SiO_2$ and Fe could have a fertilising effect and also increase $CO_2$ uptake through enhancing the biological carbon pump. | • Potentially large volumes of silicate rocks needed to be mined and processed (expensive and energy intrusive)<br>• An enormous infrastructure needed to transport mined silicate minerals. | Kohler et al. (2010)<br><br>Hartmann et al. (2013)<br><br>Beerling et al. (2020)<br><br>Beerling et al. (2018) |

| | | | | | | |
|---|---|---|---|---|---|---|
| Enhanced Weathering of Silicates-Electrolysis | Seawater HCl is electrochemically removed and then neutralized through reaction with silicate rocks. The reaction both removes HCl from the ocean and produces alkaline dissolution products (e.g. $Mg^{2+}$) which are then released into the ocean. | 0.84 moles of $CO_2$ uptake for each mole of HCl removed and neutralized. | Silicate rock dissolution products (e.g. $SiO_2$, Mg, Ni, Fe)<br><br>Halogenated organics<br><br>$H_2$ | • The process can be run anywhere in the world It works equally well for all sources of $CO_2$<br>• It can be powered by zero and low carbon power sources.<br>• $H_2$ and $Cl_2$ produced could be sold to offset the cost<br>• Increased $SiO_2$ and Fe could have a fertilising effect and also increase $CO_2$ uptake through enhancing the biological carbon pump. | • Requires large amounts of HCl to be removed to offset an appreciable quantity of $CO_2$ emissions (e.g. $10^{14}$ moles for 15% of emissions).<br>• Expensive process.<br>• Potentially large volumes of silicate rocks needed to be mined and processed (expensive and energy intrusive).<br>• Dissolution products could potentially impact on marine biology.<br>• An enormous infrastructure needed to transport mined silicate minerals. | House et al. (2007) |
| Lime (CaO) addition | Limestone is first calcinated into lime (CaO) and then the dissolution products ($Ca^{2+}$) are released into the oceans, increasing TA. | 1.79 moles of $CO_2$ uptake per mole of CaO dissolved | $Ca^{2+}$ | • Limestone is abundant and already mined on a large scale.<br>• Ca added likely to be quite small relative the total quantity already dissolved in the oceans. | • The thermal decomposition of limestone to lime (CaO) is an energy intensive process.<br>• An enormous infrastructure needed to transport mined limestone. | Kheshgi (1995) |

| | | | | | | |
|---|---|---|---|---|---|---|
| Enhanced Weathering of Limestone | React $CO_2$ rich power-plant gases with seawater to produce a carbonic acid ($H_2CO_3$) solution which then is reacted with limestone and then the dissolution products ($Ca^{2+}$) are then released into the ocean causing TA to increase. | 1 mole of $CO_2$ uptake per 1.5 mole of carbonate mineral dissolved | $Ca^{2+}$ | • Limestone is abundant and already mined on a large scale.<br>• Ca added likely to be quite small relative the total quantity already dissolved in the oceans | • A large scale operation would be an energy intensive process and would require infrastructure to mine, transport, crush and dissolve the minerals as well as substantial pumping of seawater.<br>• An enormous infrastructure needed to transport mined limestone | Rau and Caldeira (1999) |
| $CaCO_3$ addition | Limestone powder applied to the mixed layer of the surface ocean and then dissolves directly in surface seawater releasing cations (e.g. $Ca^{2+}$) which cause TA to increase. | 0.79 moles of $CO_2$ uptake for every mole of $CaCO_3$ dissolved | $Ca^{2+}$ | • Limestone is abundant and already mined on a large scale.<br>• Ca added likely to be quite small relative the total quantity already dissolved in the oceans. | • Requires large amounts of limestone to be mined to offset an appreciable quantity of $CO_2$ emissions (e.g. each year would require 4 Gt of limestone to capture 0.48 Gt C).<br>• Mining and grinding of limestone are energy intensive and expensive processes.<br>• An enormous infrastructure needed to transport mined limestone | Harvey (2008) |

| | | | | | | |
|---|---|---|---|---|---|---|
| Electrochemical Splitting of Calcium Carbonate | Calcium carbonate ($CaCO_3$) is electrochemically split into $Ca^{2+}$ and $HCO_3^-$ (producing $H_2$) by putting electrodes and carbonate penetrate surface seawater from either stationary (e.g., docks) or mobile vessels (e.g. ships). $Ca^{2+}$ is directly released into the seawater causing TA to increase. | 1 mole of $CO_2$ can be captured per mole of $H_2$ generated | $Ca^{2+}$<br>$H_2$ | • $H_2$ produced could be sold as an energy source to offset the cost<br>• Ca added likely to be quite small relative the total quantity already dissolved in the oceans.<br>• Potential to be powered by zero and low carbon power sources.<br>• Limestone is abundant and already mined on a large scale. | • Expensive process.<br>• Lots of water required to dilute enough to stop the precipitation of $CaCO_3$.<br>• Mining and grinding of limestone are energy intensive and expensive processes.<br>• Supplying and operating such an electrochemical system could produce more $CO_2$ emissions than it captures (unless electricity produced renewably) | Rau (2008) |

## 1.3. The marine carbonate system

To explain how increasing ocean TA can lead to an increase in ocean $CO_2$ storage, a review of the marine carbonate system is presented. The ocean is a natural atmospheric $CO_2$ sink and contains 50 times more carbon than the atmosphere (Schrag 2007). Over the past 200 years, the ocean has taken up approximately one third of anthropogenic $CO_2$ emissions (Sabine et al. 2004). $CO_2$ it taken up through the diffusion of $CO_2$ from the atmosphere into the water, based on the differences of $CO_2$ partial pressure between the atmosphere and the ocean, similarly the ocean degasses into the atmosphere through a reverse in this pressure gradient. A decrease in aqueous $CO_2$ concentration is caused by photosynthesis of marine phytoplankton (often referred to as the biological carbon pump)(Riebesell et al. 2009). Some of this biomass sinks into the deeper ocean and is remineralised back into $CO_2$. When these deeper waters are cycled back to the surface their elevated concentration of $CO_2$ degasses into the atmosphere. OAE involves an alternative means by which to decrease the partial pressure of $CO_2$ in ocean wasters (or terrestrial waters that drain into the ocean).

Marine carbonate chemistry is governed by the following reactions (when considering a simple overview of the marine carbonate system which only comprises the components: $CO_2$, $HCO_3^-$, $CO_3^{2-}$ , $H^+$, $OH^-$).

$$CO_{2_{atm}} \rightleftharpoons CO_{2_{(aq)}} \quad \text{(Equation 1)}$$

$$H_2O_{(l)} \rightleftharpoons H^+ + OH^- \quad \text{(Equation 2)}$$

$$CO_{2_{(aq)}} + H_2O \rightleftharpoons H_2CO_3 \quad \text{(Equation 3)}$$

$$H_2CO_3 \rightleftharpoons HCO_3^- + H^+ \quad \text{(Equation 4)}$$

$$HCO_3^- \rightleftharpoons CO_3^{2-} + H^+ \quad \text{(Equation 5)}$$

$$k_H = \frac{[CO_2]_{(aq)}}{[CO_2]_{atm}} \quad \text{(Equation 6)}$$

$$k_{H_2O} = \frac{[H^+][OH^-]}{[H_2O]_{(l)*}} * [H_2O] = 1 \quad \text{(Equation 7)}$$

$$k_1 = \frac{[HCO_3^-][H^+]}{[CO_2](aq)} \quad \text{(Equation 8)}$$

$$k_2 = \frac{[CO_3^-][H^+](aq)}{[HCO_3^{2-}](aq)} \quad \text{(Equation 9)}$$

When $CO_2$ moves from the atmosphere into the ocean, atmospheric $CO_2$ equilibrates with aqueous $CO_2$ in surface waters (Equation 1). Once dissolved, aqueous $CO_2$ ($CO_{2(aq)}$) reacts with water to form carbonic acid ($H_2CO_3$; Equation 3) which, then quickly dissociates into bicarbonate ($HCO_3^-$; Equation 4) and carbonate ($CO_3^{2-}$; Equation 5) ions. The relative quantities of $HCO_3^-$ and $CO_3^{2-}$ ions are given by Equations 8 and 9 respectively.

From these equilibria, six main carbonate chemistry parameters have been determined:

- Dissolved Inorganic Carbon (DIC)
- Alkalinity
- pH
- Partial pressure of CO2 ($pCO_2$)
- Calcium carbonate saturation state of calcite ($\Omega_{Ca}$) and aragonite ($\Omega_{Ar}$)

Each of these will be discussed in more detail below.

### 1.3.1. Dissolved inorganic carbon (DIC)

As Equations 1-5 show, once $CO_2$ enters the ocean, it exists in three different inorganic forms: $HCO_3^-$, $CO_3^{2-}$ and $CO_{2(aq)}$ and the sum of these of is defined as dissolved inorganic carbon (DIC; Equation 10). In the literature, DIC is also sometimes referred to as total $CO_2$ ($TCO_2$ or $C_T$). Because $H_2CO_3$ dissociates quickly, the stoichiometric concentration (denoted by square brackets from herein) of $H_2CO_3$ is ~0.3% that of $[CO_{2(aq)}]$. This makes it is difficult to measure and so $H_2CO_3$ is conventionally expressed as $CO_{2(aq)}$ and not included in Equation 10 (Zeebe and Wolf-Gladrow 2001).

$$DIC = [HCO_3^-] + [CO_3^{2-}] + [CO_2] \quad \text{(Equation 10)}$$

### 1.3.2. pH

An important part of the carbonate system is water ($H_2O$) and its dissociation products $H^+$ and $OH^-$(Equation 2). Free hydrogen ions ($H^+$) do not exist in any significant amount in aqueous solutions (Zeebe and Wolf-Gladrow 2001) but rather exist as hydrate complexes associated with $H_3O^+$ and $H_9O_4^+$. However, for the sake of this thesis, $[H^+]$ will refer to hydrogen ion concentration from herein.

pH can be simply defined as the negative common logarithm of $[H^+]$ (Equation 11).

$$pH = -\log [H^+] \quad \text{(Equation 11)}$$

At normal seawater pH (8.2), the relative proportions of $HCO_3^-$, $CO_3^{2-}$ and $CO_{2(aq)}$ are approximately 89%, 10.5% and 0.5% respectively (Doney et al. 2009). Therefore, the majority of the dissolved $CO_2$ in the ocean is in the form of $HCO_3^-$, not $CO_{2(aq)}$. Because of the equilibria between these species (Equations 1-6), seawater is buffered with respects to changes in $[H^+]$.

The buffering capacity of the ocean can be explained by the following equation:

$$CO_{2(aq)} + H_2O + CO_3^{2-} \leftrightarrow 2HCO_3^- \quad \text{(Equation 12)}$$

$$k = \frac{[HCO_3^{2-}](aq)}{[CO_3^-][CO_2](aq)} \quad \text{(Equation 13)}$$

Equation 12 is an equilibrium reaction occurring between the different carbonate species. When $CO_2$ increases in seawater, it produces $[H^+]$ ions (Equations 1-5). This "excess" of $[H^+]$ would then cause pH to decrease. However, the $CO_3^{2-}$ ions present in the seawater can use up this excess $[H^+]$ to form stable $HCO_3^-$ (Equation 14).

$$CO_3^{2-} + H^+ \rightarrow HCO_3^- \quad \text{(Equation 14)}$$

### 1.3.3. Saturation state

Another important constituent of the marine carbonate system is calcium carbonate ($CaCO_3$). The formation or dissolution of solid $CaCO_3$ is closely related to the control of atmospheric $CO_2$ on various time scales. $CaCO_3$ has two common polymorphs, calcite and aragonite, and whether $CaCO_3$ precipitates or dissolves is determined by both the saturation state of calcite ($\Omega_{Ca}$) and aragonite ($\Omega_{Ar}$) in seawater. Both of which are a function of $[CO_3^{2-}]$, $[Ca^{2+}]$, and $K_{sp}$ (Equation 15).

$$\Omega = \frac{[Ca^{2+}][CO_3{}^{2-}]}{K_{sp}} \quad \text{(Equation 15)}$$

$K_{sp}$ is the apparent solubility product (a discreet value for each mineral phase) and depends on temperature, salinity, and pressure. The crystal structure of calcite is rhombohedral whereas the structure of aragonite is orthorhombic and this difference in structures results in differences in physical and chemical properties. For example, aragonite is more soluble than calcite at a given temperature, salinity and pressure and so has a higher $K_{sp}$ than calcite (e.g. $10^{-6.19}$ $mol^2$ $kg^{-2}$ compared to $10^{-6.37}$ $mol^2$ $kg^{-2}$ when T = 25ºC, S = 35, P = 1 atm) and this means that calcite is the more stable polymorph of $CaCO_3$ at these conditions.

When $\Omega_{Ca/Ar} > 1$, then the solution is supersaturated with respect to calcite or aragonite and precipitation is more likely to occur. Whereas when $\Omega_{Ca/Ar} < 1$, the solution is undersaturated

with respect to calcite or aragonite and dissolution is more likely to occur. Variations in seawater [$Ca^{2+}$] are small and closely related to variations in salinity (Zeebe and Wolf-Gladrow 2001), therefore both $\Omega_{Ca}$ and $\Omega_{Ar}$ are mainly determined by changes to seawater [$CO_3^{2-}$]. This means that when seawater [$CO_3^{2-}$] is higher, precipitation rather than dissolution of $CaCO_3$ is more likely to occur.

Assuming average surface water TA of 2200 µmol $L^{-1}$ (Fine et al., 2017), salinity of 35%, and atmospheric $pCO_2$ of 400 µatm (Le Quere et al. 2018; Friedlingstein et al. 2019), modern surface seawater $\Omega_{Ca}$ ranges between 2.20 – 5.11 depending on seawater temperature (3-28℃) (Feely et al. 2009). Therefore, surface seawater is supersaturated with respect to calcite by a factor of 5 in some regions (and aragonite by ~2.5 times). However, spontaneous precipitation of $CaCO_3$ does not occur because of the presence of other elements in seawater (Berner 1975).

## 1.3.4. $CO_2$ partial pressure

The partial pressure of $CO_2$ ($pCO_2$) of seawater refers to the partial pressure of $CO_2$ in the gas phase that is in equilibrium with the seawater. Henry's law and $pCO_2$ can be used to calculate the concentration of dissolved $CO_2$ in solution ([$CO_{2(aq)}$] (Equation 16):

$$\left[CO_{2(g)}\right] = k * pCO_2 \qquad \text{(Equation 16)}$$

Where k is Henry Law's constant.

Henry's Law states that (at a constant temperature) the amount of atmospheric $CO_2$ that dissolves into the ocean is directly proportional to the partial pressure of the atmospheric $CO_2$ in equilibrium with the ocean water. This means that it is possible to use the differences in $pCO_2$ between the ocean and atmosphere to estimate the net air-sea gas $CO_2$ flux. For example, if there is a higher concentration of $CO_2$ in the atmosphere, $CO_2$ will move from the atmosphere into the ocean and if the ocean has a higher $CO_2$ concentration, $CO_2$ will move from the ocean into the atmosphere.

## 1.3.5. Alkalinity

The term alkalinity has previously been attributed many different definitions, two of which (total alkalinity and conservative alkalinity) will be discussed below.

### *1.3.5.a Total alkalinity*

Dickson (1981) defined TA as a measure of the proton ($H^+$) deficit of a solution relative to a "zero level of protons". For example, the zero level of protons species for the carbonate system

could be $CO_2$ (i.e., there is no net charge) and then the other species in the system can either be above or below this zero-level. If they are below, they accept protons and if they are above they donate protons, and subsequently converted to the zero level species. For the carbonate system, $HCO_3^-$ is one proton below the zero level of protons and $CO_3^{2-}$ is two protons below. This means they are both proton acceptors. TA is the excess of proton acceptors over proton donors (Dickson 1981).

$$TA = proton\ acceptor - proton\ donors \quad \text{(Equation 17)}$$

Therefore, for a simple carbonate chemistry system including the species $CO_2$, $H_2O$, $HCO_3^-$, $CO_3^{2-}$, $OH^-$, $H^+$, then TA may be simplified to 'carbonate alkalinity' (CA):

$$CA = [HCO_3^-] + 2[CO_3^{2-}] + [OH^-] - [H^+] \quad \text{(Equation 18)}$$

In seawater there are many more proton acceptors and donors such as silicate ($SiO(OH)_3^-$) and borate ($B(OH)_4^-$) and Dickson (1981) defined TA as:

$$TA = [HCO_3^-] + 2[CO_3^{2-}] + [B(OH)_4^-] + [OH^-] + [HPO_4^{2-}] + 2[PO_4^{3-}] + [SiO(OH)_3^-] + [HS^-] + 2[S] + [NH_3] - [H^+] - [HSO_4^-] - [HF] - [H_3PO_4]$$

(Equation 19)

However, because the concentration of $HCO_3^-$ and $CO_3^{2-}$ are much greater in seawater (pH = 8.2) than the other proton acceptors and donors, then CA is often used (Wolf-Gladrow et al. 2007). TA is a conservative quantity which means it remains unchanged with pressure or temperature. This, and because it is relatively easy to measure, makes it a useful parameter for investigating marine carbonate chemistry.

*1.3.5.b Conservative alkalinity*

Another important alkalinity concept is conservative alkalinity, which considers alkalinity from a physical perspective. Natural seawater contains many ions both positive (cations) and negative (anions) and because the principle of electroneutrality applies to seawater, the sum of the charges of all ions present in seawater must equal zero. Figure 1.1 displays the charge balance of the major ions in seawater. Figure 1.1 shows that there is a small excess positive charge from the conservative cations. Because of the law of electroneutrality, this must be balanced by $[HCO_3^-]$, $[CO_3^{2-}]$, and boric acid, $[B(OH)_4^-]$, the second most important contribution to seawater alkalinity after CA but not shown in Figure 1.1 for simplicity). Therefore, from Figure 1.1, conservative alkalinity ($TA_{con}$) can be defined by Equation 20. For average seawater salinity (35 psu), the total charge concentration for cations is ~605 mmol $L^{-1}$ and for anions is 602.8 mmol $L^{-1}$. The

difference between the two (2.2 mmol $L^{-1}$) is equal to the TA of average seawater and so explains why ambient ocean TA varies from 2.1-2.4 mEq$L^{-1}$ (Fine et al. 2017).

$$TA_{con} = [Na^+] + 2[Mg^{2+}] + [Ca^{2+}] + [K^+] - [Cl^-] - 2[SO_4{}^{2-}] \quad \text{(Equation 20)}$$

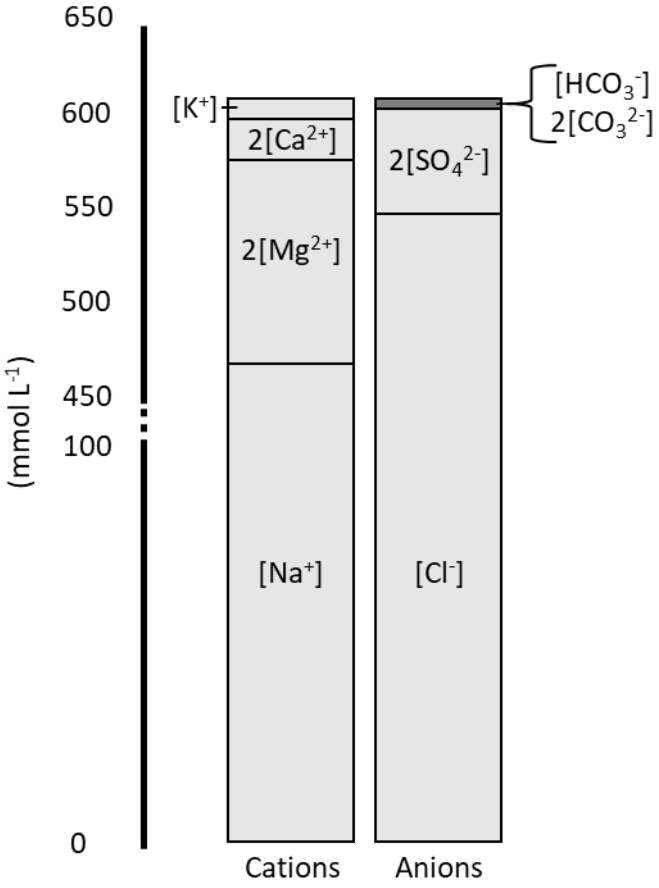


*Figure 1.1. Concentration and charge balance of the major cations and anions in seawater adapted from Zeebe and Wolf-Gladrow (2001).*

## 1.4. How does increasing alkalinity increase oceanic uptake of atmospheric $CO_2$?

The overall objective of OAE is to accelerate the natural weathering reactions which would otherwise take tens to hundreds of thousands of years to remove atmospheric $CO_2$ by increasing ocean TA (Archer 2005; Lord et al. 2016). Because of the law of electroneutrality, carbonate alkalinity has to increase when conservative alkalinity increases, therefore, a shift towards $HCO_3^-$ and $CO_3^{2-}$ can be induced by increasing the amount of positive conservative ions such as

$Ca^{2+}$ (e.g. by adding quicklime to the ocean) and $Mg^{2+}$ (e.g. by enhanced silicate weathering) (Pokrovsky and Schott 2000; Wolf-Gladrow et al. 2007; Oelkers et al. 2018). Figure 1.2 shows the increase in $[HCO_3^-]$ and $[CO_3^{2-}]$ needed to charge balance an increase in seawater $[Mg^{2+}]$.

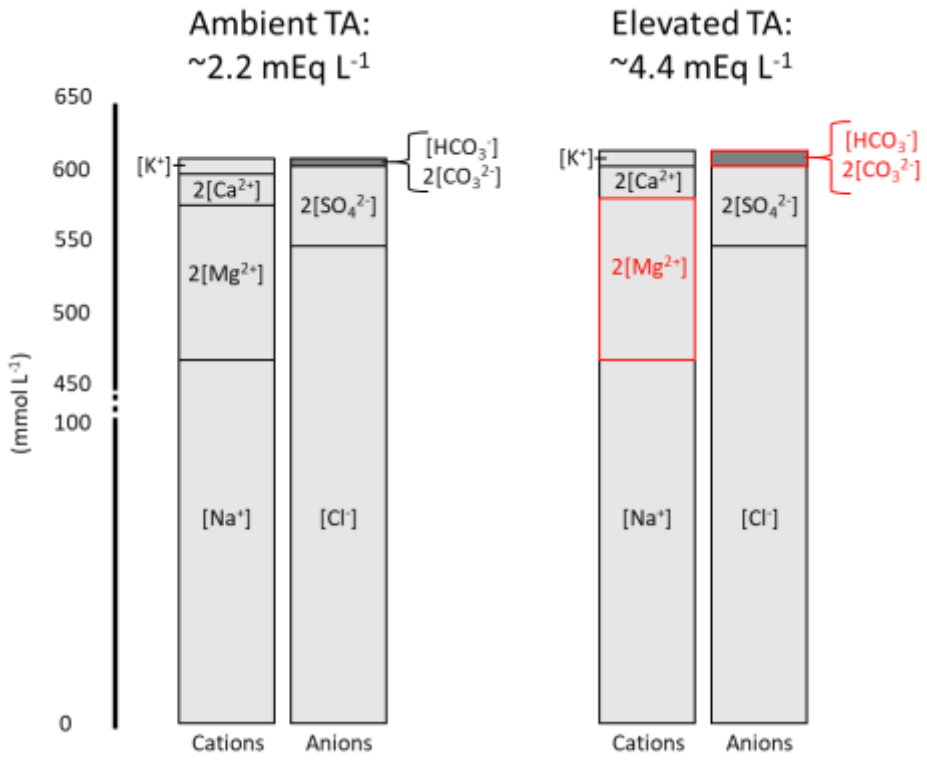


*Figure 1.2. Comparison between the concentration and charge balance of the major cations and anions in seawater for an ambient and elevated TA scenario.*

When TA is higher, more DIC is held as $CO_3^{2-}$ and less as $CO_{2(aq)}$. Therefore, by increasing TA, $pCO_2$ decreases, which then allows the ocean to take up more atmospheric $CO_2$. In other words, increasing ocean TA, increases the "buffering capacity" of the ocean so even though the ocean is taking up more atmospheric $CO_2$, the dissolved $CO_2$ is being held as stable $CO_3^{2-}$ and $HCO_3^-$ instead of aqueous $CO_2$ (Figure 1.3).

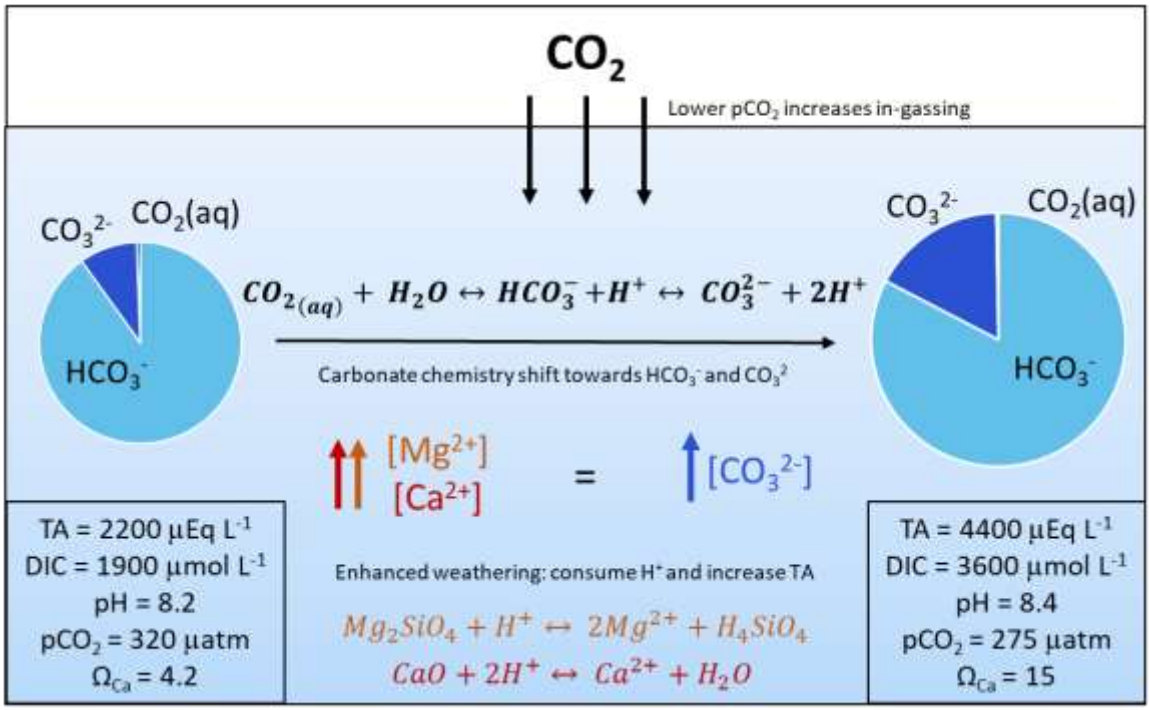


*Figure 1.3. Schematic summarising the main differences in marine carbonate chemistry between an ambient (2200 µEq $L^{-1}$) and elevated (4400 µEq $L^{-1}$) TA scenario. When alkaline dissolution products such as $Mg^{2+}$ and $Ca^{2+}$ are released into solution they consume protons which shifts the carbonate chemistry equilibrium away from $CO_2$ to $HCO_3^-$ and $CO_3^{2-}$. This lowers seawater $pCO_2$ and if surface seawater $pCO_2$ is undersaturated relative to the surrounding atmosphere, then atmospheric $CO_2$ can replenish it, causing a reduction in atmospheric $CO_2$.This results in seawater with higher total alkalinity (TA), dissolved inorganic carbon (DIC), pH, and $CaCO_3$ saturation state ($\Omega_{Ca}$).*

## 1.5. Potential ocean alkalinity induced perturbations to ocean carbonate chemistry

The environmental impact of OAE will mostly involve perturbations to the carbonate chemistry of the ocean, mainly an increase in TA, pH, and $\Omega_{CaCO3}$ as discussed previously. Because there have not yet been any large-scale additions of TA to the ocean, the potential environmental impacts are often predicted using global biogeochemical models. TA addition is predicted to increase surface seawater pH by 0.007 – 0.07 (Kohler et al. 2013; Lenton et al. 2018) and increase surface calcite saturation state ($\Omega_{Ca}$) to above current levels to 6 - 7.4 (Ilyina et al. 2013; Paquay and Zeebe 2013; Gonzalez and Ilyina 2016). Studies by Feng et al. (2016) and Gonzalez and Ilyina (2016) highlighted regional differences in the changes of carbonate chemistry due to regional variations in ocean physical and biogeochemical properties.

It is unlikely that a homogenous distribution of TA will be applied over the global oceans and so the most likely TA addition methods will involve increasing TA in a few distinct regions such as concentrated TA addition along ship tracks (Köhler et al., 2013), releasing dissolution products from on- and offshore platforms (Rau et al. 2013), or alkaline mineral application to coastal regions (Hangx and Spiers 2009; Feng et al. 2017a; Meysman and Montserrat 2017; Montserrat et al. 2017). Those regions located close to where TA is added would likely experience greater perturbations to carbonate chemistry compared to homogenous global TA addition.

Köhler et al. (2013) investigated a variety of TA addition scenarios including homogeneous TA addition and the addition of TA along existing ship pathways. Unsurprisingly, the perturbations to sea surface pH were much more localised in the ship addition scenario. For example, sea surface pH did not change south of 40° S, due to the low number of shipping routes. Whereas the changes in sea surface pH were much greater in the Northern Hemisphere compared to due to the higher ship track density in this region. This highlights that the scale of these changes will likely depend on the method of TA addition. Table 1.2 shows the range of carbonate chemistry parameters associated with several different OAE methods.

*Table 1.2. Estimate of possible changes to marine carbonate chemistry (pH and $\Omega_{Ca}$) for different OAE scenarios ($pCO_2$ and TA) adapted from Renforth and Henderson (2017).*

| OAE Scenario | Description | $pCO_2$* | TA** ($\mu Eq\ L^{-1}$) | pH' | $\Omega_{Ca}$' |
|---|---|---|---|---|---|
| A | No OAE under business as usual emissions | 1000 | 2200 | 7.666 | 1.76 |
| B | Homogenous OAE under BAU^ emissions | 1000 | 3200 | 7.817 | 3.53 |
| C | Homogenous OAE under reduced emissions | 600 | 3200 | 8.012 | 5.23 |
| D | Homogenous OAE under negative emissions | 400 | 3200 | 8.161 | 6.91 |
| E | Localised, equilibrated OAE | 400 | 4200 | 8.260 | 10.90 |
| F | Localised, rapid, non- equilibrated OAE | 50 | 4200 | 8.901 | 26.10 |

* Independent variable. Atmospheric $CO_2$ values estimated from (Matear and Lenton 2018) simulations based on the RCP pathways 8.5, 4.5, and 2.5.
** Independent variable. TA estimated assuming a TA increase of either 1000 or 2000 $\mu Eq\ L^{-1}$.
' Calculated using CO2sys (Pierrot et al. 2006) assuming T= 16 °C and S= 35
^ BAU- Business as usual

The environment to which TA addition occurs will also control the scale of perturbation. If TA addition occurs in a poorly mixed body of water with slow air-sea gas exchange, such as the South Pacific Gyre (Jones et al. 2014), then there will likely be much greater changes to carbonate chemistry. This is because any changes to carbonate chemistry will not immediately mitigated by in-gassing $CO_2$. This scenario has been described as “non-equilibrated” TA addition

(Bach et al. 2019) and potentially raise pH to ~8.9 and $\Omega_{Ca}$ to ~26 (Table 1.2). Equilibrated alkalinity refers to the conditions within seawater in which the addition of alkalinity has resulted in a corresponding increase in DIC (Table 1.2 B-E). Whereas, non-equilibrated alkalinity is a condition in which the seawater has yet to equilibrate with atmospheric $CO_2$ (Table 1.2 F). This scale of increase would have a huge influence on modern day biota as non-equilibrated OAE raises pH and $\Omega_{Ca}$ well above modern day values and even above the pre-industrial values (Figure 1.4). These more extreme carbonate chemistry perturbations may lead to the formation of "hotspots" of impact in regions located close to where TA is added. Therefore, it is important to develop a thorough understanding of how different marine environments will respond to high and low levels of TA addition.

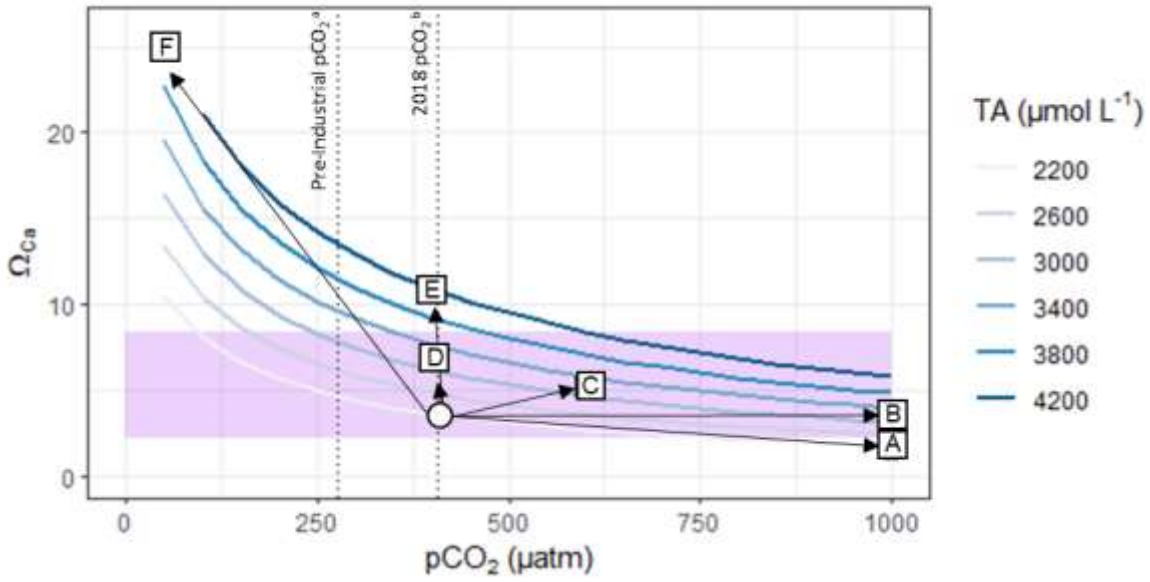


*Figure 1.4. Schematic showing the relationship between calcite saturation state ($\Omega_{Ca}$) and $pCO_2$ for the 6 ocean alkalinity enhancement scenarios described in Table1.2. The contours represent average surface ocean (0–100 m depth) TA in µEq $L^{-1}$ at 16°C and 35% salinity. The purple box shows the range of $\Omega_{Ca}$ of 23 coral reef locations (data from Cyronak et al. (2018). The black dashed lines highlight the pre-industrial and 2018 values of $pCO_2$ (a- Joos and Spahni (2008) b- Friedlingstein et al. 2019).*

Ocean TA addition across the world's oceans will likely result in asymmetrical perturbations to marine carbonate chemistry. Additionally, it may not be a simple process to reduce atmospheric $CO_2$ by the scale needed to limit global warming. Potentially large amounts of TA will need to be added (e.g. Ferrer-González and Ilyina 2016 predict that 114 Pmol of TA needs to be added to

the ocean by the end of this century to mitigate 1.5℃ of global warming) and this is likely to be costly to do so. For example, Renforth et al. (2013) and Renforth and Kruger (2013) predict it would cost approximately US$72 per 159 tonne of captured $CO_2$. Further, because of the preparation and operation processes that would be involved (e.g. mining and grinding olivine for enhanced weathering application), OAE may result in emitting $CO_2$ and so compromising the efficiency of OAE as a CDR approach.

## 1.6. Ocean alkalinity enhancement for ocean acidification mitigation

By increasing the pH buffering capacity of the ocean, OAE has the additional potential benefit of mitigating against ocean acidification. Ocean acidification is the recent, and potential future, decrease in ocean pH and $\Omega_{CaCO3}$ caused by rising atmospheric $CO_2$. The oceans are thought to take up approximately 30% of total anthropogenic atmospheric $CO_2$ to the atmosphere (Sabine et al. 2004, Gruber et al., 2019). When atmospheric $CO_2$ dissolves into seawater, $H_2CO_3$ is formed which then rapidly dissociates into $HCO_3^-$ producing hydrogen ions ($H^+$) (Equation 21) (Doney et al. 2009; Schulz et al. 2009; Schulz and Riebesell 2013).

$$CO_{2(atm)} \leftrightarrow CO_{2(aq)} + H_2O \leftrightarrow H_2CO_3 \leftrightarrow H^+ + HCO_3^- \leftrightarrow 2H^+ + CO_3^{2-}$$

(Equation 21)

Most, but not all, of these $H^+$ are then neutralised by $CO_3^{2-}$ producing more $HCO_3^-$ (Equation 21) (Doney et al. 2009; Schulz et al. 2009; Rhein et al. 2013; Doney et al. 2020). Therefore, the net result of increasing $CO_2$ in seawater is a gradual reduction of pH (increase in $H^+$), an increase in $[HCO_3^-]$ and a decrease in $[CO_3^{2-}]$ (Cao et al. 2007; Rhein et al. 2013). The increase in oceanic uptake of atmospheric $CO_2$ has resulted in a 30% increase in $[H^+]$ relative to pre-industrial times, which in turn has resulted in a decrease in global average ocean pH of 0.1 (Doney et al. 2020).

Seawater carbonate chemistry changes from ocean acidification influences the marine environment in many ways from promoting growth of certain algal species over others to altering carbon cycling in the ocean (Riebesell 2004). It is the decrease in $[CO_3^{2-}]$ which has had one of the biggest influences on the marine environment. As discussed in Section 1.3.3, a reduction in $[CO_3^{2-}]$ would result in lower $\Omega_{CaCO3}$ (both calcite and aragonite). Oceanic uptake of atmospheric $CO_2$ has reduced present day surface $[CO_3^{2-}]$ by more than 10% compared to the pre-industrial (Orr et al. 2005). Decreased $\Omega_{CaCO3}$ has already influenced the marine environment by making it more difficult for some marine calcifers to produce their calcium carbonate ($CaCO_3$) shells (Doney et al. 2009). Over the last 20 years or so, there have been a huge number of ocean acidification papers published, the majority of which focussed on biological responses

(Riebesell and Gattuso 2015). These ocean acidification studies have investigated a range of calcifying organisms such as coccolithophores (e.g. Riebesell et al. 2000; Engel et al. 2005; Lohbeck et al. 2012; Muller et al. 2015), bivalves (e.g. Cubillas et al. 2005), corals (e.g. Gattuso et al. 1998; Langdon et al. 2000; Form and Riebesell 2012), and pteropods (e.g. Comeau et al. 2009) and non-calcifying organisms such as seagrasses (e.g. Koch et al. 2013; Garrard and Beaumont 2014)), diatoms (e.g. Wu et al. 2010; Valenzuela et al. 2018).

Artificially increasing ocean TA means that more DIC is held as $CO_3^{2-}$ which mitigates against ocean acidification by firstly because the increased [$CO_3^{2-}$] means more $H^+$ are neutralised and so preventing further pH decline and secondly by increasing $\Omega_{CaCO3}$. Therefore, OAE would likely have the opposite effect on marine calcifiers than ocean acidification by making it easier to calcify (Feng et al. 2016; Renforth and Campbell, 2021).

## 1.7. Biological response to ocean alkalinity enhancement

### 1.7.1. Calcifying organisms

These carbonate chemistry perturbations from OAE could potentially have a substantial influence of marine biology. Marine calcifiers that are particularly sensitive to changes in ocean carbonate chemistry because they require $CO_3^{2-}$ ions (along with $Ca^{2+}$) to build their shells and skeletons will be particularly susceptible to these changes. Therefore, marine calcifiers would be disproportionally impacted by these changes compared to other marine organisms. To date, the majority of research into the impact of changing pH or $\Omega_{CaCO3}$ on calcifying organisms has focussed on the effect of decreased pH or $\Omega_{CaCO3}$ (ocean acidification studies, see Section 1.6). The general consensus is that lower pH and $\Omega_{CaCO3}$ will negatively affect marine calcifiers (Orr et al. 2005; Kroeker et al. 2010) by making it harder for them to calcify (Jokiel 2011; Bach et al. 2015; Waldbusser et al. 2015; Cyronak et al. 2016). However, some studies suggest that calcifying species will benefit from ocean acidification (Iglesias-Rodriguez et al., 2008, Riebesell et al., 2008). Ries et al. (2009) showed that there were mixed responses to $CO_2$ induced reduced $\Omega_{CaCO3}$. Of the 18 different benthic marine organisms tested, only 10 exhibited reduced net calcification rates due to increased $pCO_2$.

Unlike ocean acidification, OAE would have a different effect on marine carbonate chemistry conditions: pH and $\Omega_{CaCO3}$ would increase. There have been relatively few studies, which have explored the effect this would have on marine calcifiers. Albright et al. (2016) investigated the response increased TA on a coral reef flat and found that net community calcification increased when pH was raised to 8.3 and $\Omega_{Ar}$ was raised to ~6). This increase in calcification could have a

considerable impact on the marine carbon cycle because the formation of $CaCO_3$ produces $CO_2$ (Equation 22) (Schmittner et al. 2008).

$$Ca^{2+} + 2HCO_3^- \rightarrow CaCO_3 + CO_2 + H_2O \quad \text{(Equation 22)}$$

The formation of $CaCO_3$ by calcifying plankton in surface waters and then the subsequent sinking to the deep ocean is sometimes referred to the carbonate counter pump or alkalinity pump (Heinze et al. 1991). The carbonate counter pump lowers surface water DIC and TA and so causes an increase in surface water $pCO_2$. Consequently, if OAE caused a large enough increase in calcification to considerably increase surface water $pCO_2$ (to more than atmospheric $pCO_2$), this could act to have the opposite impact on air–sea $CO_2$ exchange than OAE intended and cause the ocean to become a source rather than a sink for atmospheric $CO_2$. Therefore, it is important to better understand what the potential response to marine calcification rates are to elevated TA before OAE can be deployed on a global scale.

Another study by Cripps et al. (2013) showed that there may also be other effects of increasing TA apart from just increased calcification. In their study, Cripps et al. (2013) found that increased TA (raising pH up to 8.8 and $\Omega_{CaCO3}$ up to 12.6) caused abnormal acid base balance and increased haemolymph pH in the marine calcifer, *Carcinus maenas.* Finally, Gim et al. (2018) studied the ecotoxicological effects of increased $HCO_3^-$ on various marine organisms, including both marine calcifiers and non-calcifiers. Their results showed a species-specific response to elevated $HCO_3^-$, suggesting that the ecosystem's response to increased TA may be similar to that of ocean acidification and will not be easy to predict. As such, there are still many unanswered questions regarding the environmental impacts of increasing the ocean's TA.

## 1.7.2. Non-calcifying organisms

Gross primary productivity (the total amount of energy produced by photosynthesis) of marine photosynthetic organisms could also be affected by changes in seawater carbonate chemistry. As discussed in Section 1.3, elevated TA results in increased pH and decreased $pCO_2$. Low seawater $pCO_2$ could potentially drive primary production of both calcifying and non-calcifying organisms into $CO_2$ limitation (Riebesell et al., 1993). However, seawater $pCO_2$ is already relatively low (e.g., at pH 8.2 [$CO_{2(aq)}$] only makes up 0.5% of total DIC) and as a result, marine plants have developed carbon concentrating mechanisms (CCMs), so that they can utilize $HCO_3^-$ for carbon fixation (Giordano et al. 2005). However, the decrease in $pCO_2$ could be more severe if, for example, TA addition occurs in a poorly mixed body of water with slow air-sea gas exchange and so equilibration with atmospheric $CO_2$ will occur much slowly. In these cases,

growth rates and primary productivity could be affected. Therefore, OAE induced perturbations to seawater DIC could cause substantial changes to ocean biomass.

As well as changing marine carbonate chemistry, OAE has the potential to increase other molecules or elements such as calcium ($Ca^{2+}$) and magnesium ($Mg^{2+}$); and if TA is increased via enhanced weathering of silicate minerals then also silicic acid ($Si(OH)_4$), iron ($Fe^{2+}$), and nickel ($Ni^{2+}$) may be introduced. Bach et al. (2019) predict that by increasing surface water TA by ~400 µEq $L^{-1}$ (by dissolving 10 Gt rock per year), the maximum increase in surface seawater Ca by the year 2090 could be ~240 µmol $L^{-1}$ and the maximum increase in Mg could be ~160 µmol $L^{-1}$. However, due to the natural high concentrations of $Ca^{2+}$ and $Mg^{2+}$ already in seawater (~10 000 µmol $L^{-1}$ and ~50 000 µmol $L^{-1}$ for $[Ca^{2+}]$ and $[Mg^{2+}]$ respectively (Takahashi et al. 2014), the relative change in their concentrations through OAE would only be small (<2.5%). The relative potential increase in the trace metals $Fe^{2+}$ and $Ni^{2+}$, which have much lower natural background concentrations, may be much more substantial. The potential increase in $[Fe^{2+}]$, and $[Ni^{2+}]$ could be sufficient enough to have either a fertilizing or potentially a toxic effect on marine organisms (Hartmann et al. 2013; Moore et al. 2013; Hauck et al. 2016). Further, Bach et al. (2019) estimate that the enhanced weathering of dunite (or other silicate minerals) would result in an input of dissolved [Si] into the ocean which is approximately five times greater than the natural input. Because $[Si(OH)_4]$ is an essential nutrient for silicifying organisms such as diatoms (NELSON et al. 1995; Dugdale and Wilkerson 1998; Ragueneau et al. 2006), enhanced weathering could influence diatom productivity. Köhler et al. (2013) suggest that enhanced olivine could promote a 14% increase in diatom primary productivity.

These potential changes to both marine calcifying and non-calcifying organisms could then have a substantial influence on biogeochemical cycles, carbon export and even food web dynamics within the ocean. For example, Köhler et al. (2013) predict that the increase in diatom primary productivity resulted in a 1% increase in annual export of organic matter and a 5% decrease in annual $CaCO_3$ export. Therefore, there is a need to understand how an increase in TA will affect marine ecosystems and carbon cycling in the ocean. Further, the rate of $CaCO_3$ precipitation and dissolution also influences how long the ocean can store atmospheric $CO_2$ as TA. Therefore, a better understanding of how an increase in TA affects $CaCO_3$ precipitation and dissolution is also needed.

## 1.8. Research justification

As OAE is still a relatively new area of research, it is sensible to focus the initial research on organisms which will be most sensitive to the changes to carbonate chemistry and those which

can act as indicator species for induced impacts on other marine organisms. Further, by concentrating on photosynthetic organisms, the impact of TA addition on photosynthesis and the relationship between chemical and biological carbon sequestration can also be investigated. It is the long-term response of ecosystems to potential carbonate chemistry perturbations, which is of more interest to scientists, citizens, and policymakers (Riebesell and Gattuso 2015). To constrain the wider ecosystem impacts and better understand how OAE might influence trophic interactions, multiple calcifying and non-calcifying species from many different habitats should be investigated. However, it would be impossible to study the response of every single calcifying marine taxa and so the decision was made to focus on taxa found in coastal environments. Coastal environments are a favourable site for TA addition by providing geochemical and environmental benefits over open ocean OAE (Schuiling and de Boer 2010; Meysman and Montserrat 2017). For example, the added minerals would have to be ground fine for open ocean OAE in order to stop them sinking to the deep ocean (Köhler et al. 2013), and this grinding process can be an energy and cost intensive. Also, the environmental impact of OAE may be more acute in coastal environments (Feng et al. 2017). Further, coastal regions are also often well mixed from the surface to seabed on at least an annual basis, suggesting that seawater in these areas would more likely encounter the atmosphere and so increase the efficiency of ocean carbon uptake compared to OAE in the deeper open ocean (Feng et al. 2017).

Two “end member” taxa were chosen: *Corallina* spp., a benthic, sessile calcifying macroalgae which is found on rocky shores of the continental shelf and *Synechococcus* PCC 8806, a calcifying pico-sized phytoplankton which is found in the surface of deeper waters of the continental shelf. Comparing these two different species gives an insight into two different coastal ecologies and, as such, it is possible to explore whether the size of the organism, how they calcify, and what habitat they live in affects how a species responds to increased TA. Also, by looking at two physiologically different species which inhabit different coastal ecosystems, it is possible to investigate how OAE will impact the wider ecosystem and food web dynamics. Finally, the *Corallina* spp., and *Synechococcus* PCC 8806 have different roles in the marine carbon cycle and so investigating their response to elevated TA will allow a better understand the longevity of ocean carbon storage via OAE.

### 1.8.1. Corallinales

Red calcifying macroalgae (Corallinales) are an important organism in temperate coastal regions (Akioka et al. 1999). Corallinales are found globally, most commonly in warm-temperate seas but are also found in tropical and subtropical seas (Garbary and Johansen (Johansen 1970;

Garbary and Johansen 1982). Corallinales are important ecologically and often described as "ecosystem engineers" because they maintain habitats, provide shelter from the full impact of intertidal physical stresses, and provide a "mini-ecosystem" for microphytobenthos (Williamson et al. 2014a). Therefore, global OAE would likely impact both Corallinales and their "mini-ecosystems".

Corallinales are some of the most prolific producers of $CaCO_3$, particularly in temperate shallow coastal waters (Martin et al. 2007) and global coralline algae inorganic carbon production is estimated to be 900 g $CaCO_3$ $m^{-2}$ $yr^{-1}$ (van der Heijden and Kamenos 2015). There is some evidence that suggests Corallinales growth and calcification are sensitive to changes to $\Omega_{CaCO3}$ (Martin and Gattuso 2009; Hofmann et al. 2012a; Hofmann et al. 2012b; Williamson et al. 2014a). Therefore, carbonate chemistry perturbations induced by OAE could substantially influence $CaCO_3$ production rates in coastal regions. However, Corallinales appear to be efficient at maintaining the pH of their internal environment in which they calcify and so could be less sensitive to changes in carbonate chemistry of the ambient environment (Borowitzka 1987; Ries 2009). Further, Corallinales grow in dynamic environments and so are used to relatively large daily and seasonal changes in carbonate chemistry which could promote resilience to change (Egilsdottir et al. 2013; Noisette et al. 2013). These variable results indicate that Corallinales sensitivity to changing ocean carbonate chemistry is complex.

### 1.8.2. *Synechococcus*

*Synechococcus* and *Prochlorococcus* numerically dominate oceanic phytoplanktonic communities (Partensky et al. 1999; Scanlan et al. 2009) and are key global photosynthesisers and substantially contribute to global chlorophyll biomass (Partensky et al. 1999; Agawin et al. 2000; Garcia-Pichel et al. 2003). Further, *Synechococcus* and *Prochlorococcus* contribute 25% to net global marine primary productivity (Flombaum et al. 2013). *Synechococcu*s spp. occur ubiquitously across the ocean but are most abundant in coastal regions and in the surface mixed layer of the open ocean habitats (Partensky et al. 1999; DuRand et al. 2001; Rocap et al. 2003; Zwirglmaier et al. 2007; Zwirglmaier et al. 2008; Mackey et al. 2009; Scanlan et al. 2009; Flombaum et al. 2013; Hunter-Cevera et al. 2016). Whereas *Prochlorococcus* are more often abundant in the deeper, stratified oligotrophic open ocean of the tropics and subtropics (Partensky et al. 1999; Zubkov et al. 2000; Johnson et al. 2006). Therefore, *Synechococcus* are the more interesting picocyanobacterial to investigate because they would likely be impacted by globally homogenous applied enhanced ocean TA addition and coastal applications of OAE.

Calcifying cyanobacteria have been important throughout Earth's history (Riding 2006). There are widespread recordings of calcified cyanobacteria in stromatolites throughout the Cambrian and in shallow marine carbonates during the Paleozoic and Mesozoic (Riding 2006). However, during the Late Cretaceous and throughout the Eocene, when marine $\Omega_{CaCO3}$ started to decrease, calcified cyanobacteria preservation became increasingly rare (Riding 2006). In the modern marine environment, calcifying cyanobacteria are bsent, which is likely due to the higher saturation states compared to the past (Riding 2006). Even though there are no naturally occurring calcifying marine cyanobacteria, there are calcifying strains of the marine species *Synechococcus* and *Synechocystis* that can calcify in laboratory conditions (Lee et al. 2004). Because it is possible for *Synechococcus* strains to calcify under experimental conditions (Lee et al. 2004), it may be possible for these pico-sized cyanobacteria to start calcifying if OAE causes global increases in ocean $\Omega_{CaCO3}$ and pH.

## 1.9. Aims, objectives & hypotheses

Determining the impact of OAE on coastal environments is important for the future of OAE as a carbon dioxide removal approach. Coastal calcifying organisms would be strongly impacted by future OAE because coastal regions are a favourable location for TA addition and calcifying organisms are more sensitive to changes to carbonate chemistry. Two equally important but physiologically different coastal taxa are sessile coralline algae and pelagic *Synechococcus.* Therefore, to facilitate predictions of how marine coastal environments will respond to future OAE, this thesis aims to investigate the impact of elevated seawater TA on the physiology of the red calcifying macro algae *Corallina* spp. and the calcifying strain of *Synechococcus*, *Synechococcus* PCC 8806. Specifically, the objectives were:

1. Determine how elevated TA and the resulting carbonate chemistry perturbations affect *Corallina* spp. physiology.
2. Determine how increasing TA by olivine dissolution impacts *Corallina* spp. physiology.
3. Determine the photophysiological response of *Synechococcus* 8806 to changes in TA.
4. Determine the physiological response of *Synechococcus* 8806 in terms of growth and $CaCO_3$ precipitation rates to elevated TA.

To achieve objectives 1 & 2, two short term laboratory experiments were performed using *Corallina* spp., samples harvested from a tidal rock pool and subjected to elevated TA seawater either by $Na_2CO_3$ addition (Chapter 2) or olivine dissolution (Chapter 3). Objective 3 was achieved by culturing *Synechococcus* 8806 to a low to high TA gradient from low and monitoring photophysiology through fluorescence analysis (Chapter 4). For objective 4,

*Synechococcu*s 8806 cultures were exposed to three different TA treatments, where cell growth and changing carbonate chemistry was monitored (Chapter 5). In Chapter 6, the outcomes of these studies (Chapters 2 – 5) have been synthesised to consider the overall impact of OAE on coastal biogeochemistry and efficiency of OAE as a carbon capture and ocean mitigation approach.

# Chapter 2.

# The physiological impact of increasing ocean alkalinity on a calcifying red algae, *Corallina* Spp.

## 2.1 Summary

*Corallina* spp., was harvested from a tidal rock pool and subjected to elevated TA (3454 ± 105 µEq $L^{-1}$) seawater in a three-week laboratory experiment. The physiological response of *Corallina* spp. was monitored either every other day (net calcification rates) or weekly (primary productivity rates, respiration rates, and photophysiology). Results show that the net calcification rate of *Corallina* spp. increased significantly under elevated TA (increased by 60% compared to the net calcification rate under ambient TA). This due to both an increase in light calcification rate and an increase in dark calcification rate. Further, $CaCO_3$ content of *Corallina* spp. increased by ~ 3% when exposed to elevated TA. This suggests that OAE would not be detrimental to *Corallina* spp. and that OAE could be used to mitigate against the effects of future ocean acidification. Further, *Corallina* spp. net primary productivity may have at least doubled when exposed to elevated TA compared to ambient TA. Therefore, despite the increase in calcification potentially increasing sweater $pCO_2$, the parallel increase in photosynthetic uptake of $CO_2$ suggests that overall *Corallina* spp. could still potentially act as a sink for $CO_2$ under elevated TA. However further investigation is needed to better quantify this.

## 2.2. Introduction

As discussed in the previous chapter, OAE would likely cause an increase in marine pH and $\Omega_{CaCO3}$ and so an additional benefit of OAE, is that it could alleviate regions from ocean acidification. Coastal environments are potentially important to investigate in the context of ocean acidification mitigation because coastal regions typically have higher $pCO_2$ and lower pH due to increased upwelling (Feely et al. 2008; Feely et al. 2018); low TA freshwater influx from rivers and ice meltwater (Evans and Mathis 2013; Gledhill et al. 2015; Rheuban et al. 2019); and excess nutrient and organic carbon inputs from land runoff (Feely et al. 2010; Feely et al. 2018). Therefore, coastal environments may face stronger challenges associated with ocean acidification and so would be important sites for mitigation.

Although increasing OAE could be a way of alleviating ocean acidification, it could also increase ocean pH and $\Omega_{CaCO3}$ well above preindustrial values, particularly in the regions where the alkaline minerals were added (Renforth and Henderson 2017; Feng et al. 2017). Therefore,

ecosystems located close to where TA addition occurs could face significant changes. However, coastal ecosystems tend to experience large variations in seawater carbonate chemistry on smaller time and space scales compared to the open ocean (Waldbusser et al. 2014; Williamson et al. 2014a). Therefore, although coastal calcifiers could experience more extreme acidified conditions they might also be better able to adapt to these conditions.

Red calcifying macroalgae (Corallinales), are a key feature of temperate coastal ecosystems (Akioka et al. 1999). Corallinales form complex, dense turfs made up of many branches (Kolzenburg et al. 2019) (Figure 2.1a-b). Each branch consists of both calcified segments (intergenicula) and noncalcified segments (genicula) (Figure 2.1c-d). Having both calcified and non-calcified segments allow the branches to be more flexible (Martone and Denny 2008a,b). Calcification takes place in cell walls of the thallus and $CaCO_3$ occurs as high magnesium calcite (Basso 2012). High magnesium calcite is conventionally defined as calcite containing >4 wt% $MgCO_3$ (Ries 2009) and is the most soluble form of calcite in the marine environment. High magnesium calcite is less stable than low magnesium calcite because the strength of the ionic bond between Ca and Mg ions is weaker compared to two Ca ions (Stanienda-Pilecki 2018).

The increased solubility of high magnesium calcite suggests that high magnesium calcite producers such as the Corallinales could be particularly vulnerable to ocean acidification (Andersson et al. 2008). Kroeker et al. (2013) suggest that calcifying benthic macroalgae such as the Corallinales, are one of the major groups affected by ocean acidification. There is some evidence that suggests Corallinales have reduced growth and calcification rates when subjected to a reduction in $\Omega_{CaCO3}$ (Martin and Gattuso 2009; Hofmann et al. 2012a; Hofmann et al. 2012b; Hofmann and Bischof 2014; Williamson et al. 2014b). However, due to the dynamic nature of the inter-tidal environment, where Corallinales are found, coralline algae are suggested to have a good ability to adapt to great and rapid changes in to carbonate chemistry which can fluctuate tidally, diurnal, monthly, and seasonally (Egilsdottir et al. 2013; Hofmann and Bischof 2014; Noisette et al. 2013; Williamson et al. 2014). Being exposed to these variable environments has been suggested to promote resilience to changes caused by ocean acidification (Egilsdottir et al. 2013; Noisette et al. 2013). Further, Corallinales appear to be efficient at maintaining the pH of their internal environment in which they calcify and so could be less affected by changes in carbonate chemistry of the ambient environment (Borowitzka 1987; Reis et al. 2009). These variable results indicate that Corallinales sensitivity to ocean acidification is complex and suggests that predicting Corallinales sensitivity to OAE could be equally challenging.

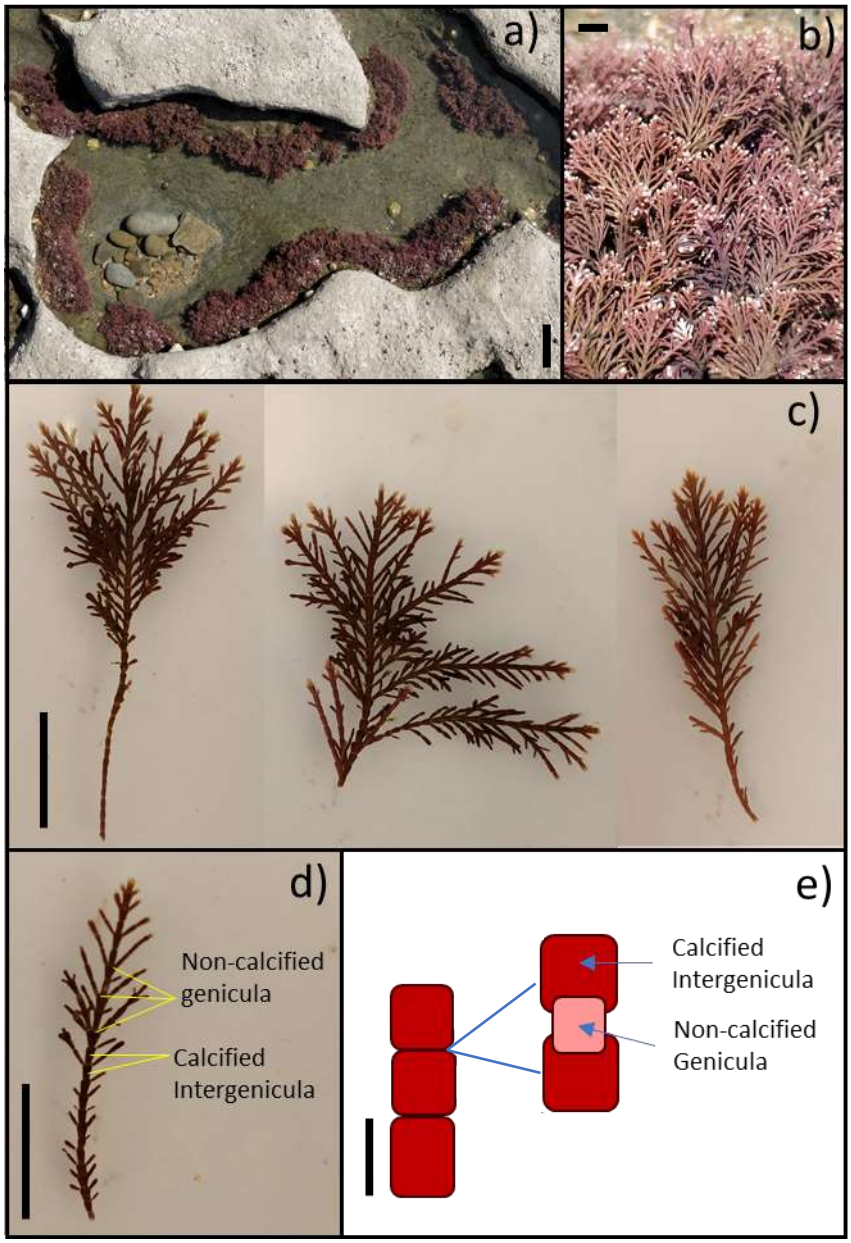


*Figure 2.1. Photographs taken at Dunraven Bay of Corallina spp. (insets a-b). Close up of Corallina spp. branches (inset c). Photograph (inset d) and schematic (inset e) showing non-calcified genicula and calcified intergenicular sections of each branch. Scale bar measurements as follow: inset a: 10cm, inset b: 0.5cm, c: 2cm, d: 1cm, e: 1mm*

How Corallinales respond to future changes to carbonate chemistry (either reduced or elevated TA, pH, and $\Omega_{Ca}$) will have an important consequences for coastal ecosystems where Corallinales are present. Corallinales are "ecosystem engineers" as they provide habitats for many other coastal macrofauna and epiphytes. There is vast literature on the crucial role Corallinales have in rocky coastal zones (Jones et al. 1994; Kelaher et al. 2001; Benedetti-Cecchi 2006; Laure et al. 2009; Nelson 2009; Williamson et al. 2014b; van der Heijden and Kamenos

2015). Corallinales can host abundant and diverse macrofaunal assemblages. Kelaher et al. (2001) estimated that each square mile of Coralline turf can host up to 250,000 individuals. Therefore, it is essential that the response of Corallinales to these potential carbonate chemistry changes is better understood. Because most studies to date focus on what effect a decrease in pH and $\Omega_{CaCO3}$ will have on marine ecosystems (ocean acidification studies) and few have investigated the biological response to an increase in pH and $\Omega_{CaCO3}$, this chapter aims to explore the response of *Corallina* spp. (of the family Corallinales) physiology (calcification, primary productivity, respiration, and photophysiology) to seawater TA and pH increase. It was hypothesised that:

1. Increasing TA will create more energetically favourable conditions for $CaCO_3$ precipitation and so *Corallina* spp. calcification rates will increase under elevated TA.
2. Because photosynthesis and calcification are closely related processes in calcifying organisms, elevated TA will also cause net primary productivity and photophysiology rates to increase.

## 2.3. Methods

### 2.3.1. Sample collection

*Corallina* spp. samples were collected from Dunraven Bay, a rocky shore near Southerndown, South Wales (51°44.65′ N, 03°60.73′ W) during February 2018. The samples were carefully removed from their substrate making sure to obtain their encrusting base. Dunraven Bay consists of a heavily pitted limestone wave cut platform with rock pools. The rock pool temperature, pH, and salinity were measured on site using a temperature and pH combination electrode and refractometer. Photochemically active radiation (PAR) was measured at the water depth at which the *Corallina* spp. was growing using a 4-pi LI-COR cosine-corrected quantum sensor respectively. The chemical and physical properties of the rock pool water are summarised in Table 2.1.

*Table 2.1. Average ± standard error chemical and physical properties of Dunraven Bay rock pool water.*

| Parameter | During Collection |
|---|---|
| Salinity (psu) | 30 |
| Temperature (ºC) | 6.5 ± 0.05 |
| Photochemically active radiation (PAR) (µmol photons $m^{-2}$) | 150-740 |
| pH | 8.17 ± 0.05 |

*Corallina* spp. samples were randomly selected from the rock pools found in the intertidal region of Dunraven Bay. Two common species of red calcifying macroalgae (Corallinales) found in the UK are *Corallina officinalis* and *Corallina elongata* (Williamson et al. 2014). Frond morphology of the samples collected closely matched that of *C. officinalis*; therefore, the samples collected were decided to be most likely *C. officinalis.* However, morphological characters alone are often not sufficient enough to identify the Corallinales to subfamily taxonomic levels (Bailey and Chapman 1998) and because no formal identification was made (e.g., using DNA comparisons), the samples will be referred to as simply *Corallina* spp. herein.

The *Corallina* spp. samples and ~ 100 L of site water were transported back to Cardiff University. The site water was filtered using the methodology of (Walsh et al. 2009) then stored in a flow-through chamber within a greenhouse. Twelve undamaged *Corallina* spp. samples that were visually free from epiphytes were chosen. Each sample had a similar number of fronds (8–10) and frond length (4–6 cm) and weight ~ 1 g (wet). The 12 *Corallina* spp. samples were submerged in 1 L glass chambers containing 400 mL of site water. Two blank 1L bottles containing 400 mL of original seawater but no *Corallina* spp. sample were also prepared. These control bottles were used to account for any differences in carbonate chemistry not caused by the *Corallina* spp. samples

## 2.3.2. Experimental set up

The experimental set up consisted of two TA treatments, an elevated TA treatment (elevated alkalinity) and an ambient TA treatment (ambient alkalinity). Every 48 hours, each glass chamber was refreshed with 400 mL of filtered site water from the flow-through chamber. For the elevated alkalinity treatment, TA was increased by ~1000 µEq $L^{-1}$ by adding 0.5 mol $L^{-1}$ $Na_2CO_3$ and bubbling with ambient air for two hours, to ensure that $\Omega_{Ca}$ did not exceed 10. This was carried out before being added to the *Corallina* spp. chambers. For the ambient alkalinity treatment, TA was unmodified but was still bubbled with ambient air for two hours to allow for consistency between the treatments. The carbonate chemistry for both the ambient and elevated alkalinity treatments is summarised in Table 2.2 and Figure 2.2. Figure 2.2 shows that measured salinity and TA do not vary in proportion as expected, which suggests there must be some error in the salinity measurements or TA measurements. However, of the two, the TA measurements are more robust and reliable therefore, it is most likely that the error came from the salinity measurements. Salinity was measured reading a refractometer, which is associated with more human error compared to the TA measurements which is calculated using a computer program

(see Section 2.3.3 for more details). This error has consequences with regards to the other calculated carbonate chemistry parameters ($pCO_2$, $[HCO_3^-]$, $[CO_3^{2-}]$, $[CO_2]$, $\Omega_{Ca,}$ $\Omega_{Ar}$). However, changing salinity by 10% (results in changes in these parameters by 1-7% (Appendix A) which is well within the quoted error in Table 2.2. This also has implications for the pH calibrations and measurements, however a 10% change in salinity resulted in salinity values to change by +/-3% and as long as the salinity is within 5% of the of the buffer's salinity, then the likely error is less than 0.01 in pH (Riebesell et al., 2010, Whitfield et al., 1985). Therefore, the potential error in salinity measurements is not thought to have considerably altered the pH values.

For the first seven days, four out of the 12 glass chambers containing *Corallina* spp. samples were refreshed with elevated TA (elevated 1) water and eight were refreshed with ambient TA water (ambient). On day eight (and for the remainder of the experiment), four of the ambient TA *Corallina* spp. samples were then subjected to elevated TA water instead (elevated 2). Of the two blank chambers with no *Corallina* spp. samples, one was refreshed with elevated alkalinity water and the other with ambient alkalinity water every 48 hours. It was intended to place each glass chamber was placed in a 10 ºC temperature-controlled fridge. However, the fridge's thermostat was not very effective resulting in a temperature to range from 11.2 to 16.7 ºC over the course of the experiment. Irradiance above the glass chambers was adjusted to ~200 µmol photons $m^{-2}$ $s^{-1}$. The light source consisted of 39 W LED tubes (JBL Solar Ultra Marin Day, JBL Aquaria, Nelson, New Zealand) placed above the aquaria, and the photoperiod was adjusted to 12 h/12 h light/dark period. The samples were kept alive for three weeks.

*Table 2.2. Average carbonate chemistry ± standard deviation for High and Low TA treatments. TA= total alkalinity (µEq $L^{-1}$), DIC = dissolved inorganic carbon (µmol $L^{-1}$), $pCO_2$ = atmospheric partial pressure of $CO_2$ (µatm), $[HCO_3^-]$ = bicarbonate ion concentration (µmol $L^{-1}$), $[CO_3^{2-}]$ = carbonate ion concentration (µmol $L^{-1}$), $[CO_2]$ = aqueous $CO_2$ concentration (µmol $L^{-1}$), ΩCa = calcite saturation state, and ΩAr = aragonite saturation state.*

| Treatment | TA (µEq $L^{-1}$) | DIC (µmol $L^{-1}$) | pH | $pCO_2$ (µatm) | $[HCO_3^-]$ (µmol $L^{-1}$) | $[CO_3^{2-}]$ (µmol $L^{-1}$) | $[CO_2]$ (µmol $L^{-1}$) | $\Omega_{Ca}$ | $\Omega_{Ar}$ |
|---|---|---|---|---|---|---|---|---|---|
| Elevated | 3454 ± 105 | 2999 ± 114 | 8.2 ± 0.1 | 364 ± 85.5 | 2632 ± 151 | 362 ± 64 | 13 ± 3 | 8.8 ± 1.6 | 5.6 ± 1 |
| Ambient | 2694 ± 114 | 2479 ± 71 | 7.97 ± 0.08 | 581 ± 111 | 2288 ± 48 | 171 ± 34 | 21 ± 4 | 4.1 ± 0.8 | 2.7 ± 0.5 |

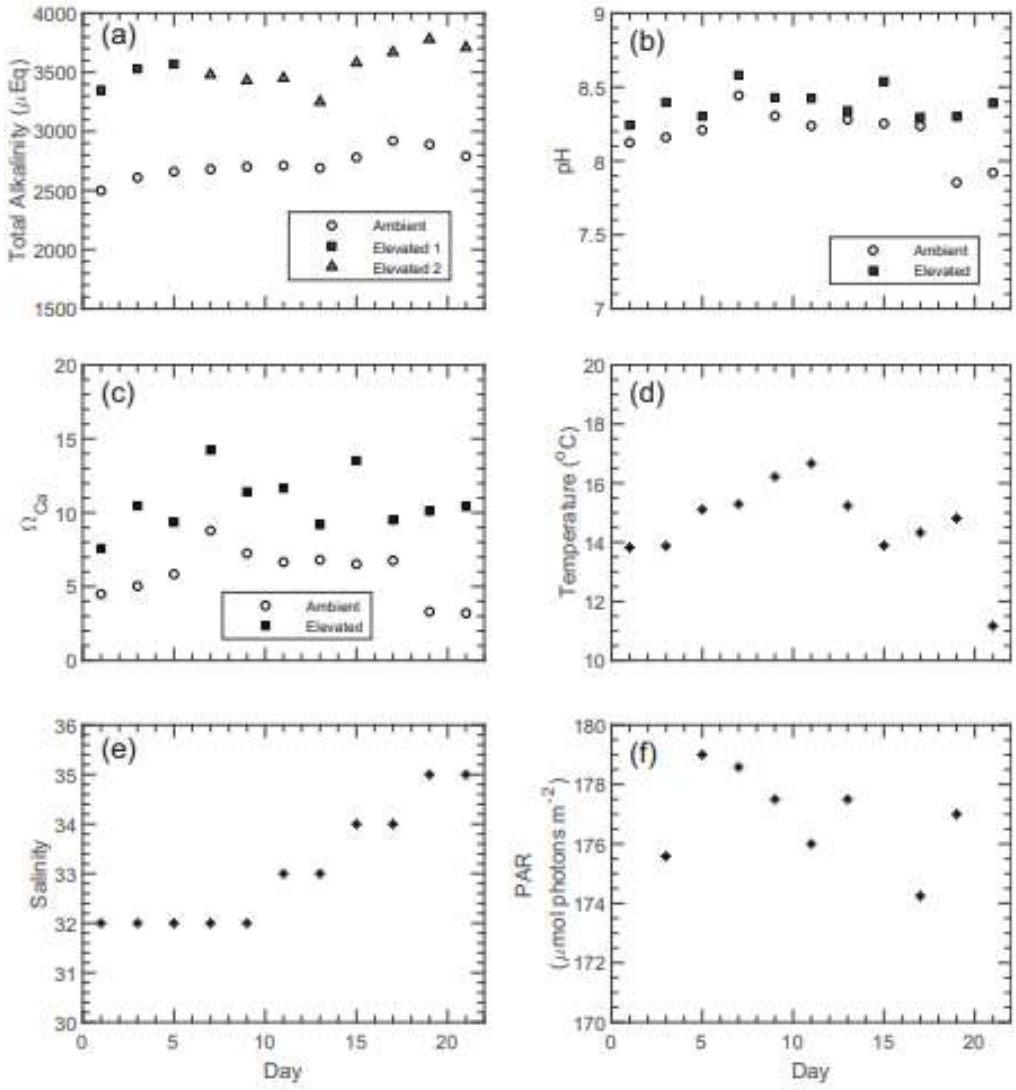


*Figure 2.2. Physical and carbonate chemistry properties of the experimental set up (a) average TA (µEq L-1), (b) pH, (c) $\Omega_{Ca}$, (d) temperature (ºC), (e) salinity, and (f) Photochemically active radiation (PAR; µmol photons m−2). Carbonate chemistry properties are divided into Low TA treatment (empty circles) and Elevated TA treatment (which is further divided into High 1 (filled diamonds) and High 2 (filled squares)). For Elevated 1, TA was increased on day 1 and for Elevated 2, TA was increased on day 8. For more information see Section 2.3.2*

## 2.3.3. Net calcification, primary productivity, and respiration

Before refreshing the seawater, 100 mL of the solution from the glass chambers was collected and filtered through 0.02 µm filters (Minisart syringe filters, Sartorius, Germany). 100 mL of both elevated and ambient alkalinity treatment seawater was also collected. The pH of each water sample was measured using a pH electrode (Mettler Toledo™, U.K.) calibrated with TRIS and AMPD seawater buffer solutions according to Dickson et al. (2007).

The TRIS and AMPD buffer solutions were prepared at Cardiff University following the best practice protocol of Dickson et al. (2007). The pH of each buffer solution was calculated using Equation 23 (TRIS) and Equation 24 (AMP) where T is temperature in kelvin and S is salinity in %. The e.m.f. (mV) of each buffer solution was measured using the pH electrode, making sure the electrode response (s, Equation 25) was within 0.3% of the ideal Nerst value (RTln10/F where R is the universal gas constant, T is temperature in kelvin, and F is the Faraday constant). Following this the measured electromotive force (e.m.f ) and calculated pH of each buffer solution was used to calibrate the measured e.m.f. values of seawater samples into accurate pH according to Dickson et al. (2007) and Equations 25 and 26.

$$pH\ (TRIS) = (11911.08 - 18.2499S - 0.039336S^2)\frac{1}{T} - 366.27059 + 0.53993607S + 0.00016329S^2 + (64.52243 - 0.084041S(\ln(T) - (0.11149858(T) \quad \text{Equation 23}$$

$$pH\ (AMP) = (111.35 + 5.44875S)\frac{1}{T} + 41.6775 - 0.015683S - 6.20815(\ln(T) - log_{10}(1 - 0.00106S) \quad \text{Equation 24}$$

$$s = \frac{E_{AMP} - E_{TRIS}}{pH_{TRIS} - E_{AMP}} \quad \text{Equation 25}$$

$$pH\ (sample) = pH_{TRIS} + \frac{E_{TRIS} - E_{sample}}{s} \quad \text{Equation 26}$$

Gran titration (907 Titrando, Metrohm tiamo™, Switzerand), used to measure TA, was calibrated using reference measurements of carefully prepared $Na_2CO_3$ standards (0.5, 1.0 and 1.25 mmol $L^{-1}$) in 0.7 mol $L^{-1}$ NaCl background medium according to Dickson et al. (2007). Accuracy and precision were determined by six titrations of a TA standard (Batch 126) supplied by the University of California San Diego. The absolute error of the TA measurements was $\pm$20 µEq $L^{-1}$. Afterward, pH, TA, water temperature, and salinity were used to determine the other carbonate chemistry parameters (DIC, $pCO_2$, $[CO_2]$, $[HCO_3^-]$, $[CO_3^{2-}]$, $\Omega_{Ar}$, and $\Omega_{Ca}$), by inputting the values into CO2SYS v2.1 (Pierrot et al. 2016). CO2SYS was run using the constants of Mehrbach et al. (1973) refitted by Dickson and Millero (1987).

The net calcification rate (NCR = µmol $CaCO_3$ $gDW^{-1}$ $h^{-1}$) was calculated from the change in TA before and after refreshing with the Low/High TA water (Equation 27).

$$NCR = \frac{\Delta TA * v}{2 * gDW * h} \quad \text{(Equation 27)}$$

Where "v" is the volume of water in the glass chamber (400 mL), "gDW" is the dry weight of the *Corallina* spp. samples in grams, and $h^{-1}$ is time elapsed in hours (48 h). The amount of

$CaCO_3$ precipitated (µmol $CaCO_3$) was estimated using the alkalinity anomaly technique (Smith and Key 1975; Chisholm and Gattuso 1991) which assumes a decrease in TA by two µEq equals one µmol of $CaCO_3$ precipitated. Nitrogen uptake during primary productivity can also influence TA. However, the change in TA due to nitrogen uptake was calculated using calculation 39 in Wolf-Gladrow et al. (2007) and was found to be <4% of the overall TA change therefore was ignored. The blank chambers were used to account for any changes in TA not produced by *Corallina* spp.

Calcification rates (CR) for light and dark periods were also determined during week one and week two. The twelve *Corallina* spp. chambers and two blank chambers, were refreshed with 200 mL of elevated/ambient TA seawater then left in either in light or dark conditions for six hours. The pH was measured at the start of the six hours (after the seawater had been bubbled with ambient air) and again at the end of the six hours. The pH and TA measured at the start and at the end of the six-hour experiment were then used to calculate how DIC changed over the course of the six hours. DIC was calculated using CO2SYS v2.1 (Pierrot et al. 2006). The change in DIC and the light and dark CRs were then used to estimate net primary productivity (NPP = -ve µmol DIC $gDW^{-1}$ $h^{-1}$) and respiration (NR = +ve µmol DIC $gDW^{-1}$ $h^{-1}$) values (Equation 28).

$$NPP\ or\ NR = \frac{\Delta DIC * v}{gDW * h} - CR(\text{dark})/(\text{light}) \qquad \text{(Equation 28)}$$

Where CR(dark) is the CR calculated from the change in TA in dark conditions and CR(light) is the CR calculated from the change in TA in light conditions. Because the light and dark experiments occurred in an open system, there may have been changes. The blank chambers were used to account for any changes in TA and pH not produced by *Corallina* spp. and used to correct light/dark CR, NPP, and NR for these changes.

The *Corallina* spp. dry weight (gDW) used in Equations 27 and 28 is an average of the *Corallina* spp. dry weight measured at the beginning of the experiment and measured at the end of the experiment to account for any changes in weight that occurred due to *Corallina* spp. growth. At the end of the experiment, the *Corallina* spp. samples were dried at 100 ºC for 24 hours to obtain the dry weight. The dry weight of *Corallina* spp. at the beginning of the experiment was estimated using the *Corallina* spp. "tapped weight". The dry weight of *Corallina* spp. was found to be ~56% less than the tapped weight when dried at 100 ºC for 24 hours immediately after measuring the tapped weight.

The $CaCO_3$ and organic carbon content of the *Corallina* spp. samples were also measured. First, the organic carbon ($C_{org}$) content of the samples was measured by the loss in mass of the samples after combustion at 500 °C for 6 h. Then, the $CaCO_3$ content of the remaining ash was estimated using a FOGII Digital Calcimeter (BD Inventions P.C., Greece). Primary productivity rates (mg $C_{org}$ $gDW^{-1}$ $h^{-1}$) were calculated assuming the ratio of $CaCO_3$ to $C_{org}$ content of the *Corallina* spp. did not change throughout the experiment and were equivalent to the measured cumulative TA change.

### 2.3.4. Photophysiology

The photophysiology of the *Corallina* spp. samples was determined using Pulse Amplitude Modulation (PAM) fluorometry. Rapid Light Curves (RLC) were performed using a Walz Water-PAM fluorometer, after the chambers were refreshed with new site seawater, following the methodology of Perkins et al. (2006). Four replicate light curves were performed for both the elevated and ambient alkalinity treatments. RLC measurements were made on the tips of the upper facing *Corallina* spp. fronds to avoid sampling potentially self-shaded frond regions and to minimise differential photoacclimation (i.e. due to differences in light history between upper and lower surfaces of fronds). RLCs were preformed after each *Corallina* spp. sample was dark adapted for 5 minutes.

Analysis of RLC was done using R v.3.4.1 (R Core Team, 2017) and followed that described by Perkins et al. (2006) with curve fitting following the iterative solution of Eilers and Peeters (1988) to determine coefficients *a*, *b* and *c* and hence calculation of light curve parameters of relative maximum electron transport rate ($rETR_{max}$), coefficient of light use efficiency (α) and light saturation coefficient ($E_k$). The shape of the RLC ($rETR_{max}$, α, $E_k$) gives an indication to how efficient photosynthesis is. The first part of the RLC (the rise of the curve in the light limiting region) is proportional to efficiency of light capture (effective quantum yield or α) (Schreiber 2004). Where the RLC peaks is used to determine the maximum photosynthetic capacity ($rETR_{max}$) (Schreiber 2004). The interception of $rETR_{max}$ and α determines the minimum saturating irradiance ($E_k$) (Sakshaug et al. 1997). $E_k$ is related to how much light energy is either used for photosynthesis (photochemical quenching) or is emitted as fluorescence or converted to heat (non-photochemical quenching). The higher the $E_k$ value, the more energy is used for photochemical quenching (Henley 1993). In the simplest terms, an increase in $rETR_{max}$, α, and $E_k$ suggests more efficient photosynthesis and a decrease in these values could suggest the *Corallina* spp. is becoming stressed.

The Genty parameter ($F_v/F_m$) which is the approximate maximum light use efficiency in the dark-adapted state (Genty et al. 1989) and therefore gives an overall indication of the health of the *Corallina* spp. samples. $F_v/F_m$ was calculated using R v.3.4.1 (R Core Team, 2017). The Genty parameter is defined as:

$$F_v/F_m = (F_m - F_o)/F_m \quad \text{(Equation 29)}$$

where $F_m$ is the maximum yield, and $F_o$ is the minimum fluorescence yield in the dark-adapted state.

### 2.3.4. Data analysis

Where averages are given, the error is quoted as standard error (∓S.E.) in text, figures or tables unless otherwise stated. All statistical analyses were performed using R v.3.4.1 (R Core Team, 2017). Prior to all analyses, normality of data was tested using the Shapiro-Wilk test and examination of frequency histograms. Differences in parameters (NCR, NPP, NP, $rETR_{max}$, $\alpha$, $E_k$ and $F_v/F_m$) between the two TA treatments were examined using student's *t*-test. Where data were not normally distributed, a Mann-Whitney U test was preformed instead. Differences were deemed significant if $p < 0.05$. Linear regressions were preformed to determine any significant relationships between NCR, $rETR_{max}$, $\alpha$, $E_k$, and $F_v/F_m$ and TA, pH, temperature and irradiance (PAR). Additional linear regressions models were run to determine any significant relationship between NCR and photophysiology ($rETR_{max}$, $\alpha$, $E_k$, and $F_v/F_m$).

## 2.4. Results

### 2.4.1. Net calcification rates

Throughout the experiment, TA, pH, $\Omega_{Ca}$ were consistently higher in the elevated alkalinity treatment compared to the ambient alkalinity treatment (Figure 2.2). *Corallina* spp. NCR was significantly higher (60%) in the elevated alkalinity treatment compared to the ambient alkalinity treatment throughout the study period (Table 2.3, Figure 2.3a). Average *Corallina* spp. NCR for elevated alkalinity was $8.51 \pm 0.55$ µmol $CaCO_3$ $gDW^{-1}$ $h^{-1}$ compared to $5.32 \pm 0.61$ µmol $CaCO_3$ $gDW^{-1}$ $h^{-1}$ for ambient alkalinity.

*Corallina* spp. NCRs were significantly higher ($p < 0.05$) in the elevated 2 alkalinity treatment, where TA was increased after day 8, compared to the elevated 1 alkalinity treatment, where TA was increased straight away (Figure 2.3a). Average *Corallina* spp. NCR for the elevated 1 alkalinity treatment was $8.14 \pm 0.82$ µmol $CaCO_3$ $gDW^{-1}$ $h^{-1}$ and for the elevated 2 alkalinity

treatment was 9.28 ± 0.83 µmol $CaCO_3$ $gDW^{-1}$ $h^{-1}$. There was substantial temporal variation in *Corallina* spp. NCR for the ambient alkalinity treatment throughout the experiment. There was an initial increase of 74% from day 1 to 16 but then decreased back to the starting values by day 21, compared to a 40% increase in *Corallina* spp. NCR in the elevated 1 alkalinity treatment during the same time-period (Fig. 2.3a). There was a significant positive linear relationship between NCR and TA, NCR and pH, and NCR and PAR (Table 2.4) with the strongest relationship between NCR and TA ($R^2 = 0.3254$, $p < 0.001$)

*Table 2.3 Average Corallina spp. physiology values and results from one-way ANOVA (NCR (µmol $CaCO_3$ $gDW^{-1}$ $h^{-1}$), LCR =light CR (µmol $CaCO_3$ $gDW^{-1}$ $h^{-1}$), DCR= dark CR (µmol $CaCO_3$ $gDW^{-1}$ $h^{-1}$), NPP (µmol DIC $gDW^{-1}$ $h^{-1}$), NR (µmol DIC $gDW^{-1}$ $h^{-1}$), $rETR^{max}$,, $F_v/F_m$ α, and $E_k$ . Significant codes: ns= not significant, p<0.001 ***.*

| | No. of measurements | | Average Value | | Standard Error | | |
|---|---|---|---|---|---|---|---|
| Parameter | Elevated | Ambient | Elevated | Ambient | Elevated | Ambient | Significance |
| NCR | 60 | 47 | 8.51 | 5.32 | 0.55 | 0.61 | *** |
| CR (light) | 8 | 8 | 12.40 | 8.80 | 1.01 | 0.64 | ns |
| CR (dark) | 8 | 8 | 2.75 | -0.02 | 0.34 | 0.36 | ns |
| NPP | 8 | 8 | -11.83 | -5.85 | 1.46 | 0.79 | ns |
| NR | 8 | 8 | 0.645 | -0.045 | 0.29 | 0.15 | ns |
| $rETR_{max}$ | 47 | 45 | 35 | 36 | 2 | 2 | ns |
| $F_v/F_m$ | 47 | 45 | 0.68 | 0.69 | 0.02 | 0.02 | ns |
| $\alpha$ | 47 | 45 | 0.13 | 0.13 | 0.01 | 0.01 | ns |
| Ek | 47 | 45 | 287 | 271 | 20 | 12 | ns |

*Corallina* spp. had higher rates of both light CR and dark CR when exposed to elevated alkalinity compared to the ambient alkalinity treatment. On average the light CR was 12.43 ± 1.01 µmol $CaCO_3$ $gDW^{-1}$ $h^{-1}$, which was 40% higher than the ambient alkalinity treatment (8.83 ± 0.64 µmol $CaCO_3$ $gDW^{-1}$ $h^{-1}$; Table 2.3). *Corallina* spp. dark CR also substantially increased when exposed to the elevated alkalinity treatment compared to the ambient alkalinity treatment (2.75 ± 0.34 µmol $CaCO_3$ $gDW^{-1}$ $h^{-1}$ compared to -0.02 ± 0.36 µmol $CaCO_3$ $gDW^{-1}$ $h^{-1}$ respectively; Table 2.3). There was no significant difference between the alkalinity treatments for both the ambient and elevated alkalinity treatments (Table 2.3). The rates for *Corallina* spp. light and dark calcification increased from week 1 to week 2 (Figure 2.3b).

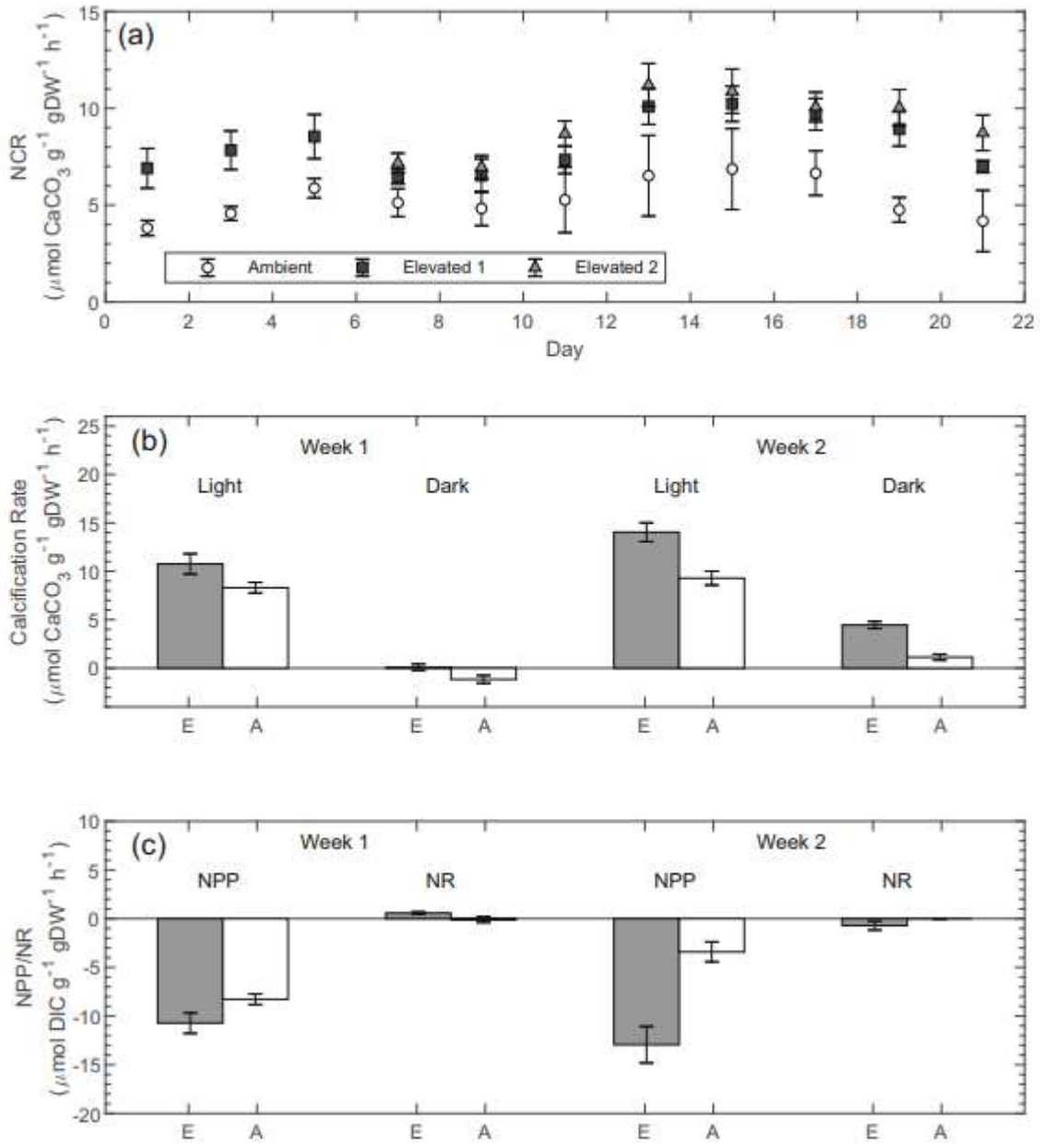


Figure 2.3. *Average Corallina spp. (a) net calcification rate (NCR; µmol $CaCO_3$ $gDW^{-1}$ $h^{-1}$), (b) light and dark Corallina spp. calcification rates (light/dark CR; µmol $CaCO_3$ $gDW^{-1}$ $h^{-1}$), and (c) Corallina net primary productivity and net respiration (NPP/NR; µmol DIC $gDW^{-1}$ $h^{-1}$) for the High and Low TA treatments. High TA is further divided in (a) into High 1 and High 2. For High 1, TA was increased on day 1 and for High 2, TA was increased on day 8.*

.

*Table 2.4. Results from linear regression analysis of (a)* Corallina *spp. NCR (µmol $CaCO_3$ $gDW^{-1}$ $h^{-1}$), $F_v/F_m$, $E_k$, α, and $rETR_{max}$ in relation to TA (µEq $L^{-1}$), and pH and (b)* Corallina *spp. NCR (µmol $CaCO_3$ $gDW^{-1}$ $h^{-1}$) in relation to Corallina spp. $rETR_{max}$, α, $E_k$,and $F_v/F_m$. Relationship explained by the regression ($R^2$), overall significance (sig), and number of observations (N). Significant codes: p<0.05 *, p<0.01 **, p<0.001 ***.*

| **a)** | TA | | | pH | | |
|---|---|---|---|---|---|---|
| | $R^2$ | sig | N | $R^2$ | sig | N |
| NCR | 0.3998 | *** | 106 | 0.1141 | *** | 106 |
| $F_v/F_m$ | 0.1563 | ** | 56 | 0.0689 | ns | 56 |
| $E_k$ | 0.0039 | ns | 56 | 0.0039 | ns | 56 |
| $rETR_{max}$ | 0.0058 | ns | 56 | 0.0203 | ns | 56 |
| α | 0.0008 | ns | 56 | 0.0648 | ns | 56 |

| **b)** | $rETR_{max}$ | | | α | | | $E_k$ | | | $F_v/F_m$ | | |
|---|---|---|---|---|---|---|---|---|---|---|---|---|
| | $R^2$ | sig | N | $R^2$ | sig | N | $R^2$ | sig | N | $R^2$ | sig | N |
| NCR | 0.0996 | * | 56 | 0.0814 | * | 56 | 0.004 | ns | 56 | 0.210 | *** | 56 |

## 2.4.2. Net primary productivity and respiration rates

After *Corallina* spp. were exposed to light conditions for six hours, there was a substantial increase in pH for both the elevated and ambient alkalinity treatment seawater (increase of 0.57 and 0.67 respectively). This change in pH and change in TA was used to estimate the rate of *Corallina* spp. NPP, which almost doubled when exposed to elevated alkalinity compared to the ambient alkalinity treatment. On average, the elevated alkalinity treatment NPP rate was -11.86 $\pm$ 1.46 µmol DIC $gDW^{-1}$ $h^{-1}$ and the ambient alkalinity treatment NPP rate was -5.87 $\pm$ 0.79 µmol DIC $gDW^{-1}$ $h^{-1}$. The negative values indicate that $CO_2$ was used up in photosynthesis. After the *Corallina* spp. were exposed to dark conditions for six hours, there was a decrease in pH for both the elevated and ambient alkalinity treatment seawater (decrease of 0.30 and 0.19 respectively). Both the elevated and ambient alkalinity treatments resulted in low rates for NR ($-$ 0.29 $\pm$ 0.39 µ mol DIC $gDW^{-1}$ $h^{-1}$ and 0.58 $\pm$ 0.20 µmol DIC $gDW^{-1}$ $h^{-1}$ respectively). There was a marked decrease in NPP rates for the ambient alkalinity treatment and a slight increase for the elevated alkalinity treatment going from week 1 to week 2 (Fig. 2.3c). Like the light and dark calcification rates, there was no significant difference between the elevated and ambient alkalinity treatments for NPP or NR.

From the combustion data and the $CaCO_3$ to $C_{org}$ ratio, it was estimated that, on average, a total of 0.09 g of $C_{org}$ was produced by the *Corallina* spp. exposed to elevated alkalinity treatment and 0.07 g of $C_{org}$ was produced by the *Corallina* spp. exposed to ambient alkalinity treatment (Table 2.5). Primary productivity was also estimated using the $CaCO_3$ to $C_{org}$ content ratio of the *Corallina* spp. samples. The primary productivity rates for *Corallina* spp. were ~ 50% higher for the elevated alkalinity treatments (elevated 1 and elevated 2) compared to that for the ambient alkalinity treatment (Table 2.5). The calculation of primary productivity was assumed that the rates were equivalent to the measured cumulative alkalinity change and that there was no variation in the ratio of $CaCO_3$ to $C_{org}$ content of the *Corallina* spp. throughout the experiment. However, as much as > ± 30% variation in the ratio of inorganic to organic carbon for calcareous algae may be possible (Meyer et al. 2015). Therefore, this error (± 30%) has also been taken into account for the primary productivity rates calculated using this ratio (Table 2.5).

*Table 2.5 Results from $CaCO_3$ and organic carbon ($C_{org}$) analysis of Corallina spp. samples and primary productivity rates (mg C $gDW^{-1}$ $h^{-1}$) estimated from these values where $gDW^{-1}$ is the average dry weight of the Corallina spp. samples and h is time in hours. Error (±) estimated using error from Meyer et al. (2015)*

| Treatment | % of total weight | | Ratio | Cumulative (g) | | Primary Productivity | |
|---|---|---|---|---|---|---|---|
| | $C_{org}$ | $CaCO_3$ | $CaCO_3$: $C_{org}$ | $C_{org}$ | $CaCO_3$ | mg $C_{org}$ $gDW^{-1}$ $h^{-1}$ | |
| Ambient | 26 | 58 | 0.45 | 0.07 | 0.15 | 0.21 | ±0.06 |
| Elevated 1 | 24 | 60 | 0.4 | 0.09 | 0.23 | 0.31 | ±0.09 |
| Elevated 2 | 26 | 59 | 0.44 | 0.09 | 0.21 | 0.33 | ±0.1 |

## 2.4.3. Photophysiology

*Corallina* spp. showed no significant difference in $rETR_{max}$, $F_v/F_m$, $\alpha$, and $E_k$ between the elevated and ambient alkalinity treatments (Table 2.3). There was a positive linear relationship between $F_v/F_m$ and TA ($R^2 = 0.1563$, $p < 0.01$), $rETR_{max}$ and temperature ($R^2 = 0.09817$ $p < 0.05$), and $\alpha$ and PAR ($R^2 = 0.0779$, $p < 0.05$) (Table 2.4). Both elevated and ambient alkalinity *Corallina* spp. $F_v/F_m$ remained relatively constant throughout the study period, decreasing by 6% and 11% from the day 1-21 respectively (Figure 2.4a). Elevated alkalinity *Corallina* spp. $E_k$ also remained relatively constant throughout the study period, only decreasing by 2% from day 1-21 whereas ambient alkalinity *Corallina* spp. $E_k$ decreased by 47% from day 1-21 (Figure 2.4b). *Corallina* spp. $rETR_{max}$ and α saw similar decreases throughout the study period; elevated alkalinity *Corallina* spp. $rETR_{max}$ and α decreased by 67% and 55% respectively and ambient alkalinity *Corallina* spp. $rETR_{max}$ and α decreased by 38% and 57% respectively (Figure 2.4c,d). There was a positive linear relationship between NCR and both $rETR_{max}$ ($R^2 = 0.09212$, $p < 0.05$) and $F_v/F_m$ ($R^2 = 0.213$, $p < 0.001$) (Table 2.4).

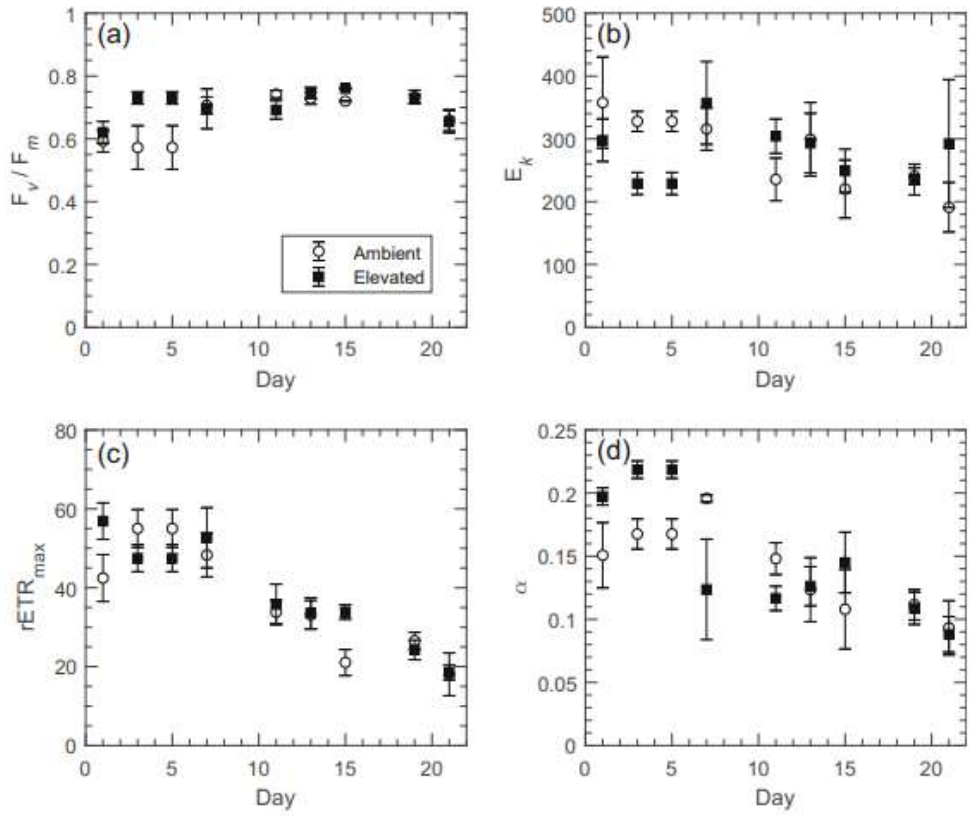


*Figure 2.4. Average High TA (filled circles) and Low TA (empty circles) Corallina spp. $F_v/F_m$ (a), $E_k$ (b), $rETR_{max}$ (c), and $\alpha$ (d) over the study period. Error bars show standard error. All parameters are dimensionless.*

## 2.5. Discussion

Results from this study show that elevated TA does influence *Corallina* spp. physiology. *Corallina* spp. net calcification rate significantly increased by 60% when exposed to elevated TA compared to the ambient alkalinity treatment. This is in part due to an increase in both light and dark calcification rates under elevated TA. However, due to the small sample sizes, there was no significant difference between the TA treatments for light and dark calcification rates. Other, non-statistically significant, physiology changes included *Corallina* spp. net primary productivity increasing and net respiration rates decreasing when exposed to elevated TA compared to ambient TA. There was no significant difference between the alkalinity TA for *Corallina* spp. photophysiological parameters. These results have important implications constraining the environmental impact and efficiency of CDR methods such as OAE.

### 2.5.1. Calcification

The strongest regression relationship for *Corallina* spp. NCR was with TA ($R^2 = 0.3998$, $p < 0.001$) suggesting that the higher rates of calcification for the elevated alkalinity treatment was due to the increase in TA. The increase in TA caused $\Omega_{Ca}$ to increase by 114%. Higher $\Omega_{Ca}$ creates more favourable conditions for *Corallina* spp. to produce $CaCO_3$. This finding is consistent with that of Hofmann et al. (2012) where *C. officinalis* growth rate and inorganic carbon content increased by ~50% and ~3% respectively when $\Omega_{Ca}$ increased by 194% (due to a decrease in $pCO_2$). A similar response was seen for a coral reef flat where the $\Omega_{Ar}$ increased by approximately 50% (due to increased TA) resulting in an increase of NCR by approximately 7% (Albright et al., 2016).

Contrary to this, Williamson et al. (2017) found that *C. officinalis* light calcification rates decreased by ~65% when $\Omega_{Ca}$ increased by 34.2%. This discrepancy between the investigations may be explained by their different methodologies. This study and the investigations by Hofmann et al. (2012a) and Albright et al. (2016) purposely altered the carbonate chemistry compared to Williamson et al. (2017) who did not. Instead, Williamson et al. (2017) investigated the response of *C. officinalis* to a tidal emersion. Williamson et al. (2017) concluded that factors such as temperature and light levels had the strongest influence on *C. officinalis* calcification rates, not the carbonate chemistry. Therefore, in an ex-situ environment where temperature and light levels were held constant, like this study, carbonate chemistry may have more influence over calcification rates.

In-situ light and dark calcification rate (CR) values from Williamson et al. (2017) are summarised and compared to values from this study in Table 2.6. The in-situ values are from *C. officinalis* in Combe Martin, North Devon and were sampled during winter when in-situ temperature and PAR were most similar to the temperature and irradiance values of this study. Both elevated and ambient alkalinity treatment *Corallina* spp. light and dark CR were higher compared to the in-situ values. This could be explained by the higher TA values at Dunraven Bay (2694 $\mu Eq\ L^{-1}$) compared to north Devon (~2300 $\mu Eq\ L^{-1}$).

Negative values for calcification rates suggest that instead of calcification, dissolution occurred. Based on previous studies, as summarised in Table 2.6, this is not unheard of for *Corallina* spp. and can be explained by an increase in respiration occurring when dark. At the

organism level, respiration can generate internal $CO_2$ which lowers internal $\Omega_{Ca}$ and so can promote $CaCO_3$ dissolution over calcification (Koch et al. 2013). However, dark dissolution (negative values), rather than calcification (positive values) only occurred for the ambient alkalinity treatment in week one (Figure 2.3b). Dark calcification, rather than dissolution, has previously been documented for *Corallina* spp. (Pentecost 1978; Lee and Carpenter 2001; Williamson et al. 2017). Whether calcification or dissolution occurs is believed to be strongly related to the rock pool $\Omega_{Ca}$ (Williamson et al. 2017). In the elevated alkalinity treatments (and ambient alkalinity treatment in week two) $\Omega_{Ca}$ was higher, so despite internal $CO_2$ increasing due to respiration, the seawater $\Omega_{Ca}$ would have remained high enough to promote calcification rather than dissolution. This is supported by the substantial increases between elevated and ambient alkalinity treatment dark CR for both week one and week two (Figure 2.3c).

*Table 2.6. Comparison of Corallina spp. physiology (LCR =light CR (µmol $CaCO_3$ $gDW^{-1}$ $h^{-1}$), DCR= dark CR (µmol $CaCO_3$ $gDW^{-1}$ $h^{-1}$), NPP (µmol DIC $gDW^{-1}$ $h^{-1}$), NR (µmol DIC $gDW^{-1}$ $h^{-1}$), $rETR_{max}$, α, $E_k$ , and $F_v/F_m$ to in-situ winter C.officinalis physiology. LCR, DCR, NPP, and NR values are the averages from week 1 and week 2.*

| | In-situ | | This study | |
|---|---|---|---|---|
| | max | min | Elevated | Ambient |
| LCR | 4[a] | 2[a] | 11 | 9 |
| DCR | -0.40[a] | -0.25[a] | 1.40 | 0.14 |
| NPP | -15[a] | -5[a] | -11 | -5 |
| NR | 5[a] | 5[a] | -0.27 | 0.50 |
| $rETR_{max}$ | 120[b] | 100[b] | 35 | 36 |
| α | 0.11[b] | 0.1[b] | 0.13 | 0.13 |
| $E_k$ | 800[b] | 700[b] | 287 | 271 |
| $F_v/F_m$ | 0.3[b] | 0.2[b] | 0.68 | 0.69 |

[a] *from Williamson et al. (2017)*
[b] *from Williamson et al. (2014)*

## 2.5.2. Photophysiology

The relatively constant values in $F_v/F_m$ values suggest little decline in *Corallina* spp. "health" throughout the experiment. However, there was a reduction in *Corallina* spp. $rETR_{max}$, α, and $E_k$ for both the elevated and ambient alkalinity treatments. This suggests less effective

photosynthesis at the end of the experiment compared to the start, which may be expected for a multi-week ex-situ experiment.

In-situ photophysiology values from Williamson et al. (2014) were used for comparison to the ex-situ values from this study (Table 2.6). Williamson et al. (2014) investigated the photophysiology of *C. officinalis* in Combe Martin, North Devon during winter 2013 (when in-situ temperature and PAR were most similar to the temperature and irradiance values of this study). However, caution should be taken with comparing the photophysiology values as the weather and light conditions would not be exactly the same as those at Dunraven Bay at the time of sampling of this study. For both the elevated and ambient alkalinity treatments, *Corallina* spp. had lower values of $rETR_{max}$ and $E_k$ than in-situ *C. officinalis*. The higher in-situ values suggest that there was some culture effect on the *Corallina* spp. photochemistry. However, there was no accompanying decrease in $F_v/F_m$ and $E_k$. Also, in-situ *C.Officinalis* $F_v/F_m$ values were lower than *Corallina spp.* values from this study (~0.2 compared to ~0.7 ; Table 2.6) and in-situ *C.Officinalis* α values were also slightly lower than the α values of the *Corallina spp.* samples in this study (~0.12 compared to ~0.13 ; Table 2.6). Further, *Corallina* spp. NPP rates were similar to in-situ *C.officinalis* NPP rates (Table 2.6). Because the *Corallina* spp. sample from this study had relatively higher α compared to $rETR_{max}$ and $E_k$, this suggests that the *Corallina* spp. were acclimated to low light (Perkins et al. 2016). During the experiment, the *Corallina* spp. were subjected to PAR values between 100-200 µmol photons $m^{-2}$ which are towards the lower end of the measured PAR values at Dunraven Bay (150-740 µmol photons $m^{-2}$).

There was no statistically significant difference in *Corallina* spp. $rETR_{max}$, α, $E_k$ and $F_v/F_m$ between the elevated and ambient alkalinity treatments (Table 2.4). However, there was a significant positive linear relationship between $F_v/F_m$ and TA ($R^2 = 0.1563$, $p < 0.01$) suggesting that increasing TA could have influenced *Corallina* spp. photosynthetic rates. However, because the *Corallina* spp. are low-light acclimated (relatively low $rETR_{max}$ compared to α), the low light levels may have had a stronger influence on the photophysiology than TA. This could partly explain why there was no similar increase in $rETR_{max}$, α and $E_k$ when TA was increased.

### 2.5.3. Primary productivity, and respiration

Despite there being little difference in photophysiology between alkalinity treatments, *Corallina* spp. primary productivity rates (NPP) did increase under elevated TA. However, a

note of caution is due here since the chambers were an open system and so DIC would have been lost as $CO_2$ through gas-solution diffusion. This means that there are significant uncertainties regarding the productivity calculations given the impact of $CO_2$ ingassing and outgassing on pH. Therefore, primary productivity was also estimated using the $CaCO_3$ to $C_{org}$ content ratio of the *Corallin*a spp. samples. The primary productivity rates estimated this way were approximately ten times larger than the NPP rates estimated using Equation 28 (once converted to mg C $gDW^{-1}$ $h^{-1}$ from µmol DIC $gDW^{-1}$ $h^{-1}$). This is most likely due to buffering of $CO_2$ from ambient air during the experiment which would mean a smaller change in pH than what would otherwise occur in a closed system. However, both the primary productivity rates estimated from the $CaCO_3$ to $C_{org}$ content ratio and from Equation 28 were higher for the elevated alkalinity treatment compared to the ambient alkalinity treatment (30% higher for Equation 28 calculated NPP rates and 52% for the $CaCO_3$ to $C_{org}$ content ratio calculated NPP rates). Therefore, even when the large errors associated with the productivity calculations (resulting from both the pH measurements and open system experimental set up), these results suggest that increasing TA does increase *Corallina* spp. primary productivity.

Increasing TA resulted in a greater increase in dark calcification rate (~900% increase from ambient to elevated) compared to light calcification (20% increase from ambient to elevated). This suggests that the increase in *Corallina* spp. NCR was due to higher $\Omega_{Ca}$ (from increasing TA) preventing dissolution occurring at night (increased dark calcification) rather than an increase in photosynthesis removing $CO_2$ in the day causing an increase in $\Omega_{Ca}$ (increased light calcification). Supporting this, in-situ *C.Officinalis* primary productivity rates were slightly less than the *Corallina* spp. primary productivity rates in this study for both the elevated and ambient alkalinity treatments (Table 2.6). This suggests that *Corallina* spp. was not fully productive in this experimental set up despite having higher calcification rates compared to in-situ values.

The near zero and slightly negative values of *Corallina* spp. respiration rates (NR) for the elevated alkalinity treatment (-0.21 µmol DIC $gDW^{-1}$ $h^{-1}$) are unusual. Respiration produces $CO_2$ therefore DIC would be expected to increase and positive values for NR were expected. The decrease in pH which occurred after the *Corallina* spp. were exposed to dark conditions for six hours also implies that $CO_2$ was being produced due to respiration. However, because the respiration and primary productivity experiments took place in an open system, they can only give an estimation of NR and NPP values and so these results need to be interpreted with caution.

## 2.6. Conclusions and implications for ocean alkalinity enhancement

This study set out to investigate the biological and environmental impact of increasing ocean TA as a CDR approach. This investigation has shown that increasing TA did not significantly affect *Corallina* spp. respiration or photophysiology but did cause a significant increase in calcification rates (NCR increased by 60% compared to a control) and a substantial, if not significant, increase in primary productivity. The increase in net calcification was due to both increased $\Omega_{Ca}$ preventing dissolution occurring at night and, to a lesser extent, an increase in photosynthesis leading to an increase in light calcification. The results from this study suggest that OAE would not be detrimental to *Corallina* spp. and that OAE could be used to mitigate against the effects of future ocean acidification. Also, despite the increase in calcification potentially driving an increase in dissolved $CO_2$ in the ocean, the parallel increase in primary productivity suggests that overall *Corallina* spp. may still act as a sink for $CO_2$ under high alkalinities. Therefore, OAE still appears to be an effective method at removing atmospheric $CO_2$ even if it does cause an increase in calcification rate. However, despite these results, questions still remain. To develop a more in-depth understanding of the environmental response to OAE, additional studies will be needed that investigate the impact of increasing TA on other marine calcifiers under different TA addition scenarios.

# Chapter 3.

# Ocean alkalinity enhancement through olivine dissolution and the physiological impact this has on *Corallina* spp.

## 3.1 Summary

Enhanced weathering (EW) is the artificially simulated weathering of silicate rich or carbonate minerals and is a method of elevating ocean TA. The aim of this chapter is to improve the understanding of the impact of olivine dissolution in coastal environments. There are two parts to this study. The first consists of an olivine dissolution experiment where Mg-rich olivine sand (Forsterite, $Mg_2SiO_4$) was mixed with seawater collected from Dunraven Bay for one month. The change in seawater chemistry (including dissolved element composition and carbonate chemistry) was determined and samples of olivine sand were taken both at the start and at the end of the experiment and analysed for mineralogy (XRD) and elemental composition (XRF). Results show that TA, pH, DIC, $\Omega_{Ca}$, and $\Omega_{Ar}$ decreased following olivine dissolution and XRD analysis of the olivine samples suggest that this was caused by hydrated magnesite precipitating out of solution. This suggests that EW of forsterite would not be an effective CDR approach because the increase in seawater TA, which is needed for ocean uptake of atmospheric $CO_2$ did not occur.

The second part consists of another *Corallina* spp. ex-situ experiment where *Corallina* spp. samples were subjected to three different treatments: ambient TA (control), elevated TA, and elevated TA + olivine dissolution. The experiment lasted for two weeks and *Corallina* spp. calcification, primary productivity, and photophysiology were monitored periodically. At the end of the experiment, *Corallina* spp. samples were also taken for XRF and XRD analysis. Results show that *Corallina* spp. exposed to olivine dissolution seawater had higher [CuO], $[FeO]_{total}$, [NiO], $[Cr_2O_3]$, and [ZnO] compared to the samples not exposed to the olivine dissolution products. The *Corallina* spp. samples from the elevated TA treatment had the highest calcification and primary productivity rates, followed by the samples from the elevated TA + olivine dissolution treatment. The *Corallina* spp. samples from the control treatment had the lowest calcification and primary productivity rates suggesting that it is changes to seawater TA, not dissolved element composition which has the stronger influence on *Corallina* spp. physiology. Therefore, demonstrating that as long as EW causes seawater TA to increase, it can be used as an ocean acidification mitigation approach.

## 3.2. Introduction

One method for increasing ocean TA for carbon storage is EW, which is the artificially simulated weathering of silicate rich or carbonate minerals (Seifritz 1990; Lackner 2002; Lenton and Britton 2006; Schuiling and Krijgsman 2006; Kohler et al. 2010; Hartmann et al. 2013; Williamson 2016). Naturally occurring Mg-rich olivine silicates ($Mg_2SiO_4$) are abundant in the Earth's crust, have relatively fast weathering reaction times, do not require energy-intense processing before their dissolution, and are commercially mined across the globe (Schuiling and Krijgsman 2006; Renforth 2012; Meysman and Montserrat 2017; Renforth and Henderson 2017). This makes them an ideal mineral for EW. When applied in an aqueous environment, the dissolution of olivine increases TA and so $CO_2$ uptake (Equation 30; Hartmann et al. 2013; Köhler et al. 2010; Köhler et al. 2013). According to Equation 30, for every mol of olivine dissolved, four mols of atmospheric $CO_2$ are taken up as $HCO_{3(aq)}$. However, because of the natural buffering effects of the ocean carbonate system, this ratio is closer to 3.0 – 3.5 in reality (Kohler et al. 2010; Renforth et al. 2013; Renforth and Kruger 2013).

$$Mg_2SiO_4 + 4H_2O + 4CO_2\,(g) \rightarrow 2Mg^{2+} + 4HCO_3^- + H_4SiO_4 \qquad \text{(Equation 30)}$$

The weathering of olivine and the other minerals found in rocks is a natural process which removes 1.1 Gt atmospheric $CO_2$ $year^{-1}$ (Ciais et al. 2014). However, this rate is not fast enough to mitigate the temperature change associated with current climate emergency. By increasing the surface area of minerals, such as olivine, the rate at which atmospheric $CO_2$ is consumed may be increased (Schuiling and Krijgsman 2006; Beerling et al. 2018). Exposure can be increased by applying olivine to terrestrial soils (Beerling et al. 2018; Dietzen et al. 2018), to the open ocean (Köhler et al. 2010), or to coastal regions (Schuiling and de Boer 2010; Meysman and Montserrat 2017). These different methods are summarised in Table 1.1, in Chapter 1. Applying olivine to coastal environments has geochemical and environmental benefits over applying minerals to the open ocean (Schuiling and de Boer 2010; Meysman and Montserrat 2017;). For example, if olivine were to be added to the surface open ocean, they would have to be ground fine in order to stop them sinking to the deep ocean (Köhler et al. 2013) which would be an energy and cost intensive process. Further, coastal regions are also often high energy, well mixed environments, which has two benefits for EW. First, the olivine grains would undergo frequent agitation increasing and the increased abrasion would rub off Mg depleted surface layers, which have been found to slow down the weathering

process (Olsson et al. 2012; Wang and Giammar 2013). Secondly, well-mixed seawater means that mineral saturation effects are limited and gas exchange with the atmosphere is maximised (Feng et al. 2017).

As well as increasing TA by releasing positive ions into solution such as $Ca^{2+}$ $Mg^{2+}$, $K^{+}$, etc., the dissolution of olivine would also release dissolved silica (dSi), and trace metals such as $Fe^{2+}$, $Ni^{2+}$, $Cu^{+}$, $Zn^{2+}$. Because trace metals occur at low concentrations in seawater, any perturbations from global EW application are likely to be sufficient to have either a fertilizing or potentially a toxic effect on marine organisms (Hartmann et al. 2013; Moore et al. 2013; Hauck et al. 2016). Further, increases in the concentration of the phytoplankton limiting nutrients dSi and $Fe^{2+}$ from EW could increase the biological carbon pump through dSi or Fe fertilisation (Hauck et al. 2016). However, in coastal regions, nutrient and trace metal concentrations are often higher than the ocean average because of a regular supply of solutes from land sources such as rivers, and ground water (Paerl 1997; Tovar-Sánchez et al. 2014). For example, the open ocean concentration of $Fe^{2+}$ is 0.02-2 nmol $L^{-1}$ and $Ni^{2+}$ concentration is 2-12 nmol $L^{-1}$ (Bruland et al. 2008) whereas the coastal waters of north west Portugal had much larger $Fe^{2+}$ concentrations of 8-72 nmol $L^{-1}$ (Reis et al. 2017)and $Ni^{2+}$ concentration can reach ~40 nmol $L^{-1}$ in the Rhine delta. However, the high concentrations of $Ni^{2+}$ in the Rhine delta are is still an order of magnitude lower than the predicted $Ni^{2+}$ perturbation from olivine dissolution in the study by Montserrat et al. (2017). Therefore, trace metals released into solution from EW could still impact marine biota in some way.

If EW was applied in coastal regions, then these areas may experience bigger perturbations as the dissolution products accumulate before being exported offshore (Meysman and Montserrat 2017). Therefore, it is sensible to investigate the response of a coastal species to EW. As discussed previously in Chapters 1 and 2, Corallinales are an important group to investigate with regards to OAE. Additionally, several studies found that macroalgae growth rate and photophysiology were negatively affected when grown with elevated metal concentrations (Matsunaga et al. 1999; Mamboya 2007).

Currently, little is known about the potential impact EW would have on the marine environment. Consequently, it is essential that the biological response to olivine dissolution is better understood. Therefore, this chapter aims to determine how olivine dissolution changes seawater chemistry (in terms of dissolution products and changes to carbonate chemistry) and how these changes then affect the physiology of *Corallina* spp. It was hypothesised that:

1. Olivine dissolution:
    a. As olivine dissolves, TA, pH, DIC and $\Omega_{Ca}$, and $\Omega_{Ar}$ would all increase due to Equation 30.
    b. As olivine dissolves, trace metals such as Cu, Fe, Ni, Cr, and Zn will be released into the solution.
2. *Corallina* spp. response:
    a. *Corallina* spp. grown under elevated TA + olivine treatment will have lower calcification and primary productivity rates due to toxicity effects of the trace metals released into solution.

## 3.3. Methods

There were two experimental segments to this investigation: the olivine dissolution experiment and the *Corallina* spp. culture experiment. The purpose of the olivine dissolution experiment was to examine how seawater chemistry changes during olivine dissolution and what dissolution products are released into solution. The aim was to dissolve olivine in seawater by repeating the experiment by Montserrat et al. (2017) but on a larger scale and then to monitor the increase in TA and pH and analyse the seawater after dissolution for trace metal content. Then, the aim was to use this same seawater for *Corallina* spp. culture experiment as an olivine treatment. However, after completing the olivine dissolution experiment, it was discovered that TA did not increase as expected and so samples of the olivine sand were also collected from before and after the dissolution experiment and chemical composition was analysed with the aim of aiding the explanation of why olivine dissolution did not lead to an increase in seawater TA. The seawater left over from the olivine dissolution experiment seawater was still used for the *Corallina* spp. culture experiment, but TA also had to be increased by $NaCO_3$ addition.

### 3.3.1 Olivine dissolution experiment

#### *3.3.1.a Experimental set up*

Two treatments were set up: one with 2.2kg of olivine added to 10 L of seawater and one control with 10 L of seawater and no added olivine. Both the olivine and control treatment seawater were held in separate 25 L sealed, plastic container each with a flow through system and left for 27 days. The flow through system was achieved using a water pump to ensure the seawater was continuously mixed to promote olivine dissolution (Figure 3.1). Table 3.1 outlines the key details of the dissolution experiment.

*Table 3.1. Olivine dissolution experiment details.*

| **Experiment Details** | |
|---|---|
| Olivine molar Mg:Fe | 0.94:0.06 |
| Olivine mineralogy | Forsterite |
| Total olivine added (kg) | 2.2 |
| Concentration (mol $L^{-1}$) | 1.56 |
| Total seawater (L) | 10 |
| Initial TA (µEq $L^{-1}$) | 2550 |
| Initial pH | 8.15 |
| Source of seawater | Dunraven Bay |
| Solution agitated by? | Flow-through system |
| Length of experiment (days) | 27 |

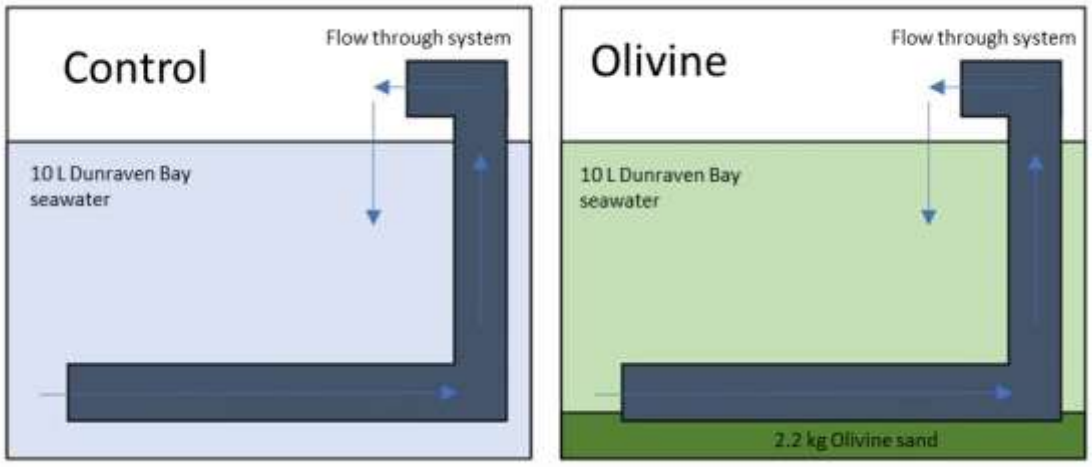


*Figure 3.1. A schematic showing the experimental set up of the olivine dissolution experiment including two flow through chambers one with olivine sand (Olivine treatment) and one without (Control treatment).*

The olivine used was the same as that used in the experiment by Renforth et al. (2015). It was commercially available Mg-rich olivine sand (Forsterite, $Mg_2SiO_4$) obtained from the Åheim plant in Møre og Romsdal county (Western Norway, from Minelco Ltd.) and then ground

using a tungsten carbide tema mill at the University of Birmingham by Renforth et al. (2015). Renforth et al. (2015) also analysed the olivine sand and the chemical composition and physical properties of the olivine are summarised in Table 3.2. The seawater used for the experiment was collected from Dunraven Bay a few days before the start the experiment, and filtered through a 0.2 µm filter, using the same technique described in Section 2.3.1, and stored in a dark container until use. 50 mL samples were collected (after being filtered through a 0.2 µm filter) periodically for TA and pH analysis. The other carbonate chemistry parameters (DIC, $pCO_2$, $\Omega_{Ar}$ and $\Omega_{Ca}$) were then calculated by inputting pH, TA, water temperature, and salinity into CO2SYS v2.1 (Pierrot et al. 2016). The standard error was determined by analysing six samples of seawater from both the control and olivine treatments at the start and end of the experiment.

*Table 3.2 Characterisation of olivine sand. Analysis performed by Renforth et al. (2015)*

| BET surface area ($m^2$ $g^{-1}$) | 3.04 ± 0.03 |
|---|---|
| Particle size distribution | Mass % |
| >500 µm | 7.4 |
| 500–212 µm | 27.5 |
| 212–125 µm | 50 |
| 125–63 µm | 11.1 |
| 63–45 µm | 3.1 |
| <45 µm | 0.8 |
| Total | 99.9 |
| XRF analysis | Mass % |
| $SiO_2$ | 41.64 |
| $TiO_2$ | 0.02 |
| $Al_2O_3$ | 0.75 |
| FeO (total) | 7.39 |
| MnO | 0.11 |
| MgO | 47.73 |
| CaO | 0.38 |
| $Na_2O$ | <0.01 |
| $K_2O$ | 0.05 |

| | |
|---|---|
| $P_2O_5$ | 0.01 |
| $SO_3$ | <0.01 |
| Loss on ignition | 2.27 |
| Total | 100.29 |

*3.3.1.b. Olivine and seawater chemical composition*

At the end of the experiment, six seawater 100 mL samples were taken from both the control and olivine treatments. The samples were filtered through a 0.2 µm polycarbonate filters, acidified, and then analysed for dissolved Si, Mg, Fe, Ni, Zn, Cu, and Cr concentrations using a Perkin Elmer Optima 2100 DV ICP-OES instrument (Cardiff University). Calibration standards (20, 40, 60, 80 and 100 mg/L) were prepared in 1% nitric acid from 1000 mg $L^{-1}$ ICP standards.

Triplicate olivine samples were taken both at the start and at the end of the experiment and were oven dried at ~100°C for 24 hours prior to X-ray diffraction (XRD) and X-ray fluorescence (XRF) analysis at Cardiff University. XRD was used for mineralogy analysis and XRF was used to determine the elemental composition of the samples. For XRD, the olivine sand samples were placed into aluminium holders, then analysed using a copper *K*α radiation source operating at 35 kV and 40 mA. The samples were scanned from 0 to 70 °2θ, at a step size of 0.02 °2θ, with a counting time of 1 s per step using a Philips PW1710 Automate Powder Diffractomer. The diffraction patterns were analysed using PW1876 PC-Identify software, version 1.0b and compared with JCPDS cards of standard materials. After XRD analysis, the same samples were analysed using XRF using an Olympus X-5000 instrument. The accuracy of the XRF data was determined to be on average ±7% by the analysis of silicate rich reference materials (Certified Reference Material: Stream Sediment STSD-1 31 and STSD-4 from Canmet Mining and Mineral Sciences, Ottawa, Canada).

## 3.3.2 *Corallina* spp. response

*3.2.3.a. Experimental set up*

*Corallina* spp. samples were collected during August 2019 using the same method as in Chapter 2 and the experimental program was identical to that used in Section 2.3.1 except that the experiment consisted of three TA treatments: Control, Elevated TA, and Elevated + Olivine each with five *Corallin*a spp. replicates. For the Control treatment, seawater from the

olivine dissolution control treatment was used. For the Elevated TA treatment, the TA of the olivine dissolution control treatment seawater was increased to 3467 µEq $L^{-1}$ using the same method as in Chapter 2. For the Elevated + Olivine treatment, the seawater from the olivine treatment was used. The seawater was collected at the end of the olivine dissolution experiment and then filtered through a 2 µm filter and then through a 0.2 µm filter and transferred to a ~10 litre container. The TA was gradually (over 60 minutes) increased to 3746 µEq $L^{-1}$ using the same method in Chapter 2. Table 3.3 summarises the starting carbonate chemistry parameters of each treatment. The experiment lasted for 15 days.

*Table 3.3. Average carbonate chemistry ± standard deviation for each treatment: Control, Elevated TA, Elevated TA + Olivine. TA= total alkalinity (µEq $L^{-1}$), DIC = dissolved inorganic carbon (µmol L-1), $pCO_2$ = atmospheric partial pressure of $CO_2$ (µatm), $\Omega_{Ca}$ = calcite saturation state, and $\Omega_{Ar}$ = aragonite saturation state.*

| Treatment | Sal | T (ºC) | pH | | TA (µmol $L^{-1}$) | | DIC (µmol $L^{-1}$) | | $pCO_2$ (µatm) | | $\Omega_{Ca}$ | | $\Omega_{Ar}$ | |
|---|---|---|---|---|---|---|---|---|---|---|---|---|---|---|
| | | | Av | ± | Av | ± | Av | ± | Av | ± | Av | ± | Av | ± |
| Elevated TA + Olivine | 35 | 19.8 | 8.31 | *0.005* | 3476 | *83* | 2893 | *5* | 280 | *4* | 10.9 | *0.09* | 7.1 | *0.06* |
| Elevated TA | 32 | 19.8 | 8.41 | *0.022* | 3467 | *456* | 2784 | *21* | 206 | *14* | 12.6 | *1.20* | 8.2 | *0.78* |
| Control | 32 | 19.6 | 8.12 | *0.004* | 2144 | *160* | 1856 | *3* | 294 | *4* | 4.7 | *4.57* | 3.1 | *2.97* |

### *3.3.2.b. Net calcification, primary productivity, and photophysiology*

Net calcification rates (NCR), net primary productivity (NPP) were calculated for each *Corallina* spp. sample from all three treatments using the same methods outlined in Chapter 2. On days 3, 6, 11, 15, the photophysiology of the *Corallina* spp. samples was determined using PAM fluorometry using the same method as Section 2.3.4.

### *3.3.2.c. Chemical composition*

Following the experiment, the *Corallina* spp. samples were carefully washed using milli-Q to remove all traces of seawater and were subsequently dried at ~100°C for 24 hours. The samples were then crushed into a fine powered using a pestle and mortar and analysed for elemental analysis using XRF and XRD using the same procedure in Section 3.2.1.b.

# 3.4. Results

## 3.4.1 Olivine dissolution experiment

### *3.4.1.a. Carbonate chemistry*

The results from olivine dissolution experiment are displayed in Figure 3.2. There was minimal change in all the carbonate chemistry parameters for the control treatment. However, there was a slight and gradual increase in $\Omega_{Ca}$ and $\Omega_{Ar}$ from ~ 4 - 7 and ~3 - 4 respectively (Figure 3.2 e-f). There was minimal change in $pCO_2$ from day 0-27 in both the olivine dissolution and control experiment. $pCO_2$ remained at ~230 ± 52 µatm for the olivine experiment and ~400 ± 67 µatm for the control experiment (Figure 3.2 d). Where olivine dissolution did take place, there was a change in TA, pH, DIC, in $\Omega_{Ca}$, and $\Omega_{Ar}$. There was a decrease in TA and DIC between day 0 and day 17 from 2550 to 1720 µEq $L^{-1}$ for TA and 2200 to 1450 µmol $L^{-1}$ for DIC, which was followed by a more gradual decrease to day 27 to final values of 1660 µEq $L^{-1}$and 1420 µmol $L^{-1}$ for TA and DIC respectively (Figure 3.2 a,c). There was a decrease in pH, $\Omega_{Ca}$, and $\Omega_{Ar}$ from the start of the experiment to the end of the experiment (day 0-27; Figure 3.2 b, e-f) from 8.14, 6.39, and 4.17 to 8.05, 3.85, and 2.53 for pH, $\Omega_{Ca}$, and $\Omega_{Ar}$ respectively. A similar response was seen in two other olivine dissolution experiments (Appendix B).

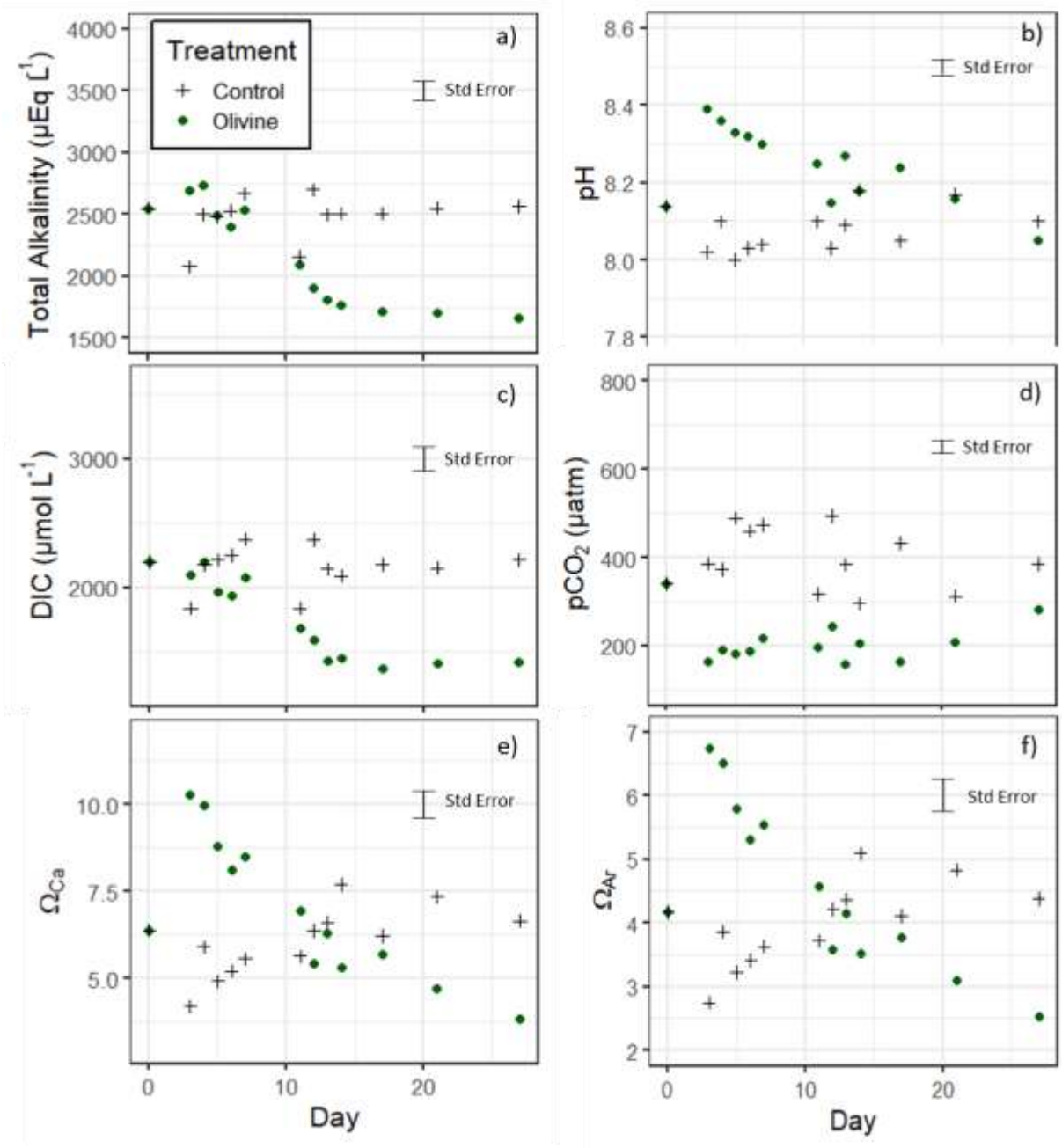


*Figure 3.2. Carbonate chemistry properties of the olivine dissolution experiment. the black crosses show the results from the control experiment (no olivine dissolution) and dark green closed circles show result from olivine dissolution. (a) Total alkalinity (µEq $L^{-1}$), (b) pH, (d) dissolved inorganic carbon (DIC, µmol $L^{-1}$), (d) atmospheric partial pressure of $CO_2$ ($pCO_2$, µatm), (e) calcite saturation state($\Omega_{Ca}$), (f) aragonite saturation state ($\Omega_{Ar}$). Standard error (Std error) for each value showed by error bar in upper left corner. A similar response was seen in two other olivine dissolution experiments- Appendix B.*

*3.4.1.b. Olivine and seawater chemical composition*

After the olivine dissolution experiment, the chemical composition of the seawater of each treatment (olivine and control) was analysed for [$SiO_2$], [Mg], [Fe], [Ni], [Zn], [Cu], and [Cr]. However, only [$SiO_2$], [Mg], [Zn], and [Cu] were above the level of detection (Figure 3.3a). When the seawater from the olivine treatment was compared to the seawater from the control treatment, there was a 10%, 105%, and 163% increase in [Cu], [Mg], and [$SiO_2$] respectively. Further, the olivine treatment seawater had [Zn] of 0.6 ± 0.2 µmol $L^{-1}$, whereas the control seawater had no detectable [Zn] present. Samples of olivine from before and after the dissolution in seawater were analysed by XRF and the results are shown in Figure 3.3b. There was a large increase in [Cl], [$K_2O$] and [$SO_3$] (~80, ~180, ~200% respectively) and a small increase in [$Cr_2O_3$] and [Cu] (~20 and ~5% respectively). There was a decrease in concentration for all other oxides analysed (Figure 3.3b). Most notably, there was a ~10% decrease in [$SiO_2$] and iron oxides ([$Fe_2CO_3$] +[FeO]; expressed as $[FeO]_{total}$ from herein) and a ~15% decrease in [NiO] and [ZnO].

XRD analysis confirmed that the main composition of the olivine sample before the experiment was forsterite (Figure 3.4). Other minerals present included fayalite ($Fe_2(SiO_4)$) crystolite ($Mg_3(Si_2O_5)(OH)_4$), enstatite ($Mg_2Si_2O_6$), brucite ($Mg(OH)_2$), and hydrated magnesite ($Mg_5(CO_3)_4(OH)_2.4H_2O$) (Figure 3.4). The composition of the olivine samples taken before and after the dissolution experiment were similar, however, the hydrated magnesite peaks were only found in the olivine samples taken after the dissolution experiment (Figure 3.4). Further, there is a forsterite peak at 23.5˚on the diffractogram from the olivine sand sample taken after the dissolution sample which is not present in the sample taken before the dissolution experiment.

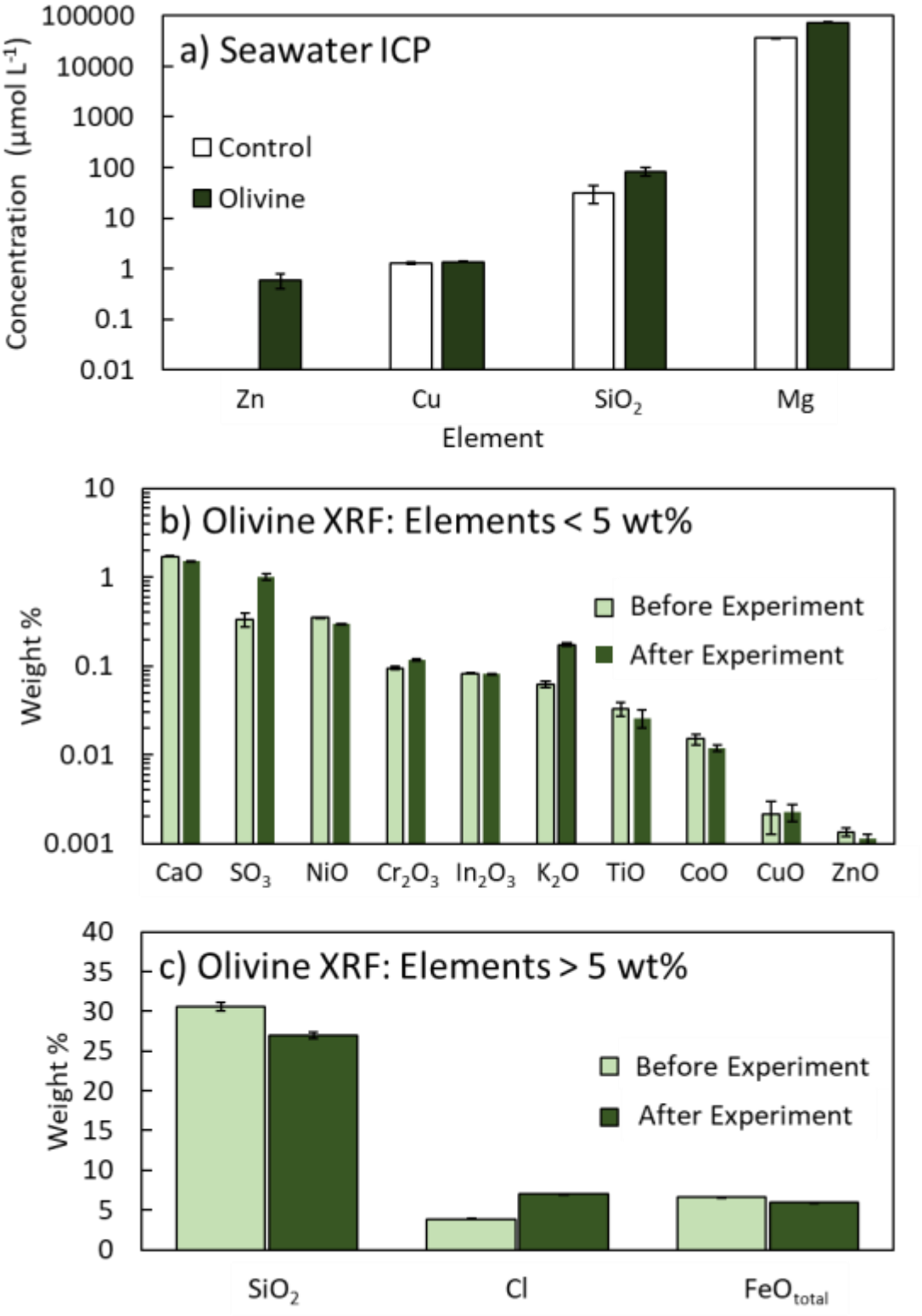


*Figure 3.3 Results from elemental analysis of olivine dissolution experiment. (a) ICP-OES results of control seawater (white) and olivine dissolution seawater (green) samples taken at the end of the olivine dissolution experiment. (b) Results from XRF analysis of olivine sand before (pale green) and after (dark green) the dissolution experiment.*

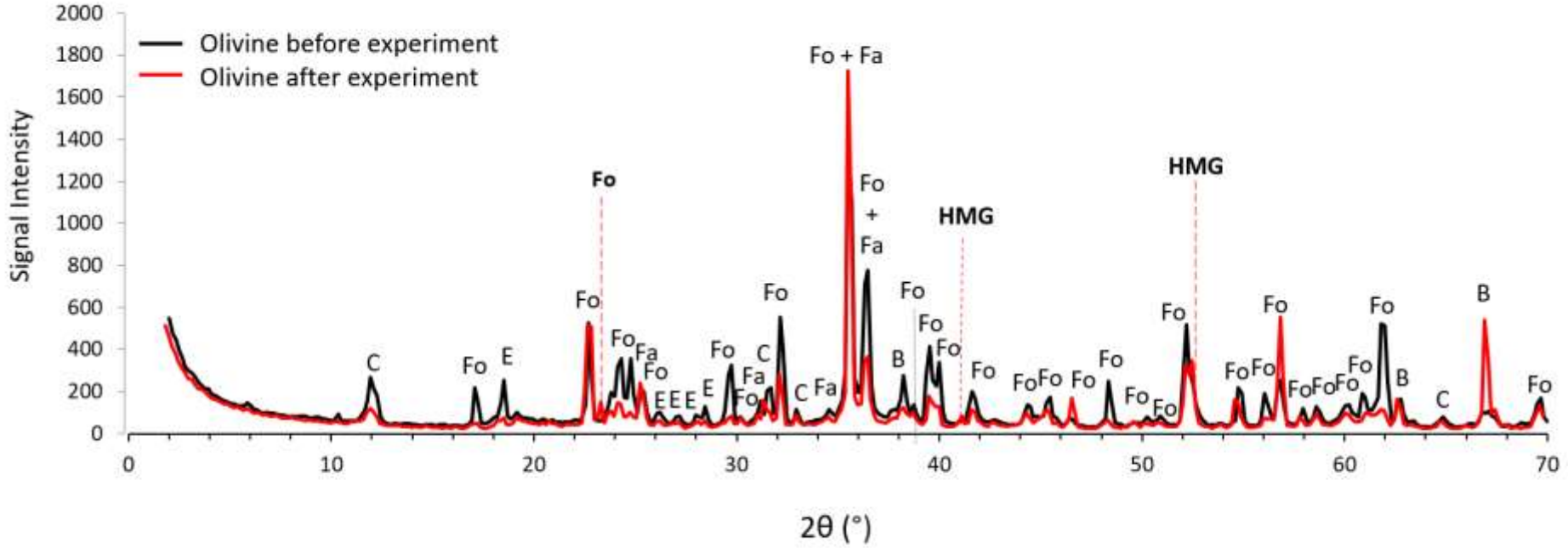


*Figure 3.4 XRD diffractograms of olivine sand from before (black) and after (red) the dissolution experiment. C = crystolite, Fo = forsterite, E = enstatite, Fa = fayalite, B= brucite, HMG = hydrated magnesite.*

## 3.4.2 *Corallina* spp. response

### *3.4.2.a. Net calcification, primary productivity, and photophysiology*

There was a statistically significant difference in both *Corallina* spp. NCR and NPP between the three treatments (Table 3.4). Calcification and primary productivity rates were on average higher when *Corallina* spp. were cultured under the Elevated TA treatment compared to both the Elevated + Olivine and Control treatments (Figure 3.5). *Corallina* spp. NCR was 3.96 ± 0.61 µmol $CaCO_3$ $gDW^{-1}$ $hr^{-1}$, 2.73 ± 0.47 µmol $CaCO_3$ $gDW^{-1}$ $hr^{-1}$, and 2.37 ± 0.22 µmol $CaCO_3$ $gDW^{-1}$ $hr^{-1}$ when grown under the Elevated TA, Elevated TA + Olivine, and Control treatments respectively. *Corallina* spp. NPP was -10.21 ± 1.59 µmol DIC $gDW^{-1}$ $hr^{-1}$, -8.06 ± 1.73 µmol DIC $gDW^{-1}$ $hr^{-1}$, and -7.20 ± 0.74 µmol DIC $gDW^{-1}$ $hr^{-1}$ when grown under the Elevated TA, Elevated TA + Olivine, and Control treatments respectively. However, there was no statistically significant difference between the photophysiological parameters ($F_v/F_m$, $_rETR_{max}$, $E_k$, and α) between the three treatments (Table 3.4, Figure 3.6).

*Table 3.4 Results from one-way ANOVA analysis of* Corallina *spp. physiology (NCR net calcification rate; µmol $CaCO_3$ $gDW^{-1}$ $h^{-1}$), NPP (net primary production; µmol DIC $gDW^{-1}$ $h^{-1}$), $rETR_{max}$, $F_v/F_m$, α, and $E_k$ . Significant codes: p<0.05: *, p<0.01: **, p<0.001: ***, not significant: NS.*

| Variable | | Df | Sum Sq | Mean Sq | F | Sig |
|---|---|---|---|---|---|---|
| NCR | Treatment | 2 | 3.17E+01 | 1.58E+01 | 60.48 | *** |
| | Res. | 75 | 1.96E+01 | 2.62E-01 | | |
| NPP | Treatment | 2 | 1.26E+02 | 6.32E+01 | 14.17 | *** |
| | Res. | 83 | 3.70E+02 | 4.46E+00 | | |
| $F_v/F_m$ | Treatment | 2 | 4.51E-01 | 2.26E-02 | 0.604 | NS |
| | Res. | 61 | 2.28E-01 | 3.74E-03 | | |
| $_rETR_{max}$ | Treatment | 2 | 6.06E+02 | 8.02E+02 | 0.512 | NS |
| | Res. | 61 | 9.56E+04 | 1.57E+04 | | |
| $E_k$ | Treatment | 2 | 8.02E+04 | 4.01E+04 | 1.317 | NS |
| | Res. | 62 | 1.86E+06 | 3.04E+04 | | |
| α | Treatment | 2 | 5.56E-03 | 2.78E-03 | 1.774 | NS |
| | Res. | 64 | 1.00E-01 | 1.57E-03 | | |

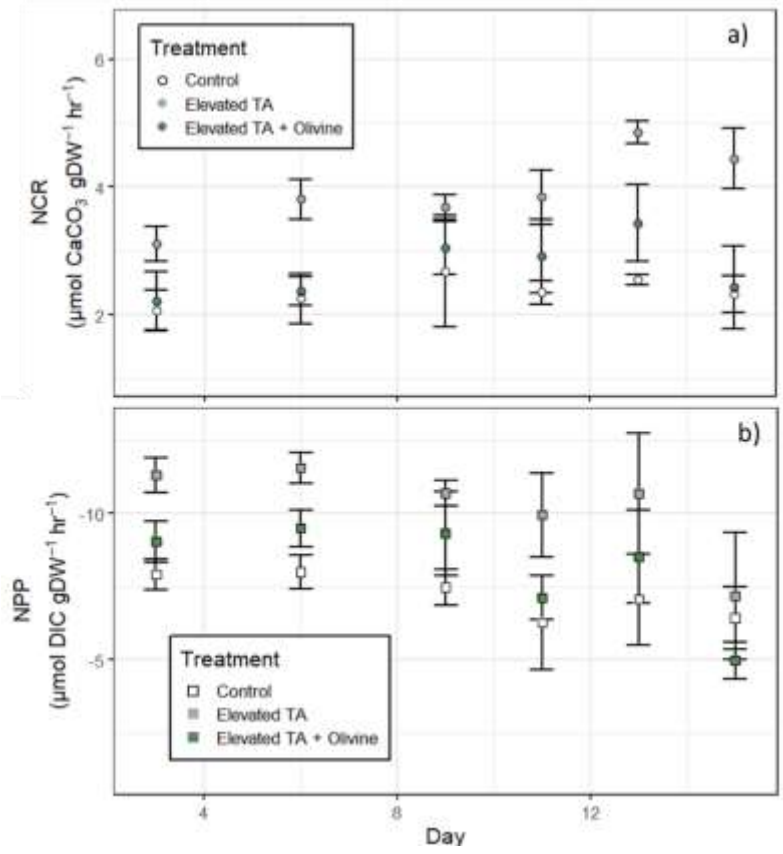


*Figure 3.5 Average (± standard error) Corallina spp. (a) net calcification rate (NCR; µmol $CaCO_3$ $gDW^{-1}$ $h^{-1}$), and (b) Corallina spp. net primary productivity (NPP; µmol DIC $gDW^{-1}$ $h^{-1}$) for the three treatments: Control (white), Elevated TA (grey), and Elevated TA +Olivine (green).*

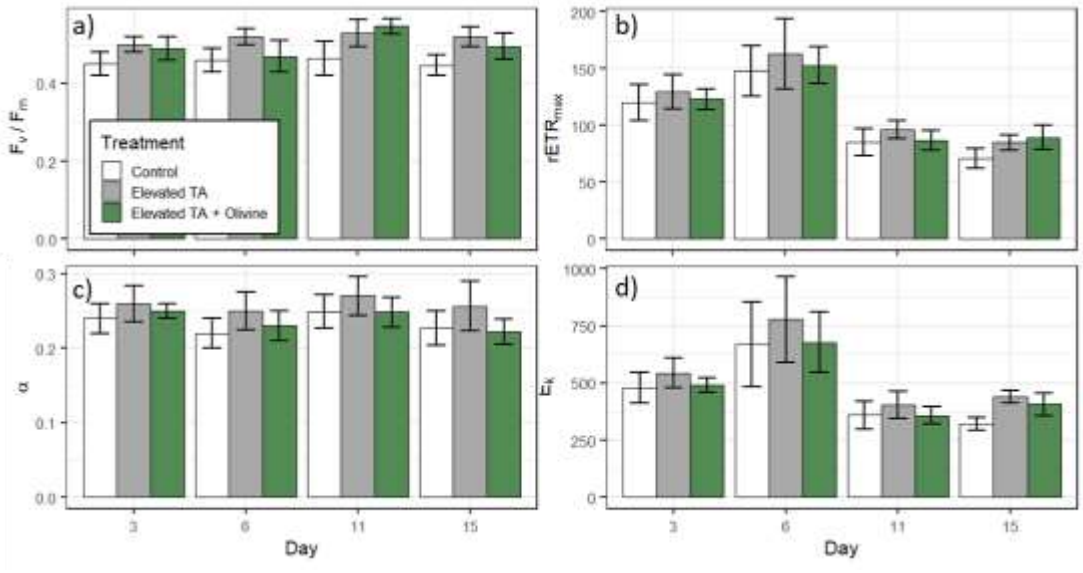


*Figure 3.6. Average (± standard error) Corallina spp. $rETR_{max}$ (a), α (b), $E_k$ (c), and $F_v/F_m$ (d) over the study period for the three treatments: Control (white), Elevated TA (grey), and Elevated TA +Olivine (green). All parameters are dimensionless.*

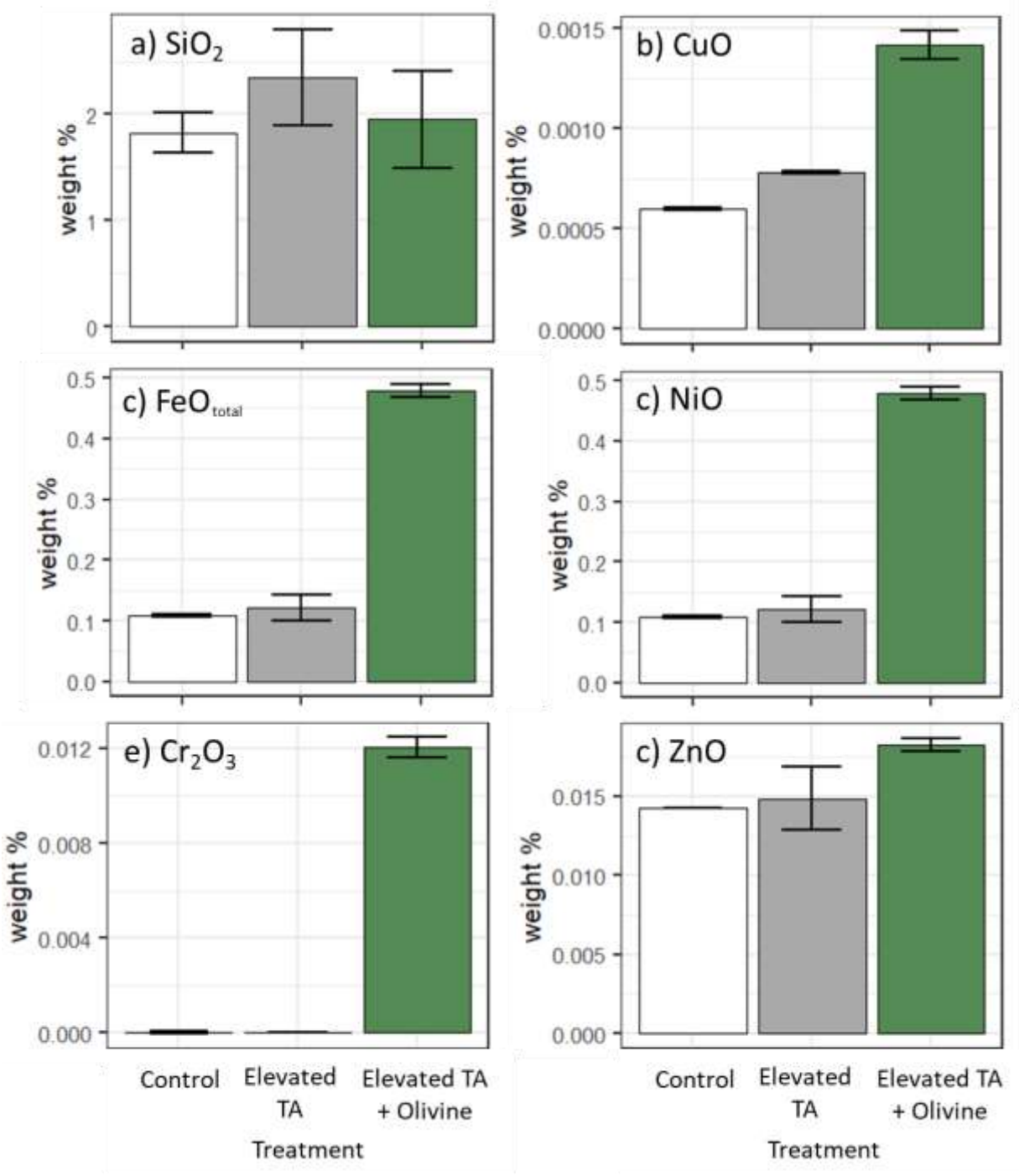


*Figure 3.7 Results from XRF elemental analysis of Corallina spp. samples from the three treatments: Control (white), Elevated TA (grey), and Elevated TA +Olivine (green)*

### *3.4.2.b. Chemical composition*

XRD analysis confirmed that the main composition of *Corallina* spp. was high magnesium calcite (Appendix C). There was no difference in *Corallina* spp. mineralogy between the TA treatments. XRF analysis revealed that there were similar concentrations of CaO, $SO_3$, $K_2O$,

$SiO_2$, CuO, $FeO_{total}$, NiO, $Cr_2O_3$, and ZnO in the *Corallina* spp. samples cultured exposed to the Control and Elevated TA treatments (Table 3.5, Figure 3.7). However, there were higher concentrations in the *Corallina* spp. samples from the Elevated TA treatment. *Corallina* spp. samples exposed to the Elevated TA + Olivine treatment had 23-28% higher [ZnO], 82-137% higher [CuO], 294-341% higher [FeO], and ~1800-3500% higher [NiO] than the samples exposed to elevated TA and control treatments. Further, the *Corallina* spp. samples grown under the olivine dissolution treatment had 0.012% [$Cr_2O_3$] where there was no detectable [$Cr_2O_3$] in the samples exposed to the elevated TA and control treatments (Table 3.5, Figure 7 b-f).

*Table 3.5. Metal oxide content (wt% and standard error) of Corallina spp. samples from the control, elevated TA, and elevated TA + Olivine treatments.*

| Treatment | Oxide | Average (wt %) | Std Error |
|---|---|---|---|
| Control | CaO | 5.28E+01 | 8.01E+00 |
| Elevated TA | | 5.24E+01 | 6.61E+00 |
| Elevated TA + Olivine | | 6.31E+01 | 0.00E+00 |
| Control | $SO_3$ | 4.15E+00 | 7.01E-01 |
| Elevated TA | | 3.98E+00 | 7.53E-01 |
| Elevated TA + Olivine | | 2.07E+00 | 4.27E-01 |
| Control | $K_2O$ | 1.43E+00 | 1.96E-01 |
| Elevated TA | | 1.53E+00 | 3.22E-01 |
| Elevated TA + Olivine | | 8.94E-01 | 2.73E-01 |
| Control | $Cr_2O_3$ | 0.00E+00 | 5.85E-05 |
| Elevated TA | | 0.00E+00 | 0.00E+00 |
| Elevated TA + Olivine | | 1.20E-02 | 4.38E-04 |
| Control | $SiO_2$ | 1.83E+00 | 1.84E-01 |
| Elevated TA | | 2.35E+00 | 4.53E-01 |
| Elevated TA + Olivine | | 1.95E+00 | 4.56E-01 |
| Control | $FeO_{total}$ | 1.09E-01 | 1.81E-03 |
| Elevated TA | | 1.22E-01 | 2.18E-02 |
| Elevated TA + Olivine | | 4.79E-01 | 1.08E-02 |
| Control | NiO | 1.57E-03 | 4.41E-04 |

| | | | |
|---|---|---|---|
| Elevated TA | | 8.34E-04 | 1.07E-03 |
| Elevated TA + Olivine | | 3.02E-02 | 9.33E-04 |
| Control | | 5.98E-04 | 5.00E-06 |
| Elevated TA | CuO | 7.79E-04 | 6.00E-06 |
| Elevated TA + Olivine | | 1.42E-03 | 7.00E-05 |
| Control | | 1.43E-02 | 2.60E-05 |
| Elevated TA | ZnO | 1.49E-02 | 1.96E-03 |
| Elevated TA + Olivine | | 1.83E-02 | 4.05E-04 |

## 3.5. Discussion

There were two notable results from this study. The first is that TA did not increase as expected during olivine dissolution. Olivine dissolution resulted in lower TA, pH, DIC, $\Omega_{Ca}$, and $\Omega_{Ar.}$ Even though TA did not increase, analysis of the olivine sand and seawater samples taken after the dissolution experiment show that olivine dissolution did occur. Therefore, this suggests there was some other process occurring which stopped TA from increasing. The second main result was that *Corallina* spp. samples grown under the olivine dissolution treatment had higher [CuO], $[FeO]_{total}$, [NiO], $[Cr_2O_3]$, and [ZnO] compared to the samples not exposed to the olivine dissolution products and this significantly influenced *Corallina* spp. physiology. The first part of this section outlines a potential explanation to why seawater TA did not increase and what this means for the efficiency of EW as a carbon dioxide removal approach. The next section will then explain how trace metal uptake can influence *Corallina* spp. physiology and what this means with regards to biological impact of EW.

### 3.5.1. Olivine dissolution: why was there no increase in total alkalinity?

It was hypothesised that olivine dissolution in seawater would cause TA to increase. However, the opposite occurred and so this hypothesis was rejected. Olivine dissolution causes seawater TA, pH, DIC, $\Omega_{Ca}$, and $\Omega_{Ar}$ to decrease and this was also seen in other olivine dissolution experiments performed (Appendix B). Even though TA did not increase, ICP-OES analysis of the seawater and XRF analysis of the olivine samples suggest that metals from olivine were released into solution, indicating that olivine dissolution did occur. Further evidence of olivine dissolution comes from XRD analysis of the olivine sand samples taken before and after the dissolution experiment. The olivine samples had different XRD diffractograms and there were some peaks present in the diffractogram of the olivine samples

taken after the dissolution experiment, which were not present in the samples taken before the experiment (Figure 3.4). For example, there is a forsterite peak at 23.5 ° on the diffractogram from the olivine sand sample taken after the dissolution sample which is not present in the sample taken before the dissolution experiment. This difference could be caused by surface alteration of the olivine grains caused by partial or complete dissolution grains changing the crystallographic structure of the olivine and so creating different peaks. There were also peaks which suggested that different minerals were present in the sample taken after the dissolution experiment, which suggests that secondary mineral precipitation could have occurred (discussed in more detail further below). Therefore, the decrease in TA was likely a result of carbonate minerals precipitating out of solution.

One theory of how TA decreased is that the olivine sand acted as a nucleation site for $CaCO_3$ precipitation, and so initially (between day 0-4) as olivine dissolved and increased TA, $\Omega_{Ca}$ and $\Omega_{Ar}$, it creating more and more favourable conditions for $CaCO_3$ precipitation so that by day 4 onwards $CaCO_3$ began to precipitate taking TA out of the solution. However, there was no evidence of $CaCO_3$ precipitates (e.g., calcite, aragonite, dolomite, high Mg-calcite) from the XRD analysis performed on the olivine sand samples taken after the dissolution experiment. Further, XRF analysis of the olivine samples, showed that there was no increase in Ca content of the olivine sand after the dissolution experiment. In fact [Ca] was lower in the olivine sand sample taken at the end of the dissolution experiment. Although, these results show that it is unlikely that the olivine grains acted as a nucleation site for $CaCO_3$ precipitation, they could have acted as a nucleation site for precipitation of other secondary minerals.

In a thermodynamic equilibrium modelling study, Griffioen (2017) showed that theoretically TA decreases when forsterite reacts with seawater in a closed system and produces magnesite as a secondary mineral (Equation 31).

$$Mg_2SiO_{4(s)} + 2H_2O + CO_{2(g)} \rightarrow 2MgCO_{3(s)} + H_4SiO_{4(aq)} \quad \text{(Equation 31)}$$

Griffioen (2017) investigated many different dissolution scenarios with variable mineralogical composition of olivine and the formation of different secondary precipitates and found that TA only decreased when there was a closed system and magnesite was formed. However, the olivine samples from before and after the dissolution experiment showed no evidence of magnesite. This is unsurprising because magnesite precipitation at ambient temperatures and $pCO_2$ is rare (Saldi et al. 2009; Gregg et al. 2015; Montes-

Hernandez and Renard 2016). This is because of the slow dehydration kinetics of $Mg^{2+}$ (Saldi et al. 2009; Gautier et al. 2014) and so temperatures generally need to be at least 40 °C for precipitation to occur (Deelman 1999; Hanchen et al. 2008; dos Anjos et al. 2011; Hopkinson et al. 2012; Swanson et al. 2014).

Unlike, magnesite, Berninger et al. 2014 showed that it is possible for hydrated magnesite to precipitate from the dissolution of olivine at ambient temperatures (25 ̊C) via the following equation:

$$5Mg_2SiO_{4(s)} + 20H_2O + 8CO_{2(g)} \rightarrow 2Mg_5(CO_3)_4(\mathrm{OH})_2 \cdot 4\mathrm{H_2O}_{(s)} + 5H_4SiO_{4(aq)}$$

(Equation 32)

Supporting this theory, XRD analysis showed there was evidence of hydrated magnesium carbonate ($Mg_5(CO_3)_4(OH)_2.4H_2O$) present in the olivine sample after the dissolution experiment which was not present in the samples from before the experiment (Figure 3.4). Therefore, one possible explanation to why TA decreased is that as olivine dissolves, TA initially increases between days 0-4 but then this promotes hydrated magnesite to precipitate out of solution, removing $Mg^{2+}$ from solution. This would not explain the decrease in TA, if it was just the dissolution products of forsterite and seawater which were being used in hydrated magnesite formation. This would just explain why there is no increase in TA. For decreased TA, $Mg^{2+}$ already present in the seawater would need to be removed from solution. Therefore, it may be that the dissolution of forsterite increasing the $Mg^{2+}$ content of seawater started the precipitation of hydrated magnesite but then the increased nucleation sites provided by the olivine grains promoted further precipitation of hydrated magnesite, removing even more $Mg^{2+}$ out of solution.

In both dissolution experiments, after ~10 days, TA and DIC levels stopped decreasing. This suggests that the continued precipitation of hydrated magnesite was inhibited. The rate limiting step of the precipitation of hydrated magnesite is the dissolution of forsterite (Berninger et al. 2014) and so by day 10, olivine dissolution may have slowed down enough to prevent further precipitation hydrated magnesite. Olivine dissolution could have been slowed down if the hydrated magnesite precipitated as a coating around the olivine surface (Oelkers et al. 2018). It should be noted that although TA and DIC remained constant after day 10, $\Omega_{Ca}$ and $\Omega_{Ar}$ continued to decrease, which can be explained by the increase in $pCO_2$ for these days. This most likely occurred because the flow through chamber was not a 100% closed system and so allowed in gassing of $CO_2$ to occur.

Monsterrat et al. (2017) performed a similar olivine dissolution experiment using the same stock of olivine sand. Like this study, Monsterrat et al. (2017) did not see a continuous increase in TA with olivine dissolution, however they did not see a decrease in TA either. Initially TA increased from ~2400 to 2500 µEq $L^{-1}$ within a couple of days but and then plateaued for the remainder of their ~90-day experiment. Monsterrat et al. (2017) used a similar experimental set up to the one that was used in experiment 1 from this study, however, there were a few differences such as, they added a smaller amount of olivine sand to 1 kg of seawater (0.15 kg compared to 2.2 kg added in this study). This could explain the why there was a decrease TA in this study but not in the one by Monsterrat et al. (2017) because the higher quantity of olivine added, would allow for more nucleation sites and so potentially causing more precipitation to occur.

Hydrated magnesite precipitating out of solution can explain why there was a decrease in TA, however it does not explain the substantial increase in [Cl], [$K_2O$] and [$SO_3$]. The increase could have occurred due to salt residue from the seawater remaining on the olivine sample. It is possible for sulphate ($SO_4^{2-}$) to replace $CO_3^{2-}$ in marine carbonates (Takano 1985). Therefore, the increase in [$SO_3$] in the olivine sample after the dissolution experiment could be explained by the substitution of $CO_3^{2-}$ by $SO_4^{2-}$ in hydrated magnesite. The precipitation of phyllosilicate clay minerals can occur from the chemical combination of seawater and marine sediments, a process known as “reverse weathering” (Mackenzie and Kump 1995). Therefore, the increase in [$K_2O$] could be explained by the formation of potassium containing clay minerals such as glauconite ($(K, Na)(Fe^{3+},Al, Mg)_2(Si, Al)_4O_{10}(OH)_2$). This would also explain the reduction in TA. However, there was no evidence for any clay minerals from the XRD analysis of the olivine samples taken after the dissolution experiment.

### 3.5.2 *Corallina* spp. response

It was hypothesised that as olivine dissolves, trace metals such as Cu, Fe, Ni, Cr, and Zn would be released into solution and if taken up by *Corallina spp.*, would reduce NCR, NPP and photophysiology rates. Results from both the ICP-OES and XRF analyses suggest that after olivine dissolution there was an increase in [Cu], [Mg], [$SiO_2$], and [Zn] in the seawater and results from XRF analysis of the olivine samples show that there was also a decrease in the amount of SiO, $FeO_{total}$, NiO, and ZnO present in the olivine sand after the dissolution experiment. Further, the *Corallina* spp. grown under elevated TA had higher [CuO], $[FeO]_{total}$, [NiO], [$Cr_2O_3$], and [ZnO] than the samples grown under the elevated TA and control

treatments. There was no statistically significant difference in *Corallina spp.* photophysiology ($F_v/F_m$, $_rETR_{max}$, $E_k$, and α) between those grown under elevated TA + olivine treatment and the control. However, these treatments had lower NCR, NPP and $F_v/F_m$ than the *Corallina* spp. grown under the elevated TA treatment. This indicates that the incorporation of trace metals had a negative influence on *Corallina* spp. physiology then what would be expected at the same TA values, and an acceptance of the hypotheses.

*3.5.2.a. Trace meatal uptake*

The *Corallina* spp. grown under the Elevated TA + olivine treatments had considerably higher [CuO], $[FeO]_{total}$, [NiO], $[Cr_2O_3]$, and [ZnO] than the *Corallina* spp. samples cultured under the other treatments. This shows that there was there was increase in these metals in the seawater (although below the level of detection of ICP-OES analysis) of the elevated TA + olivine treatment and that the *Corallina* spp. samples incorporated these extra metals into their biomass. However it is unclear whether the trace metals were taken up into Corallina spp. organic matter or into their HMC skeleton. This is because the Corallina spp. samples analysed by XRF contained both organic and inorganic matter.

A similar result was found in a study by Couto et al. (2010), who discovered that *Corallina elongata* found near hydrothermally active sites had higher [Ca], [Mg], [Zn], [Rb], and [Mn] when compared to *Corallina elongate* from other more typical seawater sites. As hydrothermal activity releases heavy metals into surrounding seawater, hydrothermal vents could be considered analogous to EW application sites. Although, an important difference between EW and hydrothermal activity, is that hydrothermal vents also increase the surrounding seawater temperature, which EW is unlikely to do. Increasing seawater temperature can increase the incorporation of metals into the calcium carbonate structure of calcifying marine organisms (Mohamed and Khaled 2005; Kamenos et al. 2008). As such, the metal assimilation rates of algae found near hydrothermal vents are likely to be higher than those found near (hypothetical) EW application sites.

Furthermore, Chakraborty et al. (2014), found a strong positive correlation between metal concentrations in *Rhodophyta* algae with respect to trace metal concentrations in seawater ($R^2$= 0.85-0.95), However, out of the 12 algal species studied, the species from the *Rhodophyta* (red algae) group generally had the lowest concentrations of Cu, Ni, Fe, Zn, and Cr compared to species from the *Phaoephyceae* or *Chlorophyceae* groups (brown and green algae). Further, because they contain a high percentage of calcium carbonate, calcifying algae

have slower metabolic rates compared to non-calcifying algae (Littler et al. 1983). This means that calcifying algae generally have a lower assimilation rate and *Corallina* spp. have often been shown to have lower metal accumulation rates when compared with non-calcified algae (Jordanova et al. 1999; Kut et al. 2000; Stengel et al. 2004; Wallenstein et al. 2009). This implies that calcifying red algae such as *Corallina* spp. may be less sensitive to trace metal perturbations than non-calcifying or green or brown algae groups.

*3.5.2.b. Influence of trace metal uptake on* Corallina *spp. physiology*

Increased metal assimilation had little impact on *Corallina* spp. photophysiology. This is the opposite to what Wilson et al. (2004) found. In their study, the coralline red algae, *P calcareum* had significantly reduced $F_v/F_m$ when grown with elevated Zn + Pb + Ni + Cu + Cd concentrations. The discrepancy may be explained because Wilson et al. (2004) increased [Pb] and [Cd], whereas in this study there was no evidence of the uptake of Pb nor Cd by *Corallina* spp.. Additionally, Bielmyer et al. (2010) reported mixed results in coral zoothanthellae photophysiological response to increased Cu incorporation. For one species, $F_v/F_m$, ${}_rETR_{max}$, $E_k$, and α all decreased with increasing Cu exposure. However, in another species, $F_v/F_m$ and α decreased, $E_k$ increased, and ${}_rETR_{max}$ remained unchanged. Therefore, demonstrating the response to increased metal assimilation is complicated.

Results from the work presented here suggest that increasing TA had a stronger influence on of *Corallina* spp. NCR and NPP than trace metal content. This is because even though the *Corallina* spp. grown under the Elevated TA + olivine treatment had lower NCR and NPP than the *Corallina* spp. grown under the Elevated TA treatment, the net calcification and NPP rates were still higher than those of the *Corallina* spp. grown under the control treatment. Therefore, increasing TA caused NCR and NPP to increase despite the increased assimilation of trace metals. This is similar to the findings of Couto et al. (2010). Although they did not directly investigate the impact of increased trace metal incorporation on *Corallina* spp. calcification rates, they did find that despite the increased metal uptake, the *Corallina elongate* cell walls were thicker in organisms found near hydrothermal vents compared to the samples found away from the vents. The thicker cell walls were attributed to higher calcification rates caused by the increased temperatures. This suggests that increasing temperature had a stronger impact on *Corallina elongate* calcification rates than the impact of trace metal content had on calcification rates. The results from this study and the study by Couto et al. (2010) suggest that other seawater properties such as TA or temperature, rather than trace metal concentration, more strongly control *Corallina* spp. calcification rates.

However, the highest NCR and NPP were from the Elevated TA treatment with no olivine dissolution, suggesting that trace metal incorporation does have some negative impact on *Corallina* spp. physiology.

The *Corallina* spp. grown under the Elevated TA + Olivine treatments had considerably higher concentrations of [CuO], $[FeO]_{total}$, [NiO], $[Cr_2O_3]$, and [ZnO] compared to the *Corallina* spp. samples cultured under the Elevated TA treatment, therefore it was likely the incorporation of either Cr, Fe, Zn, Cu, or Ni which impacted *Corallina* spp. productivity and calcification rates. This rest of this section will explore in further detail the impact [CuO], $[FeO]_{total}$, [NiO], $[Cr_2O_3]$, and [ZnO] could have had on *Corallina* spp. physiology.

Nickel has been shown to inhibit microbial carbonate precipitation in an experiment by Isik (2008). However, Ni enrichment can also increase coral calcification rates (Biscéré et al. 2017; Biscéré et al. 2018). Ni is needed for the urease enzymes to work efficiently. Urease catalyses urea hydrolysis, releasing ammonia and inorganic carbon, thus increasing pH (Krajewska 2009). This increase in pH could act to stimulate the calcification process (Crossland and Barnes 1974). However, a study by Mallick et al. (1990) found that when combined with iron, urease activity was greatly inhibited in macro algae, *Chlorella vulgaris* (Cu + Fe also inhibited urease activity). The same study also suggests that when Cu + Fe, and Ni + Fe were added simultaneously, there was a stronger toxicity effect than when added sequentially. Olivine dissolution increases numerous trace metals as the same time, and particularly to much larger perturbations of [Ni] than investigated by Biscéré et al. (2017), Biscéré et al. (2018), and Mallick et al. (1990). Although, ICP-OES analysis from this study did not measure the [Ni] in the Elevated TA + Olivine treatment, a similar experiment by Montserrat et al. (2017) found that [Ni] increased by ~3.5 µmol $L^{-1}$, which is approximately 2000 times higher than the "elevated" [Ni] used in both Biscéré et al. (2017) and Biscéré et al. (2018). Therefore, it is still possible that Ni at these high levels and combined with other trace metals such as Cu and Fe, had a toxic rather than beneficial influence on *Corallina* spp. NCR and NPP in this study.

Chromium, iron, zinc, and copper have also been shown to reduce calcification rates. Firstly, Gomes and Asaeda (2013) showed that the calcifying macro-algae, *Nitella pseudoflabellata* grown under elevated [Cr] had ~30% lower calcification rates compared to the samples grown without Cr. Secondly, Ferrier-Pagès et al. (2001) found that the growth rate of the coral, *Stylophora pistillata* decreased when incubated with elevated [Fe] and Matsunaga et al.

(1999) has also shown that increased Fe can inhibit the growth of the red coralline algae, *Lithophyllum spp.* Thirdly, Bautista-Chamizo et al. (2016) showed how increasing [Zn] caused a reduction in the growth and Chl-*a* content of the coccolithophore, *Pleurochysis roscoffensis*. Next, Collén et al. (2003) found that there was a substantial decrease in growth in the red macroalga, *Gracilaria tenuistipitata* when exposed to elevated [Cu]. They explained the reduction in growth due to oxidative stress including the oxidation of lipids and increased oxidative damage to proteins. Finally, Bielmyer et al. (2010) showed that the growth rate of the corals *Acropora cervicornis* and *Pocillopora damicornis* were reduced after five weeks of exposure to increased [Cu]. They also found that CA enzyme activity was also reduced under elevated [Cu]. A reduction in CA activity caused by increased [Cu] could explain why there was a reduction in NCR because CA facilitates the formation of $CO_3^{2-}$ used for mineral carbonate formation. Therefore, it is possible that it was either the incorporation of Cr, Fe, Zn, Cu, Ni, or a combination of all five which resulted in the reduced *Corallina* spp. calcification and primary productivity rates.

## 3.5.3. Implications for enhanced weathering as a carbon dioxide removal approach

Results from the olivine dissolution experiments suggest that due to the precipitation of secondary minerals, the dissolution of olivine may not result in an increase in seawater TA but could still cause certain metal concentrations to increase in seawater. This has important consequences with regards to EW efficiency as a CDR approach and to the response by *Corallina* spp.

### *3.5.3.a. Carbon dioxide removal potential*

For EW to work as a CDR approach, surface seawater $pCO_2$ needs to decrease so that atmospheric $CO_2$ can be taken up by the ocean (see Section 1.4. for more details). Therefore, whether EW causes ocean TA to increase or decrease will control how seawater $pCO_2$ will respond and so how much atmospheric $CO_2$ can be taken up by surface waters. The results from the olivine dissolution experiment show that olivine dissolution does not cause seawater TA to increase and $pCO_2$ to decrease, likely because of the formation of hydrated magnesite as a secondary mineral, and so that the EW of forsterite would not be an effective CDR approach. Mg rich silicates such as forsterite are thought to be one of the best minerals for EW because they have faster weathering reaction times and so do not require energy-intense processing before their dissolution (Schuiling and Krijgsman 2006; Renforth 2012; Meysman

and Montserrat 2017; Renforth and Henderson 2017). However, there are other minerals apart from olivine which could be used, such as wollanstonite or augite (Renforth 2012) and if they do not promote secondary mineral precipitation during dissolution, might turn out to be a better option for EW.

#### *3.5.3.b. Influence on* Corallina *spp. physiology*

These results also show that EW does have some negative impact on *Corallina* spp. NCR and NPP due to trace metal uptake. However, the results also show that increasing TA has a stronger influence on *Corallina* spp. NCR and NPP than trace metal uptake. Therefore, as long as EW causes seawater TA to increase, any potential detrimental impacts could be minimised and EW could still be an effective method for ocean acidification mitigation. However, as discussed in the above section, the results from this study suggest that EW will not cause seawater TA to increase and, in this case, if there is just increased metal uptake, then EW could have a stronger negative impact on *Corallina* spp. calcification and productivity rates.

Furthermore, it is mostly agreed that the algal uptake of metals increases with increasing seawater pH (Darnall et al. 1986; Fourest and Roux 1992; Holan et al. 1993; Ricou et al. 1998; Sheng et al. 2004; Papageorgiou et al. 2006). Therefore, whether EW causes seawater pH to increase or decrease could also influence the response of *Corallina* spp. to olivine dissolution. Seawater pH can impact algal trace metal uptake because algal cell walls contain a lot of carboxyl groups, which can be affected by changes to seawater pH (Matheickal and Yu 1999). Prasher et al. (2004) found that increasing pH from 2-7 greatly increased the uptake of Cu by the red algae, *P. palmata.* The low uptake rates at low pH were explained by the high $H^+$ concentrations which compete for Cu binding sites on the cell surface (Tobin et al. 1984). Further, Peterson et al. (1984) discovered that the toxicity of Cd and Cu uptake by the green algae, *Scenedesmus quadricauda*, increased with increasing pH again as a result of increased competition between $H^+$ and metal cations for cellular binding sites. However, the influence of increased pH at values relevant to EW (~pH 8) were not explored by these studies. A study by Ibrahim (2011) investigated the metal uptake rates over the pH range 2-8 found that the uptake of Co, Cr, Cd, and Pb by *Corallina mediterranea* and other red algae species peaked at pH ~5 and actually decreased when pH increased from 5-8. They explained that this was because of the formation of anionic hydroxide complexes at higher pH levels

decrease the dissolved metal concentration in solution and so competition for active binding sites also decreases.

The results from the olivine dissolution experiments in this present study suggest that if EW causes the precipitation of hydrated magnesite, pH will decrease and so increase the trace metal uptake potential of *Corallina* spp. Therefore, if the incorporation of trace metals into *Corallina* spp. biomass has a negative impact on their physiology, which the results from this study suggest it does, it is important to understand the direction which ocean pH will change due to EW to fully understand the impact increased metal assimilation will have on calcifying marine organisms such as *Corallina* spp. However, the results from the olivine dissolution experiments in this present study suggest that pH will only decrease by ~0.1 pH units and the experiments by Peterson et al. (1984), Prasher et al. (2004), and Ibrahim (2011) investigated much larger changes to pH. Therefore, even if EW causes the precipitation of secondary minerals such as hydrated magnesite, it is unlikely that pH will decrease enough to impact the assimilation rate of trace metals by *Corallina* spp. Similarly, in the olivine dissolution experiment by Montserrat et al. (2017) pH only increased by ~0.1 units before decreasing back to the initial value and Köhler et al. (2010), predicted that in a "strong" EW scenario, pH would increase globally by 0.1 by the year 2100. Therefore, if there is no precipitation of secondary minerals and EW does cause seawater pH to increase, then it is also unlikely there will be any impact on the trace metal uptake rate of *Corallina* spp.

Another important issue to consider is the exposure time of *Corallina* spp. to the trace metals. Experiments by Prasher et al. (2004), Wilson et al. (2004), Ibrahim (2011), and Tonon et al. (2018) all suggest that initially (within the first 10-60 minutes) the uptake rate and toxicity of trace metals increases as exposure time increase but after the first hour, the uptake rate remains stable and algal tolerance to the metals increases. Wilson et al. (2004) suggest that the increase in tolerance with time is due to the absorption of heavy metals onto the wall matrix or some other non-metabolic component of the algae. If this is the case, algae are more likely to be negatively impacted by long-term, constant perturbations rather than one single event. This has important implications for EW because it is likely that for EW to work on the scale needed to address the current climate emergency, then TA will need to be continuously added to the ocean as $CO_2$ continues to be emitted (Ilyina et al. 2013; Feng et al. 2017). The continued addition of silicate minerals to increase TA may not allow enough time between additions for *Corallina* spp. to fully adapt to the increased metal concentrations. Further, if the majority of metal assimilation occurs within the first 60 minutes of exposure, this

suggests that the region where silicate minerals are applied is well mixed so that the increased metal concentrations may be quickly diluted, any negative impacts they could have on algal physiology will be less severe. This may be another advantage to coastal application of silicate minerals rather than open ocean application.

## 3.6. Conclusions and further work

This chapter set out to investigate how olivine dissolution changes seawater chemistry and how these changes then go on to influence *Corallina* spp. physiology. Olivine dissolution did not cause TA, pH, DIC, $\Omega_{Ca}$, and $\Omega_{Ar}$ to increase as expected, but actually caused these parameters to decrease. Although seawater TA did not increase, and so could not be used as evidence that olivine dissolution did occur, there was evidence from the ICP-OES analysis of seawater that there was an increase in [$SiO_2$] which indicates that olivine did dissolve. Further, XRD analysis showed that there was some hydrated magnesite present in the olivine samples taken after the dissolution experiment which suggests that TA decreased because hydrated magnesite was being precipitated out of solution. This has important implications with regards to how well EW works as a CDR approach and so whether olivine dissolution results in the precipitation of secondary minerals is an important question to answer. Unfortunately, because the aim of this work was not to investigate secondary mineral precipitation, the olivine dissolution experiment was not the best design for this purpose. Therefore, to investigate this further, the olivine dissolution experiment should be repeated but using smaller volume of seawater and more olivine sand. This would make it easier to find evidence of secondary mineral precipitates such as clay minerals using XRD analysis. Furthermore, research should focus on the carbonate chemistry response and secondary mineral formation from long-term meso-scale experiments investigating the dissolution of olivine and other silicate minerals to more accurately predict the impact of large-scale coastal EW would on the marine environment.

The other aim of this chapter was to understand the response of *Corallina* spp. to elevated TA from EW of olivine. Results from the *Corallina* spp. culture experiments showed that when grown under the olivine treatment, *Corallina* spp. had higher [CuO], [$FeO]_{total}$, [NiO], [$Cr_2O_3$], and [ZnO] compared to the *Corallina* spp. samples cultured under the other treatments. The results showed that the *Corallina* spp. grown under the elevated TA + olivine treatment had higher NCR and NPP than the *Corallina* spp. grown under the control treatment. This demonstrates that the effect of increasing TA had a stronger influence on

*Corallin*a spp. calcification and productivity rates than the incorporation of trace metals and so EW can be used as an ocean acidification mitigation approach. However, these results also suggest that there may be better AOE methods than EW with regards to biological impact because *Corallina* spp. calcification and productivity rates were lower when exposed to elevated TA and trace metal increase compared to when exposed to elevated TA without trace metal perturbations suggesting that the trace metal impact had detrimental impact on *Corallina* spp. physiology.

This study is one of the first attempts to thoroughly examine the influence of EW on *Corallina* spp. physiology. However, further research is needed to explore how TA and pH will change due to global application of EW and whether increasing or decreasing TA and pH has any influence of the toxicity of trace metal uptake by calcifying species such as *Corallina* spp. Additionally studies should set out to investigate the long-term impact of continuous olivine dissolution compared to a one-off application.

# Chapter 4.

# The impact of increasing ocean alkalinity on the growth and photophysiology of a calcifying strain of *Synechococcus*.

## 4.1 Summary

The previous two Chapters focussed on a sessile, benthic coastal calcifier whereas this and Chapter 5 will now focus on the response of a pelagic coastal calcifying phytoplankton, *Synechococcus* 8806 to elevated TA. In particular, this study aims to explore how elevated TA induced changes to seawater TA affects *Synechococcus* 8806 photophysiology. *Synechococcus* 8806 was cultured under a TA gradient of 10 distinct TA values ranging from ~900-3700 µEq $L^{-1}$. *Synechococcus* 8806 growth rates were monitored over eight days and once the cultures reach exponential growth, fast repetition rate fluorometry was used to assess the overall acclimation to the changing carbonate chemistry. Results show that elevated TA increased *Synechococcus* 8806 growth rates. Further, changes to seawater TA caused significant changes to photophysiology. The relationship between *Synechococcus* 8806 photophysiology and TA was not a simple, linear increase and the results from this study have led to the new hypothesis that the magnitude of changes to $pCO_2$ due to changes in TA result in differing effects to *Synechococcus* 8806 photophysiology. Large decreases to $pCO_2$ appear to cause a reduction in photochemical efficiency whereas smaller changes in $pCO_2$ causes an increase in photochemical efficiency. However, no robust estimates of $pCO_2$ were made and so this hypothesis has not yet been fully tested. Therefore, more work needs to be carried out to better constrain the relationship between increasing TA, decreasing $pCO_2$ ,and *Synechococcus* 8806 photophysiology.

## 4.2 Introduction

As well as increasing seawater $\Omega_{Ca}$, OAE could also alter seawater $pCO_2$. At pH 8.2, the current proportions of $HCO_3^-$, $CO_3^{2-}$ and $CO_{2(aq)}$ which make up seawater DIC are approximately 89%, 10.5% and 0.5% respectively (Doney et al. 2009). Therefore, the majority of ocean DIC is in the form of $HCO_3^-$ and little is in the form of $CO_{2(aq)}$. This means that marine algae have evolved to survive environments with low $CO_{2(aq)}$. For example, marine algae have developed carbon concentrating mechanisms (CCMs) to acclimate to $CO_2$ limitation (Giordano et al. 2005). However, CCMs cannot fully compensate for reduced $CO_{2(aq)}$ (Rost et al. 2006) and phytoplankton growth rates are thought to be affected if $CO_2$ goes below ~100 µatm (Riebesell et al. 1993; Goldman 1999; Hansen 2002; Bach et al. 2011b; Sett et al. 2014). One example of when this could occur is during non-equilibrated OAE where TA is added quickly (for example over days rather than months) to an area of slow air-sea gas exchange, the seawater at the site of addition may not have time to fully equilibrate with the atmosphere and mitigate the perturbation with $CO_2$ in-gassing (see Chapter 1, Table 1.2). Other examples of naturally low $pCO_2$ include coastal areas where carbonate chemistry can fluctuate substantially and low $pCO_2$ waters are possible (Hofmann et al. 2012; Williamson et al. 2014), or during a phytoplankton bloom (Schulz et al. 2013; Engel et al. 2014). In these examples, the low seawater $pCO_2$ could potentially drive primary production into $CO_2$ limitation (Riebesell et al. 1993).

Bloom forming *Synechococcus* are abundant in coastal regions (Partensky et al. 1999; Zwirglmaier et al. 2008; Moisan et al. 2010; Flombaum et al. 2013). Therefore, it is likely that *Synechococcus* could experience low seawater [$CO_{2(aq)}$]. Further, coastal regions are a potential site of OAE addition, which would reduce $CO_2$ even more. This means that coastal, bloom forming *Synechococcus* strains may experience large perturbations in seawater [$CO_{2(aq)}$] under OAE. *Synechococcus* could be particularly sensitive to these potential changes to seawater $CO_2$ because some *Synechococcus* strains possess genes which suggest they have high-affinity $CO_2$ uptake systems (Badger et al. 2006) and is it thought that algal groups which actively use $CO_2$, will be more sensitive to the availability of $CO_2$ (Burkhardt et al. 1999).

Changes to *Synechococcus* biomass and productivity could substantially influence global net primary productivity because *Synechococcus* (along with *Prochlorococcus)* contribute 25%

to net global marine primary productivity (Flombaum et al. 2013). Further, in the past marine cyanobacteria, such as *Synechococcus,* have had a big control on ocean chemistry and are believed to be responsible for the increase in atmospheric oxygen concentrations during the Archaean and Proterozoic Eras (Knoll 2008). Consequently, potential changes to *Synechococcus* growth and productivity from OAE could have a significant impact on the marine environment. Therefore, this chapter aims to explore how the *Synechococcus* productivity is impacted by reduced seawater [$CO_{2(aq)}$] caused by elevating TA. One way to investigate the response of *Synechococcus* productivity is to use fluorescence measurements.

Fluorescence provides information of the "light harvesting" steps of photosynthesis and provides a way of evaluating the efficiency with which absorbed light is used for photosystem II (PSII) photochemistry (Krause and Weis 1991). These "light harvesting" reactions takes place within the photosystems of cyanobacteria thylakoid membranes. The light harvesting complexes absorb the photon's energy, become excited and then decay to the ground state either by transferring this excitation energy to reaction centres within PSII (leading to photosynthesis), heat dissipation, transfer of energy to an adjacent pigment, or emission of a fluorescence photon (Oxborough and Baker 1997a,b). Information on photosynthesis from fluorescence analysis can be determined by assuming that changes in fluorescence yield reflect proportional changes in these four competing de-excitation routes (Campbell et al. 1998). For cyanobacteria, the principal light-harvesting complexes are phycobilisomes, rather than Chlorophyll-*a* (Chl-*a*) which capture light in plants. Once excited, the electrons in the phycobilisomes then move through the electron transport chain. There are multiple interacting and flexible paths of electron flow including both linear flow from the oxidation of water to the formation of NADPH and cyclic pathways around subsections of the transport system (Campbell et al. 1998). Following, these light dependent reactions NADPH is then used in the subsequent dark reactions for carbon metabolism (Suggett et al. 2009). Because these photosynthetic systems in cyanobacteria occur in close proximity to other principal metabolic pathways such as carbon fixation (Campbell et al. 1998), carbon metabolism can strongly influence electron transport in cyanobacteria. There have been several studies which have shown the strong link between electron transport and carbon uptake in cyanobacteria (Ogawa and Inoue 1983; Ogawa et al. 1985; Price et al. 1998). Therefore, fluorescence analysis can also be used as a proxy for carbon fixation and photosynthesis.

One type of fluorescence analysis is fast repetition rate fluorometry (FRRf) which generates fluorescence rise (induction) and reaction centre reopening (relaxation) curves, and can be used to derive photosynthetic parameters related to PSII* (Kolber et al. 1998). These include effective PSII cross section absorbance ($\sigma_{PSII}$ (measured in the dark) or $\sigma_{PSII}$' (measured in the light)), the energy transfer between PSII units (reaction centre connectivity; ρ or ρ'), the rapid and slow kinetic phase lifetimes for PSII reopening (τ1 and τ2, respectively), quantum efficiency of PSII (Y(SPII)), electron transport rate (ETR) (Kolber et al. 1998). FRRf has previously been used to measure the stress response of marine phytoplankton to increased $pCO_2$ in several ocean acidification studies (Hoppe et al. 2015; Hoppe et al. 2017; Trimborn et al. 2017; Hoppe et al. 2018a; Hoppe et al. 2018b; Kvernvik et al. 2020; White et al. 2020). The changes to seawater carbonate chemistry (such as a decrease in $[CO_{2(aq)}]$ from increasing ocean TA, may influence *Synechococcus* photosynthesis and so result in changes to the above photosynthetic parameters. For example, if there was less available inorganic carbon for photosynthesis from OAE, then *Synechococcus* might have slower downstream electron transport resulting in slower reaction centre opening times ($\tau_1$), less light capture to the cross section of PSII ($\sigma_{PSII}$), and fewer connected PSII reaction centres (p') and so reduced photochemical efficiency of PSII (Y(PSII)).

In this chapter, FRRf is used to investigate whether increasing TA and the subsequent changes to carbonate chemistry has any effect on *Synechococcus* photophysiology and overall acclimation to the changing carbonate chemistry. To achieve this, the calcifying cyanobacteria strain, *Synechococcus* 8806 was cultured under an TA gradient and photophysiological state was monitored. It was hypothesised that increasing TA will cause $[CO_{2(aq)}]$ to decrease and so cause:

1. *Synechococcus* 8806 growth rates to decrease.
2. *Synechococcus* 8806 photosynthetic efficiency to decrease therefore decreasing ETR and Y(PSII) through changes to $\sigma_{PSII}$' and ρ' and $\tau_1$.

# 4.3. Methodology

## 4.3.1. Experimental set up

To investigate the photophysiological response to increasing TA, a calcifying strain of cyanobacteria, *Synechococcus* 8806 was cultured under an TA gradient of 10 distinct TA values. Stock cultures of *Synechococcus* 8806 (ordered from Collection of Cyanobacteria;

Department of Microbiology, Biological Resource Center of the Institut Pasteur) were cultured at Mount Allison University, Sackville, Canada, where all measurements were performed. The cultures were grown at 20 °C and at a light intensity of 200 μmol photons $m^{-2}$ $s^{-1}$, with a light/dark cycle of 12 h:12 h. The cultures were grown in ASN3+ media (Rippka et al. 1979) with adjusted salinity in 24 well plates (see Appendix D for more for details) and each well contained 0.5 mL of culture and 2 mL of media.

The TA of the growth media were manipulated by adding different volumes of sterile 0.25M $Na_2CO_3$ solution. Temperature and pH were measured using a combination temperature/pH electrode (Mettler Toledo™, U.K.). It was not possible to measure TA at the laboratory at Mount Allison University and so TA (and other carbonate chemistry parameters including DIC, $[CO_{2(aq)}$, and $CaCO_3$ saturation states) of each step of the TA gradient was calculated using was calculated using PHREEQC v2 (using the Phreeqc.dat database, (Parkhurst and Appelo 1999) from the measured pH, temperature, and media elemental concentrations. The calculated TA ranged from ~900 - 4000 μEq $L^{-1}$ and Figure 4.1 and Table 4.1 show the associated carbonate chemistry parameters for each well.

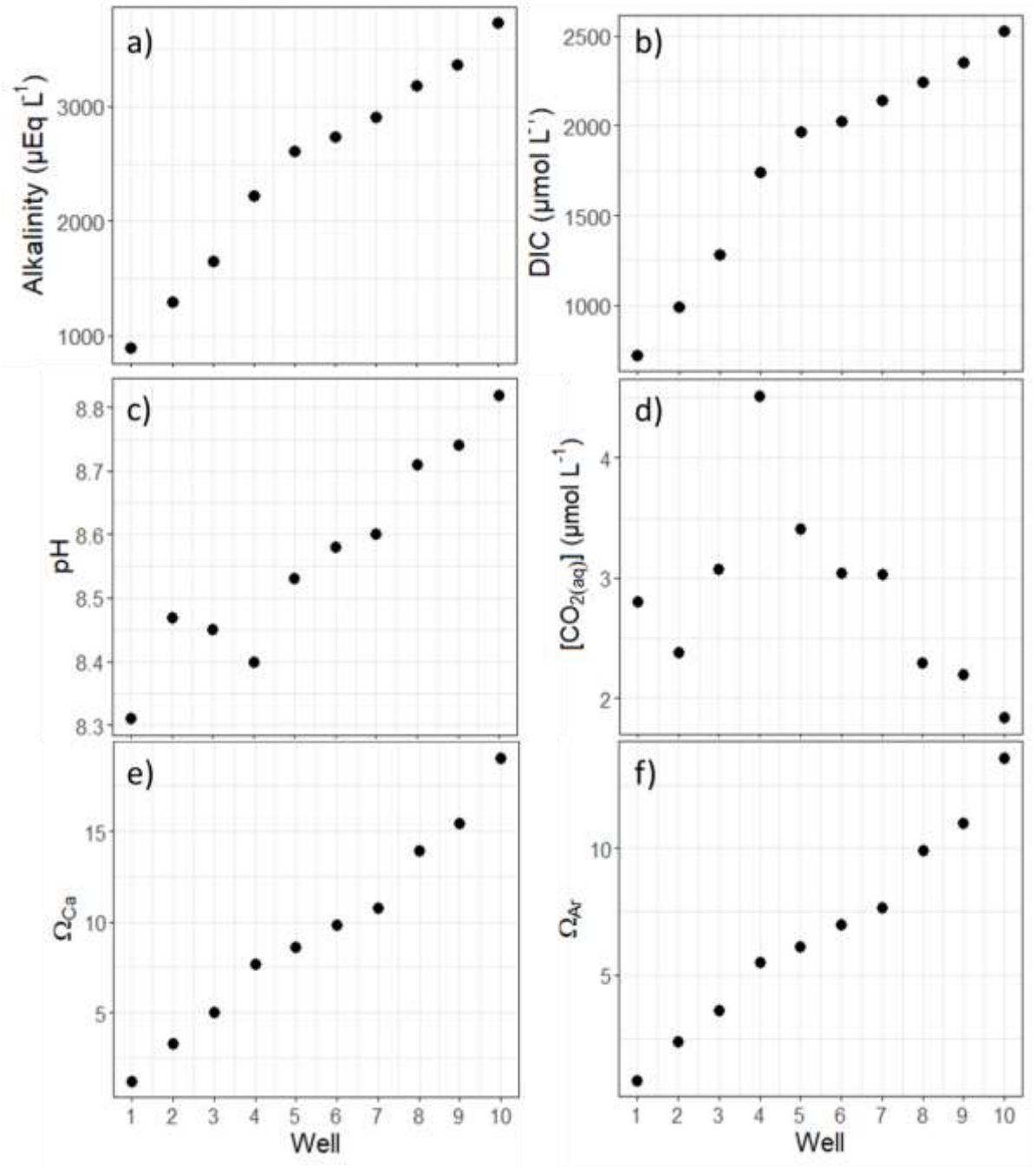


*Figure 4.1. Graphical representation of each of the carbonate chemistry parameters from the TA growth gradient including: a- TA (total alkalinity, µEq L⁻ ), b- DIC (dissolved inorganic carbon, µmol L⁻¹), c- pH, d-[$CO_{2(aq)}$] (dissolved aqueous carbon dioxide concentration, µmol L⁻¹), e-$\Omega_{Ca}$ (calcite saturation state), and f-$\Omega_{Ar}$ (aragonite saturation state).*

*Table 4.1 Description of TA growth gradient carbonate chemistry parameters: TA (total alkalinity, µEq $L^{-1}$ ), DIC (dissolved inorganic carbon, µmol $L^{-1}$), pH, [$CO_{2(aq)}$] (dissolved aqueous carbon dioxide concentration, µmol $L^{-1}$), $\Omega_{Ca}$ (calcite saturation state), and $\Omega_{Ar}$ (aragonite saturation state).*

| Well | TA* µEq $L^{-1}$ | DIC* µmol $L^{-1}$ | pH | [$CO_{2(aq)}$]* µmol $L^{-1}$ | $pCO_2$* µatm | $\Omega_{Ca}$* | $\Omega_{Ar}$* |
|---|---|---|---|---|---|---|---|
| | *± 209* | *± 240* | *± 0.674* | ± 0.30 | *± 12* | *± 0.19* | *± 0.17* |
| 1 | 893 | 988.4 | 8.31 | 2.80759 | 69 | 1.22 | 0.87 |
| 2 | 1291 | 1279.63 | 8.47 | 2.38425 | 63.1 | 3.31 | 2.37 |
| 3 | 1653 | 1743.73 | 8.45 | 3.07894 | 88.5 | 5.04 | 3.6 |
| 4 | 2217 | 1968 | 8.4 | 4.5167 | 141.9 | 7.7 | 5.51 |
| 5 | 2610 | 2026 | 8.53 | 3.41093 | 112.2 | 8.61 | 6.13 |
| 6 | 2738 | 2140 | 8.58 | 3.04343 | 100.4 | 9.8 | 6.98 |
| 7 | 2906 | 2240 | 8.6 | 3.03459 | 100.2 | 10.76 | 7.66 |
| 8 | 3180 | 2351 | 8.71 | 2.29248 | 76.2 | 13.9 | 9.9 |
| 9 | 3370 | 2525 | 8.74 | 2.19602 | 73.1 | 15.41 | 10.97 |
| 10 | 3730 | 2810 | 8.82 | 1.83874 | 61.4 | 19.05 | 13.56 |

* calculated from PHREEQC v2

The DIC values calculated from TA and pH using PHREEQC cannot be correct as the change in DIC with increasing TA is not theoretically possible. According to Equation 33, the proportional change of DIC is about ~0.8 that of TA under average seawater conditions ($pCO_2$ = 400 ppmv, S = 35%, and T = 17°C; Renforth and Henderson, 2017). Whereas the change in DIC ranged from 0.15-1.28 of the change in TA (Table 4.1). This is likely due to errors associated with pH measurements. Unlike Chapters 2,3, and 5, pH measurements at Mount Allison University were not calibrated using TRIS/AMPD buffers, which results in a greater error of around 0.05 pH units. The large error arises because of the complications that arise from seawater's ionic content.

When the temperature, salinity, and pH values from this experiment are used in Equation 33, the change in DIC should be ~0.7 that of TA. Therefore, the starting DIC value (870 µmol $L^{-1}$), the change in TA (µEq $L^{-1}$) between each well, and the measured temperature and salinity were used to estimate the "theoretical change" DIC and then CO2SYS was used to estimate the other carbonate chemistry parameters. Figure 4.2 shows the new carbonate chemistry parameters for each well. Although these values are better than the previously calculated values, it should be noted the error associated with each value is great and so great care should be taken when interpretating these results. Therefore, the focus of interpretation will be on TA, the most robust parameter.

$$\frac{\Delta DIC}{\Delta TA} = n = (S * 10^{-3.009} + 10^{-1.519}) \ln(pCO_2) - (S * 10^{-2.100}) - (T * pCO_2)(S * 10^{-7.501} - 10^{-5.598}) - (T * 10^{-2.337}) + 10^{-0.102} \quad \text{(Equation 33)}$$

Where S= salinity (in %), T= temperature (in °C) and $pCO_2$ is the partial pressure of $CO_2$ in equilibrium with the solution (in µatm).

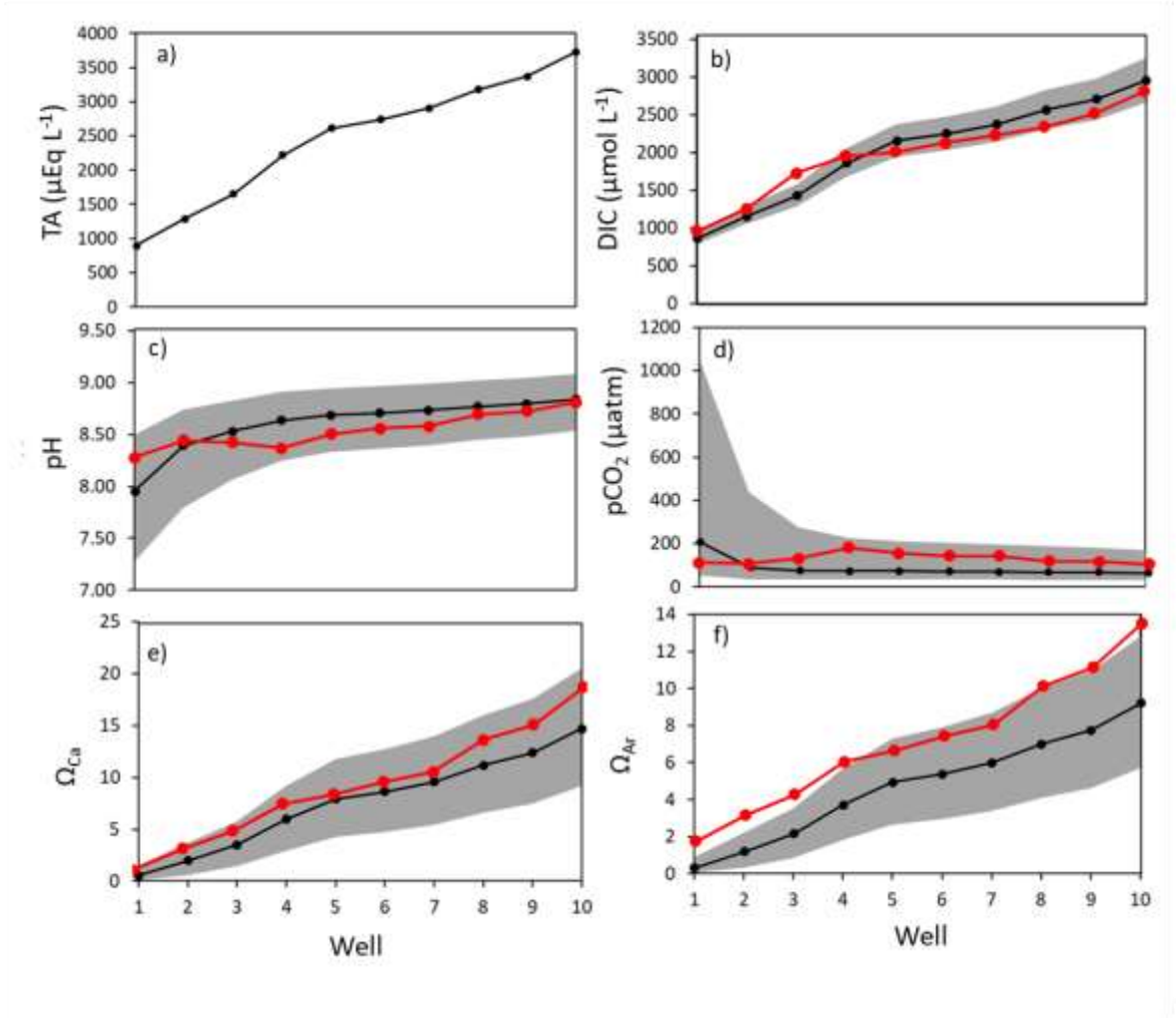


*Figure 4.2. Graphical representation of each of the carbonate chemistry parameters estimated from calculated TA and theoretical DIC: a- TA (total alkalinity, µEq $L^{-1}$), b- DIC (dissolved inorganic carbon, µmol $L^{-1}$), c- pH, d-[$CO_{2(aq)}$] (dissolved aqueous carbon dioxide concentration, µmol $L^{-1}$), e-$\Omega_{Ca}$ (calcite saturation state), and f-$\Omega_{Ar}$ (aragonite saturation state). For inset b, the grey shaded region represents the 9% error associated with the calculated theoretical DIC and for inset c-f, the grey shaded region represents the maximum and minimum carbonate chemistry parameters calculated with DIC +/- the 9% error. The red line shows the PHREEQC estimated values from Figure 4.1.*

### 4.3.2. Growth rate

The growth of the cultures was monitored by measuring the optical density at λ = 680 nm ($OD_{680}$) using a plate spectrofluorometer (SpectraMax Gemini EM, Molecular Devices, Sunnyvale, USA). The growth rate of the cells was calculated from the $OD_{680}$ during the exponential growth phase using Equation 34.

$$\mu = \frac{\ln(Chl_x) - \ln(Chl_0)}{t_x - t_0} \quad \text{(Equation 34)}$$

where $Chl_x$ is the $OD_{680}$ value at time $t_x$ (in days) and $Chl_0$ is the $OD_{680}$ value at time $t_0$ (in days).

### 4.3.3. Photophsyiology

When cultures reached mid-log phased of exponential growth, 1.5 ml aliquots were removed from the wells for chlorophyll fluorescence induction measurements. Samples were placed in a 2 ml cuvette and then dark-adapted for ~ 1 minute. A rapid light curve analysis following Perkins et al. (2006) was performed by subjecting each sample to a series of 30 s exposures of increasing actinic light levels (0 to 400 μmol photons $m^{-2}$ $s^{-1}$). An FRRf induction curve was applied to the sample using a Photon Systems Instruments FL3500 fluorometer system (Brno, Czech Republic). To induce the FRRf induction curve, a train of 40 blue (455 nm) flashlets with a duration of 1.2 μs was applied to the sample at the end of each 30 s exposure (Kolber et al. 1998). Each flashlet was separated by a 1.0 μs darkness interval. The purpose of the 40 blue flashlets was to photochemically close PSII. Therefore, the flashlet intensity was selected to be high enough to saturate the fluorescence rise within around 30 of 40 flashlets (Laney 2003; Laney and Letelier 2008). An FRRf induction curve was induced for the *Synechococcus* 8806 cells grown at every initial TA of each pH buffer treatment.

Each FRRf turnover involved 2 stages: an induction curve (fluorescence rise) and a relaxation curve (reaction centre reopening) as shown by Figure 4.3. From the induction curve, minimal fluorescence ($F_0$), maximal fluorescence ($F_M$), effective absorption cross section for PSII photochemistry (σPSII), and coefficient of excitonic connectivity (ρ) was estimated (Table 4.2, Kolber et al. 1998). From the relaxation curve the rapid kinetic phase lifetimes for PSII reopening was estimated (τ1; Kolber et al. 1998).

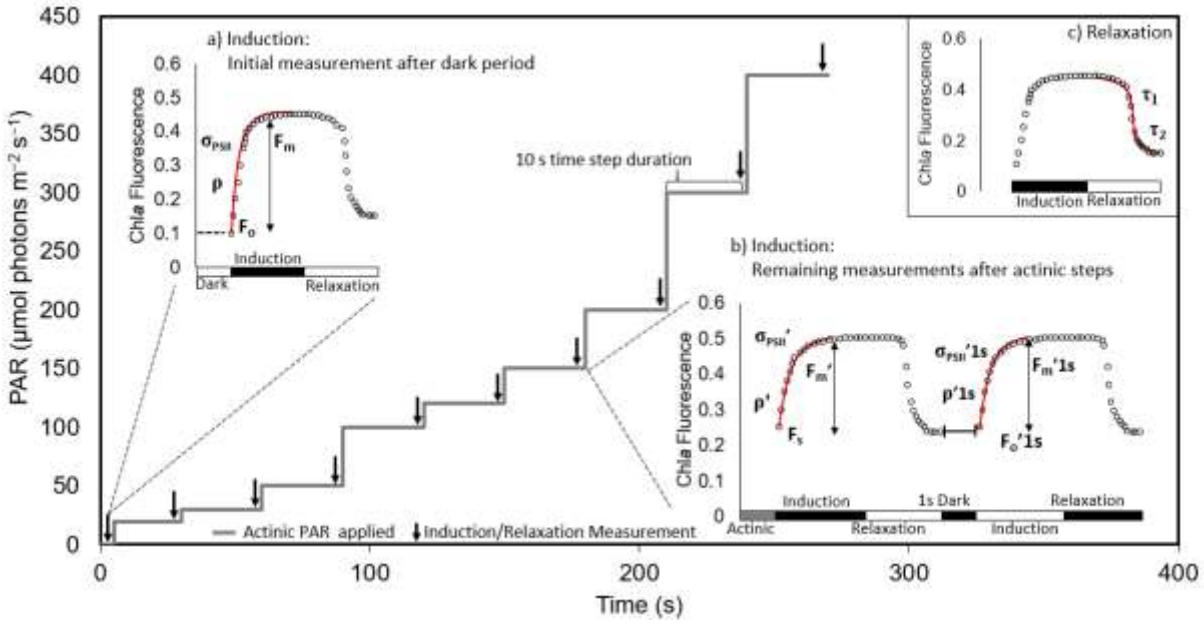


*Figure 4.3. Schematic of sequential light curve treatment and measuring protocol. Adapted from Perkins et al. 2018. The Y axis plots the levels of a sequence of light levels applied for 10 s each. The arrowheads show applications of repeated Fast Repetition and Relaxation chlorophyll fluorescence (FRRf) measurements and are demonstrated in annotated inset graphs (a,b,c). Inset (a) demonstrates the induction curve parameters derived from samples measured in the dark from the initial FRRf measurement performed following 1 minute dark adaptation ($F_0$, $F_M$, $\sigma_{PSII}$, $\rho$) Inset (b) demonstrates the induction curve parameters from all subsequent measurements performed following 10 s at respective light levels ($F_s$, $F_M$', $\sigma_{PSII}$', $\rho$') and immediately after exposure to the preceding light step the induction curve following 1 s of dark to allow re-opening of Photosystem II ($F_o$'1s, $F_M$'1s, $\sigma_{PSII}$'1s, $\rho$'1s). Inset (c) demonstrates the relaxation curve parameters ($\tau_1$ and $\tau_2$). Table 4.2. gives the definitions of all parameters mentioned.*

The initial FRRf measurement was performed in the dark following approximately 1 minute of dark adaptation of samples. The subsequent measurements were then performed following 10 s at respective increasing light levels. For each subsequent measurement, the fluorescence induction and relaxation measurements were applied both in the presence of background actinic light and following 1 s darkness immediately after exposure to the preceding light step, which allowed the reopening of photosystem II. Therefore, there are slightly different definitions for each of the four induction parameters. In the dark, $F_0$, $F_M$, $\sigma_{PSII}$, and $\rho$ were determined; under actinic light $F_S$, $F_M$', $\sigma$PSII′, and $\rho'$ were determined; and following 1s of darkness immediately after actinic light $F_0'$1s, $F_M'$1s, PSII′1s, and $\rho'$1s were determined. From these the quantum efficiency of PSII (YPSII and the electron transport rate around PSII (ETR; mol $e^-$ [mol chl a] $^{-1}$ $min^{-1}$) were calculated (Table 4.2).

*Table 4.2. FRRf abbreviations, definitions, equations and units.*

| Parameter | Equation | Definition | Units | Reference |
|---|---|---|---|---|
| $F_0$ | | Minimal fluorescence with PSII open | No units | van Kooten and Snel 1990 |
| $F_M$ | | Maximal fluorescence with PSII closed | No units | van Kooten and Snel 1990 |
| $F_S$ | | Fluorescence at an excitation level | No units | van Kooten and Snel 1990 |
| $F_M$’ | | Maximal fluorescence with PSII closed at an excitation level | No units | van Kooten and Snel 1990 |
| $F_M$’1s | | Maximal fluorescence with PSII closed 1 s after excitation | No units | Murphy et al. 2016 |
| $F_0$’ | $F_0/\{(F_M-F_0)/F_M + F_0/F_M'1s\}$ | Minimal fluorescence with PSII open, estimated for cells under excitation, excluding cumulative influence of photoinactivation. | No units | Oxborough and Baker 1997; Ware et al. 2015 |
| $F_0$’1s | | Minimal fluorescence with PSII open 1 s after excitation | No units | Murphy et al. 2016 |
| σPSII | | Effective absorption cross section for PSII photochemistry | $Å^2$ $PSII^{-1}$ | Kolber et al. 1998 |
| ρ | | Coefficient of excitonic connectivity | | Kolber et al. 1998 |
| σPSII’ | | Effective absorption cross section, for PSII photochemistry under excitation | $Å^2$ $PSII^{-1}$ | Kolber et al. 1998 |
| ρ’ | | Coefficient of excitonic connectivity under excitation | No units | Kolber et al. 1998 |

| | | | | |
|---|---|---|---|---|
| σPSII'1s | | Effective absorption cross section for PSII photochemistry 1 s after excitation | $Å^2$ $PSII^{-1}$ | Kolber et al. 1998 |
| ρ'1s | | Coefficient of excitonic connectivity 1 s after excitation | No units | Kolber et al. 1998 |
| τ1 | | Rapid kinetic phase lifetime for PSII reopening | μs | Kolber et al. 1998 |
| Y(PSII) | $(F_M'–F_S)/F_M'$ | Quantum efficiency of PSII | No units | Perkins et al. 2018 |
| ETR | $PAR * a_{PSII} *$ σPSII $*$ $(6x10^{-4})$ | Electron transport rate | mol $e^-$ [mol chl a] $^{-1}$ $min^{-1}$ | Sugget et al. 2009 |
| aPSII | | Chl-*a* specific rate of light absorption by PSII (set to 0.002) | $m^2$ [mol chl a]$^{-1}$ | Sugget et al. 2009 |

There was a strong correlation between the FRRf induction parameters applied under actinic light ($F_S$, $F_M$', σPSII′, and ρ′) and following 1 s of darkness ($F_0'$1s, $F_M'$1s, σPSII′1s, ρ′1s). Because of this and because interpretations of the 1 s re-opening FRRf curve fitting is complicated by rapid, and differential, changes in photophysiology upon the transition to darkness (Xu et al. 2018), only parameters measured under actinic light were considered from this point.

The FRRf measurements were performed on culture samples from each step of the TA gradient (10 measurements total) as well as replicates on certain samples to calculate standard error. To allow for better comparison between initial alkalinities and buffer treatment, the maximum Y(PSII) ($Y(PSII)_{max}$), $\sigma_{PSII}$' ($\sigma_{PSII}'_{max}$), ρ' ($\rho'_{max}$), and $\tau_1$($\tau_{1\ max}$) were calculated for all initial alkalinities of each buffer treatment. Because the *Synechococcus* 8806 ETR was still increasing by the end of the light curve, maximum ETR was not calculated. Instead, the

coefficient of light use efficiency (α) was estimated using curve fitting following rapid light curve fitting from Eilers and Peeters (1988).

### 4.3.4. Data analysis

The error quoted is standard error (∓S.E.) in text, figures or tables unless otherwise stated. All statistical analyses were performed using R v.4.0.1 (R Core Team, 2019). For the calculated growth rates (μ) and FRRf parameters ($\alpha$, $Y(PSII)_{max}$, $\sigma_{PSII}'_{max}$, $\rho'_{max}$, and $\tau_{1\ max}$) the standard error was calculated from five repeated measurements using the same sample (TA= 2217 μEq $L^{-1}$). Regressions analyses (GLMs) were preformed to determine any significant relationships between the μ and the only robust carbonate chemistry parameter, TA, and the FRRf parameters ($\alpha$, $Y(PSII)_{max}$, $\sigma_{PSII}'_{max}$, $\rho'_{max}$, and $\tau_{1\ max}$). Regressions analyses were also preformed to determine any significant relationships between the FRRf parameters ($\alpha$, $Y(PSII)_{max}$, $\sigma_{PSII}'_{max}$, $\rho'_{max}$, and $\tau_{1\ max}$) and only robust carbonate chemistry parameter, TA. The Relationships were deemed significant if $p < 0.05$.

## 4.4. Results

### 4.4.1 Carbonate Chemistry

From well 1-10, there is a steady increase in TA. From well 1-5, there is a bigger rate of change in TA (average increase of 30%) compared to the more gradual increase from well 6-10 (average increase of 10%). Even when error is taken into account, Figure 4.2 shows that from well 1-2, there is a substantial decrease in pH and $pCO_2$ and then from well 2-10, the change in pH/$pCO_2$ is much more gradual.

### 4.4.2 Culture growth

For *Synechococcus* 8806 growth curves see Appendix E. As TA increased, *Synechococcus* 8806 growth rate (μ, $hr^{-1}$) increased (Table 4.3). The *Synechococcus* 8806 cells grown under the highest TA (3730 μEq $L^{-1}$) had a growth rate of 0.015 $hr^{-1}$ compared to only (from 0.005 $hr^{-1}$ when cultured at the lowest TA (893 μEq $L^{-1}$). Regression analysis determined that there was a statistically significant positive linear relationship between *Synechococcus* 8806 μ and TA ($R^2 = 0.45$, $p < 0.05$; Figure 4.4 a).

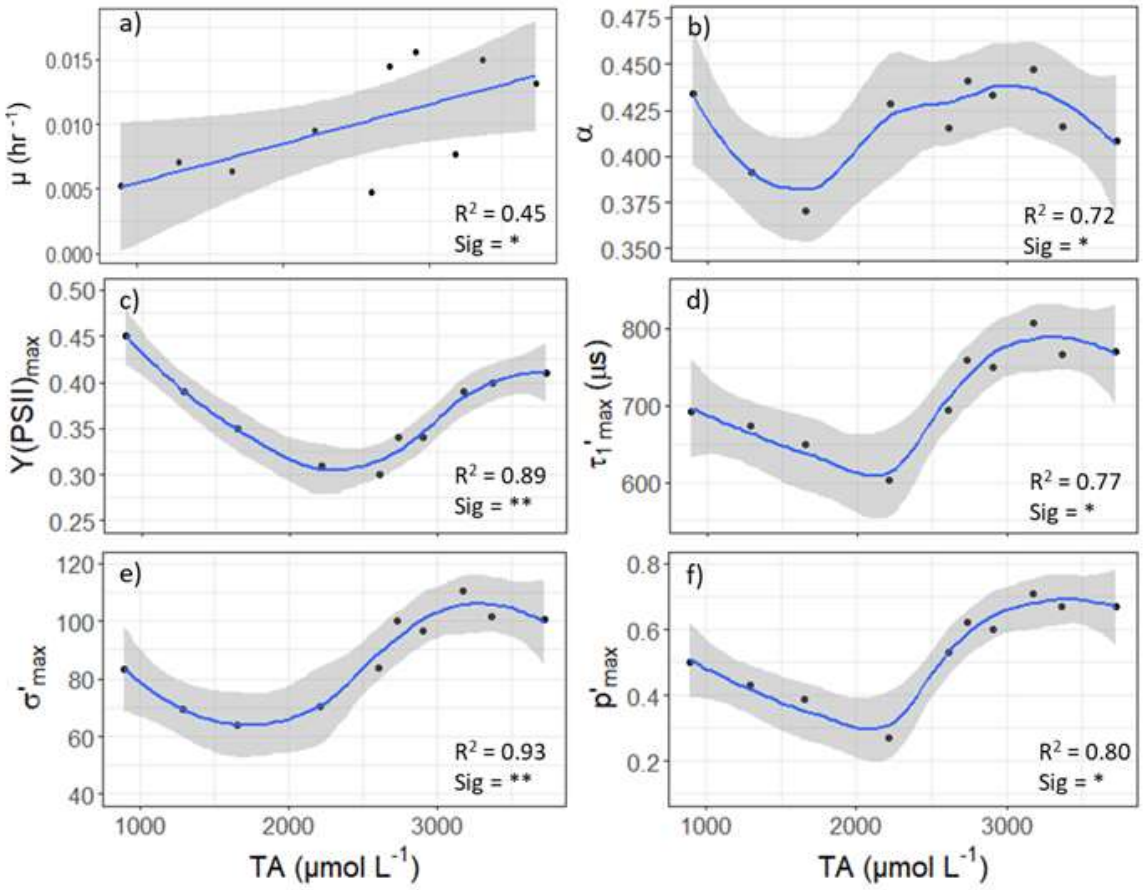


*Figure 4.4. Results from linear regression analysis between Synechococcus 8806 growth rate (μ, $hr^{-1}$) and photophysiology (α, $Y(PSII)_{max}$, $\sigma_{PSII}'_{max}$, $\rho'_{max}$, $\tau1_{max}$,) and TA (total alkalinity, μEq $L^{-1}$). Shaded grey area represents 95% confidence interval. Significant codes: <0.05: *, <0.005: **,<0.001: ***, ns: not significant.*

## 4.4.3. Photophysiology

As TA increased from 893 to 2217 μEq $L^{-1}$ (well 1-4) all five photophysiological parameters ($Y(PSII)_{max}$, $\sigma_{PSII}'_{max}$, $\rho'_{max}$,, and $\tau1_{max}$) decreased. Then as TA increased again from 2610 to 3180 μEq $L^{-1}$ (well 6-8) all five photophysiological parameters ($Y(PSII)_{max}$, $\sigma_{PSII}'_{max}$, $\rho'_{max}$,, and $\tau1_{max}$) increased before either plateauing ($Y(PSII)_{max}$) or slightly decreasing as TA increased to 3730 μEq $L^{-1}$ (well 9-10). Regression analysis revealed that the relationship between the *Synechococcus* 8806 photophysiology parameters and TA was nonlinear and that a cubic polynomial regression model best described the relationship. Figure 4.4 b-e shows the change in all five photophysiology parameters (α, $Y(PSII)_{max}$, $\sigma_{PSII}'_{max}$, $\rho'_{max}$,, and $\tau1_{max}$ ) with increasing TA. There was no statistically significant relationship between

*Synechococcus* 8806 μ and the photophysiological parameters (α, $Y(PSII)_{max}$, $\sigma_{PSII}'_{max}$, $\rho'_{max}$, and $\tau 1_{max}$; Table 4.4, Figure 4.5c).

*Table 4.3. Average ± S.E. Synechococcus 8806 physiology parameters for each step of the TA growth gradient. Parameters include growth rate (μ, $hr^{-1}$), photochemical efficiency of PSII ($Y(PSII)_{max}$), maximum light use efficiency (α), light capture to the cross section of PSII ($\sigma PSII'_{max}$), PSII reaction centres connectivity ($p'_{max}$), and reaction centre opening times ($\tau 1_{max}$).*

| Well | μ ($hr^{-1}$) | $Y(PSII)_{max}$ | *α* | $\sigma'_{max}$ | $\rho'_{max}$ | $\tau_{1\ max}$ (μs) |
|---|---|---|---|---|---|---|
| | *±0.0003* | *±0.0133* | *±0.0184* | *±2.33* | *±0.0064* | *±14* |
| 1 | 0.0052 | 0.45 | 0.434261 | 83.4 | 0.50 | 692 |
| 2 | 0.0064 | 0.39 | 0.391343 | 69.6 | 0.43 | 673 |
| 3 | 0.0071 | 0.35 | 0.370124 | 64.2 | 0.39 | 649 |
| 4 | 0.0095 | 0.31 | 0.428668 | 70.4 | 0.27 | 603 |
| 5 | 0.0155 | 0.30 | 0.415372 | 83.8 | 0.53 | 693 |
| 6 | 0.0047 | 0.34 | 0.441166 | 100.2 | 0.62 | 759 |
| 7 | 0.0144 | 0.34 | 0.433219 | 96.6 | 0.60 | 750 |
| 8 | 0.0131 | 0.39 | 0.447222 | 110.3 | 0.71 | 807 |
| 9 | 0.0077 | 0.40 | 0.416185 | 101.4 | 0.67 | 767 |
| 10 | 0.0150 | 0.41 | 0.408701 | 100.4 | 0.67 | 770 |

*Table 4.4. Results from regression analysis between Synechococcus 8806 growth rate (μ, $hr^{-1}$) and photophysiology (α, $Y(PSII)_{max}$, $\sigma_{PSII}'_{max}$, $\rho'_{max}$, and $\tau 1_{max}$) and TA (total alkalinity, μEq $L^{-1}$). Significant codes: <0.05: *, <0.005: **,<0.001: ***.*

| x | y | Relationship | *n* | $R^2$ | F | Sig |
|---|---|---|---|---|---|---|
| TA | μ | Linear | 10 | 0.45 | 6.327 | * |
| | $Y(PSII)_{max}$ | Cubic polynomial | 10 | 0.89 | 15.74 | ** |
| | α | Cubic polynomial | 10 | 0.72 | 5.23 | * |
| | $\tau_{1max}$ | Cubic polynomial | 10 | 0.77 | 6.69 | * |
| | $\sigma'_{max}$ | Cubic polynomial | 10 | 0.93 | 24.68 | *** |
| | $\rho 1_{max}$ | Cubic polynomial | 10 | 0.80 | 8.07 | * |
| μ | $Y(PSII)_{max}$ | Linear | 10 | 0.087 | 0.765 | ns |
| | α | Linear | 10 | 0.126 | 1.156 | ns |
| | $\tau_{1max}$ | Linear | 10 | 0.095 | 0.836 | ns |
| | $\sigma'_{max}$ | Linear | 10 | 0.021 | 0.171 | ns |
| | $\rho 1_{max}$ | Linear | 10 | 0.021 | 1.021 | ns |

## 4.5. Discussion

The main finding from this study is that increasing TA resulted in a linear increase in *Synechococcus* 8806 growth rates (μ, $hr^{-1}$) but a nonlinear increase in the photophysiological parameters. Although the increase was not linear, *Synechococcus* 8806 cells cultured under elevated TA, had lower values of α and $Y(PSII)_{max}$ than those cultured under lower TA. Therefore, the hypotheses that increasing TA will cause *Synechococcus* 8806 growth rates to decrease were rejected and the hypothesis that increasing TA will cause *Synechococcus* 8806 photosynthetic efficiency to decrease was accepted. The next section will address the response of *Synechococcus* 8806 growth to increasing TA. Then, Section 4.4.2 will explain how *Synechococcus* 8806 photophysiology was influenced by changes to TA.

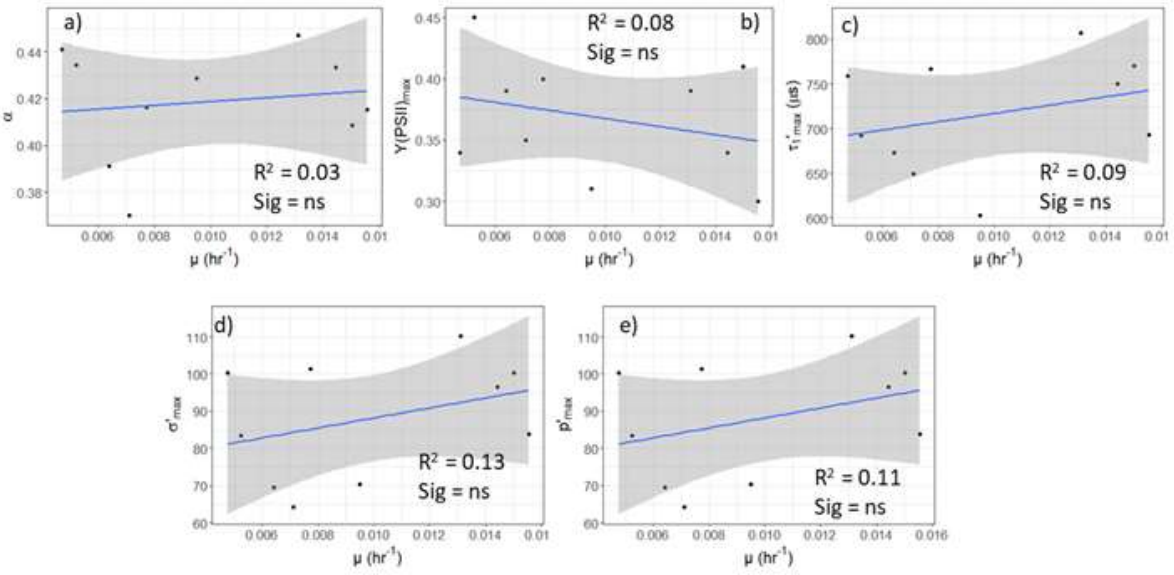


*Figure 4.5. Results from regression analysis between Synechococcus 8806 growth rate (μ, $hr^{-1}$) and photophysiology (α, $Y(PSII)_{max}$, $\sigma_{PSII}'_{max}$, $\rho'_{max}$, $\tau 1_{max}$). Significant codes: ns: not significant, < 0.05: *.*

## 4.5.1. Culture growth with increasing total alkalinity

It was hypothesised that increasing TA and so decreasing [$CO_2$(aq)] would cause *Synechococcus* 8806 growth rates (μ, $hr^{-1}$) to decrease. However, an increase in ~2500 μEq $L^{-1}$ resulted in *Synechococcus* 8806 μ to more than double (from 0.005 $hr^{-1}$ at ~900 μEq $L^{-1}$ to 0.015 $hr^{-1}$ ~3400 μEq $L^{-1}$) and so this hypothesis was rejected. Although the other carbonate chemistry parameters have also been calculated, due to the potential large error associated with them, the focus of interpretation of the results will be TA, the most robust parameter. Therefore, these results from this study do not conclusively show that the changes to *Synechococcus* 8806 growth rates were due to changes in [$CO_2$(aq)].

A similar result to this study was found in a study by Lee et al. (2004) and Lee et al. (2006) where *Synechococcus* 8806 cell density increased as TA increased. As TA increased, [$HCO_3^-$] will increase (and the $CaCO_3$ saturation states ($\Omega_{Ca}$ and $\Omega_{Ar}$)) as shown by Figure 4.2. Because *Synechococcus* 8806 is a calcifying strain of cyanobacteria, it is not surprising that growth rates increased with increasing TA. Elevated [$HCO_3^-$] conditions are more energetically favourable for $CaCO_3$ precipitation (or calcification). Further, it is widely believed there is a strong link between cyanobacteria calcification and growth rates (Riding, 2006, 2009) During photosynthesis, the uptake of inorganic carbon can raise the pH adjacent to the cyanobacteria cells, promoting $CaCO_3$ precipitation. During calcification, $pCO_2$ is increased around the cell, therefore acting as a carbon concentrating mechanism (CCM) for

photosynthesis (Riding 2006). The relationship between photosynthesis and calcification in *Synechococcus* 8806 is discussed further in Chapter 5. Although no evidence was specifically gathered to assess *Synechococcus* 8806 calcification in this study (the focus here was photophysiology), the work in Chapter 5, found a strong relationship between $\Omega_{Ca}$ and *Synechococcus* 8806 calcification rate. Further, there is considerable literature which states that both DIC and $\Omega_{Ca}$ are key external influencers on cyanobacterial calcification (Kempe (Merz 1992; Kempe and Kazmierczak 1994; Lee et al. 2004; Riding and Liang 2005; Lee et al. 2006; Riding 2006; Riding 2009). Therefore, it appears that the increase in TA caused an increase in calcification rates and in turn resulted in an increase in *Synechococcus* 8806 growth.

### 4.5.2. Influence of increasing TA on photophysiology

The results from this chapter show that the relationship between *Synechococcus* 8806 photophysiology and TA is not a simple, linear relationship but was best described by a cubic polynomial regression (Table 4.4). Increasing TA resulted an overall slight decrease in $Y(PSII)_{max}$ and $\alpha$ by (9% and 6% respectively) and an overall increase in $\sigma_{PSII}'_{max}$, and $p'_{max.}$ and $\tau 1_{max}$ (by 20%, 34%, and 11% respectively). Therefore, the hypothesis that increasing TA would decrease *Synechococcus* 8806 photosynthetic efficiency can be accepted. However, because the errors associated with the calculated carbonate chemistry parameters are too large, the results from this study do not conclusively show that the changes to *Synechococcus* 8806 photophysiology from increasing TA is due changes in $[CO_2(aq)]$.

As TA increased from 893 to 2217 µEq $L^{-1}$, all five photophysiological parameters ($\alpha$, $Y(PSII)_{max}$, $\sigma_{PSII}'_{max}$, $\rho'_{max,}$, and $\tau 1_{max}$) decreased but then as TA continued to increase again to 3180 µEq $L^{-1}$, all five photophysiological parameters started to increase before plateauing or slighlt decreasing as TA increased to 3730 µEq $L^{-1}$. One of the main differences between wells 1-4 and 5-10 is the rate of change in increasing TA. Wells 1-4 saw a much greater increase in TA compared to the increase from wells 5-10. This is reflected in the change in theoretical pH and $pCO_2$ values (Figure 4.2). Even when the large error is taken into consideration, there a substantially larger decrease in $pCO_2$ and pH between wells 1-4 compared to the decreased between wells 5-10. Therefore, this non-linear increase in TA is the most likely cause for the non-linear change in photophysiology.

From well 1-4, the decrease in *Synechococcus* 8806 $\alpha$, $Y(PSII)_{max}$, $\sigma_{PSII}'_{max}$, $\rho'_{max,}$, and $\tau 1_{max}$ is most likely due to the large increases in TA promoting a substantial decrease in media

$CO_{2(aq)}$, potentially causing photochemical efficiency to decrease. Whereas, from well 5-10, the change in $pCO_2$ appears to be much less and so the increase in *Synechococcus* 8806 photochemical efficiency. Without robust estimates of $pCO_2$, these results cannot conclusively show what caused this decrease in photochemical efficiency. However, it is hypothesised that this is due to the increase in TA and $[HCO_3^-]$ promoting an increase in *Synechococcus* 8806 calcification rates instead. This in turn would increase local $[CO_2(aq)]$ (Schmittner et al. 2008) and so promote increased rates of photosynthesis causing the increase $\alpha$ $Y(PSII)_{max}$, $\sigma_{PSII}'_{max}$, $\rho'_{max}$. The next part of this section will outline a possible explanation of how this could occur.

Cyanobacteria are well known to have efficient CCMs (Kaplan et al. 1980; Ogawa and Inoue 1983; Kaplan and Reinhold 1999; Badger and Spalding 2000). Although they can use both $HCO_3^-$ and $CO_2(aq)$ for photosynthesis (Volokita et al. 1984; Miller et al. 1990,1991; Badger and Price 2003; Badger et al. 2006), because *Synechococcus* possess *Ndh* genes this means they can actively uptake $CO_2$ and are often described as having a high affinity for $CO_2$ (Badger et al. 2006). This is in contrast to *Prochlorococcus* who do not possess these genes and so cannot actively uptake $CO_2$ (Badger et al. 2006). Because *Synechococcus* can actively uptake $CO_2$ and readily use $CO_2(aq)$ as a carbon source even at high pH values (Klughammer et al. 1999), they can thrive in both high and low $[CO_2(aq)]$ environments. However, because CCMs are an energy intensive process, *Synechococcus* preferentially uptake $CO_2$. Further, it is also thought that *Synechococcus* can more quickly uptake $CO_2$ as opposed to $HCO_3^-$ (Miyachi et al. 2003).

Photosynthetic dark reactions have been shown to be sensitive to $CO_2$ (Beardall and Raven 2004). A study by Dineshbabu et al. (2020) showed that the productivity, growth rates, and carbon fixation rates of the marine cyanobacteria, *Phormidium valderianum,* were strongly influenced by changing $CO_2$. Further, *Synechococcus* 8806 preferentially use $CO_2(aq)$ as the inorganic carbon source and so they can quickly and efficiently uptake $[CO_2(aq)]$ (Miyachi et al. 2003). Therefore, potentially explaining how an increase in TA (and decrease in $CO_2$) would cause a decrease in the photochemical efficiency of *Synechococcus* 8806 light harvesting apparatus (maximum light use efficiency ($\alpha$), and photochemical efficiency of PSII ($Y(PSII)_{max}$,)). However, unlike Perkins et al. (2018) who showed that in diatoms, higher values of Y(PSII) were driven by an increased rate of PSII reopening (lower $\tau_1$), for *Synechococcus* 8806, it appears that it is the parallel changes to the light capture to the cross

section of PSII ($\sigma_{PSII}'_{max}$), and the "connectivity" of PSII reaction centres ($p'_{max}$) which drove the decrease in α and $Y(PSII)_{max}$.

The effective absorption cross sections for open PSII reaction centres ($\sigma_{PSII}'$) measures both the capture of light to the cross section of PSII and the yield for subsequent photochemistry (Trissl and Lavergne 1995; Kolber et al. 1998; Laney 2003; Suggett et al. 2009). However, because growth light was constant in this study, changes to $\sigma_{PSII}'$ likely represented changes to the yield for subsequent photochemistry. As TA increased from well 1-4, the *Synechococcus* 8806 were potentially $CO_2$ limited and so experienced reduced carbon metabolism rates. Reduced rates of carbon fixation would mean that the *Synechococcus* 8806 cells would not need to allocate as many protein resources to upstream light capturing mechanisms of PSII resulting in reduced $\sigma_{PSII}'$ (Falkowski and Owens 1980). Further, smaller effective PSII absorption cross sections areas would decrease the sharing of excitation energy between PSII reaction centres or "connectivity" of PSII reaction centres and so result in decreased $p'_{max}$. Therefore, both the effect of reduced effective PSII absorption cross sections and less connected PSII reaction centres results in less light captured and so decreasing the photochemical efficiency of PSII (Y(PSII)) and light use efficiency (α).

The opposite effect was likely experienced by the *Synechococcus* 8806 cells in wells 5-10. Here the increase in $CO_2$(aq) from potential increased calcification rates could have caused an increase in the rates of carbon fixation meaning that the *Synechococcus* 8806 cells would have to allocate more protein resources towards the upstream light capturing mechanisms resulting increased $\sigma_{PSII}'_{max}$ and $p'_{max}$ causing the increase in α and $Y(PSII)_{max}$.

The plateau in *Synechococcus* 8806 $Y(PSII)_{max}$ and decrease in *Synechococcus* 8806 which occurred from well 9-10 could be explained by the potential decrease in $pCO_2$ (from increased TA) becoming too large so that the effect of any potential $CO_2$ released from *Synechococcus* 8806 calcification was too small to promote increased carbon fixation. Therefore, the overall effect is a decrease in $pCO_2$ and promoting *Synechococcus* 8806 to have less efficient rates of photosynthesis. However, again, because no reliable estimates of $pCO_2$ have been made during this experiment, this interpretation has to be taken with caution. In order to truly understand why *Synechococcus* 8806 photochemical efficiency declined as TA reached very high levels, this experiment needs to be repeated with better, more controlled constrains on media carbonate chemistry.

### 4.5.3. Implications for ocean alkalinity enhancement

Despite the slight overall decline in photosynthetic efficiency (by ~6-9%), the overall effect of increasing the TA of *Synechococcus* 8806 growth medium by ~300% was that *Synechococcus* 8806 growth rates increased by 57%. The increase in *Synechococcus* 8806 growth is likely a consequence of increased calcification due to increased [$CO_3^{2-}$] and [$HCO_3^-$] and suggests that potential increased calcification has a stronger effect on *Synechococcus* 8806 growth than changes to *Synechococcus* 8806 photophysiology. This could explain why there is no significant relationship between *Synechococcus* 8806 growth rate and α or $Y(PSII)_{max}$. However, it should be noted that this experiment did not directly test for *Synechococcus* 8806 calcification and so these results do not show for certain that changes to *Synechococcus* 8806 calcification rates affected *Synechococcus* 8806 growth. If changes to seawater TA do have the potential to influence *Synechococcus* 8806 growth rates by increasing calcification rates, this could have important implications for OAE because it suggests that as well as the chemical sequestration of atmospheric $CO_2$ through ocean TA, the increased growth of *Synechococcus* could also lead to an increase in the biological capture of carbon.

The aim of this study was to improve the understanding of how increasing TA and the subsequent changes to carbonate chemistry has any effect on *Synechococcus* 8806 photophysiology in order to better understand how future OAE scenarios could impact the marine environment. The only parameter from which solid conclusions can be drawn from is from increasing TA as this was the only parameter which was carefully controlled. Therefore, although the results from this chapter do show clearly that increasing TA causes an increase in *Synechococcus* 8806 growth rates and does significantly influence *Synechococcus* 8806 photophysiology. They do not for certain show that these changes were brought about from specific changes to the proportions of [$CO_3^{2-}$], [$HCO_3^-$] and [$CO_2$(aq)]. Therefore, it is acknowledged that the above conclusions drawn from these results about future OAE scenarios are limited in their scope and that further investigation is needed. The experiments from this study should be repeated but with a much greater control on constraining the carbonate system. For example, samples of media treatments of each well should be sent for DIC analysis as well as TA analysis. Further, TA should be continually measured throughout the experiment with the intention of conclusively proving whether *Synechococcus* 8806 are calcifying.

## 4.6. Conclusions

The results from this chapter show that an increase in TA significantly increases *Synechococcus* 8806 growth rates and significantly influences *Synechococcus* 8806 photophysiology. Increasing TA by 2837 µEq $L^{-1}$ caused *Synechococcus* 8806 growth rates to increase by 57% and so that increasing TA will cause *Synechococcus* 8806 growth rates to decrease was rejected. Increasing TA by 2837 µEq $L^{-1}$ caused *Synechococcus* 8806 α to decrease by 6% and $Y(PSII)_{max}$ to decrease by 9%. Therefore, the hypothesis that increasing TA will cause *Synechococcus* 8806 photosynthetic efficiency to decrease was accepted. However, the relationship between *Synechococcus* 8806 photophysiology and TA was not a simple, linear increase. The results from this study have led to the new hypothesis that when changes in TA result in substantial changes in $pCO_2$ (e.g., by 20-50%) then the effect of decreasing $pCO_2$ has the controlling influence on *Synechococcus* 8806 photophysiology and causes a reduction in photochemical efficiency. Conversely, when changes in TA result in smaller changes in $pCO_2$ (e.g., by 2-5%), increased $CO_2$ from *Synechococcus* 8806 calcification has the stronger influence on *Synechococcus* 8806 photophysiology and causes an increase in photochemical efficiency. However, no robust estimates of $pCO_2$ were made and so the results from this study do not conclusively show what the specific cause of the changes to *Synechococcus* 8806 photophysiology by changing TA was. Therefore, in order to test this new hypothesis, this experiment needs to be repeated but with better, more accurate measurements of TA, DIC and/or pH to better constrain the carbonate chemistry. Also continued TA measurements should be taken throughout the experiment in order to test whether the *Synechococcus* 8806 cells were calcifying.

.

# Chapter 5.

# The physiological impact of increasing ocean alkalinity on $CaCO_3$ precipitation by a calcifying strain of *Synechococcus*.

## 5.1. Summary

Calcifying cyanobacteria are absent from the modern marine environment because seawater $\Omega_{Ca}$ is too low, therefore elevated seawater TA from OAE may rise seawater $\Omega_{Ca}$ enough for modern strains of cyanobacteria to start calcifying again. Therefore, this chapter focusses on the response of *Synechococcus* 8806 to elevated TA in terms of $CaCO_3$ precipitation (calcification) rates. *Synechococcus* 8806 cultures were exposed to three TA treatments of ambient TA ("Ambient"), moderate TA ("E1000"), and high TA (E2000). *Synechococcus* 8806 growth rates, calcium concentration, and cell size were monitored as well as media TA, pH, DIC, $pCO_2$, $\Omega_{Ar}$, and $\Omega_{Ca.}$ Unlike the previous chapter, increasing TA had no effect on *Synechococcus* 8806 growth rates (likely due to the lower growth light used in this study). Highest $CaCO_3$ precipitation rates were associated with the higher TA treatments, and samples collected from the high TA treatment had the highest calcium concentrations. However, there was no direct evidence that it was specifically *Synechococcus* 8806 growth and physiology which resulted in the $CaCO_3$ precipitation. Although these results do not show how OAE could influence future *Synechococcus* calcification, they show that elevated TA does negatively impact on *Synechococcus* 8806 growth, they raise an interesting question regarding the role of nucleation seeds in $CaCO_3$ precipitation suggesting that under extreme TA and elevated phytoplankton cells, abiotic $CaCO_3$ precipitation could occur. However further work is needed to test this hypothesis.

## 5.2. Introduction

In the previous chapter, it was shown that as well as elevated seawater TA significantly influencing *Synechococcus* 8806 photophysiology, elevated TA also promoted *Synechococcus* 8806 growth. This was hypothesised to be due to an increase in $\Omega_{CaCO3}$

promoting $CaCO_3$ precipitation. Past examples of marine cyanobacteria $CaCO_3$ precipitation suggest that calcification was an active biological process and occurred as extracellular calcification (Riding 2006). For example, in large cyanobacteria such as *Girvanella*, $CaCO_3$ was produced as external sheaths (Riding 1977). Because cyanobacteria produced $CaCO_3$ externally, cyanobacteria calcification was also influenced by the external environment, mainly seawater $\Omega_{CaCO3}$ (Pentecost 1986). Supporting this, Riding and Liang (2005) showed that between 150-545 million years ago there was a positive correlation between cyanobacteria carbonate abundance and calculated seawater $\Omega_{Ca}$.

There is also evidence which suggests that calcification is also influenced by cyanobacteria biology. For example, Golubić (1973) showed that the extent of calcification depends on individual cyanobacteria sheath development, composition, and structure (which in turns affects Ca binding). Also, the amount of calcification is different amongst species even when their external environment had the same carbonate chemistry conditions (Lee et al. 2004). Likewise, $CaCO_3$ precipitated by cyanobacteria is closely related to the organic carbon found in the cell envelope (Riding 1991; Merz and Zankl 1993). Further, calcification is not ubiquitous in all species of cyanobacteria and some species of cyanobacteria precipitate species-specific $CaCO_3$ crystal shapes (Gleason and Spackman 1974; Krumbein and Giele 1979; Merz 1992). Finally, there are evolutionary advantages to cyanobacteria calcification such as, $CaCO_3$ precipitation can act as a buffer against extreme pH increases in alkaline environments, or act as protection against high light radiation (Merz-Preiß 2000), or enhance nutrient uptake (McConnaughey and Whelan 1997) or even help rid the cell of toxic excess Ca (Stal 2012).

The calcification process in cyanobacteria is thought to be strongly related to photosynthesis (Pentecost 1986). Evidence for this includes higher $\delta^{13}C$ isotope values in cyanobacteria $CaCO_3$ precipitate (Pentecost and Spiro 1990; Merz 1992; Andrews et al. 1997) and lower calcification rates when electron transport in photosystem II is suppressed (Badger and Andrews 1982). Merz (1992) suggested that cyanobacteria calcification occurs due to "carbon concentrating mechanisms" (CCMs). CCMs are common in cyanobacteria (Riding 2006). In fact, cyanobacteria have some of the most efficient CCMs known and their intercellular DIC can be up to 1000 times the concentration of extracellular DIC achieved by actively transporting carbon into the cell (Kaplan and Reinhold 1999). Strong CCMs can promote cyanobacteria $CaCO_3$ precipitation by concentrating $CO_2$ in the cells, which is then converted to $HCO_3^-$ by carbonic anhydrase enzymes which increases the pH. This increase in

pH then causes $HCO_3^-$ to change to $CO_3^{2-}$, raising external $\Omega_{Ca}$, and so stimulating cyanobacterial calcification. Supporting this, Yang et al. (2016) found that the extent of $CaCO_3$ precipitation in the cyanobacteria *Synechocystis* sp. was related to extracellular carbonic anhydrase and $HCO_3^-$ concentration. Further, Riding (2006) hypothesised that the development of cyanobacteria CCMs occurred around 750 Ma (which coincides with a decline in atmospheric $CO_2$) and this could explain the first occurrence of *Girvanellla* $CaCO_3$ sheaths which developed by 750-700 Mya. Just like photosynthesis enhancing calcification, calcification can enhance photosynthesis as the resulting production of $CO_2$ and protons from the calcification process could in turn promote photosynthesis (Frankignoulle et al. 1994).

Although calcifying cyanobacteria are absent from the modern marine environment, marine calcifying cyanobacteria have been important throughout Earth's history (Riding 2006) and there are calcifying strains of the marine *Synechococcus* that can calcify in laboratory conditions (Lee et. al 2004). Riding et al. (2006) hypothesises that there are no modern-day marine calcifying cyanobacteria because seawater $\Omega_{Ca}$ is too low. Therefore, it could be possible for *Synechococcus* to start calcifying if OAE causes global increases in ocean $\Omega_{Ca}$. Due to the large abundance of global *Synechococcus*, this could substantially impact marine biogeochemistry. For example, in the past, calcifying cyanobacteria have played a key role in influencing marine carbonate chemistry. Aloisi (2018) suggest that marine cyanobacteria controlled marine TA and $\Omega_{Ca}$ during the Mid Mesozoic.

This study aims to investigate the response of a calcifying strain of *Synechococcus* 8806 to elevated TA, with a particular focus on $CaCO_3$ precipitation rates. This will better constrain our understanding of how OAE could influence global marine calcification rates and in turn, how OAE could impact marine biogeochemistry. It was hypothesised that increasing TA, would cause an increase in *Synechococcus* 8806 growth rates and $CaCO_3$ precipitation rates.

# 5.3. Methods

## 5.3.1. Experimental set up

The calcifying strain of *Synechococcus* 8806 was cultured at the Earth and Ocean Sciences department, University of Oxford, where all measurements were performed. The experiment consisted of three TA treatments: "Ambient" with a starting TA of ~2100 µEq $L^{-1}$, "E1000" (Elevated 1000) treatment with a starting TA of ~3000 µEq $L^{-1}$, and "E2000" (Elevated 2000) with a starting TA of ~3600 µEq $L^{-1}$. Culture medium was prepared using Synthetic Ocean

Water (SOW) (Andersen 2005) with sterile, filtered nutrients according to L1 (Guillard and Hargraves 1993). L1 nutrient concentrations were 882 µmol/L nitrate, 36.2 µmol/L phosphate and 106 µmol/L silicate. See Appendix D for more for details. The cultures were inoculated in synthetic ocean water and L1 media. The higher TA values of the enhanced TA treatments (E1000 and E2000) were achieved by adding 0.25 M solution of $Na_2CO_3$. Each treatment consisted of triplicate 750 mL culture flasks so there were nine culture flasks in total. The culture flasks were kept in a temperature controlled (15˚C) incubator with a 12:12 light/dark light cycle. The light levels were kept at 50 µmol photons $m^{-2}$ $s^{-1}$.

## 5.3.2 Growth rates

Throughout the experiment, the cell growth of each culture flask was monitored using a Tecan SparkControl plate reader which measured the chlorophyll-*a* (Chl-*a*) florescence at γ= 680 nm ($OD_{680}$). The relative Chl-*a* florescence values were then used to calculate the instantaneous growth rate (IGR; $hr^{-1}$) and the growth rate constant (µ; $hr^{-1}$) using equations 35 and 36, where $Chl_x$ is the $OD_{680}$ value at time $t_x$ and $Chl_0$ is the $OD_{680}$ value at time $t_0$. Usually, µ is calculated during the period of exponential growth. However, there was no clear exponential growth period and there was instead a continuous growth from day 0 and 39. However, as discussed later in Sections 5.4.2 and 5.5.2, DIC was depleted by day 22 and so growth could not have occurred. Therefore, µ was calculated for the growth period from day 0-22.

$$\mathrm{IGR} = \ln\left(\frac{Chl_x/Chl_0}{t_x - t_0}\right) \quad \text{(Equation 35)}$$

$$\mu = \frac{\ln(Chl_x) - \ln(Chl_0)}{t_x - t_0} \quad \text{(Equation 36)}$$

## 5.3.3. Cell density

The cell density (cells $mL^{-1}$) of each treatment was estimated using the Chl-*a* florescence measurements and flow cytometry. After several days, when there was sufficient biomass, a serial dilution of cultures and synthetic ocean water were performed. There were five dilutions from 100% culture to 0% culture each for the Ambient and E1000 TA treatments. There was a total of 10 dilutions in all (five for E1000 and five for Ambient). The Chl-*a* florescence value was then measured for each dilution using the same technique described above. Immediately following the Chl-*a* florescence measurements, the cell density (cells $mL^{-1}$) of each dilution was measured using flow cytometry (Cytek DxP analyzer, USA). The

relationship between Chl-*a* florescence and cell density was then calculated (Figure 5.1). This relationship was then used to convert the relative Chl-*a* florescence values into cell density values (cells $mL^{-1}$).

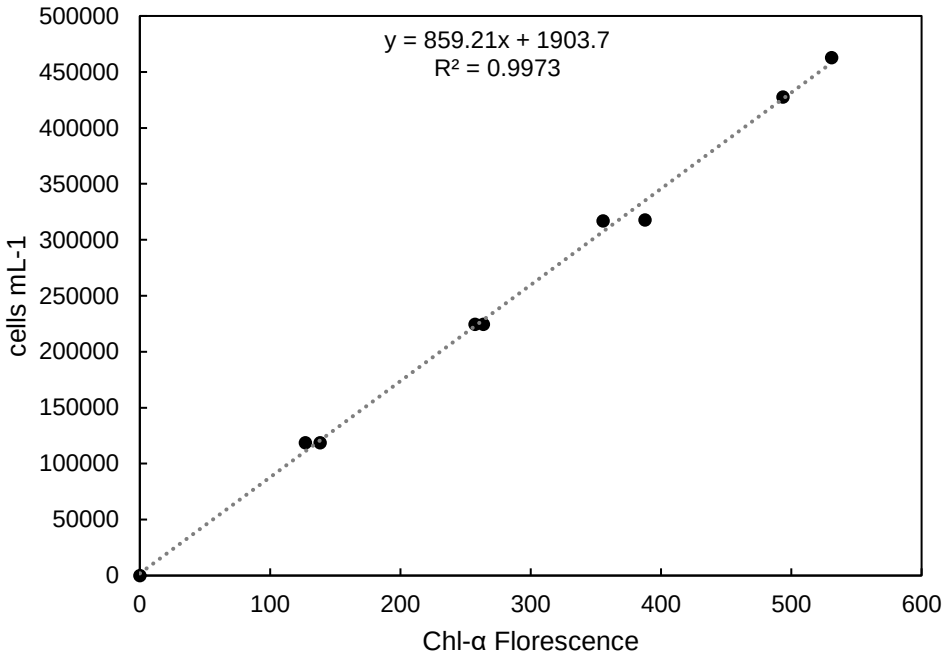


*Figure 5.1. Relationship between Synechococcus 8806 Chl-a florescence at γ= 680 nm (relative units) and cell density (cell $mL^{-1}$) measured using flow cytometry.*

## 5.3.4. Total alkalinity and pH

Periodically throughout the experiment, 20 mL samples were collected for TA and pH analysis. Each sample was filtered through a 0.22 µM polycarbonate filter and stored in an air-tight container until TA analysis was performed. Temperature and pH were measured immediately after sample collection using a combination temperature/pH electrode (Mettler Toledo™, U.K.) calibrated with TRIS and AMPD seawater buffer solutions according to Dickson et al. (2007).

Gran titration (907 Titrando, Metrohm tiamo™, Switzerand) was used to measure TA using the same method outlined in Chapter 2. For the method used, the precision is greatest when a larger sample size is used, typically at least 50 mL sample size is used. However, given the volume constraints of the culture medium, only 20 mL samples were taken. Therefore, the

samples were carefully and accurately diluted with milli Q water (TA = 0 µEq $L^{-1}$) to bring the total volume up to 50 mL. The accuracy and precision for the 20 mL samples were determined by six titrations of each sample and compared to a TA standard (Batch 175) supplied by the University of California San Diego with a known TA of 2200 µEq $L^{-1}$. The absolute error of the TA measurements was -87 $\pm$ 10 µEq $L^{-1}$. Afterward, pH, TA, temperature, and salinity were used to determine the other carbonate chemistry parameters (DIC, *p*CO2, $HCO_3^-$, $CO_3^{2-}$, $\Omega_{Ar}$, $\Omega_{Ca}$), using CO2SYS v2.1 (Pierrot et al. 2016). CO2SYS was run using the constants of Mehrbach et al. (1973) refitted by Dickson and Millero (1987), and a seawater scale for pH.

The change in TA was used to estimate the $CaCO_3$ precipitation rate (µmol $CaCO_3$ $10^6$ $cells^{-1}$ $h^{-1}$) of *Synechococcus* 8806 between day 14 and day 27 (where the change in TA was greatest) for all three TA treatments using Equation 37. The amount of $CaCO_3$ precipitated (µmol $CaCO_3$) was estimated using the alkalinity anomaly technique (Smith and Key 1975; Chisholm and Gattuso 1991) which assumes a decrease in TA by two µEq equals one µmol of $CaCO_3$ precipitated.

$$CaCO_3 \text{ precipitation rate } = \frac{\Delta TA * v}{2 * 10^6 cells * h} \quad \text{(Equation 37)}$$

Where "v" is the volume of water in the culture flask, $h^{-1}$ is time elapsed in hours, and "$10^6$ cells" is calculated from Equation 33. Where "cells $mL^{-1}$" is the average cell density and "$v_{flask}$" is the average volume of medium (mL) in the culture flask during the time period from which NCR was calculated.

$$10^6 cells = \frac{cells\ mL^{-1} * v_{flask}}{10^6} \quad \text{(Equation 38)}$$

## 5.3.5 Calcium concentration

On day 19 and day 27 of the experiment, samples were prepared for calcium concentration analysis, which was performed using the flow injection ICP-MS method for measuring $^{43}Ca$. For the preparation, 5 mL of *Synechococcus* 8806 culture from the Ambient, E1000, and E2000 treatments were filtered onto polycarbonate filters and subsequently washed with Milli Q so no synthetic ocean residue was left on the filter. The polycarbonate filters were soaked in 10% HCl for 48 hours prior to the analysis to ensure no prior trace of Ca were on the filters. Each filter was then placed into a 50 mL MF falcon tube using sterilised tweezers with 15 mL of 2% HNO3 (so that the filter was fully submerged) and centrifuged for 20 minutes at

2000 RPM. The filter was then removed from the current falcon tube and 10mL of $HNO_3$ /dissolved $^{43}Ca$ solution was carefully transferred into 15mL falcon tubes for $^{43}Ca$ analysis. The $^{43}Ca$ analysis using Indium as a carrier gas was performed on a PerkinElmer NexION 350D Inductively Coupled Plasma-Mass Spectrometer (ICP-MS) at Oxford University Trace Element Research Facility using the method from Zhang et al. (2018).

### 5.3.6. Scanning Electron Microscope

On day 22, *Synechococcus* 8806 samples were collected from each triplicate TA treatment (nine in total) and prepared for scanning electron microscope (SEM). 45 mL of each sample were placed in falcon tubes and centrifuged for one hour at 3000 RPM to increase the density. The cells were fixed onto carefully cleaned coverslips using 2.5% glutaraldehyde and 0.1 M phosphate buffer and incubated for one hour at 4 ˚C. Each sample was rinsed with 0.1 M phosphate buffer before dehydrating by rinsing in ethanol. The coverslips were finally dried overnight using HMDS. Following this, the samples were gold-coated using a Quorum Q15OR-ES sputter coater and analysed using a Zeiss-sigma Gemini and Smart SEM software.

The samples were analysed to see if there were any differences in shape, size and texture of the cells between TA treatments, which could then be used to identify $CaCO_3$ precipitation. The average cell surface area ($\mu m^2$) was estimated for each TA treatment from the SEM images using the program ImageJ and the equation below:

$$SA = 4\pi \left(\frac{(ab)^{1.6}+(ac)^{1.6}+(bc)^{1.6}}{3}\right)^{1/1.6} \quad \text{(Equation 39)}$$

Where the cell was approximated to an ellipsoid and a is half the length (µm), b is half the width (µm), and c is half the height (µm).

### 5.3.7. Data analysis

Where averages are given, the error is quoted as either standard deviation ($\mp$ S.D.) in text, figures or tables unless otherwise stated. All statistical analyses were performed using R v.3.4.1 (R Core Team, 2017). Prior to all analyses, normality of data was tested using the Shapiro-Wilk test and examination of frequency histograms. Differences in parameters ($CaCO_3$ precipitation rate, IGR, µ, and cell surface area) between the TA treatments were examined using one-way ANOVA. Where data were not normally distributed, the data were transformed using a box-cox transformation and reanalysed for normality using the Shapiro-

Wilk test. Differences were deemed significant if $p < 0.05$. Regressions models were performed to determine any significant relationships between $CaCO_3$ precipitation rate (and μ) and the initial (day 0) carbonate chemistry parameter (TA, pH, $\Omega_{Ca}$ and $pCO_2$)

# 5.4. Results

## 5.4.1. Cell density, growth rates, and cell size

Figure 5.2a shows changes in cell density (cells $mL^{-1}$) for *Synechococcus* 8806 for all three TA treatments (Ambient, E1000, and E2000). Over the 39 days which the experiment ran, the cell density of all three treatments increased from a starting density of ~ 7.8 $x10^4$ cells $mL^{-1}$ to 8.5 $x10^5 \pm 1$ $x10^5$ cells $mL^{-1}$ for the ambient treatment, 1.2 $x10^6 \pm 1.7$ $x10^5$ cells $mL^{-1}$ for the E1000 treatment, and 1.1 $x10^6 \pm 9.0$ $x10^4$ cells $mL^{-1}$ for the E2000 treatment. The instantaneous growth rates for all three treatments were similar throughout (Table 5.1, Figure 5.2), with maximum instantaneous growth rates achieved between day 0 and 6 for all treatments ($0.006 \pm 0.0005$ $hr^{-1}$, $0.007 \pm 0.0002$ $day^{-1}$, $0.006 \pm 0.0006$ $day^{-1}$ for Ambient, E1000, and E2000 respectively).

Figure 5.2b shows the μ calculated for the growth period between day 1-21. Values for μ were $0.0036 \pm 0.0002$ $hr^{-1}$, $0.0039 \pm 0.0002$ $hr^{-1}$, and $0.0035 \pm 0.0001$ $hr^{-1}$ for the Ambient, E1000, and E2000 treatments respectively. There was a weak significant difference in μ between the TA treatments ($F = 5.436$, $p < 0.05$).

*Table 5.1 Instantaneous growth rates (averages ± S.D.) of Synechococcus 8806 from each TA treatment calculated from changes in Chl-a fluorescence for growth period (days 0-19).*

| Days | Instantaneous growth rate ($hr^{-1}$) | | | | | |
|---|---|---|---|---|---|---|
| | Ambient | | E1000 | | E2000 | |
| | Average | ± | Average | ± | Average | ± |
| 0-6 | 0.0057 | 0.0005 | 0.0065 | 0.0002 | 0.0057 | 0.0006 |
| 6-12 | 0.0037 | 0.0009 | 0.0026 | 0.0003 | 0.0037 | 0.0009 |
| 12-14 | 0.0031 | 0.0011 | 0.0044 | 0.0019 | 0.0030 | 0.0008 |
| 14-19 | 0.0022 | 0.0003 | 0.0034 | 0.0003 | 0.0034 | 0.0003 |
| 19-22 | 0.0022 | 0.0008 | 0.0015 | 0.0017 | 0.0013 | 0.0012 |

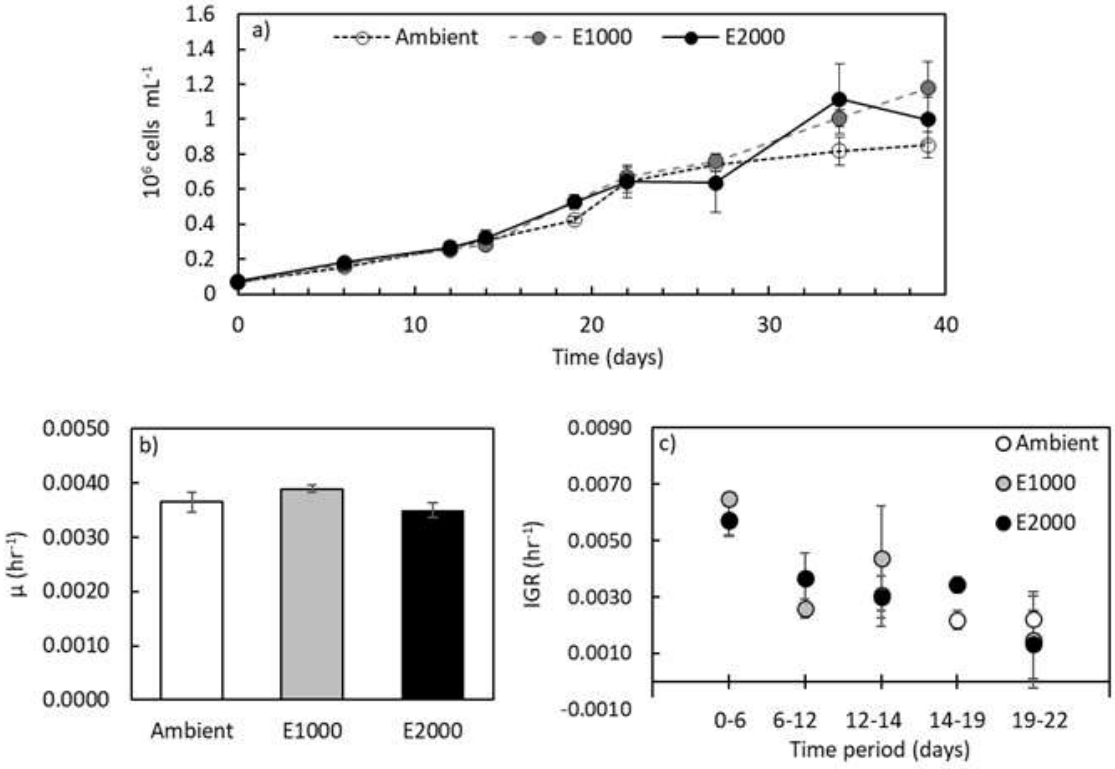


*Figure 5.2. Synechococcus 8806 cell density and growth. Inset a shows the change in cell density ($10^6$ cells $mL^{-1}$) over the course of the experiment for Synechococcus 8806 cultures from each TA treatment (Ambient- white, E1000-grey, and E2000-black). Inset b shows the growth rate constant (μ, $hr^{-1}$) for each TA treatment (Ambient- white, E1000-grey, and E2000-black) calculated from the change in cell density between day 0 and 22. Inset c shows the instantaneous growth rates (IGR, $hr^{-1}$).) for each TA treatment (Ambient- white, E1000-grey, and E2000-black) calculated for each growth period (2-6 days) between days 0 and 22.*

To investigate if there were any changes in cell size between TA treatments and for a qualitative assessment of $CaCO_3$ precipitation, SEM images were taken of the *Synechococcus* 8806 cells from all three TA treatments (Figure 5.3 d-f). Part of the SEM preparation involved centrifuging the samples to concentrate the culture and being in the centrifuge, there was evidence of a white precipitate present in the samples (Figure 5.4). There was a statistically significant difference in cell surface area ($\mu m^2$) between treatments ($F = 8.247$, $p < 0.001$). When cultured under the E2000 treatment, more cells had a smaller surface area (Figure 5.3 a-c). The average cell surface area was $14.05 \pm 1.78$ $\mu m^2$, $13.26 \pm 1.76$ $\mu m^2$, and $13.78 \pm 1.97$ $\mu m^2$ for the Ambient, E1000, and E2000 treatments respectively.

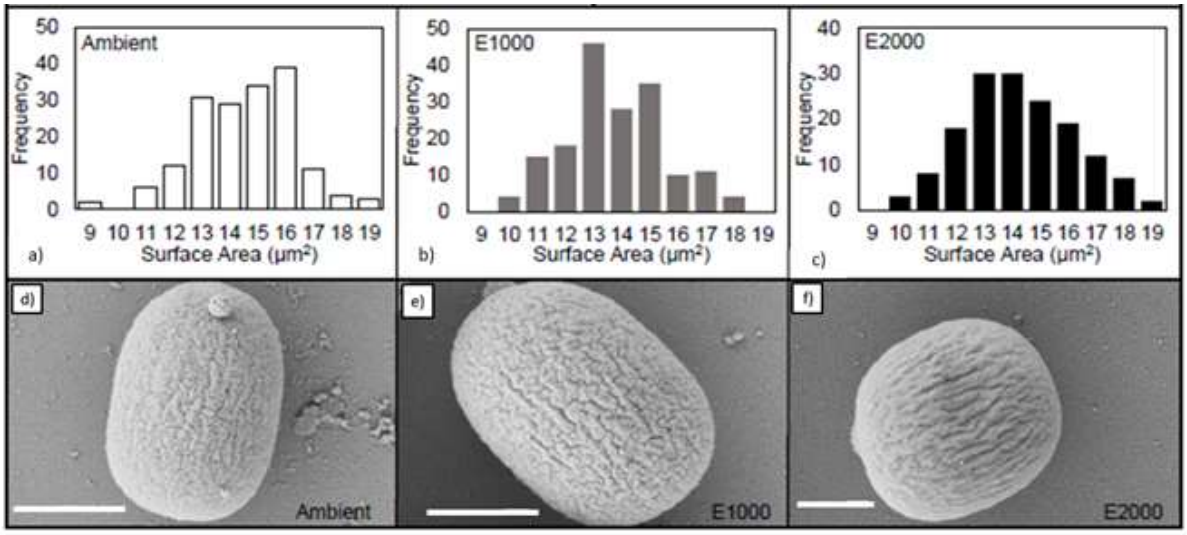


*Figure 5.3. Synechococcus 8806 cell size. Insets a-c show histograms of Synechococcus 8806 cell surface areas (µm$^2$) for each TA treatment (Ambient- white, E1000-grey, and E2000-black) measured using Image-J from SEM images taken on day 22 of the experiment (insets d-f). Scale bars show 1 µm.*

*Figure 5.4. Example of the white precipitate found in the Synechococcus 8806 culture samples from the E1000 alkalinity treatment (a white precipitate was also found in samples from the Ambient and E2000 treatments). The samples were taken on day 22 of the experiment and the white precipitate was only visible after the samples were vortexed for one hour at 3000 RPM.*

## 5.4.2. Changes to the carbonate system and $CaCO_3$ precipitation

### *5.4.2.a. Total alkalinity, calcium concentration, and $CaCO_3$ precipitation*

Changes in TA were measured throughout the experiment. The starting TA values were 2390 ± 25 µEq $L^{-1}$ for the Ambient treatment, 3396 ± 25 µEq $L^{-1}$ for the E1000 treatment and 4063 ± 25 µEq $L^{-1}$ for the E2000 treatment. For the first 19 days of the experiment, there was a small change in TA values for all three treatments (give value of small change, Figure 5.5a). After day 19, TA began to decrease and reached minimum values by day 34 of to 354 ± 11 µEq $L^{-1}$, 471 ± 82 µEq $L^{-1}$ and 378 ± 64 µEq $L^{-1}$ for the Ambient, E1000, and E2000 treatments respectively.

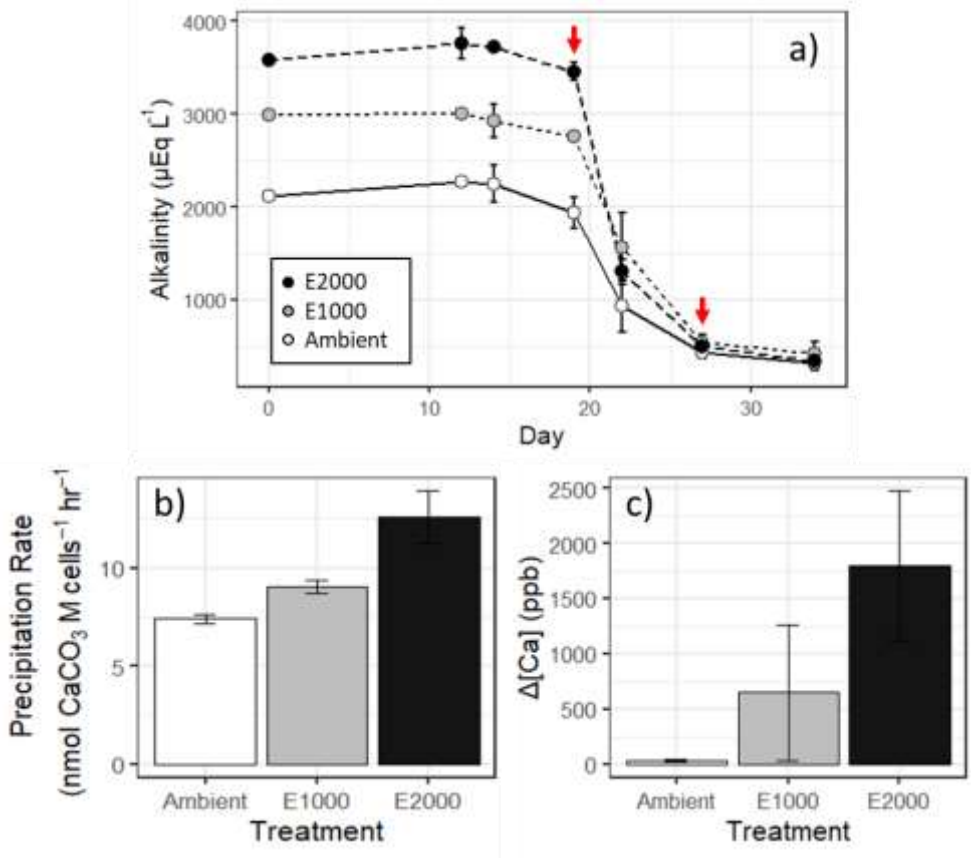


*Figure 5.5. Inset a shows the change in TA (µEq $L^{-1}$) over the course of the experiment for each of the three TA treatments (Ambient- white, E1000-grey, and E2000-black; a). The red arrows point to the start (day 19) and end (day 27) of the largest change in TA for each of the three treatments. This is the time period from which the Synechococcus 8806 $CaCO_3$ precipitation rate, and [Ca] content of the Synechococcus 8806 cells were calculated from. Insets b and c show the difference in Synechococcus 8806 $CaCO_3$ precipitation rate (nmol $CaCO_3$ $10^6$ cells $hr^{-1}$; b)and change in [Ca] content of Synechococcus 8806 cells (ppb; c) for each of the TA treatments (Ambient, E1000, and E2000).*

*Table 5.2. [$^{43}$Ca] content of Synechococcus 8806 cells (ppb) for each of the TA treatment (Ambient, E1000, and E2000) triplicates measured on day 19 and day 27 of the experiment (period of greatest change in TA).*

| Sample | [$^{43}$Ca] (ppb) | | | |
|---|---|---|---|---|
| | Day 19 | | Day 27 | |
| Blank | 57 | blank corrected | 135 | blank corrected |
| Ambient a | 72 | 15 | 190 | 55 |
| Ambient b | 47 | -9 | 132 | -4 |
| Ambient c | 48 | -8 | 157 | 22 |
| E1000 a | 49 | -7 | 110 | -25 |
| E1000 b | 48 | -9 | 1421 | 1286 |
| E1000 c | 52 | -4 | 195 | 60 |
| E2000 a | 57 | 1 | 1857 | 1722 |
| E2000 b | 73 | 17 | 3201 | 3066 |
| E2000 c | 61 | 4 | 851 | 716 |

There was a significant difference in $CaCO_3$ precipitation rate between the treatments ($F=66.78$, $p < 0.001$; Figure 5.5 b). The $CaCO_3$ precipitation rate was 6.7 ± 0.5 nmol $CaCO_3$ $10^6$cells$^{-1}$ hr$^{-1}$ for the Ambient treatment, 8.6 ± 1 nmol $CaCO_3$ $10^6$cells$^{-1}$ hr$^{-1}$ for E1000 treatment, and 12.6 ± 1.6 nmol $CaCO_3$ $10^6$cells$^{-1}$ hr$^{-1}$ for E2000 treatment. This equates to a ~28% increase in $CaCO_3$ precipitation when *Synechococcus* 8806 was cultured in the E1000 treatment compared to when they were cultured in the Ambient treatment and a ~89% increase in $CaCO_3$ precipitation when *Synechococcus* 8806 was cultured in the E2000 treatment compared to when they were cultured in the Ambient treatment.

There was a simultaneous increase in $^{43}$Ca concentration ([$^{43}$Ca], ppb) of the *Synechococcus* 8806 cells as TA decreased (Table 5.2). On Day 19 (before there was a visible decrease in TA) the [$^{43}$Ca] of the cells was near zero and by day 27 there was a marked increase in [$^{43}$Ca] for each TA treatment. Figure 5.5 c shows the difference in this increase between the TA treatments. The *Synechococcus* 8806 cells in the Ambient treatment saw an increase in of ~25

ppb between day 19 and day 27, the E1000 treatment saw an increase of ~450 ppb and the E2000 treatment saw an increase of ~ 1800 ppb (Figure 5.5 c).

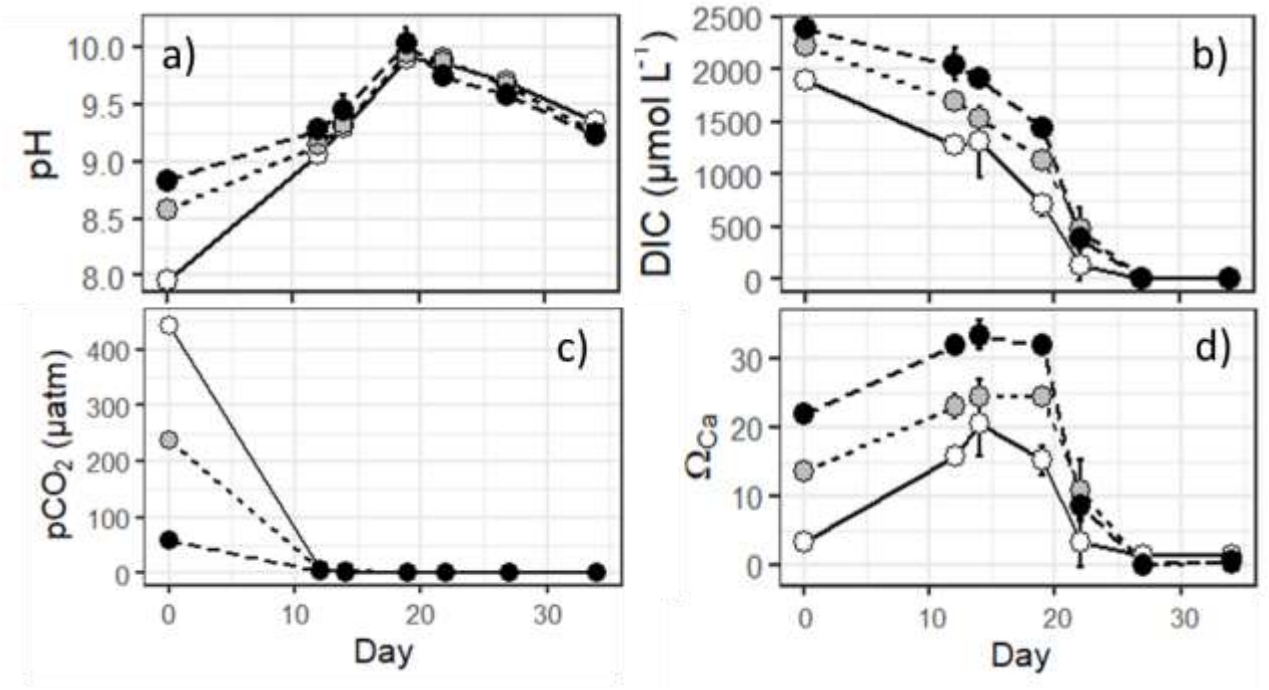


*Figure 5.6. Change in carbonate chemistry parameters (pH-a; DIC (µmol $L^{-1}$)-b; $pCO_2$ (µatm)-c; $\Omega_{Ca}$-d) over the course of the experiment for each of the three TA treatments (Ambient- white, E1000-grey, and E2000-black).*

*5.4.2.b. Dissolved inorganic carbon, pH, saturation states, and $pCO_2$*

From the start of the experiment to day 19, pH increased for all three experiments (Figure 5.6 a). Starting pH values were 7.96 ± 0.06, 8.58 ± 0.07, and 8.83 ± 0.07 and by day 19 the pH had increased to 9.98 ± 0.03, 9.95 ± 0.05, and 9.91 ± 0.09 for the Ambient, E1000, and E2000 treatments respectively. Although all three TA treatments started with substantially different pH values, after the first 12 days, the pH values for all three treatments became similar. After day 19, pH started to decrease as TA decreased and by the end of the experiment the pH was 9.35 ± 0.05, 9.25 ± 0.07, and 9.23 ± 0.08 for the Ambient, E1000, and E2000 treatments respectively.

The pH and TA values were used to calculate the change in other carbonate system parameters which are presented in Table 5.2 and Figure 5.6 a-d. Throughout the experiment there was a continuous decrease in dissolved organic carbon (DIC) for all three TA

treatments (Table 5.3, Figure 5.6 b). There was also a decrease in $pCO_2$, with all three TA treatments reaching near zero $pCO_2$ values by day 19 despite starting with different $pCO_2$ values (443 ± 8.33, 237 ± 2.97, 57 ± 0.67 µatm for the Ambient, E1000, and E2000 treatments respectively; Table 5.3, Figure 5.6 c). From day 0 to day 19, as pH increased, there was a substantial increase in $\Omega_{Ca}$ from 3.19 ± 0.06, 14.25 ± 0.18, and 24.34 ± 0.14 to 15.14 ± 2.06, 24.49 ± 0.69, and 31.96 ± 1.27 for the Ambient, E1000, and E2000 treatments respectively (Table 5.3, Figure 5.6 d). After day 19, when TA began to decrease, $\Omega_{Ca}$ also decreased to near zero values by the end of the experiment (Table 5.3, Figure 5.6 d). A similar pattern was seen in $\Omega_{Ar}$ for all three treatments (Table 5.3).

### 5.4.3. Regression relationships

Increasing TA promoted *Synechococcus* 8806 $CaCO_3$ precipitation rates but not growth. Linear regression analysis showed that there was a statistically significant positive relationship between TA and $CaCO_3$ precipitation but no statistically significant relationship between TA and µ (Figure 5.7). For the results from the linear regression analysis between $CaCO_3$ precipitation rate and µ and the other initial carbonate chemistry parameters (pH, $pCO_2$, $\Omega_{Ca}$, $\Omega_{Ar}$), see Table 5.4. There was a also a significant positive linear relationship between $CaCO_3$ precipitation rate and DIC ($R^2 = 0.8210$, $F = 32.11$, $p < 0.001$); $\Omega_{Ca}$ ( $R^2 = 0.8658$, $F = 45.18$, $p < 0.001$); and $\Omega_{Ar}$ ($R^2 = 0.8659$, $F = 45.21$, $p < 0.001$). There was a linear relationship between $CaCO_3$ precipitation rate and pH, and $pCO_2$ but these were not statistically significant. There was no statistically significant relationship between µ and any of the other carbonate chemistry parameters (pH, $pCO_2$, $\Omega_{Ca}$, $\Omega_{Ar}$)

.

*Table 5.3. Average Carbonate Chemistry parameters (± standard error) for each TA treatment (Ambient, E1000, and E2000) over the course of the experiment.*

| Day | Treatment | pH | | TA µmol $L^{-1}$ | | DIC µmol $L^{-1}$ | | $\Omega_{Ca}$ | | $\Omega_{Ar}$ | | $pCO_2$ µatm | |
|---|---|---|---|---|---|---|---|---|---|---|---|---|---|
| | | Av | ± | Av | ± | Av | ± | Av | ± | Av | ± | Av | ± |
| 0 | Ambient | 7.96 | *0.05* | 2111 | *38* | 1900 | *35* | 3.37 | *0.06* | 2.12 | *0.04* | 443 | *8.32* |
| | E1000 | 8.58 | *0.06* | 2995 | *37* | 2221 | *30* | 13.47 | *0.18* | 8.46 | *0.12* | 237 | *2.97* |
| | E2000 | 8.83 | *0.07* | 3580 | *36* | 2394 | *30* | 21.83 | *0.10* | 13.72 | *0.11* | 57 | *0.67* |
| 12 | Ambient | 9.06 | *0.06* | 2272 | *34* | 1279 | *14* | 15.88 | *0.86* | 9.98 | *0.54* | 4.90 | *1.04* |
| | E1000 | 9.14 | *0.07* | 3005 | *52* | 1698 | *34* | 23.03 | *1.54* | 14.47 | *0.97* | 4.89 | *1.57* |
| | E2000 | 9.28 | *0.07* | 3759 | *162* | 2048 | *150* | 31.98 | *1.06* | 20.10 | *0.67* | 3.30 | *1.26* |
| 14 | Ambient | 9.29 | *0.06* | 2245 | *200* | 1313 | *335* | 20.52 | *4.65* | 12.89 | *2.92* | 2.09 | *0.93* |
| | E1000 | 9.32 | *0.11* | 2926 | *182* | 1528 | *91* | 24.38 | *2.64* | 15.32 | *1.66* | 2.28 | *1.08* |
| | E2000 | 9.44 | *0.13* | 3715 | *47* | 1916 | *75* | 33.42 | *2.02* | 21.00 | *1.27* | 1.79 | *1.09* |
| 19 | Ambient | 9.89 | *0.06* | 1932 | *165* | 709 | *104* | 15.14 | *2.06* | 9.72 | *1.33* | 0.31 | *0.10* |
| | E1000 | 9.94 | *0.09* | 2762 | *34* | 1132 | *56* | 24.49 | *0.69* | 15.71 | *0.45* | 0.41 | *0.15* |
| | E2000 | 10.04 | *0.13* | 3455 | *98* | 1444 | *81* | 31.96 | *1.27* | 20.49 | *0.81* | 0.37 | *0.20* |
| 22 | Ambient | 9.87 | *0.04* | 938 | *283* | 144 | *152* | 3.28 | *3.47* | 2.06 | *2.18* | 0.00 | *0.00* |
| | E1000 | 9.90 | *0.04* | 1567 | *369* | 474 | *199* | 10.78 | *4.51* | 6.77 | *2.83* | 0.01 | *0.01* |
| | E2000 | 9.74 | *0.02* | 1303 | *136* | 393 | *67* | 8.68 | *1.51* | 5.46 | *0.95* | 0.02 | *0.00* |
| 27 | Ambient | 9.70 | *0.04* | 433 | *32* | 0.4 | *0.2* | 1.42 | *0.40* | 0.00 | *0.25* | 0.00 | *0.00* |
| | E1000 | 9.66 | *0.08* | 541 | *90* | 1 | *0.2* | 0.08 | *0.91* | 0.05 | *0.57* | 0.00 | *0.00* |
| | E2000 | 9.57 | *0.07* | 500 | *131* | 1 | *0.2* | 0.07 | *1.30* | 0.04 | *0.82* | 0.00 | *0.00* |
| 34 | Ambient | 9.35 | *0.05* | 323 | *18* | 0.3 | *0.1* | 1.30 | *0.23* | 0.82 | *0.15* | 0.02 | *0.01* |
| | E1000 | 9.25 | *0.07* | 426 | *124* | 1 | *0.2* | 0.23 | *1.27* | 0.15 | *0.80* | 0.06 | *0.05* |
| | E2000 | 9.23 | *0.08* | 344 | *98* | 1 | *0.2* | 30.00 | *0.81* | 0.36 | *0.51* | 0.05 | *0.03* |

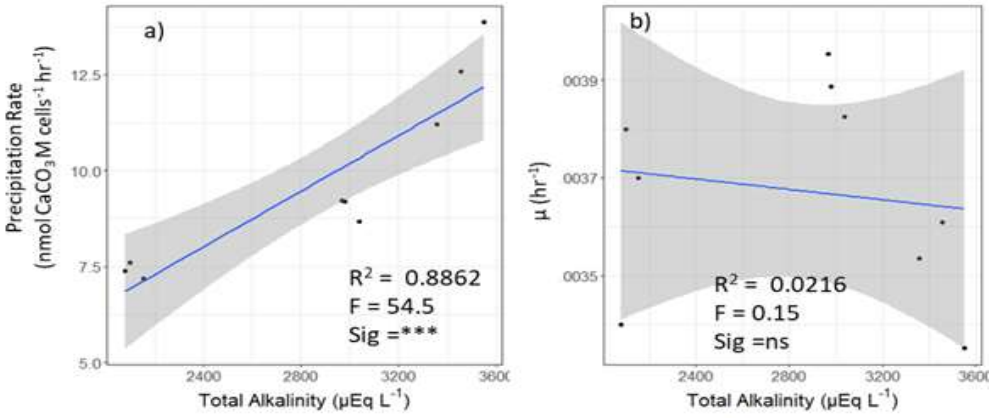


*Figure 5.7. Results from linear regression model assessing the relationship between Synechococcus 8806 $CaCO_3$ precipitation rate (nmol $CaCO_3$ million-cells $hr^{-1}$) calculated between day 19 and 27 and (a) and Synechococcus 8806 growth rate (µ, $hr^{-1}$) (b) and Total Alkalinity (µEq $L^{-1}$). Significance codes: *** = $p < 0.005$, NS = not significant.*

*Table 5.4 Results from linear regression model assessing the relationship between the dependent variables (y; Synechococcus 8806 growth rate (μ) and $CaCO_3$ precipitation rate calculated) and independent variables (x; TA, DIC, pH, $pCO_2$, $\Omega_{Ca}$, and $\Omega_{Ar}$ measured on day 19 of the experiment). Significance codes: *** = p<0.005, * = p<0.05, NS = not significant.*

| y | x | $R^2$ | F Stat | Sig |
|---|---|---|---|---|
| μ | TA | 0.0216 | 0.1547 | NS |
| | pH | 0.0012 | 0.0086 | NS |
| | DIC | 0.0541 | 0.4003 | NS |
| | $pCO_2$ | 0.0626 | 0.4677 | NS |
| | $\Omega_{Ca}$ | 0.0228 | 0.1635 | NS |
| | $\Omega_{Ar}$ | 0.0270 | 0.1942 | NS |
| $CaCO_3$ precipitation rate | TA | 0.8862 | 54.500 | *** |
| | pH | 0.4221 | 5.112 | NS |
| | DIC | 0.8210 | 32.110 | *** |
| | $pCO_2$ | 0.0008 | 0.005 | NS |
| | $\Omega_{Ca}$ | 0.8658 | 45.180 | *** |
| | $\Omega_{Ar}$ | 0.8659 | 45.210 | *** |

## 5.5. Discussion

Increasing TA had no influence on *Synechococcus* 8806 growth rate (μ) but *Synechococcus* 8806 grown under higher TA had smaller cells and higher [Ca] compared to cells grown under ambient TA. Additionally, the growth of *Synechococcus* 8806 had a large influence on the localised carbonate chemistry. As *Synechococcus* 8806 biomass first began to increase, there was a decrease in DIC and $pCO_2$ causing pH and $\Omega_{Ca}$ to increase (TA remained unchanged for the first several days). Once pH reached ~10, TA, pH, and $\Omega_{Ca}$ began to rapidly decrease suggesting that $CaCO_3$ was being precipitated out of solution. The greatest decrease in TA (and $\Omega_{Ca}$) occurred in the highest TA treatment (E2000), followed by the E1000 treatment and the lowest TA treatment (Ambient) saw the smallest change in TA (and $\Omega_{Ca}$). This is likely because there was more TA ($[HCO_3^-]$ and $[CO_3^{2-}]$) to precipitate in the elevated TA treatments compared to the Ambient treatment. It is unclear whether this $CaCO_3$ precipitation was a result of *Synechococcus* 8806 actively taking TA out of solution for their

own biological advantage, or whether *Synechococcus* 8806 were simply changing seawater chemistry so that $CaCO_3$ could spontaneously precipitate. The next part of this section will consider this by first describing and explaining the influence increasing TA had on *Synechococcus* 8806 physiology, and then by explaining the effect *Synechococcus* 8806 had on localised carbonate chemistry.

### 5.5.1. Effect of increasing total alkalinity on *Synechococcus* 8806 physiology (cell density, growth rates, cell size, calcium content)

Figure 5.2 a suggests that the *Synechococcus* 8806 culture continued growing until day 39. However, after day 22, DIC was depleted from solution meaning that the *Synechococcus* 8806 cells could not use either $CO_2$ or $HCO_3^-$ for photosynthesis and so growth should not occur. This paradox could be explained by a couple of reasons: either the DIC values were incorrect or there was an error in the Chl-*a* florescence readings. As DIC was calculated using pH values, which as discussed are the less robust measured parameter, any errors in DIC likely resulted from errors in pH. Therefore, pH was adjusted to ± 0.05 to take into account an errors associated with pH measurements. However, DIC still reached near 0 levels by day 27 when pH was adjusted to ± 0.05. Therefore, it is likely an issue with the florescence readings. A potential cause of this error could be the $CaCO_3$ precipitate formed after day 19 was interfering with the fluorescence readings making it appear that Chl- *a* biomass was increasing when in actuality it was not. Therefore, to correct for this error, growth rates were only calculated for the period it is certain growth occurred (day 0-22).

It was hypothesised that increasing TA would increase in *Synechococcus* 8806 growth. There was significant difference in *Synechococcus* 8806 μ between the three treatments (Ambient, E1000, and E2000). However, the ANOVA analysis was only weakly significant ($F = 5.436$, $p < 0.05$) and there was no significant regression relationship between TA and μ. This means that these results are not enough to confidently say that *Synechococcus* 8806 growth was influenced by increasing TA. Therefore, this hypothesis was rejected.

Because *Synechococcus* 8806 is a calcifying strain of cyanobacteria, it would make sense that increasing TA causes an increase in μ because elevated TA creates a growth environment with higher $\Omega_{CaCO3}$ and so improving the conditions for growth by making $CaCO_3$ precipitation easier. This has previously been seen in other calcifying marine species such as coccolithophores and corals (Bach et al. 2011a; Fukuda et al. 2014; Albright et al. 2016).

Therefore, it is strange that there was no increase in *Synechococcus* 8806 growth with increasing TA seen in this study, especially because there was an increase in *Synechococcus* 8806 $CaCO_3$ precipitation rate. This is opposite the results from Chapter 4, where *Synechococcus* 8806 µ increased with increasing TA. The discrepancy in results between Chapter 4 and this one may be explained because the *Synechococcus* 8806 cells never reached exponential growth in the experiment performed as part of this Chapter (Figure 5.2 a). In similar experiments performed as part of this study, the *Synechococcus* 8806 cultures did not reach exponential growth either (Appendix F). The slow growth is likely a result of the relatively low growth light (50 µmol photons $m^{-2}$ $s^{-1}$) because when grown at 200 µmol photons $m^{-2}$ $s^{-1}$ in a previous experiment (See Chapter 4), peak growth occurred after ~7 days. At lower light, the *Synechococcus* 8806 cells were probably light limited and so growth was primary influenced by light. Whereas when grown at 200 µmol photons $m^{-2}$ $s^{-1}$, the *Synechococcus* 8806 cultures were not light limited and so more strongly influenced by changing carbonate chemistry.

Contradictory to this present study, Lee et al. (2004) found that cultures of *Synechococcus* 8806 grown at higher TA (by increasing [$NaHCO_3$]) did have higher cell densities by the end of their experiment despite having a similar growth light to the one used in this study ( 28 µmol photons $m^{-2}$ $s^{-1}$). The discrepancy between this study and Lee et al. (2004) may be explained by how cell density was measured. Lee et al. (2004) monitored cell density by direct microscopic counts, however Chl-*a* fluorescence and flow cytometry was used in this study. TA may not influence the amount of Chl-*a* (or other photosynthetic pigments as there was also no difference in phycocyanin fluorescence between TA treatments) but could still influence the number of cells. In other words, cultures grown at elevated TA may have higher number of cells compared to cultures grown at low TA (which is what Lee et al. (2004) showed in their study) but each individual cell has less Chl-*a* per cell compared to cells grown at low TA. This would result in the cells grown at elevated and low TA having similar Chl-*a* fluorescence signals. The smaller cell sizes at elevated TA (Figure 5.2c, and thus lower Chl-*a*) support this hypothesis. Therefore, if the higher TA treatments have more cells but each individual cell is smaller, then that could explain why there was no change in Chl-*a* florescence overall. However, the flow cytometry data and SEM image analysis showed that there was no obvious difference in *Synechococcus* 8806 cell densities between the different TA treatments. Although, the SEM images were taken for individual cell analysis rather than culture cell counts and so there were few images that could be used for cell density

approximations. Further, the samples for flow cytometry analysis were taken at the start of the experiment, and as such *Synechococcus* 8806 cells may not have been fully acclimatised to the elevated TA. Although the results from this study imply that increasing TA results in smaller *Synechococcus* 8806 cell surfaces area, they are ambiguous on the impact of TA on the cell density/Chl-*a* ratio.

Increasing TA may have caused smaller cell surface areas due to $CO_2$ limitation. The highest TA treatment, E2000, had the lowest $pCO_2$ and Sommer et al. (2015) showed that phytoplankton cell size decreased under $CO_2$ limitation. Cyanobacteria can use both $CO_2$ and $HCO_3$ for photosynthesis (Price et al. 2008). After day 12, $pCO_2$ of all three TA treatments were near zero and the samples for SEM analysis were collected on day 22. Therefore, it could be that using $HCO_3^-$ as the inorganic carbon source meant that the *Synechococcus* 8806 cells spent more energy on photosynthesis rather than cell growth.

Another explanation could be that nutrient (nitrate, $NO_3^-$ or phosphate, $PO_4^{3-}$) stress caused the smaller cell surface of the *Synechococcus* 8806 cells grown under the E2000 treatment. A study by Peter and Sommer (2013) found that for a range of phytoplankton taxa, cell size decreased when limited by nutrients. In this study, the absolute concentrations of $NO_3^-$ and $PO_4^{3-}$ were the same in all three TA treatments (880 and 37 µmol $L^{-1}$ for $NO_3^-$ and $PO_4^{3-}$ respectively). However, when compared to total DIC, the highest TA treatment (E2000) had lower $NO_3^-$ : DIC and $PO_4^{3-}$ : DIC compared to the Ambient and E1000 treatments (Table 5.5).

*Table 5.5. Nutrient to DIC ratios for each of the TA treatments*

| Treatment | $NO_3^-$ : DIC | $PO_4^{3-}$ : DIC |
|---|---|---|
| Ambient | 0.46 | 0.019 |
| E1000 | 0.40 | 0.016 |
| E2000 | 0.37 | 0.015 |

## 5.5.2. *Synechococcus* 8806 influence on carbonate chemistry

*5.5.2.a. Influence on total alkalinity*

It was hypothesised that a higher rate of $CaCO_3$ precipitation would be induced by the highest TA treatment (E2000), followed by E1000 and the lowest TA treatment (Ambient) would have the lowest rates of $CaCO_3$ precipitation. There was a ~28% increase in $CaCO_3$ precipitation in the E1000 treatment compared to the Ambient treatment and a ~89% increase in $CaCO_3$ precipitation in the E2000 treatment compared Ambient treatment. E2000 had the highest $\Omega_{Ca}$ throughout the experiment, and so the most thermodynamically favourable conditions for $CaCO_3$ precipitation. This is supported by a statistically significant relationship between both TA and $CaCO_3$ precipitation rate ($R^2 = 0.8862$, $F = 54.5$, $p < 0.001$) and $\Omega_{Ca}$ and $CaCO_3$ precipitation rate (Figure 5.7e; $R^2 = 0.8658$, $F = 45.18$, $p < 0.001$).

Evidence for $CaCO_3$ precipitation is derived from the decrease in TA from all three treatments between days 19 and 27, which was most likely due to the precipitation of calcium carbonate ($CaCO_3$). Unfortunately, there was no direct evidence of $CaCO_3$ from the SEM images. However, white precipitate was seen in the concentrated culture samples (Figure 5.3), and there was a substantial increase in Ca content ([$^{43}$Ca]) of the *Synechococcus* 8806 cells between day 19 and 27 (which occurred simultaneously to the TA decrease). Therefore, it could be that the precipitate was lost during the SEM preparation. Either because it did not stick to the glass coverslip or was dissolved when the condensed sample was vortexed and so why no $CaCO_3$ was seen on the SEM images. Further, there was evidence of Ca on *Synechococcus* 8806 cells grown under elevated TA (Figure 5.8) from a separate culture of *Synechococcus* 8806 from a different experiment that is discussed further in Chapter 4. The cells were examined using SEM-EDS (Energy Dispersive X-ray Spectroscopy) and instead of centrifuging the samples and fixing onto coverslips using glutaraldehyde, the sample was simply filtered onto polycarbonate filters before SEM-EDS analysis. In addition, studies by Lee et al. (2004) and Lee et al. (2006) have also shown that *Synechococcus* 8806 is associated with $CaCO_3$ precipitate when cultured under high TA (by increasing [$HCO_3^-$]).

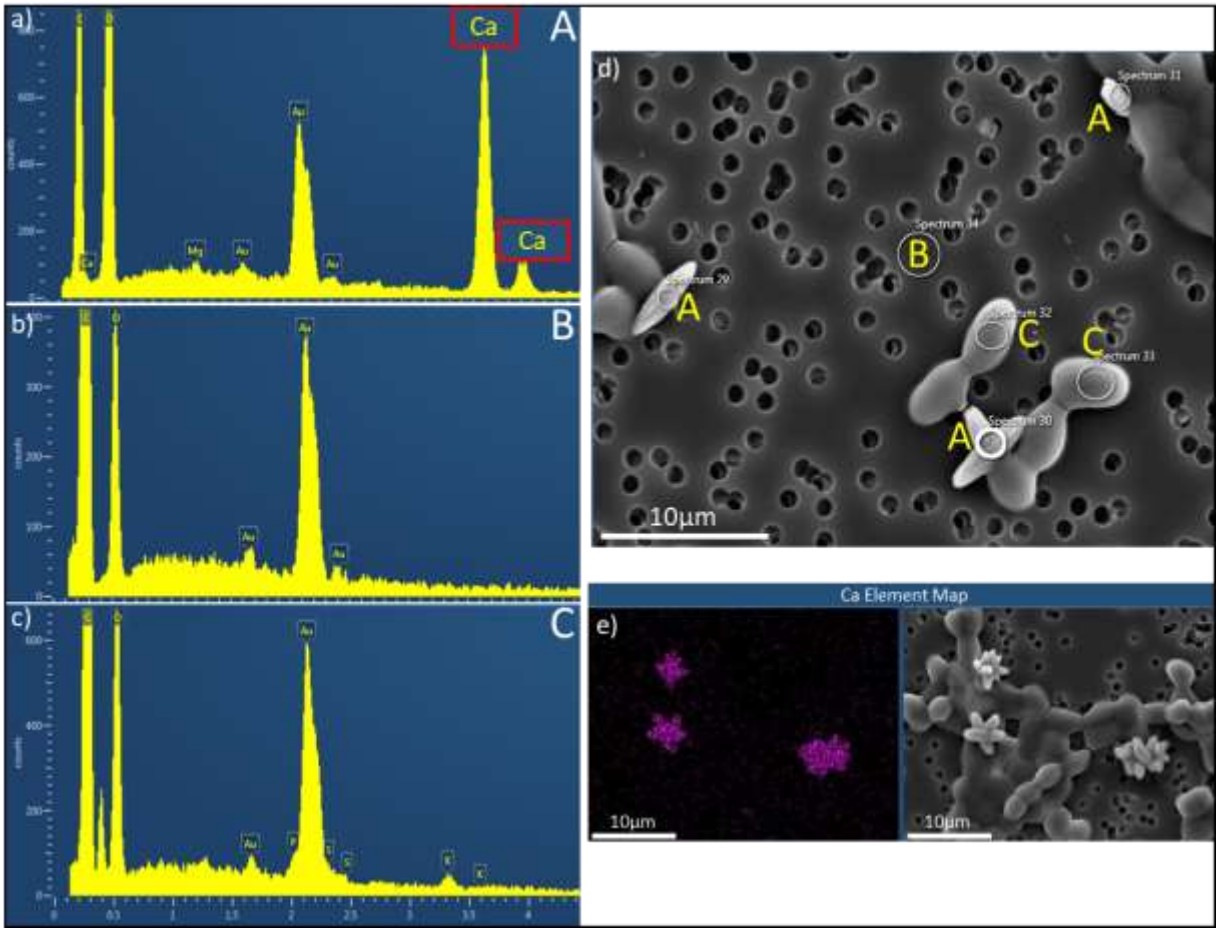


*Figure 5.8. Results from SEM-EDS analysis of Synechococcus 8806 cells cultured under elevated TA in a similar but separate experiment performed at Mount Allison University, Sackville, Canada (see Results Chapter 4 for more information). Results of elemental ID spectra of $CaCO_3$ precipitate (a), polycarbonate filter background (b), and Synechococcus cells (c) taken from SEM image of the Synechococcus 8806 culture sample (d). Ca element map of Synechococcus 8806 cells (e).*

There was little change in TA (and almost no [$^{43}$Ca] present on the cells) until after day 19 of the experiment. This delay before the start of the decrease in TA has occurred in previous studies investigating calcifying strains of *Synechococcus* (Lee et al. 2006; Xu et al. 2019). Between day 0 and 19, TA remained constant but there was an increase in pH and $\Omega_{Ca}$ and a simultaneous decrease in $pCO_2$ and DIC. This increase in pH and $\Omega_{Ca}$ would create favourable conditions for $CaCO_3$ precipitation. Xu et al. (2019) suggest that the precipitates formed by calcifying strains of *Synechococcus* are unstable and likely to be amorphous calcium carbonate. They suggest that the delay in the decrease in TA is because before local supersaturation state is reached, amorphous calcium carbonate is precipitated and

subsequently dissolves into solution. However, as *Synechococcus* spp. grows and photosynthesises, it consumes $CO_2$, increases pH and raises $\Omega_{Ca}$ such that amorphous calcium carbonate precipitates. Instead, all three TA treatments reach a maximum pH of ~10 before TA begins to decrease. Therefore, it appears that pH is a more controlling factor on $CaCO_3$ precipitation.

*5.5.2.b Influence on pH and $pCO_2$*

Each TA treatment had different starting pH. However, by day 12, the pH for all three treatments was ~9 and all increased at a similar rate to ~10 by day 19. Additionally, by day 12, $pCO_2$ had reached near-zero values in all three treatments. A similar pattern of $CO_2$ depletion was seen in the cultures of *Synechococcus* in the experiment by Lee et al. (2006). They found that after 4-5 days, pH = 10 and near zero-values of $[CO_2]$ and $pCO_2$ were reached. Because each culture flask is a closed system as the cyanobacteria grow, they photosynthesise and remove $CO_2$ from the system. As a result, pH and $\Omega_{Ca}$ increased and DIC and $pCO_2$ decreased.

Up to day 12, there was a difference in the rate of change in pH between the TA treatments. For the Ambient treatment, pH increased by 0.09 pH units per day, whereas for the elevated treatments, pH increased by 0.04-0.05 pH units per day. This change in pH is possibly due to the change in $pCO_2$ between the TA treatments. The starting $pCO_2$ value for the Ambient treatment was ~ 300% higher than the E1000 treatment and 750% higher than the E2000 treatment and by day 12, $CO_2$ was nearly fully depleted in all treatments. Implying that the *Synechococcus* 8806 culture in the Ambient treatment took up more $CO_2$ than the cultures from the other treatments and so driving the bigger increase in pH. However, there was no statistically significant difference in instantaneous growth rates between the treatments for this period (Table 5.1).

This discrepancy could be explained because even though *Synechococcus* spp. can use both $CO_2$ and $HCO_3^-$ for photosynthesis, they more readily take up $CO_2$ (Badger and Andrews 1982; Price et al. 1998; Price et al. 2008). This could explain why there was no difference in IGR but a significant difference in the uptake of $pCO_2$ and pH increase. In other words, when there is $CO_{2(aq)}$, they will rapidly use that for photosynthesis and when $CO_2$ is depleted, they then start to uptake $HCO_3^-$. Therefore, as the Ambient treatment had much more starting $CO_2$, there was there was a bigger decrease in $pCO_2$ and increase in pH between day 0-12 for the Ambient treatment compared to the elevated TA treatments (E1000 and E2000). However, as

the *Synechococcus* 8806 cultures can use both $CO_2$ and $HCO_3^-$ for photosynthesis, growth was never limited and so why there was no difference in growth rates This also explains why there was still growth even when $pCO_2$ reached near zero values by day 12 as the *Synechococcus* 8806 cultures were using $HCO_3^-$ as their source of inorganic carbon for photosynthesis.

### 5.5.3. *Synechococcus* 8806 controlled calcification or biologically induced precipitation?

There are two forms of biological calcification: biologically controlled and biologically induced (Riding and Liang 2005). Biologically controlled is when organisms closely regulate their calcification whereas biologically induced calcification is metabolically mediated but mainly dependent on ambient water chemistry (Riding and Liang 2005). The decrease in TA between day 19 and 27 is clearly due to TA being removed from solution due to $CaCO_3$ precipitation. However, because there was no significant relationship between TA and *Synechococcus* 8806 µ and there was no evidence of structural $CaCO_3$ precipitate (such as coccoliths or sheaths) attached to or next to the cells, then it is not clear whether this removal of TA was due to biologically controlled calcification by the *Synechococcus* 8806 cells. If the *Synechococcus* 8806 cells were actively controlling $CaCO_3$ precipitation, then it might be expected to see a simultaneous increase in growth rate (µ), which has previously been seen in calcifying organisms such as coccolithophores (Balch et al. 1992; Sett et al. 2014; Feng et al. 2017b). However, in this study there was no increase in µ despite an increase in $CaCO_3$ precipitation when the *Synechococcus* 8806 cultures were grown in the elevated TA treatments. Further, if the *Synechococcus* 8806 cells were actively calcifying in a similar way to how coccolithophores build their $CaCO_3$ coccoliths, it might be expected that the $CaCO_3$ precipitate found would be structurally developed and attached to the *Synechococcus* 8806 cells. Instead, the SEM-EDS analysis showed small Ca-rich forms attached to the cell rather than regularly formed structures (Figure 5.8).

Alternatively, it could be that *Synechococcus* 8806 photosynthesis raised the media $\Omega_{Ca}$ high enough so that by day 19, spontaneous abiotic precipitation of $CaCO_3$ occurred. Several studies have shown that spontaneous precipitation can occur if seawater $\Omega_{Ca}$ ~20 ((Pytkowicz 1965; Mucci and Morse 1983; Mucci 1986; Morse and He 1993). However, this is unlikely for three reasons. Firstly, in this study, all the TA treatments achieved $\Omega_{Ca}$ >20 by day 1 for the E2000 treatment and day 12 for the E1000 and Ambient TA treatments and there still was

no decrease in TA until day 19. This suggests there is more to $CaCO_3$ precipitation than surpassing a critical $\Omega_{Ca}$ threshold. Secondly, when the $CaCO_3$ precipitation rate from this experiment was compared to the $CaCO_3$ precipitation rate from abiotic precipitation studies (Figure 5.9; Mucci and Morse 1983; Mucci 1986; Mucci et al. 1989; Lopez et al. 2009), it is clear that the precipitation rate from this experiment is greater (by an order of magnitude) than what might be expected from abiotic precipitation alone. Thirdly, the Ca-rich forms in Figure 5.7 are different in morphology to the spontaneously precipitated calcite from an un-seeded experiment by Donnet et al. (2005), which were of a cuboid morphology. Instead, the Ca-rich forms in Figure 5.8 have a similar morphology to the $CaCO_3$ precipitate formed using calcite seeds in the same experiment by Donnet et al. (2005). This suggests that the *Synechococcus* 8806 cells acted as a seed for $CaCO_3$ precipitation and the reduction in TA was not a result of abiotic, spontaneous precipitation. This could also explain the why there was an increase in [Ca] of the *Synechococcus* 8806 cells grown in the elevated TA treatments (Figure 5.5 c).

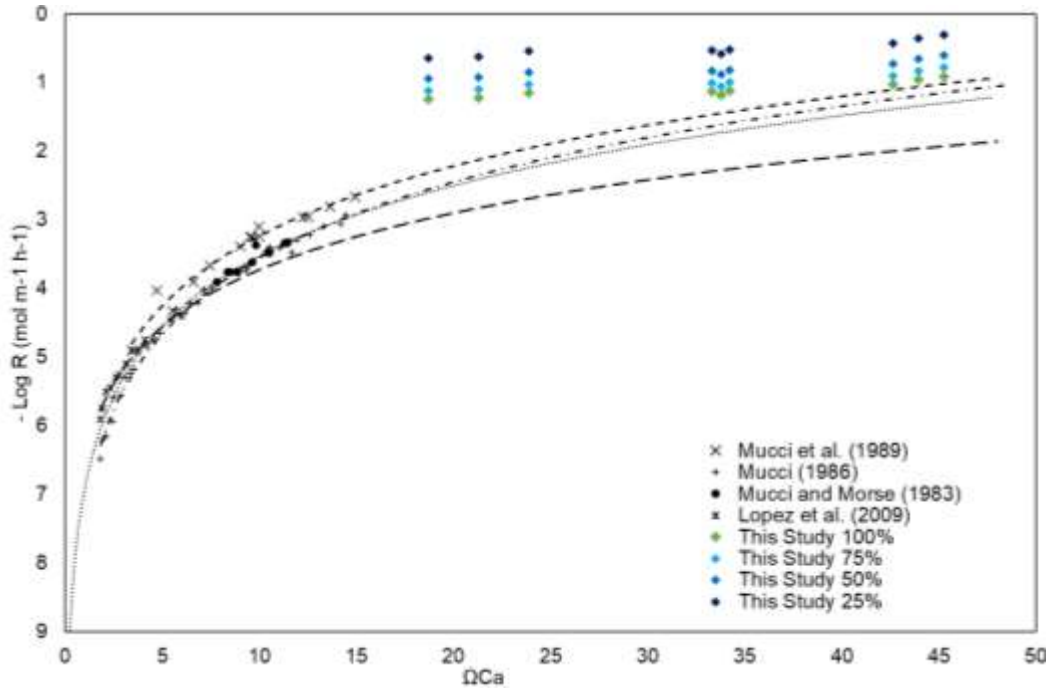


*Figure 5.9. Comparison between Log $CaCO_3$ precipitation rate (R, mol $m^{-1}$ $hr^{-1}$) from this study and from experiments by Mucci et al (1989), Mucci (1986), Mucci and Morse (1983), and Lopez et al (2009). The different percentages (e.g. This Study 100%) denote the percentage of Synechococcus 8806 cell surface area assumed to be an active nucleation site. For example, "This Study 100%" assumes that 100% of the surface area was an active nucleation site whereas "This Study 25%" assumes only 25% of the surface area was an active nucleation site.*

Although the decrease in TA between day 19 and 27 may not have resulted from direct calcification by *Synechococcus* 8806, these results suggest that $CaCO_3$ precipitation could not have occurred without the *Synechococcus* 8806 cells acting as a nucleation site or by increasing the pH and $\Omega_{Ca}$. For all three TA treatments, as *Synechococcus* 8806 grew they photosynthesised which removed $CO_2$ creating more favourable conditions for $CaCO_3$ precipitation. In addition to the increase in pH and $\Omega_{Ca}$, as cell densities increased, the number of nucleation sites for $CaCO_3$ precipitation increased. Both these factors created favourable conditions for $CaCO_3$ precipitation to occur.

The question still remains whether this was a direct result of *Synechococcus* 8806 physiology or whether it would have occurred by any other photosynthesising phytoplankton of a similar size. Cyanobacteria have efficient carbon concentrating mechanisms (CCMs) which allow them to continue growing at low $pCO_2$ levels because they can use $HCO_3^-$ as an inorganic source when $CO_2$ is depleted. This means cyanobacteria can increase the surrounding seawater pH and $\Omega_{Ca}$ much more than other phytoplankton and so create much more favourable conditions for $CaCO_3$ precipitation. Lee et al. (2004) screened several species in the genera *Seynechococcus* and *Synechocystis* and found that although all strains tested have the ability to calcify only *Synechococcus* strains PCC 8806 and PCC 8807 were able to calcify to the extent $CaCO_3$ precipitate was formed. They suggest the reason for this is because in these strains their CCMs begin working sooner and are induced at higher $CO_2$ concentrations than other cyanobacteria. Lee et al. (2004) found that that $CO_2$ removal and subsequent increase in "alkaline pH" had the greatest influence on $CaCO_3$ precipitation. Therefore, not all strains of cyanobacteria "calcify" because they don't generate enough "alkaline pH". This also could explain why the higher TA treatment had a higher rate of $CaCO_3$ precipitation because the treatment started with lower $CO_2$ and so the cultures in those treatments induced their CCMs earlier on.

Although the above evidence does appear to suggest *Synechococcus* 8806 physiology could promote $CaCO_3$ precipitation, no control was set up as part of this study and so these results do not conclusively show that it was a specific part of *Synechococcus* 8806 biology which resulted in the production of $CaCO_3$. These results simply show that the very high saturation states achieved by day 19 and the increase nucleation sites resulted in $CaCO_3$ precipitation. Therefore, the hypothesis that increasing TA would cause an increase in *Synechococcus* 8806 $CaCO_3$ precipitation rates cannot be accepted. In order to test this hypothesis and truly know whether it was the presence of *Synechococcus* 8806 in particular which caused $CaCO_3$ to

precipitate, a similar experiment needs to be performed but with other *Synechococcus* strains, other similar sized phytoplankton species, and inorganic seeds. Further, detailed analysis on *Synechococcus* 8806 photosynthesising mechanisms and CCMs is needed to test the theory proposed by Lee et al. (2004).

## 5.6. Conclusions and implications for ocean alkalinity enhancement

It was hypothesised that increasing TA would cause an increase in *Synechococcus* 8806 growth rates. The results from this investigation suggest that increasing TA does not have a significant impact on the growth of *Synechococcus* 8806. However, increasing TA did not appear to have any detrimental impacts on *Synechococcus* 8806 physiology as even though *Synechococcus* 8806 growth rates did not increase with TA, they did not decrease with TA either. However, increasing TA did cause significantly smaller cell size, which has important implications with regards to carbon export from the surface ocean. An important carbon sink is the vertical flux of organic carbon from the surface to the deep ocean, often referred to as the "biological carbon pump". The heavier and larger the cell, the deeper the cell will sink before remineralisation in surface waters, and so the more efficient the biological carbon pump. Therefore, smaller *Synechococcus* cells could mean that more organic carbon is remineralised in the surface ocean. Smaller cells would also cause substantial changes to food web dynamics as phytoplankton cell size fundamentally influences the structure and function of marine ecosystems (Finkel 2007). However, not enough evidence was collected from this experiment to prove this and so further research into how TA influences phytoplankton cell size is needed.

It was also hypothesised that increasing TA would cause an increase in *Synechococcus* 8806 $CaCO_3$ precipitation rates. Although these results show that under higher TA, higher rates of $CaCO_3$ precipitation rates occurred, they do not show that this was purely down to *Synechococcus* 8806 growth. Therefore, the hypothesis that increasing TA would cause an increase in *Synechococcus* 8806 $CaCO_3$ precipitation rates cannot be accepted. Even though these results do not show that it was specifically *Synechococcus* 8806 which caused an increase in $CaCO_3$ precipitation, they do raise an interesting question regarding the role of nucleation seeds in $CaCO_3$ precipitation. The availability of nucleation sites for $CaCO_3$ precipitation in the surface ocean is limited due to the presence of magnesium, phosphate, and sulphate ions in seawater (Burton and Walter, 1990, Mucci 1986, Bots et al., 2011, and Tand et al., 2012). It is believed that these ions inhibit $CaCO_3$ precipitation by adsorption on

to the calcite surface area. Therefore, if the phytoplankton cells can act as "seeds" for $CaCO_3$ precipitation by increase the available surface area for calcite, under elevated TA conditions from OAE could promote increased spontaneous $CaCO_3$ precipitation out of seawater.

This has important considerations regarding OAE as an increase in $CaCO_3$ precipitation would reduce the efficiency of carbon capture and could have significant implications on the marine carbon cycle. However, the media had a pH of 10 at the point at which $CaCO_3$ precipitation occurred in this experiment and in the modern ocean, pH would very rarely reach that level. This is because the removed $CO_2$ is replenished by air-sea diffusion and ocean currents. This suggests that even if OAE causes substantial perturbations to seawater carbonate chemistry, it is unlikely that marine strains of *Synechococcus*, or any phytoplankton species, will generate enough of a change in pH to induce $CaCO_3$ precipitation, even if added during a bloom.

# Chapter 6.

# General Discussion

This thesis has been one of the first to comprehensively study the response of two calcifying taxa to OAE and the findings from this thesis considerably advance knowledge in this field. The results clearly indicate that increasing seawater TA significantly increases *Corallina* spp. calcification rates. Further, elevated TA also promoted *Synechococcus* 8806 growth and increased *Corallina* spp. productivity rates. The increase in $CaCO_3$ precipitation rates has important implications for marine biogeochemistry and the efficiency of OAE as a carbon capture approach. This next chapter will go through the main conclusions and results from each results chapter and relate them to the environmental consequences of OAE and explain how they could impact the efficiency of CDR.

## 6.1. Research hypotheses and result conclusions

### 6.1.1. Chapter 2: The physiological impact of increasing ocean alkalinity on a calcifying red algae, *Corallina* spp.

The initial hypotheses were:

1. Increasing TA will create more energetically favourable conditions for $CaCO_3$ precipitation and so *Corallina* spp. calcification rates will increase under elevated TA.
2. Because photosynthesis and calcification are closely related processes in calcifying organisms, elevated TA will also cause net primary productivity and photophysiology rates to increase.

Increasing TA strongly influenced *Corallina* spp. physiology and both research hypotheses can be accepted. *Corallina* spp. net calcification rate increased significantly under elevated TA by 60% from $5.32 \pm 0.61$ µmol $CaCO_3$ $gDW^{-1}$ $h^{-1}$ when exposed to ambient TA to $8.51 \pm 0.55$ µmol $CaCO_3$ $gDW^{-1}$ $h^{-1}$ when exposed to elevated TA. This was in part due to a substantial increase in both light and dark calcification rates. Additionally, *Corallina* spp. net primary productivity appears to increase by at least ~50% from ($0.21 \pm 0.06$ mg $C_{org}$ $gDW^{-1}$ $h^{-1}$ to $0.32 \pm 0.1$ mg $C_{org}$ $gDW^{-1}$ $h^{-1}$ when exposed to elevated TA compared to ambient TA. Further, $CaCO_3$ content of *Corallina* spp. increased by ~ 3% when exposed to elevated TA.

However, increasing TA did not strongly influence *Corallina* spp. photophysiology. There was no significant relationship between $rETR_{max,}$ α, $E_k$, and TA and only a weak significant positive linear relationship between $F_v/F_m$ and TA ($R^2 = 0.1563$, $p < 0.01$).

### 6.1.2. Chapter 3: Ocean alkalinity enhancement through olivine dissolution and the physiological impact this has on *Corallina* spp.

The initial hypotheses were:

1. Olivine dissolution:
    a. As olivine dissolves, TA, pH, DIC and $\Omega_{Ca}$, and $\Omega_{Ar}$ would all increase.
    b. As olivine dissolves, trace metals such as Cu, Fe, Ni, Cr, and Zn will be released into the solution.
2. *Corallina* spp. response:
    a. *Corallina* spp. grown under elevated TA + olivine treatment will have lower calcification and primary productivity rates due to toxicity effects of the trace metals released into solution.

Olivine dissolution resulted in reduced seawater TA, therefore hypothesis 1a was rejected. Initial TA of 2550 µEq $L^{-1}$ decreased to 1660 µEq $L^{-1}$ after 27 days of olivine dissolution. Olivine dissolution also resulted in lower pH, DIC, $\Omega_{Ca}$, and $\Omega_{Ar.}$ XRD analysis provided evidence that hydrated magnesite ($Mg_5(CO_3)_4(OH)_2.4H_2O$) precipitated out of solution. Even though TA did not increase, ICP-OES analysis showed that [Zn], [Cu], [Mg], and [$SiO_2$] of seawater increased substantially after olivine dissolution. Further, XRD analysis of the olivine samples indicate that Ni and Cr were also released into the solution, leading to the acceptance of hypothesis 1b.

The aim of the second part of this chapter was to determine the physiological response of *Corallina* spp. to olivine dissolution. XRF analysis showed that there were considerably higher [CuO], $[FeO]_{total}$, [NiO], [$Cr_2O_3$], and [ZnO] in the *Corallina* spp. samples exposed to the Elevated TA + Olivine treatment. The *Corallina* spp. samples exposed to the elevated TA seawater with no dissolution products had the highest values of NCR, and NPP and (3.96 ± 0.61 µmol $CaCO_3$ $gDW^{-1}$ $hr^{-1}$ and -10.21 ± 1.59 µmol DIC $gDW^{-1}$ $hr^{-1}$ respectively). Followed by the *Corallina* spp. samples exposed to the elevated TA seawater and olivine

dissolution products (2.73 ± 0.47 µmol $CaCO_3$ $gDW^{-1}$ $hr^{-1}$ and -8.06 ± 1.73 µmol DIC $gDW^{-1}$ $hr^{-1}$ for NCR and NPP respectively). The control group (*Corallina* spp. samples exposed to ambient seawater and no dissolution products) had the lowest values of NCR and NPP (2.37 ± 0.47 µmol $CaCO_3$ $gDW^{-1}$ $hr^{-1}$ and -7.20 ± 0.74 µmol DIC $gDW^{-1}$ $hr^{-1}$ respectively). The *Corallina* spp. photophysiological parameters ($F_v/F_m$, $_rETR_{max}$, $E_k$, and α) were not significantly influenced by either changing TA or exposure to olivine dissolution products. These results indicate that the incorporation of trace metals had a somewhat toxic effect on *Corallina* spp. physiology and an acceptance of the hypothesis 2.

### 6.1.3. Chapter 4: The impact of increasing ocean alkalinity on the growth and photophysiology of a calcifying strain of *Synechococcus*.

The initial hypotheses were:

1) Increasing TA will cause $[CO_{2(aq)}]$ to decrease and so:
    a) Decrease *Synechococcus* 8806 growth rates.
    b) Decrease *Synechococcus* 8806 photosynthetic efficiency therefore decreasing ETR, Y(PSII) through changes to $\sigma_{PSII}$' and ρ' and $\tau_1$.

An increase in ~2500 µEq $L^{-1}$ resulted in *Synechococcus* 8806 µ to increase from 0.005 $hr^{-1}$ (at ~900 µEq $L^{-1}$) to 0.015 $hr^{-1}$ (at ~3400 µEq $L^{-1}$). However, the results from this study do not conclusively show that the changes to *Synechococcus* 8806 growth rates were due to changes in $[CO_{2(aq)}]$. Increasing TA resulted in a linear increase in *Synechococcus* 8806 growth rates (µ, $hr^{-1}$) but a nonlinear increase in the photophysiological parameters. Although the increase was not linear, *Synechococcus* 8806 cells cultured under elevated TA, had lower values of α and $Y(PSII)_{max}$ than those cultured under lower TA. Therefore, the hypothesis that increasing TA will cause *Synechococcus* 8806 photosynthetic efficiency to decrease can be accepted.

### 6.1.4. Chapter 5: The physiological impact of increasing ocean alkalinity on $CaCO_3$ precipitation by a calcifying strain of *Synechococcus*.

The initial hypotheses were:

1. Increasing TA will cause an increase in *Synechococcus* 8806 growth rates

2. Increasing TA will cause an increase in *Synechococcus* 8806 $CaCO_3$ precipitation.

3. *Synechococcus* 8806 growth will significantly alter the local carbonate chemistry.

Increasing TA had no significant influence on *Synechococcus* 8806 growth rates ($\mu$ day $^{-1}$) and so hypothesis 1 was rejected. However, *Synechococcus* 8806 grown under higher TA had smaller cells and higher [$^{43}$Ca] compared to cells grown under ambient TA. Evidence for $CaCO_3$ precipitation included white precipitate in concentrated culture samples, SEM-EDS detection of a Ca rich substance next to the *Synechococcus* 8806 cells, and the ~7000% increase in Ca content ([$^{43}$Ca]) of the *Synechococcus* 8806 cells cultured under the highest TA treatments compared to the lowest TA treatment, and from SEM-EDS. However, there was not enough direct evidence to suggest that this $CaCO_3$ precipitation was caused by *Synechococcus* 8806 physiology. Therefore, the hypothesis that increasing TA would cause an increase in *Synechococcus* 8806 $CaCO_3$ precipitation rates cannot be accepted. The growth of *Synechococcus* 8806 in all TA treatments had a large influence on the local carbonate chemistry, therefore hypothesis 3 was accepted. As *Synechococcus* 8806 biomass first began to increase, there was a decrease in DIC and $pCO_2$ causing pH and $\Omega_{Ca}$ to increase (TA remained unchanged for the first several days). Once pH reached ~10, TA, pH, and $\Omega_{Ca}$ began to rapidly decrease suggesting that $CaCO_3$ was being precipitated out of solution.

## 6.2. Implications for global ocean alkalinity enhancement

### 6.2.1. Implications from calcifying macroalgae and cyanobacteria

As OAE will perturb seawater carbonate chemistry parameters such as pH and $\Omega_{CaCO3}$ then calcifying organisms will likely be most impacted by these changes. The two different taxa of calcifying organism investigated in this thesis were chosen to improve the understanding of how calcifying organisms will respond to OAE despite having limited laboratory facilities and time restrictions. There are many different types of calcifying organisms such as coccolithophores, foraminifera, corals, coralline macroalgae, pteropods, bivalves, etc. However, by focussing the research on both calcifying and photosynthesising organisms, the impact of TA addition on photosynthesis and the relationship between chemical and biological carbon sequestration could also be investigated. However, it was impossible to investigate the response of every single taxa of marine calcifers and so two “end members”

were chosen: a benthic, sessile calcifying macroalgae which is found in coastal regions on the continental shelf and a calcifying pico-sized phytoplankton which is found in the surface waters of deeper open ocean waters. Comparing these two different species gives an insight into two wildly different ecologies. Therefore, it was possible to investigate whether the size of the organism, how they calcify, and what habitat they live in affects how a species responds to increased TA. Also, by looking at two physiologically different species which inhabit different ecosystems, it was possible to investigate how OAE will impact the wider ecosystem and food web dynamics compared to investigating two different types of pelagic open water phytoplankton species for example. Further, the contribution of macroalgae and phytoplankton to the marine carbon cycle are also different and so investigating the response to *Corallina* spp. and *Synechococcus* 8806 will allow a better understand the longevity of ocean carbon storage via OAE.

The next two sections will outline in more detail what this increase in calcification rates means with regards to the influence of OAE on coastal macroalgae and pelagic, open water species. First the environmental response will be discussed in terms of the impact on ecosystems, food web dynamics, ocean acidification mitigation and the impact on marine biogeochemical cycles. Secondly, the efficiency of OAE as a CDR approach will be discussed in terms of how changes to calcification rates will impact seawater $pCO_2$ and how this in turn could influence the timescales in which the ocean can store atmospheric $CO_2$ as TA.

## 6.2.2. Environmental response: implications from *Corallina* spp.

### *6.2.2.a. Increased calcification and productivity and ocean acidification mitigation*

Increasing TA was observed not to be detrimental for *Corallina* spp. with respect to calcification or photosynthesis. Results from Chapters 2 and 3 showed that calcification rates increased with increasing TA. Calcification rates were higher when *Corallina* spp. was grown under elevated TA from both $Na_2CO_3$ addition and olivine dissolution compared to when *Corallina* spp. was grown under ambient TA. However, the increase in *Corallina* spp. calcification rates was greater when TA was manipulated by added $Na_2CO_3$ to solution compared to when TA was increased by dissolving olivine. This demonstrates that trace metal uptake does have some detrimental impacts on *Corallina* spp. physiology. However, the positive impact of increased TA had a stronger influence because calcification rates still increased.

As well as increasing calcification rates, elevated TA also increased *Corallina* spp. productivity rates by ~50% compared to the control. Again, like calcification rates, the increase in *Corallina* spp. productivity rates were greater when TA was manipulated by added $Na_2CO_3$ to solution compared to when TA was increased by dissolving olivine. The similar response in calcification and productivity rates is most likely due to the strong relationship between calcification rates and photosynthesis (Pentecost 1978; Williamson et al. 2017). Therefore, these results suggest that the seawater carbonate chemistry changes induced by OAE will have two main effects on *Corallina* spp. physiology. First elevated $\Omega_{Ca}$ will promote calcification rates, which in turn will increase internal $CO_2$ which will promote photosynthesis. Secondly, decreased pH will promote photosynthesis which in turn increases $\Omega_{Ca}$ and so promotes calcification (Borowitzka 1982; Koch et al. 2013). Therefore, the findings that elevated TA promotes both *Corallina* spp. calcification and productivity rates suggest that increasing TA by $Na_2CO_3$ addition or by olivine dissolution could be used to alleviate some of the impacts of ocean acidification.

A decline in calcifying marine organisms due to ocean acidification is already being seen in certain marine environments, such as the Great Barrier Reef. Smith et al. (2020) found that between 2010 and 2016 in the Great Barrier Reef, there was a 3.1-fold decline in crustose coralline algae while non-calcifying macroalgae populations were increasing (up to 3.2-fold) due to decreasing $\Omega_{Ar}$. This highlights the importance of preventing further reductions in pH or $\Omega_{CaCO3}$ and even increasing $\Omega_{CaCO3}$ to pre-industrial values in ecosystems affected by ocean acidification through OAE. The results from Chapters 2 and 3 (showing that elevating TA causes increased $\Omega_{CaCO3}$, and pH and so creating more energetically favourable conditions for *Corallina* spp. calcification) demonstrates that OAE could help avoid further declines in calcifying coralline algae populations in ecosystems affected by ocean acidification. However, the results from Chapters 2 and 3 suggest that increasing TA without releasing trace metals might be the preferred option for OAE with regards to *Corallina* spp. physiology and ocean acidification mitigation. This is because *Corallina* spp. calcification and productivity rates did not increase by as much when TA was manipulated by dissolving olivine when compared to when TA was increased by adding $Na_2CO_3$ to solution.

*7.2.2.b. Who will benefit from elevated TA: calcifying vs non-calcifying macroalgae?*

The increase in ocean TA and $\Omega_{CaCO3}$ would cause a simultaneous decrease to ocean $pCO_2$ (see Section 1.3.). If TA is added such that it is does not have time to equilibrate with the atmosphere, ocean $pCO_2$ may decrease substantially and this will affect calcifying and non-

calcifying algae differently. If $pCO_2$ decreases much below (and if $\Omega_{CaCO3}$ increases beyond) the pre-industrial maximum due to OAE and causes disproportional changes calcifying and noncalcifying species of macro algae, there may be a significant change to macroalgae population dynamics.

In the TA addition experiments from Chapters 2 and 3, TA was increased slowly to allow atmospheric $CO_2$ to re-equilibrate with the seawater and so limit the increase in $\Omega_{Ca}$ to 8.8-12.6. However, this is still much above the pre-industrial value of $\Omega_{Ca}$, which Feely et al. 2009) predict ranged from 5.81 in the tropical Atlantic to 2.24 in the North Pacific. Further, seawater $pCO_2$ decreased to ~200-360 µatm as pH increased to 8.2 and 8.41 (TA ~3500). Low levels of $CO_2$ have been shown to negatively influence photosynthesis and growth rates in some macroalgae species (Gao et al. 1991). This is because there is less substrate being available for RubisCO, the carbon fixation enzyme under lower $CO_2$. However, there was no negative influence on *Corallina* spp. productivity or photophysiology due to this decrease in $pCO_2$. *Corallina* spp. productivity actually increased by 30-50%. For calcifying species, higher $\Omega_{CaCO3}$ results in more energetically favourable conditions for $CaCO_3$ precipitation and promotes calcification and growth. Further, the decrease in $pCO_2$ may be compensated by the increased calcification which produces $pCO_2$ as a by-product and so increases localised $pCO_2$. A similar response was seen in studies by Hofmann et al. (2012) and Gao and Zheng (2010) where *Corallina* spp. growth was higher under ambient $CO_2$ (higher $\Omega_{Ca}$) compared to elevated $CO_2$ (lower $\Omega_{Ca}$).

The results from Chapters 2 and 3 suggest that calcifying species may outcompete non-calcifying species if $\Omega_{Ca}$ increases well above preindustrial maximum values because C*orallina* spp. calcification rates increased by 60% (Chapter 2) and 70% (Chapter 3) when $\Omega_{Ca}$ was increased well above pre-industrial values ($\Omega_{Ca}$ = 8.8-12.6). This increase in calcification will likely result in a stronger skeletal structure for *Corallina* spp., faster growth, increased protection from grazers, and lower UV stress (Hofmann et al. 2012), all of which increases their potential for species dominance. Whereas, for non-calcifying species, higher $\Omega_{Ca}$ will have little influence on their physiology but lower $pCO_2$ could cause a decrease in growth and productivity because unlike calcifying species, they cannot increase internal $pCO_2$ through $CaCO_3$ precipitation. However, it should be noted that some macroalgae species have CCMs which allow them to continue photosynthesising efficiently in low $CO_2$ environments by directly using $HCO_3^-$ as the inorganic carbon source (Koch et al. 2013).

Therefore, it is possible that only macroalgae species which do not have CCMs could be outcompeted by calcifying macroalgae.

An increase in *Corallina* spp. dominance due to elevated $\Omega_{Ca}$ and decreased $pCO_2$ may cause substantial changes to coastal ecology. Changes to $CO_2$ have been shown to drive community homogenisation by the increased abundance of one or two dominant species (Kroeker et al. 2011; Inoue et al. 2013; Enochs et al. 2015) and the results from Chapters 2 and 3 suggest that *Corallina* spp. could be one of these dominating species if $pCO_2$ decreases to due to OAE. The increase in *Corallina* spp. productivity and calcification rates when cultured under elevated TA implies that potential carbonate chemistry perturbations from future OAE, will cause an increase in calcifying macroalgae in coastal ecosystems. Calcification rates increased by ~15% when TA was manipulated by dissolving olivine (compared to 60-70% when TA was increased by $Na_2CO_3$ addition). Therefore, if TA is increased via enhanced weathering (EW), these results indicate the effect would not be as pronounced.

Ecosystem processes may be compromised if there is substantial biodiversity or if there is a dominance of one species over another (Rosenfeld 2002). Especially if the species in decline has a unique role in an ecosystem's function (where function is defined in terms of energy transformation and matter cycling (Lawton and Brown 1994; Ghilarov 2000)). For a sustainable and functional ecosystem, high functional diversity is required, which means there needs to be a large number of species performing similar functions (Naeem et al. 2012; Mouillot et al. 2013; Oliver et al. 2015). This means that if one species goes into decline there are other species which can still perform that species role in the ecosystem. However, if there is only one species which can perform a role within an ecosystem and they start to decline, that role cannot be performed. Biodiversity could be reduced if OAE results in a dominance of calcifying macro algae species, such as *Corallina* spp., which the results from Chapters 2 and 3 indicate could happen. However, because *Corallina* spp. are considered "ecosystem engineers" (Johansen 1970; Jones et al. 1994; Kelaher et al. 2001; Benedetti-Cecchi 2006; Nelson 2009; van der Heijden and Kamenos 2015) it may not have such a detrimental impact on their local ecosystems if *Corallina* spp. populations increase. Increasing *Corallina* spp. populations may increase the ecosystem diversity because they often form extremely dense and highly branched turfs which can host diverse macrofaunal assemblages with up to 250,000 epiphytes per $m^2$ (Kelaher et al. 2001). Further, upright calcifying macroalgae such as *Corallina spp.* provide a niche ecological role because they offer strength and refuge to

other intertidal organisms in environments with high wave action (Stewart 1982; Coull and Wells 1983; Kelaher et al. 2001; Kelaher et al. 2003).

*6.2.2.c. Influence of increased macroalgae calcification on global biogeochemistry*

As well as potentially having a considerable influence on macroalgae community dynamics, the possible increase in calcifying macroalgae $CaCO_3$ production and decrease in noncalcifying macroalgae growth could also have a substantial influence on global biogeochemistry. Firstly, gobal coralline macroalgae inorganic carbon production is estimated to be 900 g $CaCO_3$ $m^{-2}$ $yr^{-1}$ (van der Heijden and Kamenos 2015). When the increase in *Corallina* spp. calcification rates from this thesis (60-70%) are applied to the global coralline macroalgae inorganic carbon production figure, future coralline macroalgae $CaCO_3$ production is estimated to reach between 1440-1530 g $CaCO_3$ $m^{-2}$ $yr^{-1}$. This would only be 1035 g $CaCO_3$ $m^{-2}$ $yr^{-1}$ if the 15% increase in calcification rates from EW is applied. Secondly, ecosystems where non-calcifying macroalgae species dominate such as salt marshes, mangrove forests and seagrass meadows have been identified to store 10–18% of the total ocean carbon (Kennedy and Björk 2009; Kennedy et al. 2010). Consequently, if there is a reduction to these ecosystems due to reduced $pCO_2$ from OAE then the oceanic sink for carbon could be reduced. Therefore, shifts towards a growing calcifying macroalgae population could have an important influence on marine biogeochemistry by both increasing $CaCO_3$ production through increased calcification and by decreasing carbon storage through decreasing photosynthesis of non-calcifying macro algae species.

### 6.2.3. Environmental response: implications from *Synechococcus* 8806

*6.2.3.a. Influence of light levels and carbonate chemistry on physiology*

Like *Corallina* spp., increasing TA was also observed not to be detrimental for *Synechococcus* 8806. Results from Chapter 4 showed that increasing TA promoted *Synechococcus* 8806 growth. However, the results from Chapter 5 suggested that TA had no influence on *Synechococcus* 8806 growth rates. The discrepancy between these two results is likely due to differences in experimental design. The *Synechococcus* 8806 culture experiment from Chapter 5 was performed at Oxford University using 750 mL culture flasks, a growth light of ~50 µmol photons $m^{-2}$ $s^{-1}$, using L1 media, and a TA range from ~2000-3500µEq $L^{-1}$. Whereas the experiment from Chapter 4 was performed at Mount Alison University using well plates with a media and inoculant volume of 2mL, a growth light of 200 µmol photons $m^{-2}$ $s^{-1}$, f/2 media, and an TA range of ~900-3700 µEq $L^{-1}$. Even though different media

recipes were used and different volumes of media were used in each experiment, a similar amount of inoculant was added (10-25%) and both recipes resulted in similar nutrient and salt concentrations (Appendix D). Therefore, this was unlikely to be the reason for the differing results. Similarly, the discrepancy in results is unlikely a consequence of different TA ranges investigated. When the data from the Mount Alison experiment (Chapter 4) was reanalysed using only a TA range of 1653-3370 µEq $L^{-1}$ (compared to the TA range of 1860-3550 µEq $L^{-1}$ from the Oxford University experiment in Chapter 5), there was still a positive linear regression relationship between growth rate and TA ($R^2$= 0.871, F= 33.77, p <0.01).

The most likely reason for the discrepancy between these two result chapters was the different growth lights used. It is now believed that the *Synechococcus* 8806 cells cultured at Oxford University were probably light limited and so growth was primary influenced by light. Whereas, when grown at 200 µmol photons $m^{-2}$ $s^{-1}$ at Mount Alison University, the *Synechococcus* 8806 cultures were not light limited and so more strongly influenced by changing carbonate chemistry. This would also explain why there was no obvious exponential growth period for the Oxford University *Synechococcus* 8806 growth curves. These results suggest that the primary influence of *Synechococcus* 8806 growth is light, not changing TA. Although the *Synechococcus* 8806 culture experiment from Chapter 5 was light limited, the *Synechococcus* 8806 cells still significantly altered the media carbonate chemistry and it was still possible to study the impact of *Synechococcus* 8806 growth on local carbonate chemistry and what effect elevated TA had on this.

#### *6.2.3.b. Increased growth rates and food web dynamics*

The results from Chapter 4 show that *Synechococcu*s 8806 growth rates significantly increased and biomass was higher when cultured under elevated TA. As TA increased from ~900 to ~4000 µEq $L^{-1}$ *Synechococcus* 8806 growth rates increased by 57%. However, unlike Chapter 4, the results from Chapter 5 showed that there was no significant increase in *Synechococcus* 8806 growth with increasing TA. That said, even though the results from this thesis cannot be used to predict the exact response of *Synechococcus* to OAE, they do provide an indication of the possible responses and what that means for the marine environment.

Because phytoplankton like *Synechococcus* form the foundation of the marine food, any future influence on their physiology is likely to influence the whole ecosystem by reorganising the energy flow through food webs and altering key biogeochemical processes (Dutkiewicz et al. 2015; Riebesell et al. 2017). Even slight changes to growth rates and

biomass of one species relative to another could allow one phytoplankton species to outcompete another. Phytoplankton species which will benefit from lower $pCO_2$ may become the dominant species under OAE and those in which are unresponsive to increasing TA or even negatively affected by increasing TA could be outcompeted by other species. This has been demonstrated in numerous ocean acidification studies which have shown mixed responses to changing carbonate chemistry by different phytoplankton (Tortell et al. 2002; Rost et al. 2008; Hoppe et al. 2012; Bach et al. 2017). Therefore, the increase in *Synechococcus* 8806 growth rates from elevated TA seen in Chapter 4, suggest that future changes due to OAE could potentially disrupt whole ecosystem dynamics.

*6.2.3.c Potential increased precipitation rates and impact on the global carbon cycle*

Unlike Chapters 2 and 3, where there was strong evidence to suggest that elevated TA causes an increase in Corallina spp. calcification rates, there was not enough strong evidence to suggest the same effect will be seen by *Synechococcus* 8806. The results from Chapter 5 show that under higher TA, higher rates of $CaCO_3$ precipitation rates occurred but they do not show that this was purely down to *Synechococcus* 8806 growth. Even though these results do not show that it was specifically *Synechococcus* 8806 which caused an increase in $CaCO_3$ precipitation, they do raise an interesting question regarding the role of nucleation seeds in $CaCO_3$ precipitation. An increase in TA of 1500 µEq $L^{-1}$ promoted $CaCO_3$ precipitation rates to almost double. An increase in $CaCO_3$ production of this magnitude would have substantial impact on the marine carbon cycle. It needs to be remembered that the carbonate chemistry conditions (pH ~10, $\Omega_{Ca}$ >20,) from the experiment in Chapter 5 are unlikely to occur in the natural world and so these findings do not show the likely response to future real world OAE scenarios. However, the results do show that it is possible for phytoplankton physiology to significantly alter marine carbonate chemistry and in certain, albeit extreme, conditions promote $CaCO_3$ precipitation. Spontaneous precipitation of $CaCO_3$ does not occur in the surface ocean and is believed to be due to the limited availability of nucleation sites for $CaCO_3$ precipitation because of presence of magnesium, phosphate, and sulphate ions in seawater (Burton and Walter, 1990, Mucci 1986, Bots et al., 2011, and Tand et al., 2012). It is believed that these ions inhibit $CaCO_3$ precipitation by adsorption on to the calcite surface area. Therefore, if the phytoplankton cells can act as “seeds” for $CaCO_3$ precipitation by increase the available surface area for calcite, under elevated TA conditions from OAE could promote increased spontaneous $CaCO_3$ precipitation out of seawater.

This would have considerable implications for the marine carbon cycle. Using the results from this thesis as an example. When TA is increased to 3600 µEq $L^{-1}$, and the availability of nucleation seeds increased by ~ 1300% (in this case *Synechococcus* 8806 cells but the same may be true for any similarly sized phytoplankton species), an extra ~6 nmol of $CaCO_3$ is produced per million seeds per hour. This reduces to ~2 nmol of $CaCO_3$ per million *Synechococcus* 8806 cells/seeds per hour when TA = 3000 µEq $L^{-1}$. The current annual global total abundance of *Synechococcus* spp. is ~ $7 \times 10^{26}$ cells across the global ocean (Flombaum et al. 2013). Therefore, if 100% of *Synechococcus* cells act as nucleation seeds, then each year an extra 120-360 billion tonnes of $CaCO_3$ could be produced each year (depending on whether ocean TA increases by ~500-1000 µEq $L^{-1}$). If only 1% of total *Synechococcus* cells acted as a nucleation seed, this would still result in an extra 1.2-3.6 billion tonnes of $CaCO_3$ produced per year. This represents either a 20% increase (when ΔTA = 500 µEq $L^{-1}$) or 70% increase (when ΔTA = 1000 µEq $L^{-1}$) in present-day marine $CaCO_3$ production (currently estimated as 5.3 billion tonnes of $CaCO_3$ per year (Milliman 1993). However, biogeochemical modelling studies suggest that using OAE as the sole response to mitigating carbon emissions global surface water calcite $\Omega_{CaCO3}$ would increase to ~6-7.5 (Paquay and Zebee 2013; Ilynia et al. 2013; Ferrer-Gonzalez and Ilyina 2016) which is substantially lower than the increase in $\Omega_{CaCO3}$ from Chapter 4 ($\Omega_{Ca}$ = ~13-20). Therefore, any potential increase in $CaCO_3$ production from an increase in nucleation seeds and elevated TA is likely to be much less than 2.76-3.99 × $10^5$ nmol $CaCO_3$ $yr^{-1}$. Therefore, in order to better constrain whether an increase in seawater TA from OAE would cause an increase in global marine precipitation, further experiments are needed to test the growth and CaCO3 precipitation of *Synechococcus* 8806 under much lower TA scenarios and should be compared to the growth of different phytoplankton and both seeded and unseeded controls (for more detail see Section 6.5). Also, this assumes that increasing TA will cause an increase in phytoplankton growth, and the results from this thesis only suggest that *Synechococcus* 8806 growth might increase due to elevated TA. Nonetheless, the results from this thesis still provides one of the first investigations into what the theoretical impacts to *Synechococcus* 8806 growth and the resulting impact on marine biogeochemistry could be from extreme TA addition.

### 6.2.4 Comparison of the impact of elevated total alkalinity on *Corallina* spp. and on *Synechococcus* 8806.

The main finding from this thesis is that increasing ocean TA and the resulting changes to seawater carbonate chemistry was not harmful physiologically to either *Corallina* spp. or *Synechococcus* 8806. However, elevated TA had differing effects on *Corallina* spp. and *Synechococcus* 8806 photophysiology. Increasing TA had no significant influence on *Corallina* spp. photophysiology in both Chapters 2 and 3 but elevated TA significantly influenced *Synechococcus* 8806 photophysiology. Previous studies have shown that macroalgal photosynthetic rates can be ~80% lower when exposed to low [$CO_2$(aq)](as a result of increasing pH to 9.3) compared to rates measured at ambient pH (8.1) (Middelboe and Hansen 2007). Further, a study by Williamson et al. (2014) suggests that a 92% reduction in $pCO_2$ contributed to a decrease in *Corallina officinalis* $rETR_{max}$. Therefore, it was expected that *Corallina* spp. photophysiology would have been affected by the decreased [$CO_2$(aq)] from elevated TA. However, in both Chapters 2 and 3, $pCO_2$ remained above 200 µatm whereas the reduction in *Corallina officinalis* $rETR_{max}$ from the study by Williamson et al. (2014) occurred when $pCO_2$ reached ~20 µatm. Therefore, it may be that *Corallina* spp. photophysiology is only affected when $pCO_2$ is low (e.g. less than 100 µatm).

Unlike the *Corallina* spp. experiments in Chapters 2 and 3, when the *Synechococcus* 8806 FRRf photophysiology measurements were made in Chapter 4, it is likely that $pCO_2$ was almost depleted. Due to the lack of robust pH measurements, the estimates of $pCO_2$ in this chapter are associated with large errors. However, even with these large errors, $pCO_2$ was likely less than 100 µatm. Therefore, this might explain why there was a statistically significant relationship between *Synechococcus* 8806 photophysiology and TA but no relationship between *Corallina* spp. physiology and TA. It indicates that photophysiology will only be significantly affected if OAE causes $pCO_2$ to substantially decrease (e.g. to below ~100 µatm). This may occur if TA is added to marine regions with naturally low $pCO_2$. For example, in coastal areas where carbonate chemistry can fluctuate substantially and low $pCO_2$ is possible (Hofmann et al. 2011; Williamson et al. 2014), or during a phytoplankton blooms (Schulz and Riebesell 2013; Engel et al. 2014). It is also possible to achieve low $pCO_2$ if TA addition occurs in a poorly mixed body of water with slow air-sea gas exchange resulting in "non-equilibrated OAE". Therefore, to ensure that OAE has as little impact on photophysiology, TA should be added in a way so that seawater can re-equilibrate with $CO_2$.

The difference in the photophysiological response between *Corallina* spp. and *Synechococcus* 8806 may also be due to their size difference. The *Synechococcus* 8806 cells

were ~1 µm long, whereas *Corallina* spp. fronds were ~1mm thick and could be up to 10 cm long. The smaller *Synechococcus* 8806 cells may have had a stronger response to decreasing [$CO_{2(aq}$] than *Corallina* spp. because they have a higher surface area to volume ratio and so more exposed to the changes to seawater carbonate chemistry.

## 6.3. Longevity of carbon storage

The increase in *Corallina* spp. calcification rates under elevated TA and the potential increase in $CaCO_3$ precipitation resulting from the potential increased $\Omega_{CaCO3}$ and calcite nucleation surface area (from the potential increase in *Synechococcus* cell numbers acting as seeds) could impact the efficiency of OAE as a carbon dioxide removal approach. $CaCO_3$ precipitation (calcification) lowers TA and DIC and causes an increase in $pCO_2$ (Equation 40) (Schmittner et al. 2008).

$$Ca^{2+} + 2HCO_3^- \rightarrow CaCO_3 + \boldsymbol{CO_2} + H_2O \qquad \text{(Equation 40)}$$

The increase in ocean $pCO_2$ would make the ocean less efficient at taking up atmospheric $CO_2$ by decreasing the concentration gradient across the air/surface boundary (Zeebe and Wolf-Gladrow 2001). Therefore, a substantial increase in calcification (and an increase ocean $pCO_2$) would act against the primary aim of OAE which is to increase the oceanic uptake of atmospheric $CO_2$. This process is sometimes referred to as the "carbonate counter pump" (Heinze et al. 1991). Over geological timescales, the carbonate counter pump acts to maintain relatively constant concentrations of atmospheric $CO_2$. However, OAE may cause a large enough increase to marine calcification to perturb this natural homeostasis.

The increase in seawater $pCO_2$ could be offset if OAE also causes an increase in photosynthesis. The "0.6 rule" states that for every mole of $CaCO_3$ precipitated approximately 0.6 moles of $CO_2$ are released (Ware et al. 1992). This assumes the physical and chemical properties of pre-industrial seawater (temperature = 15 ˚C, and salinity S = 35). However, it is thought that this ratio will increase as the oceans take up more $CO_2$ (Frankignoulle et al. 1994). A recent study by Kalokora et al. (2020) found that for every mol of $CO_2$ fixed in calcification, about 0.78 mol of $CO_2$ was released into the atmosphere. Therefore, this ratio can be used along with the *Corallina* spp. light calcification and primary productivity rates derived in Chapter 2 to estimate whether *Corallina* spp. exposed to increased TA acts as a sink or source of $CO_2$. If $CO_2$ produced by calcification is greater than that consumed by photosynthesis, the *Corallina* spp. would be a source. The results are

presented in Table 6.1. This is a simplification, and there are many other factors that can influence this balance, such as temperature which controls the amount of $CO_2$ released by calcification (Frankignoulle et al. 1994). However, it provides a useful indication of whether an increase to macroalgae calcification will act as a future sink or source of $CO_2$.

Table 6.1 shows that despite the increase in calcification rates producing $CO_2$, the increase in primary productivity consumed more $CO_2$. However, when exposed to ambient TA seawater, *Corallina* spp. act as a slight source for $CO_2$. This can be explained by the much lower NPP rates in week two (-2.42 µmol DIC $gDW^{-1}$ $h^{-1}$). If only week one is considered, *Corallina* spp. still acts as a sink for $CO_2$ (overall taking up 3.13 µmol $CO_2$ $gDW^{-1}$ $h^{-1}$). This suggests that even if OAE causes an increase in calcification rates and so $CO_2$, the parallel increase in primary productivity (and take up of $CO_2$) results in a net sink for atmospheric $CO_2$.

*Table 6.1. Comparison of $CO_2$ produced/taken up by Corallina spp.*

| Week | Treatment | $CO_2$ released<br>µmol $CO_2$ $gDW^{-1}$ $h^{-1}$ | $CO_2$ taken up<br>µmol DIC $gDW^{-1}$ $h^{-1}$ | Difference<br>µmol $CO_2$ gDW-1 $h^{-1}$ | Source or sink? |
|---|---|---|---|---|---|
| 1 | Elevated | 6.2556 | 7.99 | 1.7344 | sink |
| 1 | Ambient | 5.4288 | 6.93 | 1.5012 | sink |
| 2 | Elevated | 7.8936 | 9.4 | 1.5064 | sink |
| 2 | Ambient | 6.0294 | 2.42 | -3.6094 | source |
| Av | Elevated | 7.0746 | 8.96 | 1.8854 | sink |
| Av | Ambient | 5.7291 | 4.68 | -1.0491 | source |

Biogeochemical modelling studies suggest that using OAE as the sole response to mitigating carbon emissions would cause global surface water calcite $\Omega_{Ca}$ to increase to ~7 (Paquay and Zebee 2013), ~7.5 (Ferrer-Gonzalez and Ilyina 2016), or ~ 6 (Ilynia et al. 2013) all of which are lower than the increase in $\Omega_{CaCO3}$ in this thesis ($\Omega_{Ca}$ = ~9-20). This implies that if OAE was to be deployed on a global scale, the increase in global *Corallina* spp. calcification would be less than this study. However, if TA is added to smaller more specific regions (e.g. coastal seas) rather than homogeneously across the whole ocean, the changes in $\Omega_{Ca}$ could be much greater in these regions. Therefore, the magnitude of the increase in calcification rates would depend on the how and where TA was added.

## 6.4. Limitations of this research

One of the main limitations to this research was using pH along with TA to constrain carbonate chemistry parameters. This is particularly true for Chapter 4, where pH was not calibrated against TRIS and AMP buffers (as it was for Chapters 2, 3, and 5) and the carbonate chemistry parameters estimated in that study were not robust enough to draw solid conclusions from. Although calibrating seawater pH using TRIS and AMP buffers (the potentiometric method of measuring pH) improves the accuracy of measuring seawater compared to using only primary buffer standards (the error using potentiometric method is ~0.02 compared to ~0.05 when not, Riebesell et al., 2010). There is a third technique where a small amount pH indicator dye solution is added to the seawater sample (spectrophotometric pH measurements) only has a ~0.01 error associated with it. Therefore, a limitation in Chapters 2, 3, and 5 (and even more so for Chapter 4) is that the pH measurements have a relatively large amount of error associated with them. Further, Riebesell et al. (2010) recommends using DIC and TA measurements to constrain the carbonate chemistry of a system with even less error. However, as Dickson (1984) suggests, pH measurements do have their advantages in that it is possible to make pH measurements with a high enough level of precision and accuracy, and at a high sampling rate. Other advantages of using the potentiometric pH measuring method include: it is non-destructive, involves cheap equipment, and can be made in real-time. However, measuring pH using the potentiometric method is appropriate when investigating pH variations larger than 0.01 pH units (Rérolle et al., 2012), which is compatible with the scope of this research. The average change in pH measurements was ~0.13 pH units for Chapter 1, ~0.07 - 0.29 pH units for Chapter 3, ~0.07 pH units for Chapter 4, and ~0.40 pH units for Chapter 5. Therefore, the measurements made during this research are well within the potential error of 0.02 and even 0.05 pH units. Further, in several similar studies, such as Cripps et al. (2013), Hofmann et al. (2012b), Hoppe et al. (2015), Kalokora et al. (2020), Meyer et al. (2015), Noisette et al. (2013), White et al. (2020), and Williamson et al. (2017), pH was the measured parameter from which the other carbonate chemistry parameters were calculated.

To investigate how the potential error from the pH measurements (0.02-0.05) propagates through to the other carbonate chemistry parameters, different values of DIC, $pCO_2$, and $\Omega_{Ca}$ were calculated using CO2SYS for three different TA scenarios and the results are presented in Table 6.2. Changing pH by 0.05 units results in a change in DIC by ~1-4% (depending on

the TA scenario) whereas the DIC manipulations from the studies which make up this thesis were on the range of 16-239%. Further, the change in DIC used in the primary productivity calculations in Chapters 2 and 3 were on the magnitude of 30-40%. Therefore, it is clear that although the quality of the research conducted as part of this thesis would be improved if seawater DIC was also measured, the error resulting from the pH measurements is relatively small compared to the experimental manipulations.

*Table 6.2. Resulting errors in DIC, $pCO_2$, and $\Omega_{Ca}$ from 0.02-0.05 changes in pH, calculated using CO2SYS for three different TA scenarios and the range in DIC investigated in each research chapter and NPP calculations.*

| Treatment | DIC | $pCO_2$ | $\Omega_{Ca}$ |
|---|---|---|---|
| | 0.02 pH error | | |
| High TA | 1% | 7-8% | 2% |
| Ambient TA | 1% | 6% | 4% |
| Low TA | 0.5% | 6% | 4% |
| | 0.05 pH error | | |
| High TA | 2-4% | 20-30% | 6-12% |
| Ambient TA | 1% | 14% | 10% |
| Low TA | 1% | 14% | 10% |
| | % ΔDIC investigated | | |
| Chapter 2 | 21% | 60% | 114% |
| Chapter 3 | 55% | 42% | 168% |
| Chapter 4 | 239% | 131% | 475% |
| Chapter 5 | 16% | 67% | 297% |
| | % ΔDIC from NPP calculations | | |
| Chapter 2 | 27% | - | - |
| Chapter 3 | 43% | - | - |

A limitation to this research is that only two calcifying species were studied, in single species experiments. However, for more robust feasibility assessment of OAE, the response to as many taxa to elevated TA should be investigated, and specifically whole ecosystems. Ocean acidification studies have shown that it the indirect effects of manipulations which have a stronger impact on the whole ecosystem, rather than the direct effects. For example, Bach et al. (2017) showed that *Synechococcus* spp. (which do no calcify) were indirectly affected through enhanced grazing by picoeukaryotes under elevated $CO_2$ in a mesocosm experiment. This shows that although *Synechococcus* spp. physiology was unaffected directly by changing $CO_2$ concentrations, the *Synechococcus* spp. population was affected by the ecosystem response to increasing $CO_2$ levels. The same may be true for the experiments in this thesis. Although they show that increasing TA does not directly harm *Corallina* spp. or

*Synechococcus* 8806 physiology, the indirect effects on increasing TA on the greater ecosystem may result in indirect effects which are detrimental to *Corallina* spp. or *Synechococcus* spp. populations. Therefore, without testing and comparing the results from this thesis to the whole ecosystem response, the results presented here do not unambiguously demonstrate impact marine ecosystems from OAE. However, because two markedly different taxa were studied, the results from this thesis gives an insight into two ecologies and how OAE may impact the wider ecosystem and food web dynamics. Further, by investigating two physiologically different species, it was possible to explore whether the size of the organism and how they calcify influences their response to increased TA. Therefore, even though only two species were examined, the results from this still gives a valuable insight to the influence of elevated TA on marine calcifying organisms.

Another limitation to this thesis is that each experiment lasted for only a matter of weeks. To truly understand the response of *Corallina* spp. and *Synechococcus* 8806, longitudinal studies lasting months to years are required. However, OAE is a relatively new area of research and this has been one of the first attempts to examine its influence on calcifying organism physiology. Therefore, the results from this thesis are useful in expanding our understanding of how elevated TA may impact the marine environment despite only investigating the short-term response.

In Chapter 3, TA did not increase as expected when olivine was dissolved in seawater and so the desired "increased TA and olivine dissolution" treatment was achieved by adding $Na_2CO_3$ solution. Therefore, this method was not 100% equivalent to enhance weathering. However, the main aim of this thesis was to understand the biological response of increased TA, not to constrain olivine dissolution. Therefore, even though the method of achieving enhanced TA was not as expected, the study still provided a valuable insight to the response of *Corallina* spp. to enhanced TA through olivine dissolution.

For the experiments performed in Chapter 4, it was not possible to measure TA. Instead, TA was calculated using PHREEQ-C, media temperature and pH, and media salt concentrations. However, the focus of this study was *Synechococcus* 8806 photophysiology, rather than carbon mass balance. Therefore, the calculated TA values were sufficient for the initial TA estimates. Further, PHREEQ-C is a well-established technique and has often been used to calculate TA in ocean OAE modelling studies (Griffioen 2017; Montserrat et al. 2017). The other big limitation to this chapter is that the errors associated with the pH measurements

means that no robust measurements of the carbonate chemistry of the system apart from TA were made, which limited the conclusions drawn from the results.

Finally, in Chapter 5, there were two primary limitations. The first was that the *Synechococcus* 8806 cells were light limited and did not reach exponential growth. Therefore, the growth rate constants were estimated unconventionally using the total growth period, not the period of exponential growth. Secondly, because there was no exponential growth period, the cultures were left to grow and reached large cell abundances ($\sim 10^6$ cells $mL^{-1}$) by the end of the experiment. This meant that the carbonate chemistry of the media was different by the end of the experiment and much greater than the changes to seawater carbonate chemistry is expected to be. Further, there was no direct evidence of *Synechococcus* 8806 calcification and as no control experiments were performed, it is not possible to know whether the increase in $CaCO_3$ precipitation would have occurred with a different phytoplankton strain, or without any phytoplankton cells present. Despite these limitations, the findings from this chapter still improve our understanding of the response of *Synechococcus* 8806 to enhanced TA. Even though the *Synechococcus* 8806 growth rate constant estimates were not optimal, the focus of this chapter was to investigate the influence *Synechococcus* 8806 on carbonate chemistry and what effect increasing TA had on $CaCO_3$ precipitation and the TA and pH measurements were performed accurately. Therefore, the results provide a reliable insight to how an increase in calcite nucleation surface area (provided by *Synechococcus* 8806 cells) can influence $CaCO_3$ precipitation.

Both Chapters 4 and 5 had considerable limitations to their experimental protocol. This means that this thesis does not provide the same level of detail into to how *Synechococcus* 8806 responds to elevated TA, in the way that it does for *Corallina* spp. However, it does show that under extreme elevated TA scenarios, phytoplankton growth has the potential to promote $CaCO_3$ precipitation. Therefore, acts as a valuable starting off point for future research to investigate the response of *Synechococcus* 8806 to elevated TA.

## 6.5 Future Research

The results from this thesis serves as a base for future studies investigating the marine response to elevated TA. A natural progression to this work would be to analyse the long-term effects of elevated TA on calcifying organisms, which would allow for a better understanding of calcifying organisms acclimation to elevated TA. Further, the experiments in Chapters 2-5 should be repeated using a range of marine calcifying organisms, non-

calcifying organisms, and whole ecosystems. This will allow for a more comprehensive understanding of how OAE may affect the marine environment. Ideally, "meso-scale" in-situ experiments which involve multiple species should be undertaken to constrain the wider ecosystem impacts and better understand how OAE might influence trophic interactions.

The observation of increased *Corallina* spp. calcification and productivity rates when exposed to elevated TA provide some of the first insights into how the biological response to increased TA may influence the longevity of oceanic storage of atmospheric $CO_2$ through OAE. However, more research is needed to better quantify this. Therefore, the *Corallina* spp. culture experiments should be repeated using a more robust method for quantifying the carbon released through increased calcification and that is consumed through photosynthesis, for example by conducting the NPP experiments in a closed system and by sending samples off for DIC analysis instead of using pH measurements.

To better constrain the relationship between *Synechococcus* 8806 precipitation and TA, and so better test the hypothesis set out in Section 5.1 (that increasing TA, would cause an increase in *Synechococcus* 8806 growth rates and $CaCO_3$ precipitation rates) the *Synechococcus* 8806 experiments need to be repeated, albeit adjusted for lower cell growth. These experiments should contain methodologies which can provide more direct evidence for *Synechococcus* 8806. For example, the experiment protocol from Chapter 5 should be repeating using a culture of the calcifying strain of *Synechococcus* 8806, a noncalcifying strain of *Synechococcus,* and potentially another more prolific calcifying phytoplankton taxa such as coccolithophores. Further, several controls should be set up with no biological cells of several TA treatments both with and without abiotic nucleation seeds. Better quantification of $CaCO_3$ precipitation is also needed and so samples of the cells should be taken throughout the growth period for SEM-EDS analysis.

Further, to better understand how changing TA influences *Synechococcus* 8806 photosynthetic efficiency, the aim of Chapter 4, the experimental procedure in Chapter 4 should be repeated but using larger culture samples to allow for more accurate measurements of pH. Further pH should be measured using the methodologies of Chapters 2, 3, and 5 that is using TRIS and AMPD buffers to calibrate pH. Further, because changes in media $pCO_2$ likely strongly influenced *Synechococcus* 8806 photophysiology, a more accurate way of constraining the carbonate chemistry of the system should be used. Therefore, samples of the

media should be sent for both TA and DIC analysis. This would allow to test for the hypothesis proposed in Section 4.5.2.

Both better NPP rate estimates and $CaCO_3$ precipitation estimates (from either *Synechococcus* 8806 or other calcifying phytoplankton or both) would allow for a better estimate of how OAE could influence global marine calcification rates and the impact this has on marine $pCO_2$, thus the longevity of oceanic storage of carbon as TA.

The focus of this thesis was on the biological impact of OAE and so the olivine dissolution experiment in the first part of Chapter 3 was opportunistically undertaken when attempting to create an olivine saturated media for the growth experiment. It was not originally intended to fully constrain incongruent olivine dissolution. However, the experiment demonstrated that TA does not increase as expected following olivine dissolution. Therefore, there remains a potentially important limitation on the efficiency of coastal enhanced weathering as a CDR approach. However, more work is required to fully understand why TA does not increase as expected following olivine dissolution. The olivine dissolution experiment should be repeated with greater focus on secondary mineral precipitation and changes to solution chemistry using PHREEQC simulations. Further, similar experiments should be performed using other minerals such as wollanstonite or augite to see whether the decrease in TA still occurs.

## 6.6 Final Remarks

In summary, increasing seawater TA has been shown not to negatively affect two marine calcifiers, *Corallina spp.* and *Synechococcus* 8806, in terms of their physiology. This illustrates that the direct effect of increased seawater TA from OAE would not be detrimental to these two marine species. However, years of research into ocean acidification studies have shown that indirect effects of changing carbonate chemistry can lead to significant impacts at the ecosystem level. Therefore, without testing and comparing the results from this thesis to the whole ecosystem response, the results from this thesis does not yet provide evidence that OAE will not negatively impact marine ecosystems thus OAE could still indirectly harm *Corallina spp.* and *Synechococcus* spp. Further, elevated TA has been shown to promote increased calcification rates for *Corallina spp.*, which demonstrates that OAE would be an effective ocean mitigation approach for coastal macro algae. Although increased marine calcification rates could substantially influence the marine carbon cycle and potentially reduce the efficiency of OAE as an CDR approach by releasing $CO_2$, the results of this thesis suggest that OAE could still be an efficient CDR approach due to the parallel increase in

productivity rates. However again, more research is needed to better the carbon released through increased calcification and that is consumed through photosynthesis to fully support this.

# Chapter 7.

# 7. Thesis Conclusions

This thesis provides a detailed analysis of the physiological response of two coastal marine calcifiers: *Corallina spp.* (Chapters 2 and 3) and *Synechococcus* 8806 (Chapters 4 and 5) to elevated seawater TA. A summary of the main conclusions of this work is provided below.

The main conclusion from Chapter 2 is that when seawater TA was increased by $Na_2CO_3$ addition *Corallina* spp. net calcification rate increased significantly under elevated TA by 40% compared to a control. Further, *Corallina* spp. net primary productivity doubled when exposed to TA ~30% higher than the control. The increase in calcification rates resulted from an increase in the concentration of [$CO_3^{2-}$] ions which helped reduce dissolution at night and, to a lesser extent, an increase in photosynthesis leading to an increase in light calcification during the day. Therefore, these results show that *Corallina* spp. calcification and photosynthesis are tightly coupled processes. Despite the increase in productivity and calcification rates *Corallina* spp. photophysiology was not affected by increasing TA. These results suggest that artificially increasing ocean TA would not be detrimental for *Corallina* spp. and that it could help to mitigate future coastal ocean acidification.

The first conclusion from Chapter 3 is that olivine dissolution caused seawater TA to decrease because of the precipitation of secondary minerals such as hydrated magnesite ($Mg_5(CO_3)_4(OH)_2.4H_2O$). This highlights that more research needs to be completed before the enhanced weathering of silicate minerals can be deployed as an effective CDR approach in coastal environments or the ocean. Further, the results from this chapter show that *Corallina* spp. samples exposed to olivine dissolution products and elevated TA assimilated trace metals such as Cu, Fe, Ni, Cr, and Zn. This may have caused lower calcification and productivity rates in *Corallina* spp. compared to the samples exposed to similar seawater TA but without the olivine dissolution products. However, when compared to the *Corallina spp.* samples exposed to ambient TA, the *Corallina spp.* exposed to elevated TA + olivine dissolution products had higher calcification and productivity rates. This shows that even though the incorporation of trace metals lowered *Corallina* spp. physiology, increasing TA has a stronger influence. Therefore, as long as seawater TA increases, artificially increasing ocean TA by enhanced weathering may still result in an increase in *Corallina* spp. calcification rates.

The main conclusion from Chapter 4 is that increasing TA affects *Synechococcus* 8806 physiology in two ways. The first is that elevated TA promoted increased growth rates. Secondly, increasing TA significantly alters *Synechococcus* 8806 photophysiology. *Synechococcus* 8806 cells cultured under elevated TA had slightly reduced photosynthetic efficiencies but relationship between *Synechococcus* 8806 photophysiology and TA was not a simple, linear increase. Due to the limitations in the way carbonate chemistry was measured, there is no direct evidence to show what specifically caused the potential decrease in *Synechococcus* 8806 photophysiological efficiency. Therefore, it is difficult to predict how OAE could influence *Synechococcus* photophysiology in future scenarios. However, the results from Chapter 4 show that increasing TA significantly increased *Synechococcus* 8806 growth rates. The increase in *Synechococcus* 8806 growth is possibly a consequence of increased calcification due to increased [$CO_3^{2-}$] and [$HCO_3^-$] and so suggests that if future OAE promotes increased *Synechococcus* growth, it may also promote an increase in the biological capture of carbon. However, further work is needed to test this theory as Chapter 4 did not directly test for *Synechococcus* 8806 calcification.

In Chapter 5, unlike in Chapter 4, *Synechococcus* 8806 growth rates were unaffected by increasing TA. However, increasing TA did not appear to have any detrimental impacts on *Synechococcus* 8806 physiology as even though *Synechococcus* 8806 growth rates did not increase with TA, they did not decrease with TA either. Although these results show that under higher TA, higher rates of $CaCO_3$ precipitation rates occurred, it is not possible to attribute this to *Synechococcus* 8806 growth. The results from Chapter 5 raise an interesting question regarding the role of nucleation seeds in $CaCO_3$ precipitation suggesting that under extreme TA and elevated phytoplankton cells, abiotic $CaCO_3$ precipitation could occur. This has important considerations regarding OAE as an increase in $CaCO_3$ precipitation would reduce the efficiency of carbon capture and could have significant implications on the marine carbon cycle. However, further work is needed to test this hypothesis because at the point that $CaCO_3$ precipitation occurred, the media had a pH of 10, which is unlikely to occur in the modern surface ocean due to air-sea diffusion and ocean currents replenishing seawater with $CO^2$, lowering pH.

The results from these four research chapters show how elevated seawater TA affects the physiology of two coastal marine calcifiers: *Corallina spp.* and *Synechococcus* 8806 and provides the first insights to the practical use of OAE as a carbon dioxide removal approach in terms of the response of the marine environment. First, they show that OAE may not result

in a discernible negative impact two important marine taxa by increasing seawater TA. However, questions still remain about how OAE could influence *Corallina spp.* and *Synechococcus* spp. through indirect effects from a wider ecosystem response to increased TA. Secondly, the results from this thesis suggest that OAE has the potential to mitigate some of the effects of ocean acidification, particularly for *Corallina* spp. Finally, they suggest that OAE could still be an efficient method of capturing atmospheric $CO_2$ despite causing an increase in *Corallina* spp. calcification rates (which would cause an increase in seawater $pCO_2$), because there was a parallel increase in productivity (which would cause a decrease in seawater $pCO_2$). However, further work is needed to constrain the relationship between *Synechococcus* 8806 induced precipitation and what impact this has on the longevity of carbon storage.

# References

Agawin, N. et al. 2000. Nutrient and temperature control of the contribution of picoplankton to phytoplankton biomass and production. *Limnology and Oceanography* 45(3), pp. 591-600. doi: 10.4319/lo.2000.45.3.0591

Akioka, H. et al. 1999. Rocky shore turfs dominated by *Corallina* (Corallinales, Rhodophyta) in northen, Japan. *Phycologial Research* 47, pp. 199-206.

Albright, R. et al. 2016. Reversal of ocean acidification enhances net coral reef calcification. *Nature* 531(7594), pp. 362-+. doi: 10.1038/nature17155

Aloisi, G. 2018. A pronounced fall in the CaCO3 saturation state and the total alkalinity of the surface ocean during the Mid Mesozoic. *Chemical Geology* 487, pp. 39-53.

Andersen, R. A. 2005. *Algal culturing techniques*. Elsevier.

Andersson, A. J. et al. 2008. Life on the margin: implications of ocean acidification on Mg-calcite, high latitude and cold-water marine calcifiers. *Marine Ecology Progress Series* 373, pp. 265-273. doi: 10.3354/meps07639

Andrews, J. E. et al. 1997. The stable isotope record of environmental and climatic signals in modern terrestrial microbial carbonates from Europe. *Palaeogeography, Palaeoclimatology, Palaeoecology* 129(1-2), pp. 171-189.

Archer, D. 2005. Fate of fossil fuel $CO_2$ in geologic time. *Journal of Geophysical Research-Oceans* 110(C9), doi: Artn C09s05 10.1029/2004jc002625

Armstrong, R. et al. 2001. A new, mechanistic model for organic carbon fluxes in the ocean based on the quantitative association of POC with ballast minerals. *Deep-Sea Research Part Ii-Topical Studies in Oceanography* 49(1-3), pp. 219-236. doi: 10.1016/S0967-0645(01)00101-1

Bach, L. et al. 2017. Simulated ocean acidification reveals winners and losers in coastal phytoplankton. *Plos One* 12(11), doi: 10.1371/journal.pone.0188198

Bach, L. et al. 2011a. Distinguishing between the effects of ocean acidification and ocean carbonation in the coccolithophore Emiliania huxleyi. *Limnology and Oceanography* 56(6), pp. 2040-2050. doi: 10.4319/lo.2011.56.6.2040

Bach, L. T. et al. 2019. $CO_2$ removal with enhanced weathering and ocean alkalinity enhancement: Potential risks and co-benefits for marine pelagic ecosystems. *Frontiers in Climate* 1, p. 7.

Bach, L. T. et al. 2015. A unifying concept of coccolithophore sensitivity to changing carbonate chemistry embedded in an ecological framework. *Progress in Oceanography* 135, pp. 125-138. doi: 10.1016/j.pocean.2015.04.012

Bach, L. T. et al. 2011b. Distinguishing between the effects of ocean acidification and ocean carbonation in the coccolithophore Emiliania huxleyi. *Limnology and Oceanography* 56(6), pp. 2040-2050. doi: 10.4319/lo.2011.56.6.2040

Badger, M. et al. 2006. The environmental plasticity and ecological genomics of the cyanobacterial $CO_2$ concentrating mechanism. *Journal of Experimental Botany* 57(2), pp. 249-265. doi: 10.1093/jxb/eri286

Badger, M. R. and Andrews, T. J. 1982. Photosynthesis and inorganic carbon usage by the marine cyanobacterium, Synechococcus sp. *Plant physiology* 70(2), pp. 517-523.

Badger, M. R. and Price, G. D. 2003. $CO_2$ concentrating mechanisms in cyanobacteria: molecular components, their diversity and evolution. *Journal of experimental botany* 54(383), pp. 609-622.

Badger, M. R. and Spalding, M. H. 2000. $CO_2$ acquisition, concentration and fixation in cyanobacteria and algae.*Photosynthesis*. Springer, pp. 369-397.

Bailey, J. C. and Chapman, R. L. 1998. A phylogenetic study of the Corallinales (Rhodophyta) based on nuclear small-subunit rRNA gene sequences. *Journal of Phycology* 34(4), pp. 692-705. doi: DOI 10.1046/j.1529-8817.1998.340692.x

Balch, W. M. et al. 1992. Calcification, photosynthesis and growth of the bloom-forming coccolithophore, Emiliania huxleyi. *Continental Shelf Research* 12(12), pp. 1353-1374.

Basso, D. 2012. Carbonate production by calcareous red algae and global change. *Geodiversitas* 34(1), pp. 13-33. doi: 10.5252/g2012n1a2

Bautista-Chamizo, E. et al. 2016. Simulating CO2 leakages from CCS to determine Zn toxicity using the marine microalgae Pleurochrysis roscoffensis. *Chemosphere* 144, pp. 955-965.

Beardall, J. and Raven, J. 2004. The potential effects of global climate change on microalgal photosynthesis, growth and ecology. *Phycologia* 43(1), pp. 26-40. doi: 10.2216/i0031-8884-43-1-26.1

Beerling, D. J. et al. 2020. Potential for large-scale CO 2 removal via enhanced rock weathering with croplands. *Nature* 583(7815), pp. 242-248.

Beerling, D. J. et al. 2018. Farming with crops and rocks to address global climate, food and soil security. *Nature Plants* 4(3), pp. 138-147.

Benedetti-Cecchi, L. 2006. Understanding the consequences of changing biodiversity on rocky shores: how much have we learned from past experiments? *Journal of Experimental Marine Biology and Ecology* 338(2), pp. 193-204.

Berner, R. 1975. Role of magnesium in crystal-growth of calcite and aragonite from sea-water. *Geochimica Et Cosmochimica Acta* 39(4), pp. 489-&. doi: 10.1016/0016-7037(75)90102-7

Berninger, U. N. et al. 2014. The experimental determination of hydromagnesite precipitation rates at 22.5–75ºC. *Mineralogical Magazine* 78(6), pp. 1405-1416.

Bielmyer, G. K. et al. 2010. Differential effects of copper on three species of scleractinian corals and their algal symbionts (*Symbiodinium* spp.). *Aquatic Toxicology* 97(2), pp. 125-133.

Biscere, T. et al. 2018. Enhancement of coral calcification via the interplay of nickel and urease. *Aquatic Toxicology* 200, pp. 247-256. doi: 10.1016/j.aquatox.2018.05.013

Biscere, T. et al. 2017. Nickel and ocean warming affect scleractinian coral growth. *Marine Pollution Bulletin* 120(1-2), pp. 250-258. doi: 10.1016/j.marpolbul.2017.05.025

Borowitzka, M. 1979. Calcium exchange and the measurement of calcification rates in the calcareous coralline red alga *Amphiroa-Foliacea*. *Marine Biology* 50(4), pp. 339-347. doi: 10.1007/BF00387011

Borowitzka, M. and Vesk, M. 1978. Ultrastructure of corallinaceae .1. Vegetative cells of *Corallina-Officinalis* and *Corallina-Cuvierii*. *Marine Biology* 46(4), pp. 295-304. doi: 10.1007/BF00391400

Borowitzka, M. A. 1982. Morphological and Cytological Aspects of Algal Calcification. *International Review of Cytology-a Survey of Cell Biology* 74, pp. 127-162. doi: Doi 10.1016/S0074-7696(08)61171-7

Borowitzka, M. A. 1987. Calcification in Algae - Mechanisms and the Role of Metabolism. *Crc Critical Reviews in Plant Sciences* 6(1), pp. 1-45. doi: Doi 10.1080/07352688709382246

Bruland, K. W. et al. 2008. Factors influencing the chemistry of the near-field Columbia River plume: Nitrate, silicic acid, dissolved Fe, and dissolved Mn. *Journal of Geophysical Research: Oceans* 113(C2),

Burkhardt, S. et al. 1999. Effects of growth rate, $CO_2$ concentration, and cell size on the stable carbon isotope fractionation in marine phytoplankton. *Geochimica Et Cosmochimica Acta* 63(22), pp. 3729-3741. doi: 10.1016/S0016-7037(99)00217-3

Campbell, D. et al. 1998. Chlorophyll fluorescence analysis of cyanobacterial photosynthesis and acclimation. *Microbiology and Molecular Biology Reviews* 62(3), pp. 667-+. doi: 10.1128/MMBR.62.3.667-683.1998

Cao, L. et al. 2007. Effects of carbon dioxide and climate change on ocean acidification and carbonate mineral saturation. *Geophysical Research Letters* 34(5), doi: 10.1029/2006GL028605

Cavan, E. et al. 2017. Role of zooplankton in determining the efficiency of the biological carbon pump. *Biogeosciences* 14(1), pp. 177-186. doi: 10.5194/bg-14-177-2017

Chakraborty, S. et al. 2014. Benthic macroalgae as biological indicators of heavy metal pollution in the marine environments: A biomonitoring approach for pollution assessment. *Ecotoxicology and environmental safety* 100, pp. 61-68.

Change, U. N. F. C. o. C. 2008. Provisions of the Kyoto Protocol and decisions by the Conference of the Parties serving as the meeting of the Parties to the Kyoto Protocol relating to the means to reach emission reduction targets of Annex I Parties.

Chisholm, J. R. M. and Gattuso, J. P. 1991. Validation of the Alkalinity Anomaly Technique for Investigating Calcification and Photosynthesis in Coral-Reef Communities. *Limnology and Oceanography* 36(6), pp. 1232-1239. doi: DOI 10.4319/lo.1991.36.6.1232

Ciais, P. et al. 2014. Carbon and other biogeochemical cycles.*Climate change 2013: the physical science basis. Contribution of Working Group I to the Fifth Assessment Report of the Intergovernmental Panel on Climate Change*. Cambridge University Press, pp. 465-570.

Clark, D. and Flynn, K. 2000. The relationship between the dissolved inorganic carbon concentration and growth rate in marine phytoplankton. *Proceedings of the Royal Society B-Biological Sciences* 267(1447), pp. 953-959. doi: 10.1098/rspb.2000.1096

Collén, J. et al. 2003. Induction of oxidative stress in the red macroalga Gracilaria tenuistipitata by pollutant metals. *Archives of Environmental Contamination and Toxicology* 45(3), pp. 337-342.

Comeau, S. et al. 2009. Impact of ocean acidification on a key Arctic pelagic mollusc (Limacina helicina). *Biogeosciences* 6(9), pp. 1877-1882.

Coull, B. and wells, J. 1983. Refuges from fish predation - experiments with phytal meiofauna from the New-Zealand rocky intertidal. *Ecology* 64(6), pp. 1599-1609. doi: 10.2307/1937513

Couto, R. P. et al. 2010. Metal concentration and structural changes in *Corallina elongata* (Corallinales, Rhodophyta) from hydrothermal vents. *Marine Pollution Bulletin* 60(4), pp. 509-514.

CRED. 2009. The Psychology of Climate Change Communication: A Guide for Scientists, Journalists, Educators, Political Aides, and the Interested Public.

Cripps, G. et al. 2013. Biological impacts of enhanced alkalinity in Carcinus maenas. *Marine Pollution Bulletin* 71(1-2), pp. 190-198. doi: 10.1016/j.marpolbul.2013.03.015

Crossland, C. and Barnes, D. 1974. Role of metabolic nitrogen in coral calcification. *Marine Biology* 28(4), pp. 325-332. doi: 10.1007/BF00388501

Cubillas, P. et al. 2005. Experimental determination of the dissolution rates of calcite, aragonite, and bivalves. *Chemical Geology* 216(1-2), pp. 59-77. doi: 10.1016/j.chemgeo.2004.11.009

Cyronak, T. et al. 2018. Taking the metabolic pulse of the world's coral reefs. *Plos One* 13(1), doi: ARTN e019087210.1371/journal.pone.0190872

Cyronak, T. et al. 2016. The Omega myth: what really drives lower calcification rates in an acidifying ocean. *Ices Journal of Marine Science* 73(3), pp. 558-562. doi: 10.1093/icesjms/fsv075

Darnall, D. et al. 1986. Selective recovery of gold and other metal-ions from an algal biomass. *Environmental Science & Technology* 20(2), pp. 206-208. doi: 10.1021/es00144a018

De La Rocha, C. et al. 2008. Interactions between diatom aggregates, minerals, particulate organic carbon, and dissolved organic matter: Further implications for the ballast hypothesis. *Global Biogeochemical Cycles* 22(4), doi: 10.1029/2007GB003156

Deelman, J. C. 1999. Low-temperature nucleation of magnesite and dolomite. *Neues Jahrbuch Fur Mineralogie Monatshefte*, pp. 289-302.

Dickson, A. G. 1981. An exact definition of total alkalinity and a procedure for the estimation of alkalinity and total inorganic carbon from titration data. *Deep-Sea Research Part a-Oceanographic Research Papers* 28(6), pp. 609-623. doi: 10.1016/0198-0149(81)90121-7

Dickson, A. G. and Millero, F. J. 1987. A Comparison of the Equilibrium-Constants for the Dissociation of Carbonic-Acid in Seawater Media. *Deep-Sea Research Part a-Oceanographic Research Papers* 34(10), pp. 1733-1743. doi: Doi 10.1016/0198-0149(87)90021-5

Dickson, A. G. et al. 2007 (Eds). Guide to best practices for ocean $CO_2$ meaurements PICES Special Publication 3, 191 pp.

Dietzen, C. et al. 2018. Effectiveness of enhanced mineral weathering as a carbon sequestration tool and alternative to agricultural lime: An incubation experiment. *International Journal of Greenhouse Gas Control* 74, pp. 251-258. doi: 10.1016/j.ijggc.2018.05.007

Dineshbabu, G. et al. 2020. Elevated $CO_2$ impact on growth and lipid of marine cyanobacterium Phormidium valderianum BDU 20041- towards microalgal carbon sequestration. *Biocatalysis and Agricultural Biotechnology* 25, doi: 10.1016/j.bcab.2020.101606

Doney, S. et al. 2020. The impacts of ocean acidification on marine ecosystems and reliant human communities. *Annual Review of Environment and Resources, Vol 45* 45, pp. 83-112. doi: 10.1146/annurev-environ-012320-083019

Doney, S. C. et al. 2009. Ocean Acidification: The other $CO_2$ problem. *Annual Review of Marine Science* 1, pp. 169-192. doi: 10.1146/annurev.marine.010908.163834

Donnet, M. et al. 2005. Use of seeds to control precipitation of calcium carbonate and determination of seed nature. *Langmuir* 21(1), pp. 100-108.

dos Anjos, A. P. A. et al. 2011. Synthesis of magnesite at low temperature. *Carbonates and Evaporites* 26(3), pp. 213-215.

Dugdale, R. C. and Wilkerson, F. P. 1998. Silicate regulation of new production in the equatorial Pacific upwelling. *Nature* 391(6664), pp. 270-273.

DuRand, M. et al. 2001. Phytoplankton population dynamics at the Bermuda Atlantic Time-series station in the Sargasso Sea. *Deep-Sea Research Part Ii-Topical Studies in Oceanography* 48(8-9), pp. 1983-2003. doi: 10.1016/S0967-0645(00)00166-1

Dutkiewicz, S. et al. 2015. Impact of ocean acidification on the structure of future phytoplankton communities. *Nature Climate Change* 5(11), pp. 1002-+. doi: 10.1038/NCLIMATE2722

Egilsdottir, H. et al. 2013. Effects of $pCO_2$ on physiology and skeletal mineralogy in a tidal pool coralline alga Corallina elongata. *Marine Biology* 160(8), pp. 2103-2112. doi: 10.1007/s00227-012-2090-7

Eilers, P. H. C. and Peeters, J. C. H. 1988. A model for the relationship between light intensity and the rate of photosynthesis in phytoplankton. *Ecological modelling* 42(3-4), pp. 199-215.

Engel, A. et al. 2014. Impact of $CO_2$ enrichment on organic matter dynamics during nutrient induced coastal phytoplankton blooms. *Journal of Plankton Research* 36(3), pp. 641-657. doi: 10.1093/plankt/fbt125

Engel, A. et al. 2005. Testing the direct effect of $CO_2$ concentration on a bloom of the coccolithophorid Emiliania huxleyi in mesocosm experiments. *Limnology and Oceanography* 50(2), pp. 493-507.

Enochs, I. C. et al. 2015. Shift from coral to macroalgae dominance on a volcanically acidified reef. *Nature Climate Change* 5(12), pp. 1083-1088.

Evans, W. and Mathis, J. 2013. The Gulf of Alaska coastal ocean as an atmospheric $CO_2$ sink. *Continental Shelf Research* 65, pp. 52-63. doi: 10.1016/j.csr.2013.06.013

Falkowski, P. et al. 2004. The evolution of modern eukaryotic phytoplankton. *Science* 305(5682), pp. 354-360. doi: 10.1126/science.1095964

Falkowski, P. and Owens, T. 1980. Light-shade adaptation - 2 strategies in marine-phytoplankton. *Plant Physiology* 66(4), pp. 592-595. doi: 10.1104/pp.66.4.592

Feely, R. et al. 2009. Ocean acidification: present conditions and future changes in a high-$CO_2$ world. *Oceanography* 22(4), pp. 36-47. doi: 10.5670/oceanog.2009.95

Feely, R. et al. 2018. The combined effects of acidification and hypoxia on pH and aragonite saturation in the coastal waters of the California current ecosystem and the northern Gulf of Mexico. *Continental Shelf Research* 152, pp. 50-60. doi: 10.1016/j.csr.2017.11.002

Feely, R. et al. 2008. Evidence for upwelling of corrosive "acidified" water onto the continental shelf. *Science* 320(5882), pp. 1490-1492. doi: 10.1126/science.1155676

Feng, E. Y. et al. 2016. Could artificial ocean alkalinization protect tropical coral ecosystems from ocean acidification? *Environmental Research Letters* 11(7), doi: 10.1088/1748-9326/11/7/074008

Feng, E. Y. et al. 2017a. Model-Based Assessment of the $CO_2$ Sequestration Potential of Coastal Ocean Alkalinization. *Earths Future* 5(12), pp. 1252-1266. doi: 10.1002/2017ef000659

Feng, Y. et al. 2017b. Environmental controls on the growth, photosynthetic and calcification rates of a Southern Hemisphere strain of the coccolithophore *Emiliania huxleyi*. *Limnology and Oceanography* 62(2), pp. 519-540.

Ferrier-Pagès, C. et al. 2001. Response of a scleractinian coral, Stylophora pistillata, to iron and nitrate enrichment. *Journal of Experimental Marine Biology and Ecology* 259(2), pp. 249-261.

Fine, R. et al. 2017. Global variability and changes in ocean total alkalinity from Aquarius satellite data. *Geophysical Research Letters* 44(1), pp. 261-267. doi: 10.1002/2016GL071712

Finkel, Z. V. 2007. Does phytoplankton cell size matter? The evolution of modern marine food webs. *Evolution of primary producers in the sea*, pp. 333-350.

Flombaum, P. et al. 2013. Present and future global distributions of the marine Cyanobacteria *Prochlorococcus* and *Synechococcus*. *Proceedings of the National Academy of Sciences of the United States of America* 110(24), pp. 9824-9829. doi: 10.1073/pnas.1307701110

Form, A. U. and Riebesell, U. 2012. Acclimation to ocean acidification during long-term $CO_2$ exposure in the cold-water coral *L ophelia pertusa*. *Global change biology* 18(3), pp. 843-853.

Fourest, E. and Roux, J. 1992. Heavy-metal biosorption by fungal mycelial by-products - mechanisms and influence of pH. *Applied Microbiology and Biotechnology* 37(3), pp. 399-403. doi: 10.1007/BF00211001

Frankignoulle, M. et al. 1994. Marine calcification as a source of carbon dioxide: Positive feedback of increasing atmospheric $CO_2$. *Limnology and Oceanography* 39(2), pp. 458-462.

Friedlingstein, P. et al. 2019. Global Carbon Budget 2019. *Earth System Science Data* 11(4), pp. 1783-1838. doi: 10.5194/essd-11-1783-2019

Fu, F. et al. 2007. Effects of increased temperature and $CO_2$ on photosynthesis, growth, and elemental ratios in marine *Synechococcus* and *Prochlorococcu*s (Cyanobacteria). *Journal of Phycology* 43(3), pp. 485-496. doi: 10.1111/j.1529-8817.2007.00355.x

Fukuda, S.-y. et al. 2014. Difference in physiological responses of growth, photosynthesis and calcification of the coccolithophore *Emiliania huxleyi* to acidification by acid and $CO_2$ enrichment. *Photosynthesis research* 121(2), pp. 299-309.

Fuss, S. et al. 2018. Negative emissions-Part 2: Costs, potentials and side effects. *Environmental Research Letters* 13(6), doi: 10.1088/1748-9326/aabf9f

Gao, K. et al. 1991. Enhanced growth of the red alga *Porphyra yezoensis Ueda* in high $CO_2$ concentrations. *Journal of Applied Phycology* 3(4), pp. 355-362.

Gao, K. and Zheng, Y. 2010. Combined effects of ocean acidification and solar UV radiation on photosynthesis, growth, pigmentation and calcification of the coralline alga *Corallina sessilis* (Rhodophyta). *Global Change Biology* 16(8), pp. 2388-2398.

Garbary, D. J. and Johansen, H. W. 1982. Scanning electron microscopy of *Corallina* and *Haliptilon* (Corallinaceae, Rhodophyta): surface features and their taxonomic implicationS 1. *Journal of Phycology* 18(2), pp. 211-219.

Garcia-Pichel, F. et al. 2003. Estimates of global cyanobacterial biomass and its distribution. *Algological Studies* 109(1), p. 213.

Garrard, S. L. and Beaumont, N. J. 2014. The effect of ocean acidification on carbon storage and sequestration in seagrass beds; a global and UK context. *Marine Pollution Bulletin* 86(1-2), pp. 138-146.

Gattuso, J. et al. 1998. Effect of calcium carbonate saturation of seawater on coral calcification. *Global and Planetary Change* 18(1-2), pp. 37-46. doi: 10.1016/S0921-8181(98)00035-6

Gautier, Q. et al. 2014. Hydromagnesite solubility product and growth kinetics in aqueous solution from 25 to 75 C. *Geochimica et Cosmochimica Acta* 138, pp. 1-20.

Genty, B. et al. 1989. The Relationship between the Quantum Yield of Photosynthetic Electron-Transport and Quenching of Chlorophyll Fluorescence. *Biochimica Et Biophysica Acta* 990(1), pp. 87-92. doi: Doi 10.1016/S0304-4165(89)80016-9

Ghilarov, A. M. 2000. Ecosystem functioning and intrinsic value of biodiversity. *Oikos* 90(2), pp. 408-412.

Giles, B. 2015. Managing the Risks of Extreme Events and Disasters to Advance Climate Change Adaptation. *Weather and Climate* 35, pp. 36-39.

Gim, B. M. et al. 2018. Potential ecotoxicological effects of elevated bicarbonate ion concentrations on marine organisms. *Environ Pollut* 241, pp. 194-199. doi: 10.1016/j.envpol.2018.05.057

Giordano, M. et al. 2005. $CO_2$ concentrating mechanisms in algae: mechanisms, environmental modulation, and evolution. *Annu. Rev. Plant Biol.* 56, pp. 99-131.

Gleason, P. J. and Spackman, W. J. 1974. Calcareous periphyton and water chemistry in the Evergaldes. - In: Gleason, P.J. (ed.): Environments in South Florida, Present and Past. (34), pp. 146-181.

Gledhill, D. et al. 2015. Ocean and Coastal Acidification off New England and Nova Scotia. *Oceanography* 28(2), pp. 182-197. doi: 10.5670/oceanog.2015.41

Goglio, P. et al. 2020. Advances and challenges of life cycle assessment (LCA) of greenhouse gas removal technologies to fight climate changes. *Journal of Cleaner Production* 244, doi: 10.1016/j.jclepro.2019.118896

Goldman, J. 1999. Inorganic carbon availability and the growth of large marine diatoms. *Marine Ecology Progress Series* 180, pp. 81-91. doi: 10.3354/meps180081

Goldman, J. and Graham, S. 1981. Inorganic carbon limitation and chemical-composition of 2 fresh-water green microalgae. *Applied and Environmental Microbiology* 41(1), pp. 60-70. doi: 10.1128/AEM.41.1.60-70.1981

Golubić, S. 1973. The relationship between blue-green algae and carbonate deposits. *The biology of blue-green algae*, pp. 434-472.

Gomes, P. I. A. and Asaeda, T. 2013. Phytoremediation of heavy metals by calcifying macro-algae (Nitella pseudoflabellata): implications of redox insensitive end products. *Chemosphere* 92(10), pp. 1328-1334.

Gonzalez, M. F. and Ilyina, T. 2016. Impacts of artificial ocean alkalinization on the carbon cycle and climate in Earth system simulations. *Geophysical Research Letters* 43(12), pp. 6493-6502. doi: 10.1002/2016gl068576

Gregg, J. M. et al. 2015. Mineralogy, nucleation and growth of dolomite in the laboratory and sedimentary environment: a review. *Sedimentology* 62(6), pp. 1749-1769.

Griffioen, J. 2017. Enhanced weathering of olivine in seawater: The efficiency as revealed by thermodynamic scenario analysis. *Science of the Total Environment* 575, pp. 536-544. doi: 10.1016/j.scitotenv.2016.09.008

Guillard, R. R. L. and Hargraves, P. E. 1993. Stichochrysis immobilis is a diatom, not a chrysophyte. *Phycologia* 32(3), pp. 234-236.

Gullstrom, M. et al. 2006. Assessment of changes in the seagrass-dominated submerged vegetation of tropical Chwaka Bay (Zanzibar) using satellite remote sensing. *Estuarine Coastal and Shelf Science* 67(3), pp. 399-408. doi: 10.1016/j.ecss.2005.11.020

Gullstrom, M. et al. 2018. Blue Carbon Storage in Tropical Seagrass Meadows Relates to Carbonate Stock Dynamics, Plant-Sediment Processes, and Landscape Context: Insights from the Western Indian Ocean. *Ecosystems* 21(3), pp. 551-566. doi: 10.1007/s10021-017-0170-8

Hanchen, M. et al. 2008. Precipitation in the Mg-carbonate system - effects of temperature and CO2 pressure. *Chemical Engineering Science* 63(4), pp. 1012-1028. doi: 10.1016/j.ces.2007.09.052

Hangx, S. J. T. and Spiers, C. J. 2009. Coastal spreading of olivine to control atmospheric $CO_2$ concentrations: A critical analysis of viability. *International Journal of Greenhouse Gas Control* 3(6), pp. 757-767. doi: 10.1016/j.ijggc.2009.07.001

Hansen, P. 2002. Effect of high pH on the growth and survival of marine phytoplankton: implications for species succession. *Aquatic Microbial Ecology* 28(3), pp. 279-288. doi: 10.3354/ame028279

Hartmann, J. et al. 2013. Enhanced chemical weathering as a geoengineering strategy to reduce atmospheric carbon dioxide, supply nutrients, and mitigate ocean acidification. *Reviews of Geophysics* 51(2), pp. 113-149. doi: 10.1002/rog.20004

Harvey, L. D. D. 2008. Mitigating the atmospheric $CO_2$ increase and ocean acidification by adding limestone powder to upwelling regions. *Journal of Geophysical Research-Oceans* 113(C4), doi: Artn C04028 10.1029/2007jc004373

Hauck, J. et al. 2016. Iron fertilisation and century-scale effects of open ocean dissolution of olivine in a simulated $CO_2$ removal experiment. *Environmental Research Letters* 11(2), doi: 10.1088/1748-9326/11/2/024007

Heinze, C. et al. 1991. Glacial $pCO_2$ reduction by the world ocean: experiments with the hamburg carbon cycle model. *Paleoceanography* 6(4), pp. 395-430. doi: 10.1029/91PA00489

Henley, W. J. 1993. Measurement and interpretation of photosynthetic light-response curves in algae in the context of photoinhibition and diel changes. *Journal of Phycology* 29(6), pp. 729-739.

Hofmann, L. C. and Bischof, K. 2014. Ocean acidification effects on calcifying macroalgae. *Aquatic Biology* 22, pp. 261-279. doi: 10.3354/ab00581

Hofmann, L. C. et al. 2012a. Competition between calcifying and noncalcifying temperate marine macroalgae under elevated $CO_2$ levels. *Marine Ecology Progress Series* 464, pp. 89-105. doi: 10.3354/meps09892

Hofmann, L. C. et al. 2012b. Physiological responses of the calcifying rhodophyte, *Corallina officinalis* (L.), to future $CO_2$ levels. *Marine Biology* 159(4), pp. 783-792. doi: 10.1007/s00227-011-1854-9

Holan, Z. et al. 1993. Biosorption of cadmium by biomass of marine-algae. *Biotechnology and Bioengineering* 41(8), pp. 819-825. doi: 10.1002/bit.260410808

Hopkinson, L. et al. 2012. Phase transitions in the system $MgO$-$CO_2$-$H_2O$ during $CO_2$ degassing of Mg-bearing solutions. *Geochimica Et Cosmochimica Acta* 76, pp. 1-13. doi: 10.1016/j.gca.2011.10.023

Hoppe, C. et al. 2018a. The Arctic picoeukaryote *Micromonas pusill*a benefits synergistically from warming and ocean acidification. *Biogeosciences* 15(14), pp. 4353-4365. doi: 10.5194/bg-15-4353-2018

Hoppe, C. et al. 2015. Ocean acidification decreases the light-use efficiency in an Antarctic diatom under dynamic but not constant light. *New Phytologist* 207(1), pp. 159-171. doi: 10.1111/nph.13334

Hoppe, C. et al. 2012. Implications of observed inconsistencies in carbonate chemistry measurements for ocean acidification studies. *Biogeosciences* 9(7), pp. 2401-2405. doi: 10.5194/bg-9-2401-2012

Hoppe, C. et al. 2018b. Resistance of Arctic phytoplankton to ocean acidification and enhanced irradiance. *Polar Biology* 41(3), pp. 399-413. doi: 10.1007/s00300-017-2186-0

Hoppe, C. et al. 2017. Functional Redundancy Facilitates Resilience of Subarctic Phytoplankton Assemblages toward Ocean Acidification and High Irradiance. *Frontiers in Marine Science* 4, doi: 10.3389/fmars.2017.00229

House, K. Z. et al. 2007. Electrochemical acceleration of chemical weathering as an energetically feasible approach to mitigating anthropogenic climate change. *Environmental Science & Technology* 41(24), pp. 8464-8470. doi: 10.1021/es0701816

Hunter-Cevera, K. et al. 2016. Diversity of *Synechococcus* at the Martha's Vineyard Coastal Observatory: Insights from Culture Isolations, Clone Libraries, and Flow Cytometry. *Microbial Ecology* 71(2), pp. 276-289. doi: 10.1007/s00248-015-0644-1

Ibrahim, W. M. 2011. Biosorption of heavy metal ions from aqueous solution by red macroalgae. *Journal of Hazardous Materials* 192(3), pp. 1827-1835.

Ilyina, T. et al. 2013. Assessing the potential of calcium-based artificial ocean alkalinization to mitigate rising atmospheric $CO_2$ and ocean acidification. *Geophysical Research Letters* 40(22), pp. 5909-5914. doi: 10.1002/2013gl057981

Inoue, S. et al. 2013. Spatial community shift from hard to soft corals in acidified water. *Nature Climate Change* 3(7), pp. 683-687.

IPCC. 2018. An IPCC special report on the impacts of global warming of1.5C above pre-industrial levels and related global greenhouse gas emission pathways, in the context of strengthening the globalresponse to the threat of climate change.

Johansen, H. W. 1970. The diagnostic value of reproductive organs in some genera of articulated coralline red algae. *British phycological journal* 5(1), pp. 79-86.

Johnson, Z. et al. 2006. Niche partitioning among *Prochlorococcus* ecotypes along ocean-scale environmental gradients. *Science* 311(5768), pp. 1737-1740. doi: 10.1126/science.1118052

Joint, I. et al. 2011. Will ocean acidification affect marine microbes? *Isme Journal* 5(1), pp. 1-7. doi: 10.1038/ismej.2010.79

Jokiel, P. L. 2011. Ocean acidification and control of reef coral calcification by boundary layer limitation of proton flux. *Bulletin of Marine Science* 87(3), pp. 639-657.

Jones, C. G. et al. 1994. Organisms as ecosystem engineers.*Ecosystem management*. Springer, pp. 130-147.

Jones, D. et al. 2014. Spatial and seasonal variability of the air-sea equilibration timescale of carbon dioxide. *Global Biogeochemical Cycles* 28(11), pp. 1163-1178. doi: 10.1002/2014GB004813

Joos, F. and Spahni, R. 2008. Rates of change in natural and anthropogenic radiative forcing over the past 20,000 years. *Proceedings of the National Academy of Sciences* 105(5), pp. 1425-1430.

Jordanova, A. et al. 1999. Heavy metal assessment in algae, sediments and water from the Bulgarian Black Sea coast. *Water science and technology* 39(8), pp. 207-212.

Kalokora, O. et al. 2020. An experimental assessment of algal calcification as a potential source of atmospheric $CO_2$. *Plos One* 15(4), doi: 10.1371/journal.pone.0231971

Kamenos, N. A. et al. 2008. Coralline algae are global palaeothermometers with bi-weekly resolution. *Geochimica et cosmochimica Acta* 72(3), pp. 771-779.

Kaplan, A. et al. 1980. Photosynthesis and the intracellular inorganic carbon pool in the bluegreen alga *Anabaena-Variabilis* - response to external $CO_2$ concentration. *Planta* 149(3), pp. 219-226. doi: 10.1007/BF00384557

Kaplan, A. and Reinhold, L. 1999. $CO_2$ concentrating mechanisms in photosynthetic microorganisms. *Annual Review of Plant Physiology and Plant Molecular Biology* 50, pp. 539-+. doi: 10.1146/annurev.arplant.50.1.539

Keith, D. W. 2000. Geoengineering the climate: History and prospect. *Annual Review of Energy and the Environment* 25, pp. 245-284. doi: 10.1146/annurev.energy.25.1.245

Kelaher, B. et al. 2003. Experimental transplantations of coralline algal turf to demonstrate causes of differences in macrofauna at different tidal heights. *Journal of Experimental Marine Biology and Ecology* 282(1-2), pp. 23-41. doi: 10.1016/S0022-0981(02)00443-4

Kelaher, B. P. et al. 2001. Spatial patterns of diverse macrofaunal assemblages in coralline turf and their association with environmental variables. *Journal of the Marine Biological Association of the United Kingdom*,

Kempe, S. and Kazmierczak, J. 1994. The role of alkalinity in the evolution of ocean chemistry, organization of living systems, and biocalcification processes. *Bulletin de la Institut Océanographique (Monaco)* 13, pp. 61-117.

Kennedy, H. et al. 2010. Seagrass sediments as a global carbon sink: Isotopic constraints. *Global Biogeochemical Cycles* 24(4),

Kennedy, H. and Björk, M. 2009. Seagrass meadows. *The management of natural coastal carbon sinks* 23,

Kheshgi, H. S. 1995. Sequestering Atmospheric Carbon-Dioxide by Increasing Ocean Alkalinity. *Energy* 20(9), pp. 915-922. doi: Doi 10.1016/0360-5442(95)00035-F

Klaas, C. and Archer, D. E. 2002. Association of sinking organic matter with various types of mineral ballast in the deep sea: Implications for the rain ratio. *Global Biogeochemical Cycles* 16(4), pp. 63-61.

Klughammer, B. et al. 1999. The involvement of NAD(P)H dehydrogenase subunits, NdhD3 and NdhF3, in high-affinity $CO_2$ uptake in *Synechococcus* sp PCC7002 gives evidence for multiple NDH-1 complexes with specific roles in cyanobacteria. *Molecular Microbiology* 32(6), pp. 1305-1315. doi: 10.1046/j.1365-2958.1999.01457.x

Knoll, A. H. 2008. Cyanobacteria and earth history. *The cyanobacteria: molecular biology, genomics, and evolution* 484,

Koch, M. et al. 2013. Climate change and ocean acidification effects on seagrasses and marine macroalgae. *Global change biology* 19(1), pp. 103-132.

Kohler, P. et al. 2013. Geoengineering impact of open ocean dissolution of olivine on atmospheric CO2, surface ocean pH and marine biology. *Environmental Research Letters* 8(1), doi: Artn 01400910.1088/1748-9326/8/1/014009

Kohler, P. et al. 2010. Geoengineering potential of artificially enhanced silicate weathering of olivine. *Proceedings of the National Academy of Sciences of the United States of America* 107(47), pp. 20228-20233. doi: 10.1073/pnas.1000545107

Kolber, Z. S. et al. 1998. Measurements of variable chlorophyll fluorescence using fast repetition rate techniques: defining methodology and experimental protocols. *Biochimica et Biophysica Acta (BBA)-Bioenergetics* 1367(1-3), pp. 88-106.

Kolzenburg, R. et al. 2019. Understanding the margin squeeze: Differentiation in fitness-related traits between central and trailing edge populations of *Corallina officinalis*. *Ecology and Evolution* 9(10), pp. 5787-5801. doi: 10.1002/ece3.5162

Krajewska, B. 2009. Ureases I. Functional, catalytic and kinetic properties: A review. *Journal of Molecular Catalysis B: Enzymatic* 59(1-3), pp. 9-21.

Krause, G. and Weis, E. 1991. Chlorophyll fluorescence and photosynthesis - the basics. *Annual Review of Plant Physiology and Plant Molecular Biology* 42, pp. 313-349. doi: 10.1146/annurev.pp.42.060191.001525

Kroeker, K. et al. 2010. Meta-analysis reveals negative yet variable effects of ocean acidification on marine organisms. *Ecology Letters* 13(11), pp. 1419-1434. doi: 10.1111/j.1461-0248.2010.01518.x

Kroeker, K. J. et al. 2011. Divergent ecosystem responses within a benthic marine community to ocean acidification. *Proceedings of the National Academy of Sciences* 108(35), pp. 14515-14520.

Krumbein, W. E. and Giele, C. 1979. Calcification in a coccoid cyanobacterium associated with the formation of desert stromatolites. *Sedimentology* 26(4), pp. 593-604.

Kut, D. et al. 2000. Trace metals in marine algae and sediment samples from the Bosphorus. *Water, Air, and Soil Pollution* 118(1), pp. 27-33.

Kvernvik, A. et al. 2020. Higher sensitivity towards light stress and ocean acidification in an Arctic sea-ice-associated diatom compared to a pelagic diatom. *New Phytologist* 226(6), pp. 1708-1724. doi: 10.1111/nph.16501

Labour. 1 May 2019. J*eremy Corbyn declares environment and climate emergency [*Press release].

Lackner, K. S. 2002. Carbonate chemistry for sequestering fossil carbon. *Annual Review of Energy and the Environment* 27, pp. 193-232. doi: 10.1146/annurev.energy.27.122001.083433

Laney, S. R. 2003. Assessing the error in photosynthetic properties determined by fast repetition rate fluorometry. *Limnology and Oceanography* 48(6), pp. 2234-2242.

Laney, S. R. and Letelier, R. M. 2008. Artifacts in measurements of chlorophyll fluorescence transients, with specific application to fast repetition rate fluorometry. *Limnology and Oceanography: Methods* 6(1), pp. 40-50.

Langdon, C. et al. 2000. Effect of calcium carbonate saturation state on the calcification rate of an experimental coral reef. *Global Biogeochemical Cycles* 14(2), pp. 639-654.

Laure, M. L. J. N. et al. 2009. Grazing dynamics in intertidal rockpools: connectivity of microhabitats. *Journal of Experimental Marine Biology and Ecology* 370(1-2), pp. 9-17.

Lawrence, M. et al. 2018. Evaluating climate geoengineering proposals in the context of the Paris Agreement temperature goals. *Nature Communications* 9, doi: 10.1038/s41467-018-05938-3

Lawton, J. H. and Brown, V. K. 1994. Redundancy in ecosystems.*Biodiversity and ecosystem function*. Springer, pp. 255-270.

Le Quéré, C. et al. 2018. Global Carbon Budget 2018. *Earth System Science Data* 10(4), pp. 2141-2194. doi: 10.5194/essd-10-2141-2018

Lee, B. et al. 2004. Screening of cyanobacterial species for calcification. *Biotechnology Progress* 20(5), pp. 1345-1351. doi: 10.1021/bp0343561

Lee, B. et al. 2006. Calcium carbonate formation by *Synechococcus* sp strain PCC 8806 and *Synechococcus* sp strain PCC 8807. *Bioresource Technology* 97(18), pp. 2427-2434. doi: 10.1016/j.biortech.2005.09.028

Lee, D. and Carpenter, S. J. 2001. Isotopic disequilibrium in marine calcareous algae. *Chemical Geology* 172(3-4), pp. 307-329. doi: Doi 10.1016/S0009-2541(00)00258-8

Lenton, A. et al. 2018. Assessing carbon dioxide removal through global and regional ocean alkalinization under high and low emission pathways. *Earth System Dynamics* 9(2), pp. 339-357. doi: 10.5194/esd-9-339-2018

Lenton, T. M. and Britton, C. 2006. Enhanced carbonate and silicate weathering accelerates recovery from fossil fuel CO2 perturbations. *Global Biogeochemical Cycles* 20(3),

Lenzi, D. et al. 2018. Don't deploy negative emissions technologies without ethical analysis. Nature Publishing Group.

Lin, B. and Zhu, J. 2019. The role of renewable energy technological innovation on climate change: Empirical evidence from China. *Science of the Total Environment* 659, pp. 1505-1512. doi: 10.1016/j.scitotenv.2018.12.449

Littler, M. M. et al. 1983. Evolutionary strategies in a tropical barrier reef system: functional-form groups of marine macroalgae 1. *Journal of Phycology* 19(2), pp. 229-237.

Lohbeck, K. et al. 2012. Adaptive evolution of a key phytoplankton species to ocean acidification. *Nature Geoscience* 5(5), pp. 346-351. doi: 10.1038/NGEO1441

Lopez, O. et al. 2009. The influence of temperature and seawater composition on calcite crystal growth mechanisms and kinetics: Implications for Mg incorporation in calcite lattice. *Geochimica Et Cosmochimica Acta* 73(2), pp. 337-347. doi: 10.1016/j.gca.2008.10.022

Lord, N. S. et al. 2016. An impulse response function for the "long tail" of excess atmospheric CO2 in an Earth system model. *Global Biogeochemical Cycles* 30(1), pp. 2-17. doi: 10.1002/2014gb005074

Lui, H. et al. 2020. Intrusion of Kuroshio Helps to Diminish Coastal Hypoxia in the Coast of Northern South China Sea. *Frontiers in Marine Science* 7, doi: 10.3389/fmars.2020.565952

Mackenzie, F. T. and Kump, L. R. 1995. Reverse weathering, clay mineral formation, and oceanic element cycles. *Science* 270(5236), pp. 586-586.

Mackey, K. et al. 2009. Picophytoplankton responses to changing nutrient and light regimes during a bloom. *Marine Biology* 156(8), pp. 1531-1546. doi: 10.1007/s00227-009-1185-2

Mallick, N. et al. 1990. Impact of bimetallic combinations of Cu, Ni and Fe on growth rate, uptake of nitrate and ammonium, 14 $CO_2$ fixation, nitrate reductase and urease activity of *Chlorella vulgaris*. *Biology of metals* 2(4), pp. 223-228.

Mamboya, F. A. 2007. Heavy metal contamination and toxicity: Studies of macroalgae from the Tanzanian Coast.

Martin, S. et al. 2007. Community metabolism in temperate maerl beds. I. Carbon and carbonate fluxes. *Marine Ecology Progress Series* 335, pp. 19-29. doi: 10.3354/meps335019

Martin, S. and Gattuso, J. P. 2009. Response of Mediterranean coralline algae to ocean acidification and elevated temperature. *Global Change Biology* 15(8), pp. 2089-2100. doi: 10.1111/j.1365-2486.2009.01874.x

Martone, P. and Denny, M. 2008a. To bend a coralline: effect of joint morphology on flexibility and stress amplification in an articulated calcified seaweed. *Journal of Experimental Biology* 211(21), pp. 3421-3432. doi: 10.1242/jeb.020479

Martone, P. and Denny, M. 2008b. To break a coralline: mechanical constraints on the size and survival of a wave-swept seaweed. *Journal of Experimental Biology* 211(21), pp. 3433-3441. doi: 10.1242/jeb.020495

Matear, R. and Lenton, A. 2018. Carbon-climate feedbacks accelerate ocean acidification. *Biogeosciences* 15(6), pp. 1721-1732. doi: 10.5194/bg-15-1721-2018

Matheickal, J. and Yu, Q. 1999. Biosorption of lead(II) and copper(II) from aqueous solutions by pre-treated biomass of Australian marine algae. *Bioresource Technology* 69(3), pp. 223-229. doi: 10.1016/S0960-8524(98)00196-5

Matsunaga, K. et al. 1999. The role of terrestrial humic substances on the shift of kelp community to crustose coralline algae community of the southern Hokkaido Island in the Japan Sea. *Journal of Experimental Marine Biology and Ecology* 241(2), pp. 193-205. doi: 10.1016/S0022-0981(99)00077-5

McConnaughey, T. A. and Whelan, J. F. 1997. Calcification generates protons for nutrient and bicarbonate uptake. *Earth-Science Reviews* 42(1-2), pp. 95-117. doi: 10.1016/s0012-8252(96)00036-0

McGlashan, N. et al. 2012. High-level techno-economic assessment of negative emissions technologies. *Process Safety and Environmental Protection* 90(6), pp. 501-510. doi: 10.1016/j.psep.2012.10.004

McLaren, D. 2012. A comparative global assessment of potential negative emissions technologies. *Process Safety and Environmental Protection* 90(6), pp. 489-500. doi: 10.1016/j.psep.2012.10.005

Mehrbach, C. et al. 1973. Measurement of Apparent Dissociation-Constants of Carbonic-Acid in Seawater at Atmospheric-Pressure. *Limnology and Oceanography* 18(6), pp. 897-907. doi: DOI 10.4319/lo.1973.18.6.0897

Merz, M. U. E. 1992. The biology of carbonate precipitation by cyanobacteria. *Facies* 26(1), pp. 81-101.

Merz, M. U. E. and Zankl, H. 1993. The influence of culture conditions on growth and sheath development of calcifying cyanobacteria. *Facies* 29(1), pp. 75-80.

Merz-Preiß, M. 2000. Calcification in cyanobacteria.*Microbial sediments*. Springer, pp. 50-56.

Meyer, F. W. et al. 2015. The Physiological Response of Two Green Calcifying Algae from the Great Barrier Reef towards High Dissolved Inorganic and Organic Carbon (DIC and DOC) Availability. *Plos One* 10(8), doi: 10.1371/journal.pone.0133596

Meysman, F. J. R. and Montserrat, F. 2017. Negative $CO_2$ emissions via enhanced silicate weathering in coastal environments. *Biology Letters* 13(4), doi: ARTN 20160905 10.1098/rsbl.2016.0905

Middelboe, A. L. and Hansen, P. J. 2007. High pH in shallow-water macroalgal habitats. *Marine Ecology Progress Series* 338, pp. 107-117. doi: 10.3354/meps338107

Miller, A. et al. 1990. Physiological-aspects of $CO_2$ and $HCO_3^-$ transport by cyanobacteria - A Review. *Canadian Journal of Botany-Revue Canadienne De Botanique* 68(6), pp. 1291-1302. doi: 10.1139/b90-165

Miller, A. et al. 1991. Active $CO_2$ transport in cyanobacteria. *Canadian Journal of Botany-Revue Canadienne De Botanique* 69(5), pp. 925-935. doi: 10.1139/b91-119

Milliman, J. 1993. Production and accumulation of calcium-carbonate in the ocean - budget of a nonsteady statE. *Global Biogeochemical Cycles* 7(4), pp. 927-957. doi: 10.1029/93GB02524

Minx, J. C. et al. 2018. Negative emissions-Part 1: Research landscape and synthesis. *Environmental Research Letters* 13(6), doi: 10.1088/1748-9326/aabf9b

Miyachi, S. et al. 2003. Historical perspective on microalgal and cyanobacterial acclimation to low- and extremely high-$CO_2$ conditions. *Photosynthesis Research* 77(2-3), pp. 139-153. doi: 10.1023/A:1025817616865

Mohamed, L. A. and Khaled, A. 2005. Comparative study of heavy metal distribution in some coastal seaweeds of Alexandria, Egypt. *Chemistry and Ecology* 21(3), pp. 181-189.

Moisan, T. et al. 2010. Influences of temperature and nutrients on Synechococcus abundance and biomass in the southern Mid-Atlantic Bight. *Continental Shelf Research* 30(12), pp. 1275-1282. doi: 10.1016/j.csr.2010.04.005

Monteiro, F. et al. 2016. Why marine phytoplankton calcify. *Science Advances* 2(7), doi: 10.1126/sciadv.1501822

Montes-Hernandez, G. and Renard, F. 2016. Time-Resolved in Situ Raman Spectroscopy of the Nucleation and Growth of Siderite, Magnesite, and Calcite and Their Precursors. *Crystal Growth & Design* 16(12), pp. 7218-7230. doi: 10.1021/acs.cgd.6b01406

Montserrat, F. et al. 2017. Olivine Dissolution in Seawater: Implications for $CO_2$ Sequestration through Enhanced Weathering in Coastal Environments. *Environmental Science & Technology* 51(7), pp. 3960-3972. doi: 10.1021/acs.est.605942

Moore, C. et al. 2013. Processes and patterns of oceanic nutrient limitation. *Nature Geoscience* 6(9), pp. 701-710. doi: 10.1038/NGEO1765

Morse, J. W. and He, S. 1993. Influences of T, S and $pCO_2$ on the pseudo-homogeneous precipitation of CaCO3 from seawater: implications for whiting formation. *Marine Chemistry* 41(4), pp. 291-297.

Mouillot, D. et al. 2013. Rare species support vulnerable functions in high-diversity ecosystems. *PLoS biol* 11(5), p. e1001569.

Mucci, A. 1986. Growth kinetics and composition of magnesian calcite overgrowths precipitated from seawater: Quantitative influence of orthophosphate ions. *Geochimica et Cosmochimica Acta* 50(10), pp. 2255-2265.

Mucci, A. et al. 1989. The solubility of calcite and aragonite in sulfate-free seawater and the seeded growth kinetics and composition of the precipitates at 25 C. *Chemical geology* 74(3-4), pp. 309-320.

Mucci, A. and Morse, J. W. 1983. The incorporation of $Mg^{2+}$ and $Sr^{2+}$ into calcite overgrowths: influences of growth rate and solution composition. *Geochimica et Cosmochimica Acta* 47(2), pp. 217-233.

Muller, M. N. et al. 2015. Differing responses of three Southern Ocean Emiliania huxleyi ecotypes to changing seawater carbonate chemistry. *Marine Ecology Progress Series* 531, pp. 81-90. doi: 10.3354/meps11309

Murphy, T. et al. 2016. A Radiative Transfer Modeling Approach for Accurate Interpretation of PAM Fluorometry Experiments in Suspended Algal Cultures. *Biotechnology Progress* 32(6), pp. 1601-1615. doi: 10.1002/btpr.2394

Naeem, S. et al. 2012. The functions of biological diversity in an age of extinction. *science* 336(6087), pp. 1401-1406.

Nelson, D. et al. 1995. Production and dissolution of biogenic silica in the ocean - revised global estimates, comparison with regional data and relationship to biogenic sedimentation. *Global Biogeochemical Cycles* 9(3), pp. 359-372. doi: 10.1029/95GB01070

Nelson, W. A. 2009. Calcified macroalgae - critical to coastal ecosystems and vulnerable to change: a review. *Marine and Freshwater Research* 60(8), pp. 787-801. doi: 10.1071/mf08335

Nemet, G. F. et al. 2018. Negative emissions-Part 3: Innovation and upscaling. *Environmental Research Letters* 13(6), doi: 10.1088/1748-9326/aabff4

Nieto, J. et al. 2018. Less than 2 degrees C? An Economic-Environmental Evaluation of the Paris Agreement. *Ecological Economics* 146, pp. 69-84. doi: 10.1016/j.ecolecon.2017.10.007

Noisette, F. et al. 2013. Physiological responses of three temperate coralline algae from contrasting habitats to near-future ocean acidification. *Journal of Experimental Marine Biology and Ecology* 448, pp. 179-187. doi: 10.1016/j.jembe.2013.07.006

Oelkers, E. et al. 2018. Olivine dissolution rates: A critical review. *Chemical Geology* 500, pp. 1-19. doi: 10.1016/j.chemgeo.2018.10.008

Ogawa, T. and Inoue, Y. 1983. Photosystem i-initiated postillumination $CO_2$ burst in a cyanobacterium, *Anabaena-variabilis*. *Biochimica Et Biophysica Acta* 724(3), pp. 490-493. doi: 10.1016/0005-2728(83)90110-X

Ogawa, T. et al. 1985. Photosystem-I-driven inorganic carbon transport in the cyanobacterium, Anacystis nidulans. *Biochimica et Biophysica Acta (BBA)-Bioenergetics* 808(1), pp. 77-84.

Oliver, T. H. et al. 2015. Biodiversity and resilience of ecosystem functions. *Trends in ecology & evolution* 30(11), pp. 673-684.

Olsson, J. et al. 2012. Olivine reactivity with $CO_2$ and $H_2O$ on a microscale: Implications for carbon sequestration. *Geochimica Et Cosmochimica Acta* 77, pp. 86-97. doi: 10.1016/j.gca.2011.11.001

Orr, J. et al. 2005. Anthropogenic ocean acidification over the twenty-first century and its impact on calcifying organisms. *Nature* 437(7059), pp. 681-686. doi: 10.1038/nature04095

Oxborough, K. and Baker, N. 1997a. An instrument capable of imaging chlorophyll alpha fluorescence from intact leaves at very low irradiance and at cellular and subcellular levels of organization. *Plant Cell and Environment* 20(12), pp. 1473-1483. doi: 10.1046/j.1365-3040.1997.d01-42.x

Oxborough, K. and Baker, N. 1997b. Resolving chlorophyll a fluorescence images of photosynthetic efficiency into photochemical and non-photochemical components - calculation of qP and Fv '/Fm ' without measuring Fo '. *Photosynthesis Research* 54(2), pp. 135-142. doi: 10.1023/A:1005936823310

Paerl, H. W. 1997. Coastal eutrophication and harmful algal blooms: Importance of atmospheric deposition and groundwater as “new” nitrogen and other nutrient sources. *Limnology and oceanography* 42(5part2), pp. 1154-1165.

Palmer, C. 2019. Mitigating Climate Change Will Depend on Negative Emissions Technologies. *Engineering* 5(6), pp. 982-984. doi: 10.1016/j.eng.2019.10.006

Papageorgiou, S. K. et al. 2006. Heavy metal sorption by calcium alginate beads from Laminaria digitata. *Journal of Hazardous Materials* 137(3), pp. 1765-1772.

Paquay, F. S. and Zeebe, R. E. 2013. Assessing possible consequences of ocean liming on ocean pH, atmospheric CO2 concentration and associated costs. *International Journal of Greenhouse Gas Control* 17, pp. 183-188. doi: 10.1016/j.ijggc.2013.05.005

Parkhurst, D. L. and Appelo, C. A. J. 1999. User's guide to PHREEQC—a computer program for speciation, reaction-path, 1D-transport, and inverse geochemical calculations. *US Geological Survey Water-Resources Investigations Report* 99, p. 4259.

Partensky, F. et al. 1999. Differential distribution and ecology of Prochlorococcus and Synechococcus in oceanic waters: a review. *Bulletin-Institut Oceanographique Monaco-Numero Special-*, pp. 457-476.

Pentecost, A. 1978. Calcification and photosynthesis in *Corallina officinalis*. using the $^{14}CO_2$ method. *British phycological journal* 13(4), pp. 383-390.

Pentecost, A. 1986. Calcification in cyanobacteria. *Biomineralization in lower plants and animals*, pp. 73-90.

Pentecost, A. and Spiro, B. 1990. Stable carbon and oxygen isotope composition of calcites associated with modern freshwater cyanobacteria and algae. *Geomicrobiology Journal* 8(1), pp. 17-26.

Perkins, R. et al. 2016. Microspatial variability in community structure and photophysiology of calcified macroalgal microbiomes revealed by coupling of hyperspectral and high-resolution fluorescence imaging. *Scientific Reports* 6, doi: 10.1038/srep22343

Perkins, R. G. et al. 2006. Light response curve methodology and possible implications in the application of chlorophyll fluorescence to benthic diatoms. *Marine Biology* 149(4), pp. 703-712. doi: 10.1007/s00227-005-0222-z

Peter, K. H. and Sommer, U. 2013. Phytoplankton cell size reduction in response to warming mediated by nutrient limitation. *PloS one* 8(9), p. e71528.

Peters, G. P. et al. 2013. COMMENTARY: The challenge to keep global warming below 2 degrees C. *Nature Climate Change* 3(1), pp. 4-6.

Peterson, H. et al. 1984. Metal toxicity to algae - a highly pH dependent phenomenon. *Canadian Journal of Fisheries and Aquatic Sciences* 41(6), pp. 974-979. doi: 10.1139/f84-111

Pierrot, D. et al. 2006. MS Excel program developed for CO2 system calculations. ORNL/CDIAC-105a. Carbon Dioxide Information Analysis Center, Oak Ridge National Laboratory, US Department of Energy, Oak Ridge.

Pires, J. 2019. Negative emissions technologies: A complementary solution for climate change mitigation. *Science of the Total Environment* 672, pp. 502-514. doi: 10.1016/j.scitotenv.2019.04.004

Pokrovsky, O. S. and Schott, J. 2000. Kinetics and mechanism of forsterite dissolution at 25 degrees C and pH from 1 to 12. *Geochimica Et Cosmochimica Acta* 64(19), pp. 3313-3325. doi: 10.1016/s0016-7037(00)00434-8

Prasher, S. et al. 2004. Biosorption of heavy metals by red algae (Palmaria palmata). *Environmental Technology* 25(10), pp. 1097-1106. doi: 10.1080/09593332508618378

Price, G. et al. 1998. The functioning of the $CO_2$ concentrating mechanism in several cyanobacterial strains: a review of general physiological characteristics, genes, proteins, and recent advances. *Canadian Journal of Botany-Revue Canadienne De Botanique* 76(6), pp. 973-1002. doi: 10.1139/b98-081

Price, G. D. et al. 2008. Advances in understanding the cyanobacterial $CO_2$-concentrating-mechanism (CCM): functional components, Ci transporters, diversity, genetic regulation and prospects for engineering into plants. *Journal of experimental botany* 59(7), pp. 1441-1461.

Pytkowicz, R. M. 1965. Rates of inorganic calcium carbonate nucleation. *The Journal of Geology* 73(1), pp. 196-199.

Ragueneau, O. et al. 2006. Si and C interactions in the world ocean: Importance of ecological processes and implications for the role of diatoms in the biological pump. *Global Biogeochemical Cycles* 20(4),

Rau, G. H. and Caldeira, K. 1999. Enhanced carbonate dissolution: a means of sequestering waste $CO_2$ as ocean bicarbonate. *Energy Conversion and Management* 40(17), pp. 1803-1813. doi: 10.1016/s0196-8904(99)00071-0

Rau, G. H. et al. 2013. Direct electrolytic dissolution of silicate minerals for air $CO_2$ mitigation and carbon-negative $H_2$ production. *Proceedings of the National Academy of Sciences of the United States of America* 110(25), pp. 10095-10100. doi: 10.1073/pnas.1222358110

Reis, P. A. et al. 2017. Barnacle species as biomonitors of metal contamination in the northwest coast of Portugal: Ecological quality classification approach. *Human and Ecological Risk Assessment: An International Journal* 23(5), pp. 1219-1233.

Renforth, P. 2012. The potential of enhanced weathering in the UK. *International Journal of Greenhouse Gas Control* 10, pp. 229-243. doi: 10.1016/j.ijggc.2012.06.011

Renforth, P. and Henderson, G. 2017. Assessing ocean alkalinity for carbon sequestration. *Reviews of Geophysics* 55(3), pp. 636-674. doi: 10.1002/2016rg000533

Renforth, P. et al. 2013. Engineering challenges of ocean liming. *Energy* 60, pp. 442-452. doi: 10.1016/j.energy.2013.08.006

Renforth, P. and Kruger, T. 2013. Coupling Mineral Carbonation and Ocean Liming. *Energy & Fuels* 27(8), pp. 4199-4207. doi: 10.1021/ef302030w

Renforth, P. et al. 2015. The dissolution of olivine added to soil: Implications for enhanced weathering. *Applied Geochemistry* 61, pp. 109-118. doi: 10.1016/j.apgeochem.2015.05.016

Renforth P. and Campbell (2021, accepted) The role of soils in the regulation of ocean acidification. *Phil. Trans. R. Soc. B.*

Rérolle V.M.C. et al. 2012 Seawater-pH measurements for ocean-acidification observations. *Trends in Anaytical Chemistry*, 40, pp. 146-157

Reusch, T. and Wood, T. 2007. Molecular ecology of global change. *Molecular Ecology* 16(19), pp. 3973-3992. doi: 10.1111/j.1365-294X.2007.03454.x

Rhein, M. et al. 2013. Observations: Ocean. In: Climate Change 2013: The Physical Science Basis. Contribution of Working Group I to the Fifth Assessment Report of the Intergovernmental Panel on Climate Change. [Stocker, T.F., D. Qin, G.-K. Plattner, M. Tignor, S.K. Allen, J. Boschung, A. Nauels, Y. Xia, V. Bex and P.M. Midgley (eds.)]. Cambridge University Press, Cambridge, United Kingdom and New York, NY, USA

Rheuban, J. et al. 2019. Quantifying the effects of nutrient enrichment and freshwater mixing on coastal ocean acidification. *Journal of Geophysical Research-Oceans* 124(12), pp. 9085-9100. doi: 10.1029/2019JC015556

Richardson, T. and Jackson, G. 2007. Small phytoplankton and carbon export from the surface ocean. *Science* 315(5813), pp. 838-840. doi: 10.1126/science.1133471

Ricou, P. et al. 1998. Influence of pH on removal of heavy metallic cations by fly ash in aqueous solution. *Environmental Technology* 19(10), pp. 1005-1016.

Riding, R. 1977. Calafied plectonema (blue-green algae), a recent example of *Girvanella* from aldabra atoll. *Palaeontology* 20(1), pp. 33-46

Riding, R. 1991. Classification of microbial carbonates.*Calcareous algae and stromatolites*. Springer, pp. 21-51.

Riding, R. 2006a. Cyanobacterial calcification, carbon dioxide concentrating mechanisms, and Proterozoic-Cambrian changes in atmospheric composition. *Geobiology* 4(4), pp. 299-316. doi: 10.1111/j.1472-4669.2006.00087.x

Riding, R. 2006b. Cyanobacterial calcification, carbon dioxide concentrating mechanisms, and Proterozoic–Cambrian changes in atmospheric composition. *Geobiology* 4(4), pp. 299-316.

Riding, R. 2009. An atmospheric stimulus for cyanobacterial-bioinduced calcification ca. 350 million years ago? *Palaios* 24(9-10), pp. 685-696. doi: 10.2110/palo.2009.p09-033r

Riding, R. and Liang, L. 2005. Geobiology of microbial carbonates: metazoan and seawater saturation state influences on secular trends during the Phanerozoic. *Palaeogeography, Palaeoclimatology, Palaeoecology* 219(1-2), pp. 101-115.

Riebesell, U. 2004. Effects of $CO_2$ enrichment on marine phytoplankton. *Journal of Oceanography* 60(4), pp. 719-729. doi: 10.1007/s10872-004-5764-z

Riebesell U. et al. 2010. Guide to best practices for ocean acidification research and data reporting, pp. 20-39. Luxembourg: Publications Office of the European Union. doi: 10.2777/66906.

Riebesell, U. et al. 2017. Competitive fitness of a predominant pelagic calcifier impaired by ocean acidification. *Nature Geoscience* 10(1), pp. 19-23. doi: 10.1038/NGEO2854

Riebesell, U. and Gattuso, J.-P. 2015. Lessons learned from ocean acidification research. *Nature Climate Change* 5(1), pp. 12-14. doi: 10.1038/nclimate2456

Riebesell, U. et al. 2009. Sensitivities of marine carbon fluxes to ocean change. *Proceedings of the National Academy of Sciences of the United States of America* 106(49), pp. 20602-20609. doi: 10.1073/pnas.0813291106 doi:10.1073/pnas.0813291106

Riebesell, U. et al. 1993. Carbon-dioxide limitation of marine-phytoplankton growth-rates. *Nature* 361(6409), pp. 249-251. doi: 10.1038/361249a0

Riebesell, U. et al. 2000. Reduced calcification of marine plankton in response to increased atmospheric $CO_2$. *Nature* 407(6802), pp. 364-367. doi: 10.1038/35030078

Riebesell, U. et al. 2010 Guide to Best Practices for Ocean Acidification Research and Data Reporting. Publications Office of the European Union, Luxembourg (2010), pp. 27-31

Ries, J. B. 2009. Effects of secular variation in seawater Mg/Ca ratio (calcite-aragonite seas) on $CaCO_3$ sediment production by the calcareous algae *Halimeda, Penicillus* and *Udotea*-evidence from recent experiments and the geological record. *Terra Nova* 21(5), pp. 323-339. doi: 10.1111/j.1365-3121.2009.00899.x

Ries, J. B. et al. 2009. Marine calcifiers exhibit mixed responses to $CO_2$-induced ocean acidification. *Geology* 37(12), pp. 1131-1134. doi: 10.1130/g30210a.1

Rigopoulos, I. et al. 2018. Carbon sequestration via enhanced weathering of peridotites and basalts in seawater. *Applied Geochemistry* 91, pp. 197-207. doi: 10.1016/j.apgeochem.2017.11.001

Rippka, R. et al. 1979. Generic assignments, strain histories and properties of pure cultures of cyanobacteria. *Microbiology* 111(1), pp. 1-61.

Rocap, G. et al. 2003. Genome divergence in two *Prochlorococcus* ecotypes reflects oceanic niche differentiation. *Nature* 424(6952), pp. 1042-1047. doi: 10.1038/nature01947

Rosenfeld, J. S. 2002. Functional redundancy in ecology and conservation. *Oikos* 98(1), pp. 156-162.

Rost, B. et al. 2006. Inorganic carbon acquisition in red tide dinoflagellates. *Plant Cell and Environment* 29(5), pp. 810-822. doi: 10.1111/j.1365-3040.2005.01450.x

Rost, B. et al. 2008. Sensitivity of phytoplankton to future changes in ocean carbonate chemistry: current knowledge, contradictions and research directions. *Marine Ecology Progress Series* 373, pp. 227-237. doi: 10.3354/meps07776

Sabine, C. L. et al. 2004. The oceanic sink for anthropogenic $CO_2$. *Science* 305(5682), pp. 367-371. doi: 10.1126/science.1097403

Sakshaug, E. et al. 1997. Parameters of photosynthesis: definitions, theory and interpretation of results. *Journal of Plankton Research* 19(11), pp. 1637-1670. doi: DOI 10.1093/plankt/19.11.1637

Saldi, G. et al. 2009. Magnesite growth rates as a function of temperature and saturation state. *Geochimica Et Cosmochimica Acta* 73(19), pp. 5646-5657. doi: 10.1016/j.gca.2009.06.035

Sarmiento, J. and Gruber, N. 2002. Sinks for anthropogenic carbon. *Physics Today* 55(8), pp. 30-36. doi: 10.1063/1.1510279

Sarmiento, J. et al. 2004. Response of ocean ecosystems to climate warming. *Global Biogeochemical Cycles* 18(3), doi: 10.1029/2003GB002134

Scanlan, D. et al. 2009. Ecological Genomics of Marine Picocyanobacteria. *Microbiology and Molecular Biology Reviews* 73(2), pp. 249-+. doi: 10.1128/MMBR.00035-08

Schmittner, A. et al. 2008. Future changes in climate, ocean circulation, ecosystems, and biogeochemical cycling simulated for a business-as-usual CO2 emission scenario until year 4000 AD. *Global Biogeochemical Cycles* 22(1), doi: 10.1029/2007GB002953

Schrag, D. P. 2007. Preparing to capture carbon. *Science* 315(5813), pp. 812-813. doi: 10.1126/science.1137632

Schreiber, U. 2004. Pulse-Amplitude-Modulation (PAM) Fluorometry and Saturation Pulse Method: An Overview. 19, pp. 279-319. doi: 10.1007/978-1-4020-3218-9_11

Schuiling, R. D. and de Boer, P. L. 2010. Coastal spreading of olivine to control atmospheric $CO_2$ concentrations: A critical analysis of viability. Comment: Nature and laboratory models are different. *International Journal of Greenhouse Gas Control* 4(5), pp. 855-856. doi: 10.1016/j.ijggc.2010.04.012

Schuiling, R. D. and Krijgsman, P. 2006. Enhanced weathering: An effective and cheap tool to sequester $CO_2$. *Climatic Change* 74(1-3), pp. 349-354. doi: 10.1007/s10584-005-3485-y

Schulz, K. et al. 2013. Temporal biomass dynamics of an Arctic plankton bloom in response to increasing levels of atmospheric carbon dioxide. *Biogeosciences* 10(1), pp. 161-180. doi: 10.5194/bg-10-161-2013

Schulz, K. et al. 2009. $CO_2$ perturbation experiments: similarities and differences between dissolved inorganic carbon and total alkalinity manipulations. *Biogeosciences* 6(10), pp. 2145-2153. doi: 10.5194/bg-6-2145-2009

Schulz, K. and Riebesell, U. 2013. Diurnal changes in seawater carbonate chemistry speciation at increasing atmospheric carbon dioxide. *Marine Biology* 160(8), pp. 1889-1899. doi: 10.1007/s00227-012-1965-y

Seifritz, W. 1990. $CO_2$ disposal by means of silicates. *Nature* 345(6275), pp. 486-486.

Sett, S. et al. 2014. Temperature modulates coccolithophorid sensitivity of growth, photosynthesis and calcification to increasing seawater $pCO_2$. *PloS one* 9(2), p. e88308.

Sheng, P. X. et al. 2004. Sorption of lead, copper, cadmium, zinc, and nickel by marine algal biomass: characterization of biosorptive capacity and investigation of mechanisms. *Journal of colloid and interface science* 275(1), pp. 131-141.

Smith, S. V. and Key, G. S. 1975. Carbon-Dioxide and Metabolism in Marine Environments. *Limnology and Oceanography* 20(3), pp. 493-495. doi: DOI 10.4319/lo.1975.20.3.0493

The Royal Society. 2018. Keeping global warming to 1.5°C Challenges and opportunities for the UK.

Sommer, U. et al. 2015. Warming and ocean acidification effects on phytoplankton—from species shifts to size shifts within species in a mesocosm experiment. *PloS one* 10(5), p. e0125239.

Stal, L. J. 2012. Cyanobacterial mats and stromatolites.*Ecology of cyanobacteria II*. Springer, pp. 65-125.

Stanienda-Pilecki, K. 2018. Magnesium calcite in Muschelkalk limestones of the Polish part of the Germanic Basin. *Carbonates and Evaporites* 33(4), pp. 801-821. doi: 10.1007/s13146-018-0437-y

Stengel, D. B. et al. 2004. Zinc concentrations in marine macroalgae and a lichen from western Ireland in relation to phylogenetic grouping, habitat and morphology. *Marine Pollution Bulletin* 48(9-10), pp. 902-909.

Stewart, J. G. 1982. Anchor species and epiphytes in intertidal algal turf. *Pacific Science* 36(1): 45-59

Suggett, D. et al. 2009. Comparing electron transport with gas exchange: parameterising exchange rates between alternative photosynthetic currencies for eukaryotic phytoplankton. *Aquatic Microbial Ecology* 56(2-3), pp. 147-162. doi: 10.3354/ame01303

Swanson, E. et al. 2014. Directed precipitation of hydrated and anhydrous magnesium carbonates for carbon storage. *Physical Chemistry Chemical Physics* 16(42), pp. 23440-23450. doi: 10.1039/c4cp03491k

Tai, V. and Palenik, B. 2009. Temporal variation of *Synechococcus* clades at a coastal Pacific Ocean monitoring site. *The ISME journal* 3(8), pp. 903-915.

Takahashi, T. et al. 2014. Climatological distributions of pH, $pCO_2$, total $CO_2$, alkalinity, and $CaCO_3$ saturation in the global surface ocean, and temporal changes at selected locations. *Marine Chemistry* 164, pp. 95-125. doi: 10.1016/j.marchem.2014.06.004

Takano, B. 1985. Geochemical implications of sulfate in sedimentary carbonates. *Chemical Geology* 49(4), pp. 393-403.

Tobin, J. M. et al. 1984. Uptake of metal ions by Rhizopus arrhizus biomass. *Applied and environmental Microbiology* 47(4), pp. 821-824.

Tonon, A. et al. 2018. *Gracilaria tenuistipitata* (Rhodophyta) tolerance to cadmium and copper exposure observed through gene expression and photosynthesis analyses. *Journal of Applied Phycology* 30(3), pp. 2129-2141. doi: 10.1007/s10811-017-1360-7

Tortell, P. et al. 2002. $CO_2$ effects on taxonomic composition and nutrient utilization in an Equatorial Pacific phytoplankton assemblage. *Marine Ecology Progress Series* 236, pp. 37-43. doi: 10.3354/meps236037

Tovar-Sánchez, A. et al. 2014. Contribution of groundwater discharge to the coastal dissolved nutrients and trace metal concentrations in Majorca Island: karstic vs detrital systems. *Environmental science & technology* 48(20), pp. 11819-11827.

Trimborn, S. et al. 2017. Iron sources alter the response of Southern Ocean phytoplankton to ocean acidification. *Marine Ecology Progress Series* 578, pp. 35-50. doi: 10.3354/meps12250

T*rissl*, H. and L*avergne*, J. 1995. Fluorescence induction from photosystem-ii - analytical equations for the yields of photochemistry and fluorescence derived from analysis of a model including exciton-radical pair equilibrium and restricted energy-transfer between photosynthetic units. *Australian Journal of Plant Physiology* 22(2), pp. 183-193. doi: 10.1071/PP9950183

The United Nations Framework Convention on Climate Change (UNFCCC). 2008. Provisions of the Kyoto Protocol and decisions by the Conference of the Parties serving as the meeting of the Parties to the Kyoto Protocol relating to the means to reach emission reduction targets of Annex I Parties.

The United Nations Framework Convention on Climate Change (UNFCCC). 2015. Adoption of the Paris Agreement.

Valenzuela, J. J. et al. 2018. Ocean acidification conditions increase resilience of marine diatoms. *Nature communications* 9(1), pp. 1-10.

van der Heijden, L. H. and Kamenos, N. A. 2015. Reviews and syntheses: Calculating the global contribution of coralline algae to total carbon burial. *Biogeosciences* 12(21), pp. 6429-6441. doi: 10.5194/bg-12-6429-2015

Volokita, M. et al. 1984. Nature of the inorganic carbon species actively taken up by the cyanobacterium Anabaena variabilis. *Plant Physiology* 76(3), pp. 599-602.

Waldbusser, G. et al. 2015. Ocean Acidification Has Multiple Modes of Action on Bivalve Larvae. *Plos One* 10(6), doi: 10.1371/journal.pone.0128376

Waldbusser, G. et al. 2014. Ocean Acidification in the Coastal Zone from an Organism's Perspective: Multiple System Parameters, Frequency Domains, and Habitats. *Annual Review of Marine Science, Vol 6* 6, pp. 221-247. doi: 10.1146/annurev-marine-121211-172238

Wallenstein, F. M. et al. 2009. Baseline metal concentrations in marine algae from São Miguel (Azores) under different ecological conditions–Urban proximity and shallow water hydrothermal activity. *Mar. Chem* 87, pp. 87-96.

Walsh, D. A. et al. 2009. Large volume (20L+) filtration of coastal seawater samples. *J Vis Exp* (28), doi: 10.3791/1161

Wang, F. and Giammar, D. E. 2013. Forsterite dissolution in saline water at elevated temperature and high $CO_2$ pressure. *Environmental science & technology* 47(1), pp. 168-173.

Wang, K. et al. 2011. Abundance and distribution of Synechococcus spp. and cyanophages in the Chesapeake Bay. *Applied and environmental microbiology* 77(21), pp. 7459-7468.

Ware, J. R. et al. 1992. Coral-Reefs - Sources or Sinks of Atmospheric Co2. *Coral Reefs* 11(3), pp. 127-130. doi: Doi 10.1007/Bf00255465

World Economic Forum (WEF). 2020. The Global Risks Report 2020.

White, E. et al. 2020. The Arctic picoeukaryote Micromonas pusilla benefits from ocean acidification under constant and dynamic light. *Biogeosciences* 17(3), pp. 635-647. doi: 10.5194/bg-17-635-2020

Williamson, C. et al. 2014. *Corallina* and *Ellisolandia* (Corallinales, Rhodophyta) photophysiology over daylight tidal emersion: interactions with irradiance, temperature and carbonate chemistry. *Marine Biology* 161(9), pp. 2051-2068. doi: 10.1007/s00227-014-2485-8

Williamson, C. J. et al. 2017. The regulation of coralline algal physiology, an in situ study of *Corallina officinalis* (Corallinales, Rhodophyta). *Biogeosciences* 14(19), pp. 4485-4498. doi: 10.5194/bg-14-4485-2017

Williamson, P. 2016. Emissions reduction: Scrutinize $CO_2$ removal methods. *Nature News* 530(7589), p. 153.

Wilson, S. et al. 2004. Environmental tolerances of free-living coralline algae (maerl): implications for European marine conservation. *Biological conservation* 120(2), pp. 279-289.

Wolf-Gladrow, D. A. et al. 2007. Total alkalinity: The explicit conservative expression and its application to biogeochemical processes. *Marine Chemistry* 106(1-2), pp. 287-300. doi: 10.1016/j.marchem.2007.01.006

Wu, Y. et al. 2010. $CO_2$-induced seawater acidification affects physiological performance of the marine diatom Phaeodactylum tricornutum. *Biogeosciences* 7(9), pp. 2915-2923.

Xu, H. et al. 2019. Precipitation of calcium carbonate mineral induced by viral lysis of cyanobacteria: evidence from laboratory experiments. *Biogeosciences* 16(4), pp. 949-960.

Xu, K. et al. 2018. Phytoplankton σPSII and excitation dissipation; implications for estimates of primary productivity. *Frontiers in Marine Science* 5, p. 281.

Yang, Z.-N. et al. 2016. Insight into calcification of Synechocystis sp. enhanced by extracellular carbonic anhydrase. *RSC advances* 6(35), pp. 29811-29817.

Zeebe, R. E. and Wolf-Gladrow, D. 2001. *CO2 in Seawater: Equilibrium, Kinetics, Isotopes*. Elsevier Oceanography Series.

Zhang, L. et al. 2017. Ecological Protection and Restoration ProgramReduced Grazing Pressure in the Three-River Headwaters Region, China. *Rangeland Ecology & Management* 70(5), pp. 540-548. doi: 10.1016/j.rama.2017.05.001

Zhang, Q. et al. 2018. In-situ LA-ICP-MS trace element analyses of scheelite and wolframite: Constraints on the genesis of veinlet-disseminated and vein-type tungsten deposits, South China. *Ore Geology Reviews* 99, pp. 166-179.

Zubkov, M. et al. 2000. Picoplankton community structure on the Atlantic Meridional Transect: a comparison between seasons. *Progress in Oceanography* 45(3-4), pp. 369-386. doi: 10.1016/S0079-6611(00)00008-2

Zwirglmaier, K. et al. 2007. Basin-scale distribution patterns of picocyanobacterial lineages in the Atlantic Ocean. *Environmental Microbiology* 9(5), pp. 1278-1290.

Zwirglmaier, K. et al. 2008. Global phylogeography of marine Synechococcus and Prochlorococcus reveals a distinct partitioning of lineages among oceanic biomes. *Environmental microbiology* 10(1), pp. 147-161.

# Appendix A: Carbonate chemistry parameters with changing salinity.

*Table A.1. Carbonate chemistry parameters and associated error when salinity is changed by +/- 10%. TA = total alkalinity (µEq $L^{-1}$), DIC = dissolved inorganic carbon (µmol $L^{-1}$), $pCO_2$ = atmospheric partial pressure of $CO_2$ (µatm), $[HCO_3^-]$ = bicarbonate ion concentration (µmol $L^{-1}$), $[CO_3^{2-}]$ = carbonate ion concentration (µmol $L^{-1}$), $[CO_2(aq)]$ = aqueous $CO_2$ concentration (µmol $L^{-1}$), $\Omega Ca$ = calcite saturation state, and $\Omega Ar$ = aragonite saturation state*

| Sal | Δ% | TA (µEq $L^{-1}$) | pH | DIC (µmol $L^{-1}$) | Δ% | $pCO_2$ (µatm) | Δ % | $[HCO_3^-]$ (µmol $L^{-1}$) | Δ % | $[CO_3^{2-}]$ (µmol $L^{-1}$) | Δ % | $[CO_{2(aq)}]$ (µmol $L^{-1}$) | Δ % | $\Omega_{ca}$ | Δ % | $\Omega_{Ar}$ | Δ % |
|---|---|---|---|---|---|---|---|---|---|---|---|---|---|---|---|---|---|
| 32 | | 3454 | 8.2 | 3084 | | 400 | | 2771 | | 298 | | 16 | | 7.23 | | 4.60 | |
| 32 | | 2694 | 7.97 | 2511 | | 574 | | 2341 | | 148 | | 23 | | 3.59 | | 2.29 | |
| 35.2 | 10 % | 3454 | 8.2 | 3053 | -1% | 389 | -3% | 2722 | -2% | 316 | 6% | 15 | -5% | 7.51 | 4% | 4.82 | 5% |
| 35.2 | 10 % | 2694 | 7.97 | 2493 | -1% | 561 | -2% | 2313 | -1% | 158 | 7% | 22 | -4% | 3.76 | 5% | 2.41 | 5% |
| 28.8 | -10 % | 3454 | 8.2 | 3115 | 1% | 414 | 4% | 2820 | 2% | 279 | -6% | 17 | 5% | 6.90 | -5% | 4.35 | -5% |
| 28.8 | -10 % | 2694 | 7.97 | 2530 | 1% | 591 | 3% | 2369 | 1% | 138 | -7% | 24 | 5% | 3.41 | -5% | 2.15 | -6% |

# Appendix B: Additional olivine dissolution experiments.

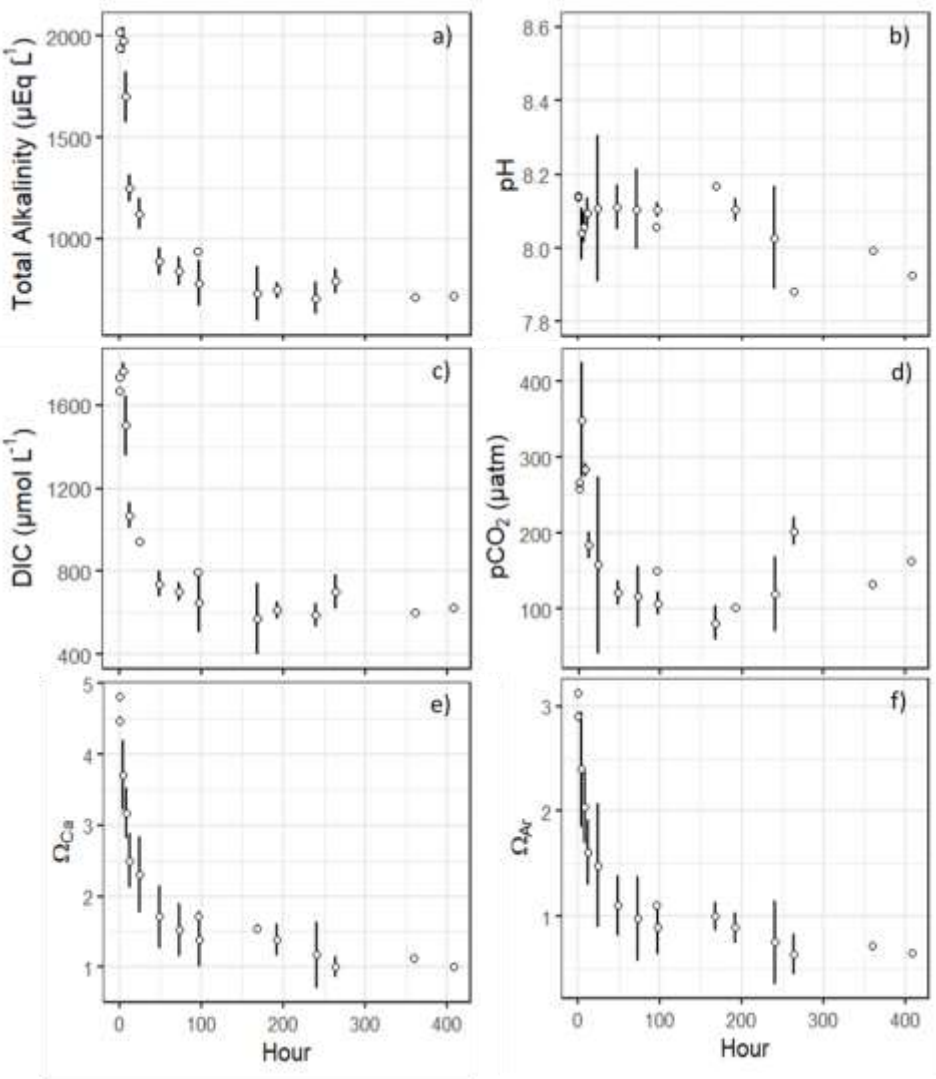


*Figure B.1. Average (± standard error) carbonate chemistry properties of the olivine dissolution experiment performed in April 2019. (a) total alkalinity (µEq L-1), (b) pH, (d) dissolved inorganic carbon (DIC, µmol $L^{-1}$), (d) atmospheric partial pressure of $CO_2$ ($pCO_2$, µatm), (e) calcite saturation state($\Omega_{Ca}$), (f) aragonite saturation state($\Omega_{Ar}$.*

In addition to the olivine dissolution experiment outlined in Chapter 3, two other olivine dissolution experiments were performed. Carbonate chemistry (TA. pH, DIC, $pCO_2$, $\Omega_{Ar}$ and $\Omega_{Ca}$) of the solution was monitored through each experiment using the same protocol outlined in Section 3.3.1.a). For the first experiment (Figure B.1), performed in April 2019, 200 g of olivine was added to 800 mL of seawater collected from Dunraven Bay (seawater was collected, filtered, and stored according to the protocol outlined in Chapter 3.3.1.a). There were three replicates and each seawater and olivine solution was held in a one litre boro-

silicate glass bottle and continuously agitated using a Heidolph shaker at ~200 rpm for ~17 days (400 hours).

The second experiment (Figure B.2) was performed in April 2018 and 200 g of olivine was added to 800 mL of seawater collected from Dunraven Bay (seawater was collected, filtered, and stored according to the protocol outlined in Section 3.3.1.a) with elevated TA (from $Na_2CO_3$ addition using the same protocol outlined in Chapter 2.3.2). Six replicates of elevated TA seawater and olivine solution were held in a one litre boro-silicate glass bottle and continuously agitated using a Heidolph shaker at ~200 rpm for 51 days.

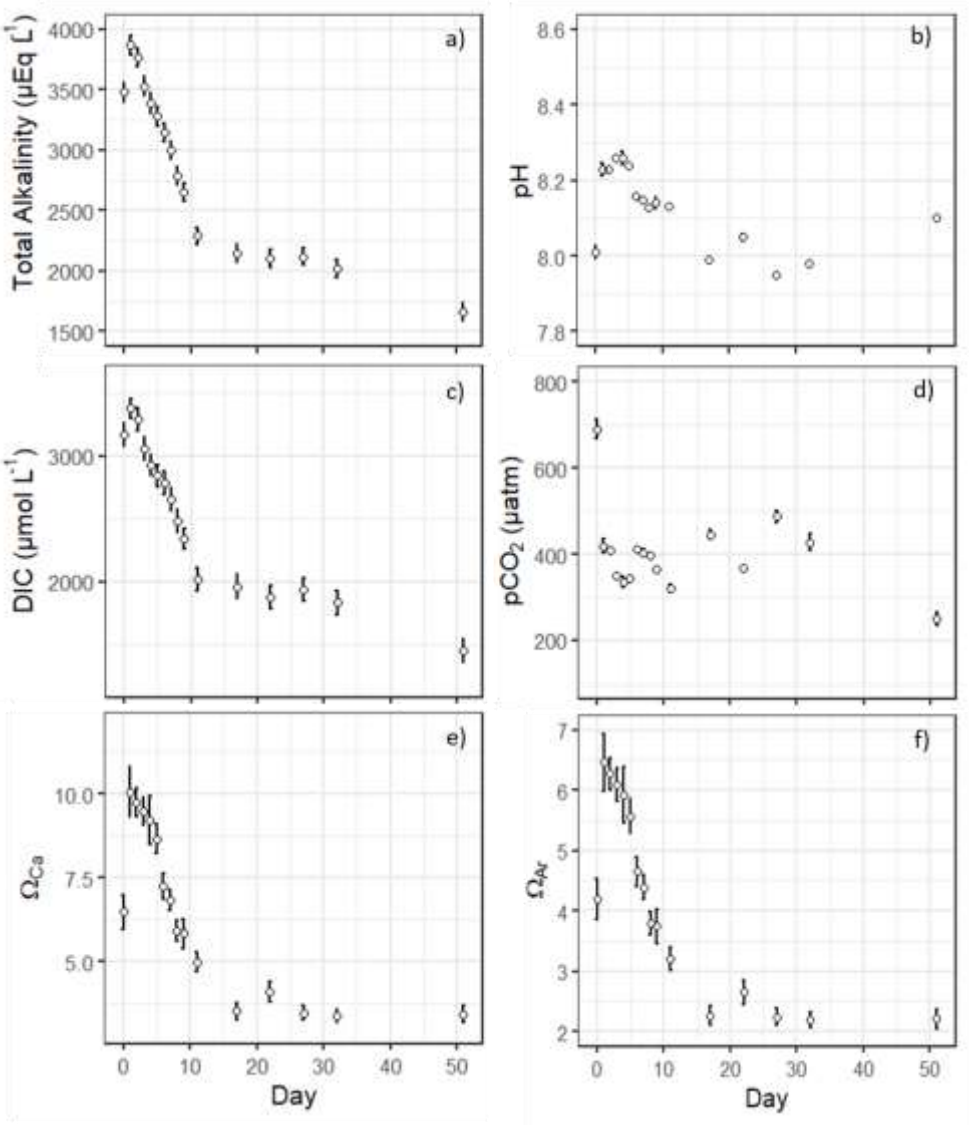


*Figure B.2. Average (± standard error) carbonate chemistry properties of the olivine dissolution experiment performed in April 2018. (a) total alkalinity (µEq L-1), (b) pH, (d) dissolved inorganic carbon (DIC, µmol $L^{-1}$), (d) atmospheric partial pressure of $CO_2$ ($pCO_2$, µatm), (e) calcite saturation state($\Omega_{Ca}$), (f) aragonite saturation state($\Omega_{Ar}$)*

# Appendix C: XRD diffractograms of *Corallina* spp. samples exposed to three different total alkalinity addition treatments.

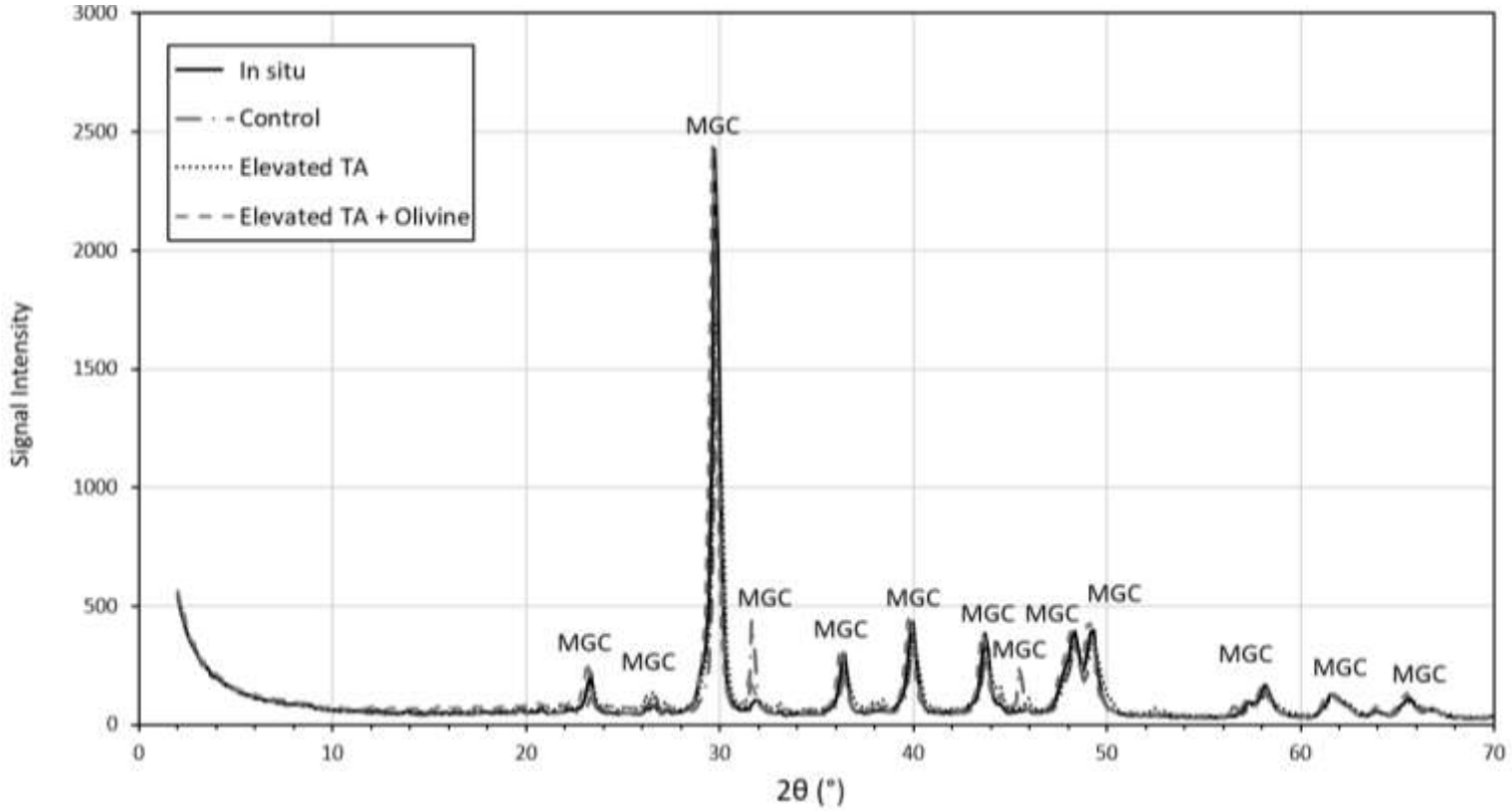


*Figure C.1. XRD diffractograms of Dunraven Bay* Corallina *spp. samples (In situ) and* Corallina *spp. samples from the experiment outlined in Chapter 3.3.1. The samples exposed to ambient total alkalinity seawater (Control), exposed to elevated total alkalinity seawater (Elevated TA) and exposed to elevated total alkalinity and olivine dissolution seawater (Elevated TA + Olivine). HMG = High Magnesium Calcite*

# Appendix D: *Synechococcus* 8806 culture media recipes

*Table D.1. ASN-III media (Rippka et al. 1979) recipe with adjusted NaCl, $MgSO_4 \cdot 7H_2O$, $CaCl_2.2H_2O$, and $Na_2CO_3$ so that salinity and total alkalinity more closely represent marine rather than fresh water.*

| ASN-III Component | Concentration (g $L^{-1}$) |
|---|---|
| NaCl | 25 |
| $MgSO_4 \cdot 7H_2O$ | 7 |
| $MgCl_2 \cdot 6H_2O$ | 2 |
| $NaNO_3$ | 0.75 |
| $K_2HPO_4 \cdot 3H_2O$ | 0.75 |
| $CaCl_2.2H_2O$ | 1.34 |
| KCl | 0.5 |
| $Na_2CO_3$ | 0.2 |
| Citric acid | 0.003 |
| Ferric ammonium citrate | 0.003 |
| Mg EDTA | 0.005 |
| Vitamin $B_{12}$ | 0.00001 |
| $H_3BO_3$ | 0.003 |
| $MnCl_2 \cdot 4H_2O$ | 0.002 |
| $ZnSO_4 \cdot 5H_2O$ | 0.0002 |
| $CuSO_4 \cdot 5H_2O$ | 0.0001 |
| $Na_2MoO_4 \cdot 2H_2O$ | 0.0004 |
| $Co(NO_3)_2 \cdot 6H_2O$ | 0.00005 |

*Table D.1. SOW (Andersen, 2005)+ L1 (Guillard and Hargraves, 1993) media recipe.*

| SOW + L1 Media Component | Concentration (g L-1) |
|---|---|
| NaCl | 24.54 |
| $Na_2SO_4$ | 4.09 |
| KCl | 0.7 |
| $NaHCO_3$ | 0.2 |
| KBr | 0.1 |
| $H_3BO_3$ | 0.003 |
| NaF | 0.003 |
| $MgCl_2$ | 5.20 |
| $CaCl_2 \cdot 2H_2O$ | 1.54 |
| $SrCl_2 \cdot 6H_2O$ | 0.017 |
| $NaNO_3$ | 0.070 |
| $NaH_2PO_4 \cdot H_2O$ | 0.004 |
| $Na_2SiO_3 \cdot 9H_2O$ | 0.03 |
| $Na_2EDTA \cdot 2H_2O$ | 3.2 |

| | |
|---|---|
| $FeCl_3 \cdot 6H_2O$ | 0.85 |
| $MnCl_2 \cdot 4H_2O$ | 0.035 |
| ZnSO4 · 7H2O | 0.007 |
| CoCl2 · 6H2O | 0.003 |
| CuSO4 · 5H2O | 0.0006 |
| Na2MoO4 · 2H2O | 0.005 |
| H2SeO3 | 0.0002 |
| NiSO4 · 6H2O | 0.0007 |
| Na3VO4 | 0.0003 |
| K2CrO4 | 0.0004 |
| Vitamin $B_1$ | 0.0001 |
| Vitamin H | 0.000001 |
| Vitamin $B_{12}$ | 0.000001 |

# Appendix E: Synechococcus 8806 growth curves from Mount Alison Experiment (Chapter 4)

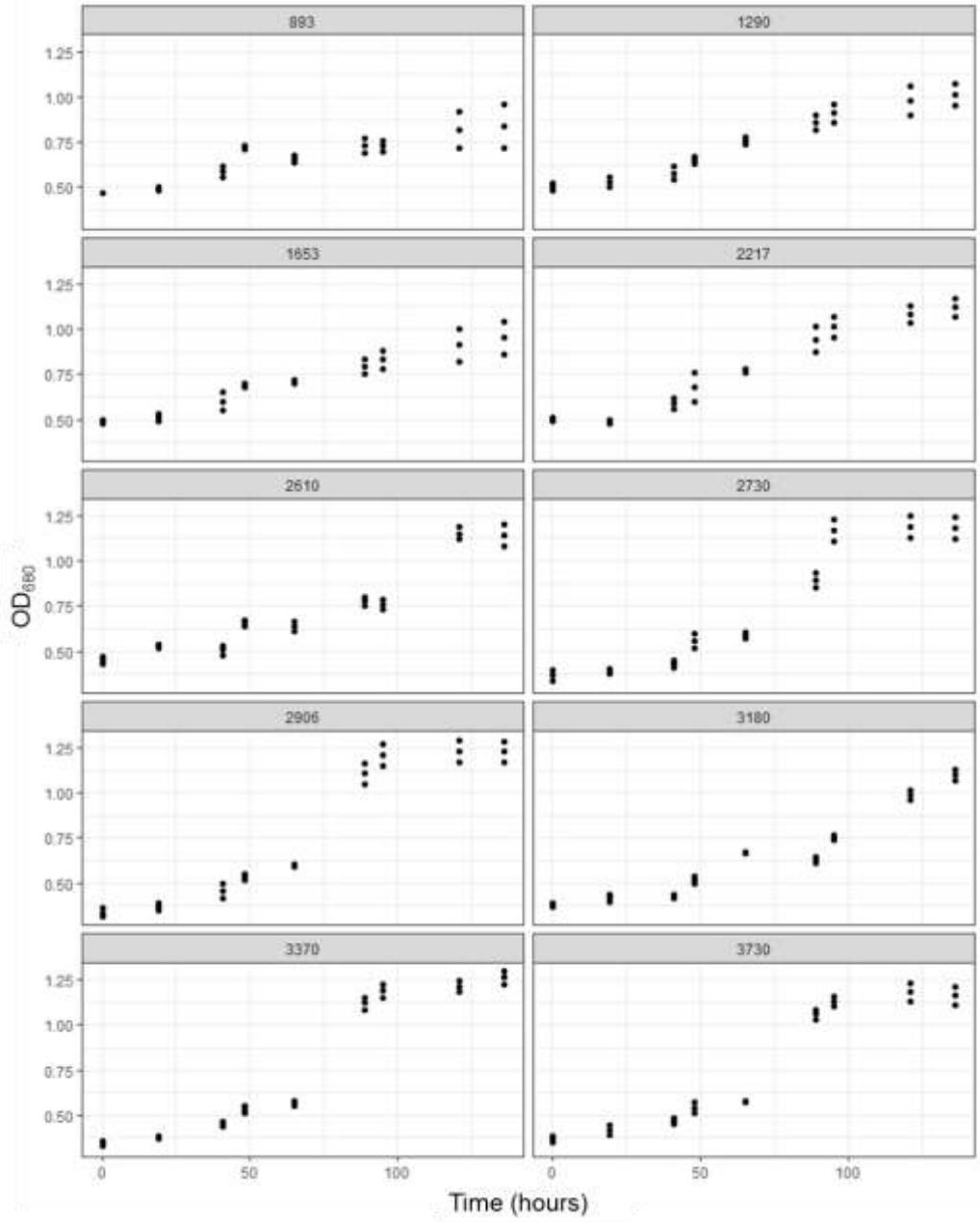


*Figure E.1. Change in* Synechococcus *8806 Chl a absorbance (optical density at λ = 680 nm; $OD_{680}$) over the course of the experiment.* Synechococcus *8806 cultures were exposed to a total alkalinity gradient from (893 µEq $L^{-1}$ to 3730 µEq $L^{-1}$). See Chapter 4.3. for methodology.*

# Appendix F: *Synechococcus* 8806 growth curves from Oxford Experiment (Chapter 5)

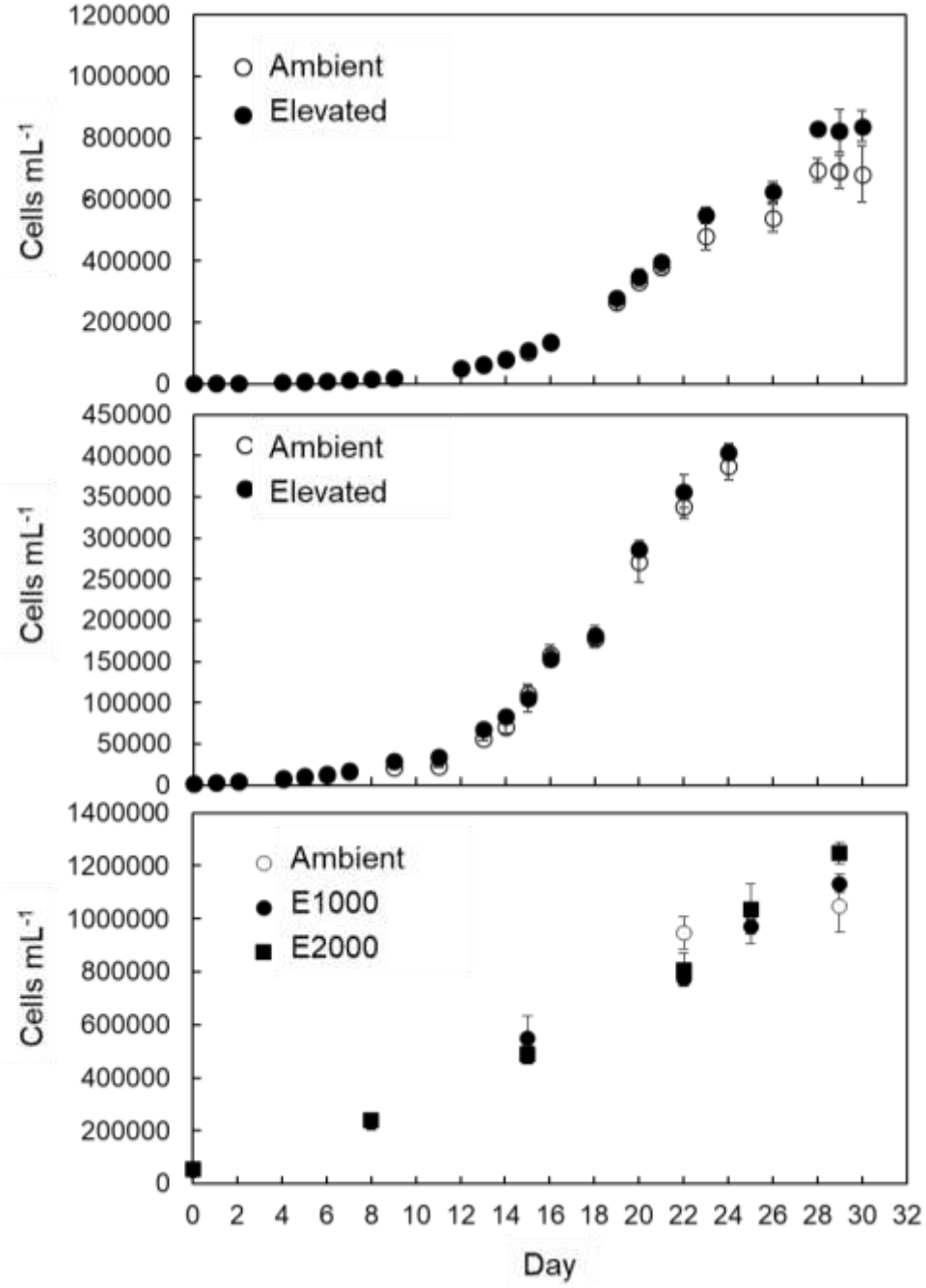


*Figure F.1. Change in Synechococcus 8806 cell density (cells mL$^{-1}$) over the course of three separate experiments performed at Oxford University as part of the work completed for Chapter 5. Synechococcus 8806 cultures were exposed to three different total alkalinity (TA) treatments: ambient TA (2640-2410 µEq L$^{-1}$; Ambient), and ~1000 elevated TA treatments (4230-3580 µEq L$^{-1}$; E1000) and ~2000 elevated TA (3980 µEq L$^{-1}$; E2000). The Experimental protocol was identical to that outlined in Chapter 5.3.*